AMRINE, CHIRAZ SOUMIA M., Ph.D. Studies on Epipolythiodioxopiperazine Alkaloids. (2019)
Directed by Dr. Nicholas H. Oberlies. 211 pp.

Natural products research remains a fertile source for drug discovery due to the complexity, chemical diversity and biological activity of compounds discovered from nature. Verticillins are members of the epipolythiodioxopiperazine (ETP) alkaloid class of fungal metabolites and are known as potent cytotoxic agents, some with IC_{50} values of less than 10 nM. Studies showed that verticillin A has activity as a selective histone methyl transferases inhibitor with important anticancer properties. However, several challenges slowed the further development of this class of compounds. The goals of this project strived to address such challenges in the development of the ETP alkaloids in three ways: (1) enhancing the production of verticillins, (2) identifying and isolating new analogues of the verticillins, and (3) developing a targeted delivery approach for the verticillins.

Aim 1 was achieved by analyzing different fungal strains under a suite of fermentation conditions. These studies were facilitated by the use of the droplet-liquid microjunction-surface sampling probe (droplet probe) coupled with UHPLC–PDA–HRMS/MS, which enables chemical analysis *in situ* directly from the surface of the cultures. These experiments showed that the production of verticillins was greatly affected by growth conditions. Using these technologies to select the best among the tested growth conditions, the production of the verticillin analogues was increased in laboratory scale fermentation.

Aim 2 was achieved via using a precursor-directed biosynthesis approach that was monitored *in situ* via droplet probe. To characterize the generated series of "non-natural natural products", a suite of NMR and mass spectrometry data were collected. This approach yielded novel compounds that would be difficult to generate via synthesis. Furthermore, and in a collaborative manner, the generation of new analogues was also achieved via semisynthetic approaches that generated ester, carbonate, sulfonate and carbamate derivatives of the verticillins. This synthetic process was characterized by the use of ^{1}H NMR to monitor the various reactions.

Aim 3 was achieved by encapsulating verticillin A into an expansile nanoparticles (verticillin A-eNP). This delivery system was used to circumvent two imperative issues of the drug administration of verticillins. First, the verticillin A-eNP was used to shield healthy cells, by targeting cancerous cells, as it permits the retention of the eNPs inside the cancer cells and the continuous release of the drug in their acidic environment Secondly, the verticillin A-eNP enhanced the solubility of the poorly soluble verticillins, facilitating a more straight forward approach to their delivery and testing *in vivo.*

STUDIES ON EPIPOLYTHIODIOXOPIPERAZINE ALKALOIDS

by

Chiraz Soumia M. Amrine

A Dissertation Submitted to
the Faculty of The Graduate School at
The University of North Carolina at Greensboro
in Partial Fulfillment
of the Requirements for the Degree
Doctor of Philosophy

Greensboro
2019

Approved by

Nicholas H. Oberlies
Committee Chair

To my loving
parents. I truly could
not have done any of
this without
you

APPROVAL PAGE

This dissertation, written by CHIRAZ SOUMIA M. AMRINE, has been approved by the following committee of the Faculty of The Graduate School at The University of North Carolina at Greensboro.

Committee Chair	Nicholas H. Oberlies
Committee Members	Nadja B. Cech
	Sherri A. McFarland
	Mitchell P. Croatt
	Aaron H. Colby

_____
Date of Acceptance by Committee

May 30, 2019
Date of Final Oral Examination

ACKNOWLEDGMENTS

I am thankful and greatly indebted to my parents, for giving me liberty to choose what I desired, for their care, sacrifice and patience in bearing with my long absence from home. I would like to express my gratitude to my sister Roufeïda and my brother Moussab for their sincere love, kindness, and support. I deeply thank Aqib for being my best friend, for his endless support and timely encouragements.

I am thankful to my advisor, Dr. Nicholas Oberlies, for providing me the opportunity to conduct this research, and for his advice and support. Drs. Nadja Cech, Sherri McFarland, Mitchell Croatt, and Aaron Colby, for serving as my committee and for their valuable comments and discussions. Dr. Feras Alali, for his help, support, and advice. Dr. Tamam El-Elimat for laboratory training and support. Drs. Franklin Moy and Daniel Todd for NMR and mass spectrometry training. Tyler Graf, for training in operating instrumentation. Drs. Huzefa Raja and Cedric Pearce, for mycological assistance. Drs Jerry Walsh, Norman Chiu, Shabnam Hematian and Pradyumna Pradhan for their advice and continual support.

This research was supported in part via P01 CA125066 from the National Cancer Institute/National Institutes of Health, Bethesda, MD.

TABLE OF CONTENTS

Page

LIST OF TABLES

Page

LIST OF FIGURES

Page

LIST OF SCHEMES

Page

CHAPTER I

VERTICILLINS: EPIPOLYTHIODIOXOPIPERAZINE ALKALOIDS WITH CHEMOTHERAPEUTIC POTENTIAL

This chapter is intended for submission to *The Journal of Antibiotics* and is presented in that style. Coauthors will include Doyle, M. G., Raja, H. A. and Oberlies, N. H.

Introduction

Despite considerable advances for early detection, diagnoses, and treatment, cancer remains a major public health issue,[1] resulting in over 1600 deaths in the United States daily.[2] As cancer progresses, or escapes elimination by current chemotherapeutic strategies, tumor cells often accrue mediated drug resistance.[3] This resistance can be caused by different mechanisms, such as the creation of a tumor microenvironment[4] (surrounding blood vessels, immune cells, fibroblasts, signaling molecules); the altered expression of efflux channels in the cell membrane, thereby lowering the dose of the drug reaching the target; and the alteration of the cellular drug target, rendering the drug ineffective.[5] With many cancer types, these resistance mechanisms result in an almost impossible escape from cancer, especially when metastasis develops, often after chemotherapy.[6-7] For these reasons, there is still a need to develop new chemical entities and approaches to fight against cancer.

Natural products have proven to be a diverse and reliable source for new scaffolds in the treatment of various diseases.[8-9] Of the 136 anticancer small molecule drugs on the

market from 1940 to 2014, a total of 113 (83%) came from, or were inspired by, natural products.[8, 10] This includes some of the front line drugs for the treatment of cancer, such as vincristine/vinblastine (bisindole alkaloids), taxol (paclitaxel), and irinotecan/topotecan (camptothecin derivatives).[11] The structural diversity of fungal metabolites makes them a significant source for drug discovery.[12-14] While much of that research has been in the anti-infective research space, due to the antibiotics revolution spawned by penicillin,[15-16] researchers have shown growing interest in investigating fungal metabolites for anticancer purposes.[17] Fungal species are hyper diverse, and various sources estimate 1.5 to 5.1 million species[18] or 2.2 to 3.8 million species.[19] The exact number may never been known, and regardless, only about 120,000[19] to 135,000[20] are taxonomically described in the literature. Of these, it is likely that even fewer have been studied for bioactive secondary metabolites,[21] making fungi an under investigated reservoir of pharmaceutical leads.[17, 22-23]

With over a decade of research on cytotoxic fungal metabolites, representing over 500 compounds, verticillins represent an area of emphasis for our research team, including scaled up production, new analogue development, drug delivery, and *in vitro* and *in vivo* evaluation against a range of cancer models. Even though three review papers[24-26] were published previously discussing particular aspects of the epipolythiodioxopiperazine (ETP) alkaloids, as a class, about ten years ago, none of these focused on the verticillins. Given that research on these compounds spans 50 years in 2020, we felt that a comprehensive summary was timely, particularly with the growing number of publications on them over the last 8 years.[27-37]

Structure, Biosynthesis and Fungal Origin of Verticillins

Epipolythiodioxopiperazines alkaloids (ETPs) are a class of fungal secondary metabolites[24, 30, 38] characterized by the presence of a polysulfur bridge on the dioxopiperazine moiety, and these can be subdivided into 14 groups according to distinct structural characteristics.[26] Of those 14 groups, only three of them are dimeric, specifically verticillins, chaetocins and leptosins (Figure 1). The main difference between these is that chaetocins have methyl alcohol groups on R_1 and R_2, while leptosins contain at least one isopropyl side chain. For verticillins, R_1 and R_2 can be CH_3, CH_3CHOH, CH_3CH_2, CH_2OH or acetyl. Both five membered rings in one verticillin monomer are *cis*-fused, and the hydroxys at the 11 and 11′ positions add stability to the molecule by forming a hydrogen-bonding network. Indeed, Liu et al.[39] reported the crystal structure of verticillin A (**1**), demonstrating that the O-H---O interactions between molecules facilitated the packing of crystals. All verticillins are ether and methanol insoluble, and they precipitate as an off white / yellow powder. The acetate form seems to enhance their solubility.[40-41]

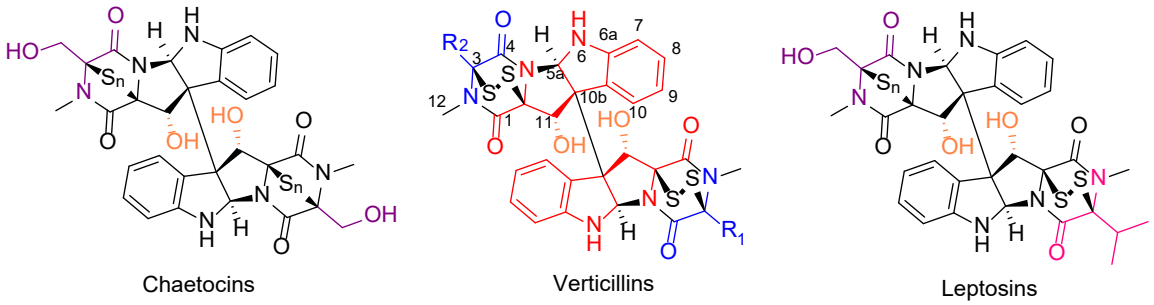

Figure 1. **The Basic Structure of Dimeric Epipolythiodioxopiperizine (ETP) Alkaloids, Showing Their Biosynthetic Origins**. The color coding is used to illustrate the building blocks of these molecules. In red is tryptophan (Trp), common to all three dimeric structural classes. For verticillins, the "blue" substituent dictates the appendage at C-3 and C-3′. For example, a methyl unit derives from alanine (Ala) or CH_2OH from serine (Ser; purple). Alternatively, a C_2H_4OH derives from threonine (Thr), which can be oxidized to the acetyl or reduced to the ethyl. The N-methylation, common to all three classes, likely derives from S-adenosyl methionine. For chaetocins and leptosins, biosynthesis often uses Ser (purple) and/or Val (pink). Moreover, in these two classes, the sulfur bridge is often greater than two atoms, whereas in the verticillins, it is almost always two sulfur atoms.

The structural diversity observed with the dimeric ETP alkaloids is due to differences in the gene clusters involved in the biosynthesis of these groups. While tryptophan (Trp) is used as a key unit in all of them, alanine (Ala), threonine (Thr) or serine (Ser) are believed to be the other building blocks used in the NRPS biosynthesis of these fungal metabolites.[24, 42]

As an additional way to classify the dimeric ETP alkaloids, the fungi producing these three classes are distinct, making their classification dependent on their fungal origin. For example, with the verticillins, their production is often noted by *Verticillium* sp., *Penicillium* sp., and *Gliocladium* sp. Alternatively, chaetocins and leptosins are biosynthesized by *Chaetomium* sp. and *Leptosphaeria* sp., respectively.[26]

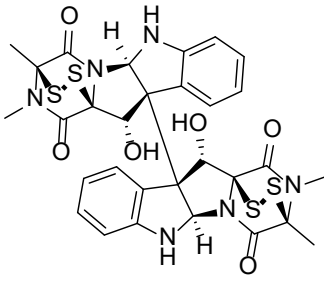

Verticillin A (1)

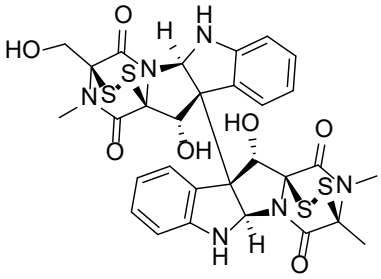

Verticillin B (2)

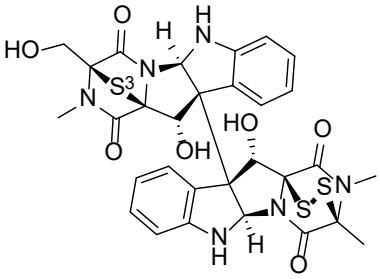

Verticillin C (3)

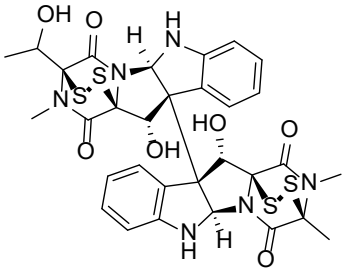

Sch 52900 (4)

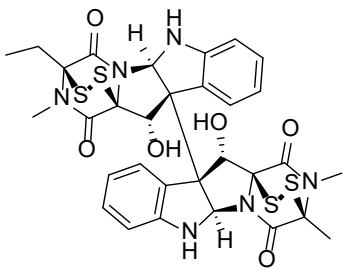

Sch 52901 (5)

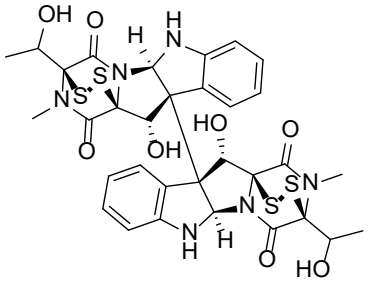

Verticillin D (6)

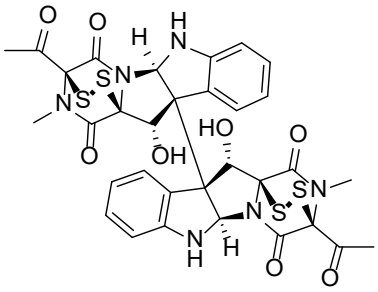

Verticillin E (7)

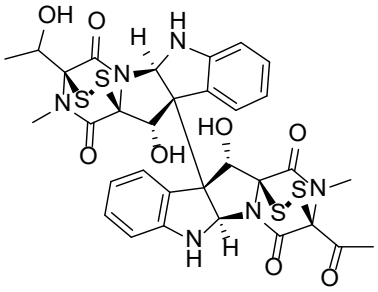

Verticillin F (8)

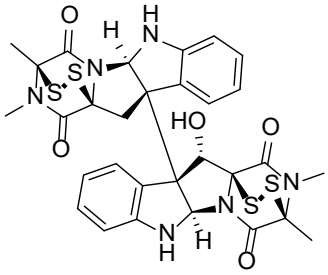

11' Deoxyverticillins A (9)

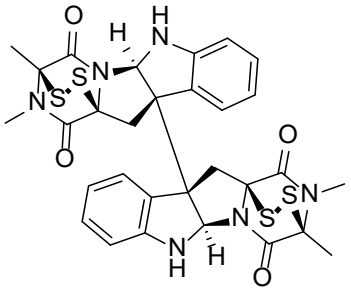

11, 11' Dideoxyverticillin A (10)

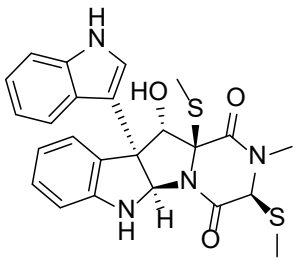

Gliocladin A (11)

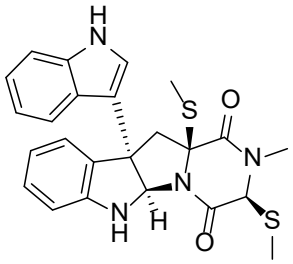

Gliocladin B (12)

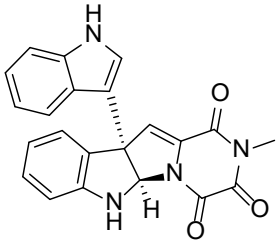

Gliocladin C (13)

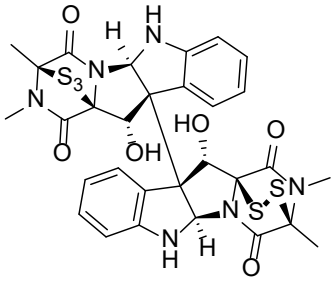

Gliocladine A (14)

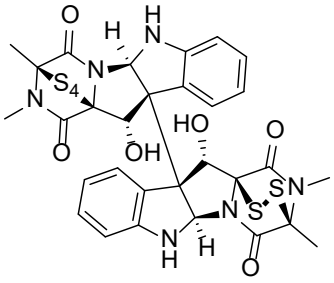

Gliocladine B (15)

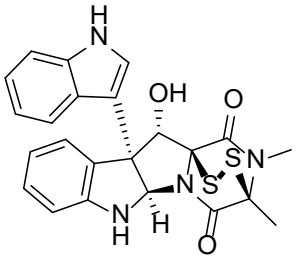

Gliocladine C (16)

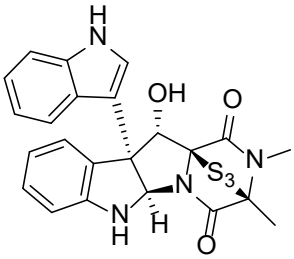

Gliocladine D (17)

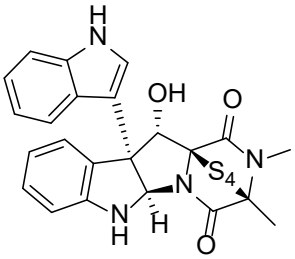

Gliocladine E (18)

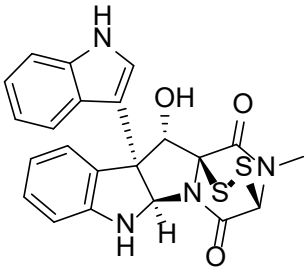

Bionectin A (19)

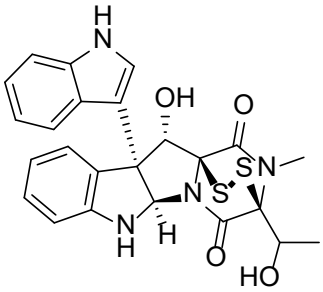

Bionectin B (20)

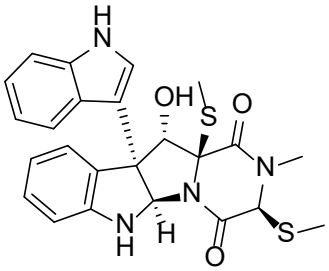

Bionectin C (21)

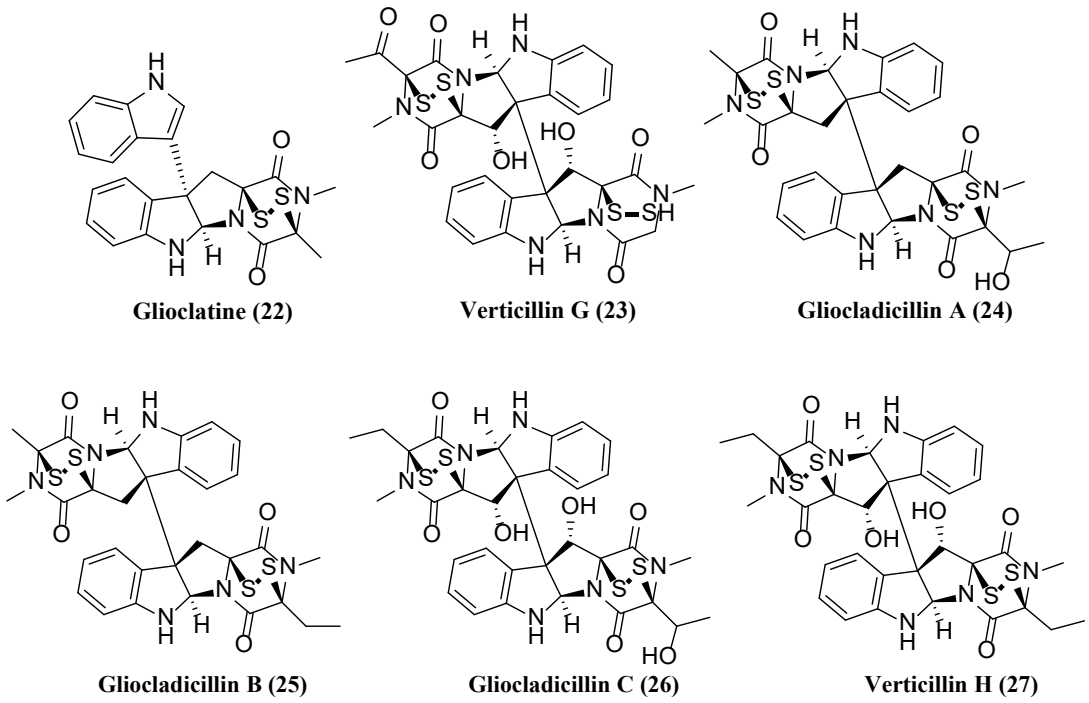

Figure 2. Structures of the 27 Verticillins in the Literature. These are ordered chronologically, based on when they were first reported.

Discovery

The first verticillin was discovered in 1970 by Katagiri and colleagues at Shionogi research laboratory from the fungus *Verticillium* sp.,[40] which was isolated from the basidiocarp of a mushroom termed "*Coltricia cinnamomea*;" this implies that the fungus was mycoparasitic. A pale yellow, ether-insoluble substance was obtained after a series of extractions followed by purification via crystallization in pyridine/acetone. This compound was analyzed using IR, MS and ^{1}H-NMR, but its structure could not be elucidated completely. During this initial report, the compound was confirmed to contain both disulfide bridged diketopiperazine and di-indolyl moieties. The name verticillin A (**1**) was ascribed to this new compound of the molecular formula $C_{30}H_{28}O_6N_6S_4$.[40] One

year later, the full structure and the absolute configuration of verticillin A (**1**) was determined using chemical and physico-chemical experiments, along with the comparisons with the close-related chaetocin (Figure 1), which was characterized previously by chemical and X-ray methods.[43] The same research team continued working on this fungus, reporting both verticillin B (**2**) and verticillin C (**3**) in 1973.[44]

No other analogues were reported for over twenty years until Sch 52900 (**4**) and Sch52901 (**5**) were disclosed by Schering-Plough, who named their new analogues with the first three letters of the institute name and a sequential serial number. Compounds (**4**) and (**5**) were isolated from the fungus *Gliocladium* sp*,* and their structures were characterized by spectral methods, including UV, IR, MS, and ^{1}H- and ^{13}C-NMR data.[45] In a separate study about sclerotium survival in soil, reported in 1999, another species of *Gliocladium* was investigated after noticing that damage was caused by this mycoparasite on its host. *G. catenulatum* was isolated from *Aspergillus flavus* sclerotia buried by the research group for two years in a Georgia cornfield.[41] This fungus was cultured and extracted to yield three new verticillins [verticillin D (**6**), E (**7**) and F (**8**)], with structures elucidated via IR, UV, HRESIMS, and 1D and 2D NMR data. In the same year, a project focused on exploring marine fungal metabolites with cytotoxic activity isolated a *Penicillium* sp. from Caribbean green algae, "*Avrainvillea longicaulis*." The cytotoxic extract was purified to yield 11′-deoxyverticillin A (**9**) and 11,11′-dideoxyverticillin A (**10**), which were both characterized by spectral methods. It could be argued that 11,11′-dideoxyverticillin A (**10**) is an outlier in the verticillin group, since its structure is neatly

identical to verticillin A (**1**) with the only difference being the absence of the hydroxy groups, classifying it to both verticillin and chaetocin groups.[46]

Gliocladin A (**11**), gliocladin B (**12**) and gliocladin C (**13**) were isolated in 2004 from *Gliocladium* sp. living in a marine environment. These metabolites lack the sulfur bridge, and gliocladin C (**13**) is considered the only trioxopiperazine isolated from the fungus.[47] One year later, five new compounds were discovered and included in the verticillin group. These latter entities were isolated from *G. roseum 1A* after a research screening freshwater fungi. Gliocladine A (**14**), B (**15**), C (**16**), D (**17**) and E (**18**) were isolated and characterized after the bioactivity directed fractionation of the a fungal culture on wheat medium.[48] Bionectin A (**19**), Bionectin B (**20**) and Bionectin C (**21**) were isolated from *Bionectria byssicola* in the same year by another research group in Korea in the course of a project screening microbial sources for antibacterial leads.[49] Glioclatine (**22**) was isolated from the fermentation of *Gliocladium roseum* grown on a wheat medium.[50] The new verticillin G (**23**) was discovered one year later by the same group in a further investigation of the same fungus.[51] Bionectin A (**19**) and B (**20**) are structurally related to gliocladine C (**16**), D (**17**) and E (**18**), as all of these have one indole ring absent in their structures, making them monomeric ETPs, which are rare compared to the usual dimer of verticillins. These monomers still belong to the verticillin group because they are produced by the same fungi that produce verticillins, and it is believed that they are produced by the same pathway, since other dimeric verticillins were isolated from the same extract as the monomers.

In a study that aims to find novel anti-tumor entities, Chen et al. published a paper in 2009 where they isolated and characterized the structure of two new dimeric ETPs isolated from *Gliocladium* sp., the same fungus from which most of the verticillins were previously isolated. Gliocladicillin A (**24**) and B (**25**) were elucidated using HRESI-MS, and 1D and 2D NMR.[52] Gliocladicillin C (**26**) was isolated by the same research group but was published in a Chinese patent.[53] Figueroa et al.[34] isolated verticillin H (**27**) along with six other verticillins after a bioactivity directed fractionation of the fermented filamentous fungus *Bionectria* sp (Figure 2).

Table 1. Chronological Data, including Year Discovered, Molecular Formula, and the Fungal Source, for the Twenty-Seven Verticillin Analogues. (*misidentified or confused with *Gliocladium* sp.)

#	*Verticillin*	*Year*	*Molecular formula*	*Molecular weight (Da)*	*Fungi*
1	Verticillin A [40, 43]	1970	$C_{30}H_{28}O_6N_6S_4$	696.83	*Verticillium sp.**
2	Verticillin B [44]	1973	$C_{30}H_{28}N_6O_7S_4$	712.83	*Verticillium sp.**
3	Verticillin C [44]	1973	$C_{30}H_{28}N_6O_7S_5$	680.77	*Verticillium sp.**
4	Sch 52900 [45]	1995	$C_{31}H_{30}N_6O_7S_4$	726.86	*Gliocladium sp.*
5	Sch 52901 [45]	1995	$C_{31}H_{30}N_6O_6S_4$	710.86	*Gliocladium sp.*
6	Verticillin D [41]	1999	$C_{32}H_{32}N_6O_8S_4$	756.88	*Gliocladium catenulatum*
7	Verticillin E [41]	1999	$C_{32}H_{28}N_6O_8S_4$	752.85	*Gliocladium catenulatum*
8	Verticillin F [41]	1999	$C_{32}H_{30}N_6O_8S_4$	754.87	*Gliocladium catenulatum*
9	11′ Deoxyverticillin A [46]	1999	$C_{30}H_{29}N_6O_5S_4$	680.83	*Penicillium sp.*
10	11,11′ Dideoxyverticillin A [46]	1999	$C_{30}H_{29}N_6O_4S_4$	664.83	*Penicillium sp.*
11	Gliocladin A [47]	2004	$C_{24}H_{24}N_4O_3S_2$	480.60	*Gliocladium sp.*
12	Gliocladin B [47]	2004	$C_{24}H_{24}N_4O_2S_2$	464.60	*Gliocladium sp.*
13	Gliocladin C [47]	2004	$C_{22}H_{16}N_4O_3$	384.40	*Gliocladium sp.*
14	Gliocladine A [48]	2005	$C_{30}H_{29}N_6O_6S_5$	664.77	*Gliocladium roseum*
15	Gliocladine B [48]	2005	$C_{30}H_{29}N_6O_6S_6$	664.77	*Gliocladium roseum*
16	Gliocladine C [48]	2005	$C_{23}H_{21}N_4O_3S_2$	464.56	*Gliocladium roseum*
17	Gliocladine D [48]	2005	$C_{23}H_{21}N_4O_3S_3$	432.50	*Gliocladium roseum*
18	Gliocladine E [48]	2005	$C_{23}H_{21}N_4O_3S_4$	432.50	*Gliocladium roseum*
19	Bionectin A [49]	2006	$C_{22}H_{18}N_4O_3S_2$	450.53	*Bionectria byssicola*
20	Bionectin B [49]	2006	$C_{24}H_{22}N_4O_4S_2$	494.58	*Bionectria byssicola*
21	Bionectin C [49]	2006	$C_{24}H_{24}N_4O_4S_3$	480.60	*Bionectria byssicola*
22	Glioclatine [50]	2006	$C_{23}H_{20}N_4O_2S_2$	448.56	*Gliocladium roseum*
23	Verticillin G [51]	2007	$C_{30}H_{28}N_6O_7S_4$	714.85	*Bionectria byssicola*
24	Gliocladicillin A [52]	2009	$C_{31}H_{30}N_6O_5S_4$	694.86	*Gliocladium sp.*
25	Gliocladicillin B [52]	2009	$C_{31}H_{30}N_6O_4S_4$	678.86	*Gliocladium sp.*
26	Gliocladicillin C [53]	2009	$C_{32}H_{33}N_6O_7S_4$	740.88	*Gliocladium sp.*
27	Verticillin H [34]	2012	$C_{32}H_{32}N_6O_6S_4$	724.88	*Bionectria sp.*

As summarized in Table 1, it is apparent that the first verticillin, verticillin A (**1**) as well as verticillins B and C were the only verticillin isolated from *Verticillium* sp.[40] A 2011 study by Schenke et al.[54] investigated the genes that were known to be responsible of the ETP verticillin like compounds. This study was performed on *Verticillium dahliae* but the authors were unable to detect any genes responsible for verticillins expression; even the extraction of a fermented culture of this fungus did not detect any verticillin, which led to uncertainties about the true ability of the fungus to be a verticillin producer. The group hypothesized the possibility that the isolated verticillin A (**1**) was from a different genus than *Verticillium* that was known to be heterogeneous. The ability of *Clonostachys* sp, the fungus from where most of the verticillins were produced, to be a mycoparasite of *Verticillium* made it possible that the original fungi was confused or contaminated with other fungi. In our research lab, we have identified the verticillin producing strains as *Clonostachys* sp. (Hypocreales, Ascomycota) that is phylogenetically similar to *C. rogersoniana*.

Biosynthesis

The investigation of the ETP class by using labeling experiments demonstrated that they were built up from amino acids.[55-56] Studies suggest that formation of the diketopiperazine ring happens during the early stages of the biosynthesis process, as feeding experiments of sulfur atoms showed incorporation from different sources (methionine, cysteine or sodium sulfate).[57] Verticillins, as the other groups of ETPs, are synthesized via a non-ribosomal peptide synthases (NRPS).[42, 58] The biosynthesis pathway of the monomeric ETP gliotoxin was thoroughly investigated for years, making

it the prototype for this class of fungal metabolites. The gene cluster, and consequently, many enzymes playing a role in its biosynthesis were determined.[59-61]

Little was known about verticillins' biosynthetic pathway until very recently when Wang et al.[32] identified the gene cluster (*ver*) from the fungus *Clonostachys rogersoniana* contributing to a better understanding of an ETP dimer's biosynthetic process. Various genes located in the *ver* cluster proved necessary to the biosynthesis, since their disruption halted the production of the verticillins. The gene *verP* is considered to be responsible for amino acid condensation to form the skeleton of the molecule. The *verA* gene is believed to serve in the transportation of verticillins, its disruption resulted in excretion of fewer secondary metabolites. The *verT* gene is believed to be accountable for the dithiol oxidation.[32]

Synthesis

Verticillins have drawn a lot of interest by synthetic chemists because of their dimeric structure, which contain sulfur bridges with eight stereocenters.[62] The high amount of stereocenters make this class very challenging for synthesis especially in the presence of basic, acidic and redox substructures.[63] The first initiative to develop a total synthesis of verticillins was in 2007, where (+)-Gliocladin C (**13**) was achieved via an enantioselective approach.[64] Movassaghi group relied on a hypothesis of the retro-biosynthesis to synthesize (+)-11,11′-dideoxyverticillin A (**10**) via 14 enantioselective steps. (+)-11,11′-Dideoxyverticillin A (**10**) was the first dimeric ETP synthesized via reductive radical dimerization, and the establishment of the disulfide bridge was elegantly added after the completion of the total carbon frame via a regioselective α hydroxylation

of the diketopiperazine rings.[62-63] The success of this synthesis strategy not only gave an insight about the probable biosynthesis but also opened the door for synthesis of other ETPs. However the yield of such synthesis was low, 0.2 g of (+)-11,11′-dideoxyverticillin A (**10**) was prepared from more than 10 g scale of commercially available amino acids derivatives.[62]

Other verticillin analogues along with closely related ETP secondary metabolites were synthesized by the same group and during the biosynthesis, they addressed some challenges like the formation of C-11/C-11′ vicinal quaternary centers, the oxidation of diketopiperazine, and the stereoselective thiolation. The study resulted in a structure-activity relationship (SAR) study and served to build a better understanding of the ETP class. Modifications were targeted on N-6, C-10b, C-3 and C-3/C-11a and results showed an increased potency when the variations were applied to C-10b and C-3/C-11a positions (Figure 3). A minimal changes in activity was observed when modification were applied on substituents on positions N-6 and C-3 make them favorable for optimizing the efficacy of the molecule.[65-66] A high potency is related to the presence of a disulfur at C-3/C-11a, while the removal of the sulfur atoms or the reduction of the sulfur bridge diminish/abolish the activity of verticillins.[49, 65, 67]

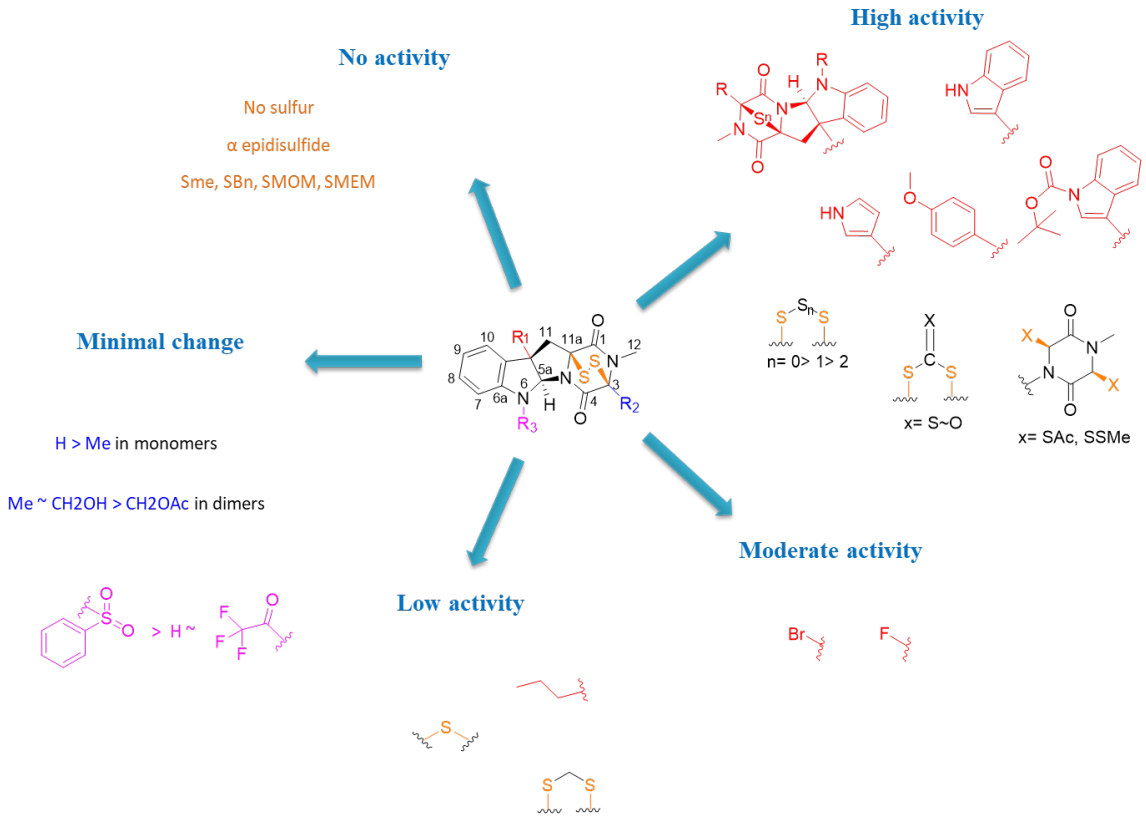

Figure 3. Structure-Activity Relationship Study. Modified from Boyer et al.[65]

Mechanism of Action

Mechanism of action studies have shown that verticillin A (**1**) is a histone methyl transferases (HMTase) inhibitor with a selective activity towards G9a, GLP, SUV39H1, SUV39H2, MLL1 and NSD2 methyltransferases. The most selectivity of verticillin A (**1**) was observed against G9a, SUV39H1 and SUV39H2 with IC_{50} values of 0.54, 0.57 and 0.48 μM, respectively.[28] Paschall et al.[35] discerned the selective role of verticillin A (**1**) in inhibiting the histone H3 lysine9 (H3K9) methylation, by reversing enzyme function displaying a decrease of H3K9me2 and H3K9me3 levels. H3K9me3 was shown to be responsible for Fas transcription silencing, which results in its loss of expression in

human colon carcinoma cells. Treatment with verticillin A (**1**) showed a decrease in H3K9me3 levels in the FAS promoter region with an increase of histone H3 lysine9 acetylation (H3K9ac), which indicates active transcriptional chromatin and is known to mediate FAS expression.[35] FAS-L ligand present on the surface of cytotoxic T lymphocyte (CTL) binding to FAS initiates an immunological reaction leading to FAS mediated apoptosis.[68-69]

H3K4me3 levels were found to be significantly high *in vitro* and *in vivo* in PANC02-H7 and UN-KC-6141 pancreatic cancer cell lines and the orthotropic tumor. MLL1 was found to be the HMTase responsible for the methylation of the H3K4. Silencing the MLL1 gene in both human and mouse pancreatic cancer cells resulted in a decrease of H3K4me3 with a decrease of PD-L1 ligand expressed by the tumor cell. Being an HMTase inhibitor, verticillin A (**1**) inhibits MLL1 with an IC_{50} of 0.8 μM. Subsequently, a decrease of H3K4me3 levels consistent with a decrease of expression in a dose dependent manner was observed in both *in vitro* and *in vivo* orthotropic tumors. The decrease of PD-L1 resulting in its reduced binding to PD-1 present in the CTL that activates the immune response against the tumor cells. The same pancreatic cancer cells that showed a potent anti-MLL1 activity, also showed that FAS-L mechanism is important in tumor growth suppression in wild mice models transplanted with pancreatic tumor.[70]

Verticillin A (**1**) was found to inhibit pancreatic ductal adenocarcinoma (PDAC) growth in a dose dependent manner and sensitized PDAC cells to gemcitabine. Mechanistically, verticillin A (**1**) caused epigenetic modification in apoptosis regulating

genes by altering H3K9me3 and H3K4me3 levels. Chromatin immunoprecipitation (ChIP) revealed that verticillin A (**1**) caused dysregulation of apoptotic genes by decreasing H3K9me3 levels at Bak , Bax and Bim promoter region and H3K4me3 level at Bcl-x, Mcl-1 and FLIP promoter region in PDAC cells.[37]

Pharmacology

Anticancer activity

Most of the isolated verticillins were discovered within projects investigating cytotoxic secondary metabolites.[40, 46] Using a *fos/lac Z* reporter gene assay, Chu et al. showed that Sch 52900 (**4**), Sch 52901 (**5**) and verticillin A (**1**) inhibited serum-stimulated transcription of human c-fos promoter.[45] Certain cancer cells were detected to produce a high level of *c-fos,* which is a proto-oncogene and plays a role in transition of cells from a quiescent to a growing state.[71] These verticillin analogues exerted potent activity in the *fos/lac* Z reporter gene assay with *in vitro* IC_{50} values of 1.5, 1.8 and 0.5 μM, respectively. Thus, verticillin A (**1**) exerted antitumor activity by inhibiting the activation of at least two signaling pathways involved in *c-fos* induction.[45]

Leukemia is characterized by an uncontrolled propagation of white blood cells (WBCs) and evasion from the terminal differentiation step leading to under-developed WBCs. One strategy of treatment in leukemia is to induce differentiation of WBCs followed by apoptosis.[72] Sch 52900 (**4**) demonstrates the ability to induce differentiation of 50-69% of HL-60 cells (human promyelocytic cells) at low concentrations (6.8-13.6 nM). Mechanistically, Sch 52900 (**4**) caused induction of the cell cycle inhibitor $p21^{WAF}$

and inhibition of the extracellular signal regulated kinase (ERK) that led to cellular apoptosis and subsequent growth arrest.[73]

11,11′-Dideoxyverticillin A (**10**) has a potent anti-tyrosine kinase activity and inhibitory activity towards epidermal growth factor receptor (EGFR), vascular endothelial growth factor receptor-1/fms-like tyrosine kinase-1 (VEGFR-1/FLT-1) and human epidermal growth factor receptor-2 (HER2/ErbB-2), being selectively more potent against EGFR and VEGFR-1 with IC_{50} values of 0.136 and 1.645 nM, respectively.[74] Verticillins have also been shown to cause cell cycle G2/M phase arrest in HCT-116 colon cancer cells using *in vitro* and *in vivo* experiments.[75] Similarly, Gliocladicillins A and B are strong anti-proliferative and pro-apoptotic agents and are demonstrated to inhibit proliferation of cancer cell lines HeLa, HepG2 and MCF-7 by cell cycle blockage in the G_2/M phase.[52] Moreover, 11,11′-dideoxyverticillin A (**10**) has an anti-angiogenic effect and inhibits proliferation of HUVECs (human umbilical vein endothelial cells) with IC_{50} values of 0.17 and 0.39 μM for VEGF (vascular endothelial growth factor) stimulated cells and serum-stimulated cells respectively.[74-76]

An important study done by Liu et al.[27] revealed that verticillin A (**1**) inhibited HepG2 (human liver carcinoma) tumor cell growth by inducing apoptosis *in vitro* and inhibited *in vivo* tumor growth at a dose of 2 mg/kg body weight. Verticillin A (**1**) showed its high potency against multiple types of cancer cells with concentrations in the nanomolar ranges. It has also been demonstrated that verticillin A (**1**) is an apoptosis sensitizer for different types of tumors resistant to TRAIL, a potent anticancer agent *in vitro* and *in vivo*. This study emphasized the importance of verticillin A (**1**) as a highly

potent, low toxicity anti-cancer agent and a strong adjuvant to overcome drug resistance in cancer treatment.[27] 11′ Deoxyverticillin A (**9**) is shown to induce autophagy in HCT116 human colon carcinoma cells leading to cell death.[29] In another study of human colorectal carcinoma (CRC) xenograft model, verticillin A (**1**) showed its efficacy in overcoming metastatic human CRC resistance to 5-fluorouracil (5-FU), which is the standard treatment for this type of cancer. The tumor size and weight were decreased significantly when the mice were treated with a combination of verticillin A (**1**) and 5-FU compared to groups that received individual treatments. The investigation of the role of verticillin A (**1**) in sensitizing the cancer cells to 5-FU revealed that the mechanism of apoptosis induction was independent of the FAS expression. Other analysis on the mice liver enzymes indicated that verticillin A (**1**) has minimal liver toxicity at a dose of 1 mg/kg body weight injected every other day during 10 days.[35]

In a study on soft tissue sarcoma (STS), that is known to be therapeutically challenging due to the genetic and histological heterogeneity, verticillin A (**1**) showed its potency in inhibiting malignant peripheral nerve sheath tumor (MPNST) and leiomyosarcoma (LMS) growth by inducing apoptosis. *In vitro* experiments demonstrated that verticillin A (**1**) inhibited colony formation in STS cells, in addition to inducing apoptosis. Mice xenografted with MPNST724 revealed tumor growth inhibition and significant reduction of tumor volumes and weights when treated with verticillin A (**1**) at a dose of 0.25 or 0.5 mg/kg of body weight.[30]

In pancreatic cancer cells, upregulation of the PD-L1 ligand increased the tumor cells viability by evading immune response.[70, 77] CTL express PD-1 receptor that binds to

PD-L1 overexpressed in cancer cells and this binding inhibits the CTL activity permitting immune checkpoint evasion. In both PANC02-H7 and UN-KC-6141 pancreatic tumors, PD-L1 was found to be expressed in significant higher levels *in vivo*, likewise, over 50% of tumor-infiltrating $CD8^+$ CTLs were $PD\text{-}1^+$. Four mice group with pancreatic tumor transplants received 0.5 mg/kg body weight of verticillin A (**1**) and 200 µg of anti-PD-L1 either alone or in combination along with a control group. Pancreatic cancer has a poor response to anti-PD-L1/PD-L1 immunotherapy[78] and the results from this study decreased tumor growth in the treated groups compared to the control. The group with combined treatment of verticillin A (**1**) and anti-PD-L1 exhibited the most significant growth suppression close to tumor eradication. Verticillin A (**1**) repressed PD-L1 expression by inhibiting MLL1 on the tumor cells and the additive effect of combining the two drugs indicates the important role of verticillin A (**1**) in increasing the efficacy of the anti-PD-L1 therapy.[70]

Verticillin A (**1**) suppressed tumor growth by inhibiting H3K9me3, resulting in a FAS-L mediated apoptosis or by inhibiting H3K4me3 leading to PD-L1 immunosuppression. A similar *in vivo* experiment was conducted with the same therapeutic strategies mentioned above where the FAS-L mechanism was excluded. The tumor growth suppression rose to be dependent on the FAS-L and CTLs,suggesting new approaches of combining epigenetic and immune checkpoint blockade immunotherapies.[36, 70]

The first pharmacokinetic and bioavailability studies were conducted on verticillin A (**1**) by Wang and colleagues who administrated the drug orally (PO),

intraperitoneally (IP) at a dose of 3 mg/kg and intravenously (IV) at a dose of 1 mg/Kg Blood plasma concentrations of verticillin A (**1**) were then calculated using liquid chromatography-tandem mass spectroscopy (LC-MS). The within and between days precision was <9% and the accuracy was between 90 to 105%. IP dosing results showed the highest systemic exposure with a maximal concentration (C_{max}) of 110 nM and sustained plasma concentrations above 10 nM for 24 hours duration. IV and PO doses achieved 73 nM and 9 nM of C_{max} values respectively. The high levels of active verticillin A (**1**) after IP and IV administration warrant further investigation of these routes for future *in vivo* studies.[31]

Nematidical activity

Verticillin analogues such as gliocladine A (**14**), B (**15**), C (**16**), D (**17**) & E (**18**), verticillin A (**1**), 11′ deoxyverticillin A (**9**), Sch 52900 (**4**) and Sch52901 (**5**) were tested for their anti-nematicidal effects against *Caenorhabditis elegans* and *Panagrellus redivivus.* The dimeric verticillins were the most effective in comparison to the monomeric forms containing the indole moiety. The number of sulfur atoms in the bridge did not influence the potency of the molecules.[48]

Antimicrobial activity

Bionectin A (**19**) and B (**20**) were tested for their antibacterial activity against *Staphylococcus aureus*, methicillin-resistant *S. aureus* (MRSA) and quinolone-resistant *S. aureus* (QRSA) and resulted in MIC values of 10-30 µg/mL whereas, Verticillin D (**6**) and G (**23**) showed a higher activity with a MIC of 3-10 µg/mL.[49, 51]

Summary and Conclusion

To date, 27 verticillin analogues have been reported in the literature. This review describes this interesting group of ETP alkaloids. What differentiates verticillins from other ETP groups appears to be primarily based on the fungal strain producer of these different entities. Verticillins are biosynthesized via NPRS, and the amino acids building blocks used for biosynthesis are specific for this group. Recently, a study of the genome of *C. rogersoniana* identified the gene cluster (*ver*) contributing to a better understanding of the biosynthetic pathway of these molecules. Verticillin A (**1**) was discovered in 1970 from the filamentous fungi *Verticillium* sp. that turned out to be a misidentification of the genus. *Gliocladium* sp., *Penicillium* sp., and *Bionectria* sp. are reported to be the main producers of verticillins. The verticillin group is characterized by its sulfur bridge, essential for the potency of the molecule. Verticillins are known to be antifungal and antibacterial and recently their anticancer activity has generated interest in the field of cancer drug discovery. Verticillin A (**1**) is shown to be a potential anti-tumor drug due to its specificity and toxicity towards cancer cells by modifying the epigenome and sensitizing cancer cells to apoptosis. This interest in the anti-cancer activity lead to a couple of *in vitro* and *in vivo* studies described in this review. The demand for new anticancer drugs and the potential shown by the verticillin group of compounds make them a good lead for drug development

CHAPTER II

MEDIA STUDIES TO ENHANCE THE PRODUCTION OF VERTICILLINS FACILITATED BY *IN SITU* CHEMICAL ANALYSIS

This chapter has been published in *The Journal of Industrial Microbiology & Biotechnology* and is presented in that style. Amrine, C. S. M., Raja, H. A., Darveaux, B. A., Cedric J. Pearce, C. J., Oberlies, N. H. *J Ind Microbiol Biotechnol*. **2018**, 45 (12), 1053–1065.

Introduction

Fungi are a rich resource for biologically active and structurally diverse secondary metabolites.[12-14] As such, a number of authors have noted the value of investing in fungi as a source of new drug leads, especially to treat cancer and overcome its resistance.[11, 21] Cancer is a worldwide problem, and in the USA alone, over one million new cases were estimated for 2016, resulting in more than half a million cancer-related deaths.[79]

As part of ongoing studies to discover new anticancer leads from filamentous fungi,[11, 34, 80] our team has isolated hundreds of fungal metabolites over the last decade.[14] Of these, verticillins are one of the most interesting for a variety of reasons.[27, 30, 34-35, 70] This class of bioactive fungal secondary metabolites (as exemplified by compounds **1-7**) is characterized by a dimeric structure[26] and is a key member of the epipolythiodioxopiperazine (ETP) alkaloids. Biologically, these compounds display potent antitumor activity,[38, 46, 52, 74, 76] along with antibacterial,[41, 43, 49, 51] nematicidal [48] and immune induction properties.[73]

The lead compound of this class, verticillin A (**1**), was first discovered in 1970,[40] and since then, 27 verticillin analogues have been characterized,[34] even 30 years ago, their cytotoxic potential was noted.[38] At the time of discovery, verticillin A (**1**) showed an ED_{50} of 0.2 μg/mL (0.27 μM) against HeLa cells.[40] In another study, verticillin A (**1**), along with the closely related analogues, Sch 52900 (**5**) and Sch 52901 (**2**), showed potential in preventing the transcription of *c-fos* promoter gene, which is a proto-oncogene found overexpressed in a variety of cancers.[45] Two analogues, 11,11′-dideoxyverticillin A (**6**) and 11′-deoxyverticillin A (**7**), demonstrated *in vitro* cytotoxicity against HCT-116 (human colon carcinoma) cells in the nanomolar range.[46] These later compounds also demonstrated an inhibitory effect of tyrosine kinase on the growth factor receptor, thereby leading to anti-tumor activity.[74] Verticillin A showed potent activity in sensitizing human colorectal cancer cells to apoptosis both *in vitro* and *in vivo*, as well as, the ability to induce cell-cycle arrest at the G_2 phase.[27]

Biologically, interest has been growing in the verticillins, particularly after verticillin A (**1**) was shown to be a selective histone methyl transferases (HMT) inhibitor.[35] The HMT inhibitory activity resulted in the demethylation of H3K9me3 of the silenced FAS gene, [35] thereby allowing its transcription, such that FAS was re-expressed, triggering apoptosis mediated cell death.[81] Moreover, verticillin A (**1**) induced apoptosis selectively against malignant tumor cells, while minimal effect was exhibited against healthy cells.[30] Verticillin A (**1**) showed potential to overcome metastatic colon carcinoma resistance to 5-fluorouracil. Mice transplanted with SW620-5FU-R cells were treated with a combination of verticillin A (**1**) and 5-fluorouracil and displayed

significantly smaller tumors compared to the groups receiving only one of these two treatments.[35] In a recent study conducted on pancreatic cancer by Lu et al.,[70] verticillin A was given to two groups of mice transplanted with either PANC02-H7 or UN-KC-6141 cells. Verticillin A was administrated alone or in combination with anti PD-L1 (programmed death ligand) treatment to provide immunotherapy. The results demonstrated that verticillin A (**1**), in conjugation with anti PD-L1 ligand, markedly reduced tumor size and viability. In summary, a suite of pharmacological studies over the last five years has increased the interest surrounding this class of compounds.

Despite the promising activities that verticillins have shown *in vitro* and *in vivo*, research has been hindered by the lack of material. In previous work, 0.66 to 1.72 mg of verticillin analogues (**1-3**) per g of extract could be isolated from large scale fermentations of fungal cultures containing 150 g of rice (with a total isolated of 1.6 to 5.5 mg).[34] Similarly, 0.37 to 0.85 mg of verticillin analogues were isolated per g of extract (with a total isolated of 3.5 to 8.0 mg).[41] Based on the literature, the yields of these compounds were not improved greatly when grown in liquid cultures. For example, from a 73 L fermentation, the yield of verticillin G was 0.58 mg per g of extract (with a total isolated of 2.9 mg).[51] In another study that used 20 L fermentations, compounds **1**, **6** and **7** were isolated with a yield of 0.25 mg, 0.61 mg and 1.14 mg per g of extract, respectively (with a total yield of 3.5 mg, 8.5 mg and 16 mg, respectively).[46] Furthermore, although elegant synthetic approaches have been reported for the preparation of various epipolythiodioxopiperazine alkaloids,[62, 65-66] these processes require numerous reactions steps, making the large-scale production of these compounds

challenging. About 0.2 g of (+)-11,11′-dideoxyverticillin A was prepared in 14 steps from >10 g scale of commercially available amino acids derivatives.[62] In summary, the production of the verticillins in the literature, whether using liquid-based or solid-based fermentations, has been largely on the scale of only a couple mg, and most of the verticillins have never been synthesized. For these reasons, the adequate supply of key analogues must be addressed before the full pharmacological potential of these compounds can be realized.

Many studies have shown the influence of media and environmental factors on fungal biosynthesis,[82-83] where optimal nutrition is required for ideal fungal growth.[84-85] The OSMAC approach is a prominent strategy to probe the importance of fungal fermentation conditions, potentially generating broader chemical diversity [86-87] and/or targeting the enhanced production of a distinct a class of secondary metabolites. In this study, several fungal strains were selected from the Mycosynthetix library. These cultures were grown on a suite of different solid media, and productivity was assessed by taking advantage of new instrumentation that facilitates the screening of the chemistry of the cultures. The droplet-liquid microjunction-surface sampling probe (droplet probe) permits the *in situ* analysis of targeted secondary metabolites directly from the surface of cultures.[88-89] Our goal was to enhance the biosynthesis of verticillins by identifying a strain that produces the highest quantity of the analogues under appropriate fermentation conditions in the shortest period of time.

Materials and Methods

Mycology

Fungal cultures were provided by Mycosynthetix, Inc., via an ongoing project to identify diverse natural product study material as a source of anticancer drug leads.[11] Over the last decade, we have analyzed the chemistry and biological activity of thousands of cultures from the Mycosynthetix library, and among these, ten cultures were identified as being able to biosynthesize verticillin A and its analogues (compounds **1-5**) based on published dereplication protocols.[90-91] Accordingly, the following strains were chosen for this study: MSX74391, MSX71844, MSX58124, MSX75296, MSX75281, MSX45374, MSX70777, MSX59553 and MSX79542 (Table 2S). In a previous study, fungal strains MSX59553 and MSX79542 were both identified as *Clonostachys rogersoniana.*[90]

Identification of fungal strains

The different MSX strains utilized in the present study were identified to the genus and/or species level using the fungal ITS region (ITS1-5.8S-ITS2) of the nuclear ribosomal operon, which was amplified with primer combination ITS5 and ITS4 with primers ITS5/ITS1F and ITS4.[92-93] Methods for BLAST search in NCBI GenBank and Maximum Likelihood phylogenetic analysis, as utilized to identify fungal strains, have been detailed recently.[94] The BLAST search and phylogenetic analysis using taxon sampling.[95] revealed that MSX59553, MSX79542, MSX74391, MSX58124, MSX75296, MSX75281, MSX45374, and MSX70777 belong to the genus *Clonostachys* (Ascomycota, Hypocreales, Bionectriaceae), while MSX71844 was identified as *Purpureocillium lavendulum* (Ascomycota, Hypocreales, Ophiocordycipitaceae) (Figure

1S). Phylogenetic analysis using the ITS region also showed that strains MSX59553, MSX45374, MSX74391, MSX79542, MSX7077, and MSX 58124 had phylogenetic affinities with *C. rogersoniana.*[96] Our results were in agreement with a recent genomic study identifying the biosynthetic gene clusters for verticillins in *C. rogersoniana.*[32] As the ITS region alone is not informative to identify species in certain orders of the Ascomycota, including Hypocreales,[97] future taxonomic and molecular phylogenetic studies will incorporate sequence data from protein-coding regions to more precisely identify species names for verticillin-producing strains.[98] The sequence data were deposited in GenBank (accession numbers: KX845687, KX845688, MH421853, MH421854, MH421855, MH421856, MH421857, MH421858, MH421859, and MH421860).

For verticillin producing strains, there has been some confusion on the fungal taxonomy.[54] Earlier studies on the chemistry of verticillin analogues have identified the verticillin-producing fungi as belonging to the genera *Gliocladium, Penicillium,* and *Verticillium*.[40-41, 46] The morphology of the flask shaped phailide in all three genera can be a cause of confusion for non-mycologists. Moreover, fungal taxonomic names have been rapidly changing due to the use of molecular sequence data in the past 20 years.[94] In addition, the name *Bionectria* (sexual state) has been used previously in the literature for a fungal strain producing verticillin G;[51] which was accurate, but the use of name *Bionectria* is now phased out due to the adoption of One Fungus = One Name,[99-100] in accordance with the recent changes concerning pleomorphic fungi in the *International Code of Nomenclature for algae, fungi, and plants*. For pleomorphic names (sexual and

asexual) in the family Bionectriaceae, Rossman et al.[101] have proposed the use and protection of the asexual morph (*Clonostachys*) rather than the sexual morph (*Bionectria*). Despite the adoption of the name *Clonostachys*, the subgenus *Bionectria* is still being used in the literature. Based on our recent identification of fungal strains that make verticillin and its analogues, we have identified two fungal genera, *Clonostachys* spp. and *Purpureocillium lavendulum*,[102] that biosynthesize the epipolythiodioxopiperazine-type alkaloids.

Media and fermentations

For the analysis of fungal cultures in Petri dishes, seven types of agar media were used, and ingredients to make these were purchased from Difco, ACROS, and Research Products International (RPI): malt extract agar, potato dextrose agar, yeast extract soy peptone dextrose agar, Spezieller Nährstoffarmer agar, Sabouraud dextrose agar, potato dextrose mushroom and oatmeal agar (See Table 1S for compositions). A small piece (~0.5 cm^2) of fresh culture grown on potato dextrose agar was cut from the leading edge of 2-week old colony from strains MSX59553 and MSX79542 and was used to inoculate various types of agar media in duplicate, respectively. The plates were then incubated at room temperature until the cultures showed good growth as noted by the expansion of the colony over the surface of the medium (~3 to 4 weeks).

Rice fermentations [(1:1 commercial white rice (variety: Carose Botan; 5 g) and (variety: Sona Masoori; 5 g)] were prepared by adding 10 g of rice to a Petri dish or a 250 mL flask with 25 mL of DI-H_2O, followed by autoclaving at 221 °C for 30 min. Oatmeal media (Old fashioned Quaker oats) was prepared using 10 g of rolled oats and ~17 mL of

DI-H_2O, followed by autoclaving at 221 °C for 30 min. The flasks containing the rice or oatmeal media were inoculated with a seed culture grown in 10 mL of YESD broth media (2% soy peptone, 2% dextrose and 1% yeast extract) for about 5 days with agitation (100 rpm) at room temperature. The inoculated cultures were grown at room temperature for ~4 to 5 weeks, except for the time progression studies, where each duplicate of the oatmeal culture was extracted every few days, from days 2 to 35. Strains were scaled-up in a similar way, using 2.8 L Fernbach flasks (Corning, Inc., Corning, NY, USA). The medium was prepared using 150 g of either rice or oatmeal, with 300 mL or 250 mL of DI-H_2O added for rice medium and oatmeal medium, respectively, and both sterilized at 221 °C for 30 min. In addition, and as noted in more detail in the supplement (Figure S7), augmenting the oatmeal media with amino acids was also examined. However, this did not result in significant differences in the biosynthesis of verticillins, and thus, this line of inquiry was not pursued further.

Extraction of fungal cultures

Each culture was chopped with a spatula to ensure thorough extraction. For the cultures grown on Petri dishes, the chopped pieces were transferred into 150 mL flasks. Solutions of 60 mL of 1:1 chloroform:methanol ($CHCl_3$:MeOH) were poured in each flask, followed by overnight shaking (100 rpm) at room temperature. The cultures were filtered by vacuum, and then the filtrates were mixed with 90 mL of $CHCl_3$ and 150 mL of H_2O and stirred for 30 min. The mixtures were transferred into a separatory funnel, where the bottom organic layer was evaporated *in vacuo* and reconstituted with 100 mL

of 1:1 acetonitrile:methanol (CH_3CN:MeOH) and 100 mL hexanes. Again, the defatted organic layers were collected and evaporated *in vacuo*.

***In situ* analysis of fungal metabolite profiles via the droplet probe coupled with UPLC-PDA-HRMSMS/MS**

The use of the droplet probe with fungal cultures has been detailed previously [89] and several examples have been published.[103-107] A CTC/LEAP HTC Pal auto-sampler was converted to a droplet probe with assistance from colleagues at Oak Ridge National Laboratories.[108-109] Microextractions (3-5 µL) were performed on precise spots directly on fungal cultures using a 1:1 solution of MeOH:H_2O. The extractions were injected onto a UPLC, and the chromatographic method followed previous protocols [91] used in the dereplication of fungal extracts. A Waters Acquity UPLC system was used with a BEH C_{18} column (Waters; 50 mm x 2.1 mm x 1.8 µm) heated to 40 °C and a mobile phase using a gradient from 15% to 100% CH_3CN; the other solvent was 0.1% formic acid-H_2O. The run utilized a flow rate of 0.3 mL/min for 10 min. UV data were collected from 190 to 500 nm and the eluent was split into a Thermo Fisher Scientific Q Exactive Plus mass spectrometer via electrospray ionization (ESI). MS data were collected from 150-2000 *m*/z at a resolution of 70,000 while alternating between positive and negative modes. MS/MS was performed with an HCD value of 35, and Xcalibur software was used for the primary analysis.

Analysis of fungal metabolite profiles via UPLC-PDA-HRMSMS/MS

Extracts of the plates and flasks were dissolved separately in 1:1 MeOH:dioxane to elaborate concentrations of $2.5x10^{-2}$, 0.5 or 2.0 mg/mL; 3 µL were injected directly

onto the UPLC-PDA-HRMSMS/MS system. In addition to HRMS and MSMS data, retention times and UV data were used as mutually supportive data. The relative peak areas of each targeted secondary metabolite were measured (Figure 4).

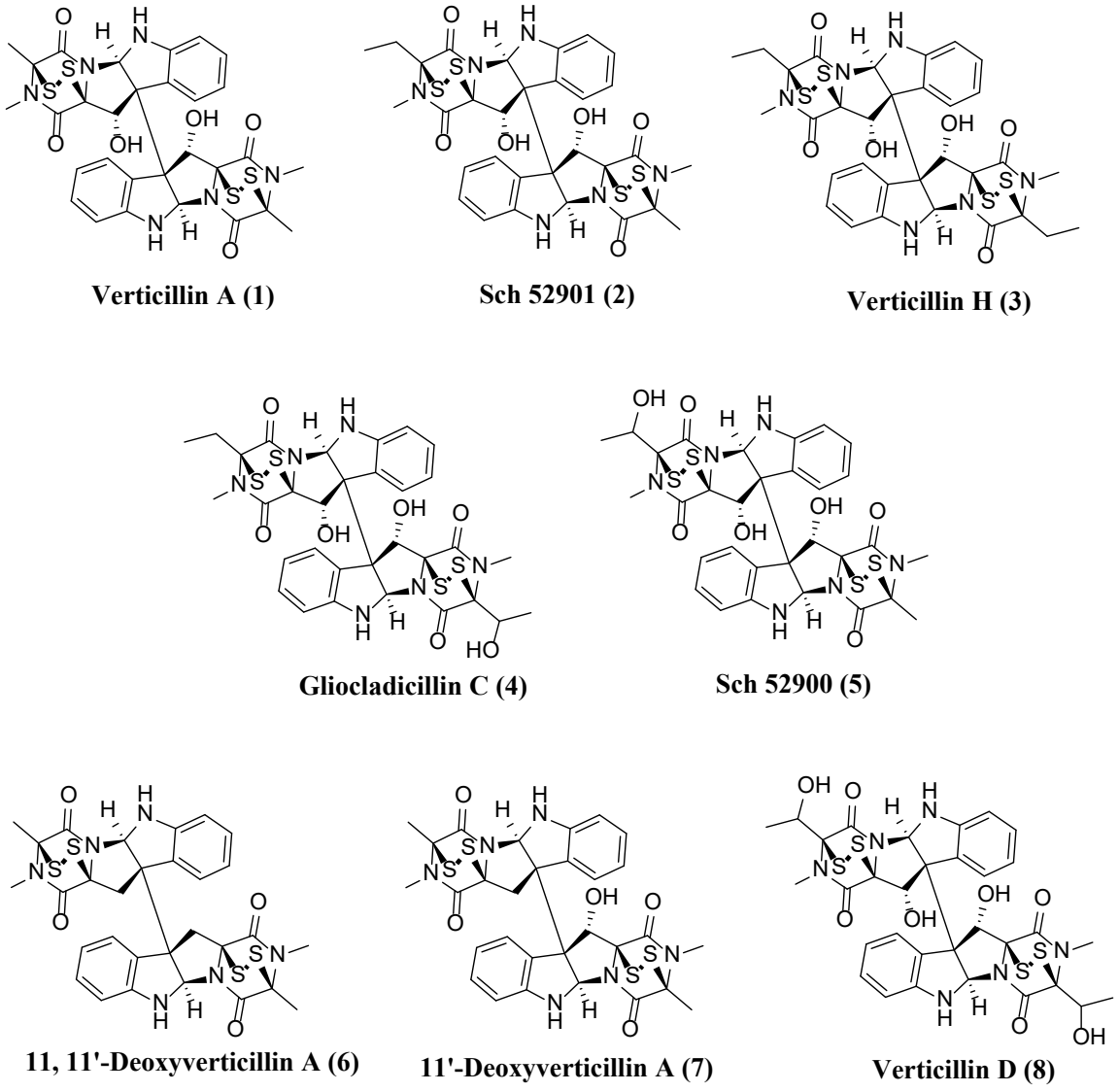

Figure 4. Structures of Verticillin A and Related Analogues. Compounds **1-5** were the target for the biosynthetic optimization studies.

Results and Discussion

Different fungal strains biosynthesize distinct patterns of verticillin analogues

The dereplication protocol was used to identify fungal strains that produced verticillins [91] (Table 2S). Extracts of suspected verticillin producing strains from our library were screened using UPLC-HRMS, revealing a higher production of verticillin analogues within the organic extracts of both strains MSX59553 and MSX79542 (Figure 5). The graph shows the relative percentage of the targeted verticillin analogues as measured in triplicate. In order to more accurately compare the total production of the secondary metabolites, the calculations were normalized to the largest value and multiplied by the total mass of the defatted organic extract of each strain. Interestingly, some strains produced higher amounts of verticillin D (**8**) but only low levels of verticillin A (**1**) and related analogues (and *vice versa*), suggesting that the biosynthetic pathway for these analogues were somewhat different, even though the fungi were presumably all using non-ribosomal peptide synthesis to produce these metabolites.[42]

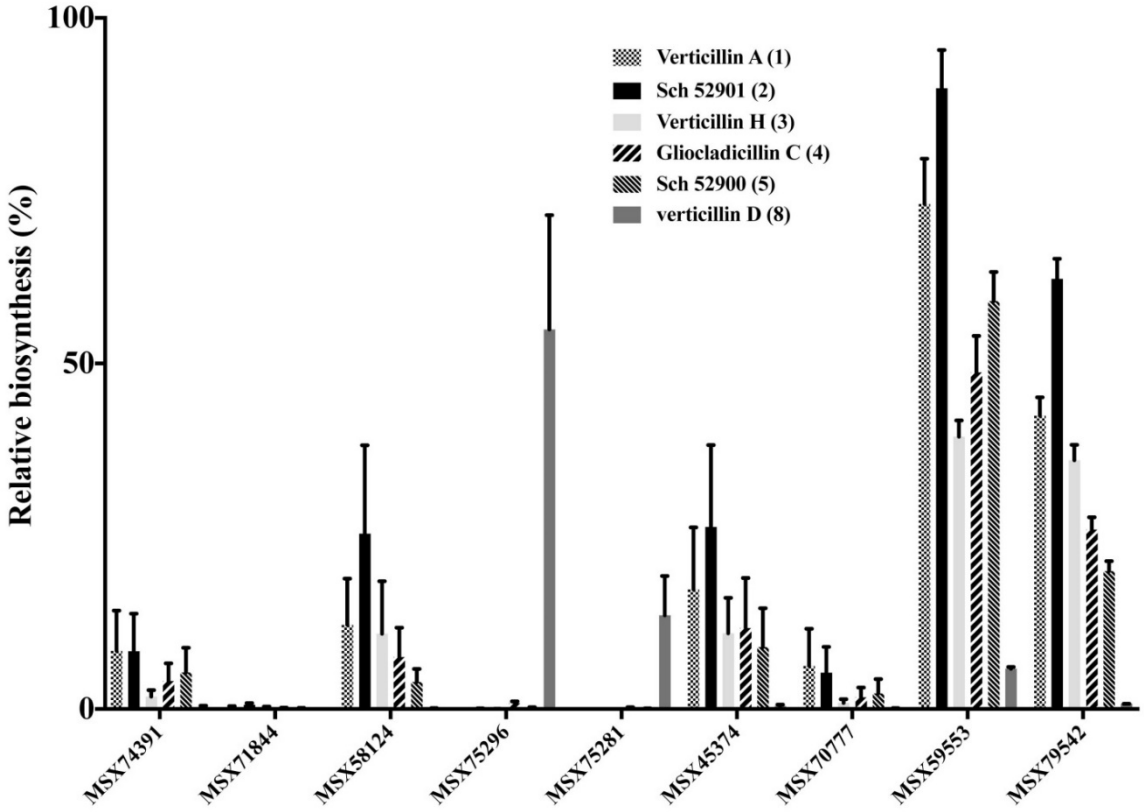

Figure 5. Relative Production of Various Verticillin Analogues grown on rice for four weeks across ten different fungal strains as measured by LC-HRMS in three replicates. Strains MSX59553 and MSX79542 demonstrated the highest relative biosynthesis of the targeted verticillin analogues (compounds **1-5**). Interestingly, specific strains (such as MSX75296 and MSX75281) showed the biosynthesis of higher amounts of verticillin D (**8**), corresponding to low to minimal production of the other analogues.

Use of the droplet probe for *in situ* chemical analysis to optimize the production of verticillins

Optimization of fermentation parameters is a well-established approach to enhance the yield of compounds biosynthesized by microorganisms.[110-111] The alteration of media parameters had an important role in varying the biosynthesis of secondary metabolites in numerous fungal strains.[112-115] In most cases investigations of optimal

fermentation conditions are targeted for specific active compounds, such as antibiotics.[116-118]

Toward this end, the variation of culture media showed the most immediate results. A visual difference in the growth of the two fungal strains (MSX59553 and MSX79542) was noted (Figure 6). Guttates, which we and others hypothesize concentrate secondary metabolites,[103, 119-121] were noted when these were grown on Oat-A, YESDA, and PD-mushroom agar (Figure S6), but not found on the fungi grown on the other nutrient media.

During this study solid media were chosen over submerged liquid media, despite the advantages of the latter in offering control over the fermentation parameters and the simplification of scale up for industrial purposes.[122] Pragmatically, we do not have the facilities for large-scale liquid fermentation, and moreover, liquid media for the production of verticillins did not show promise in the literature.[45-46, 51] Furthermore, the chemistry of the cultures grown on solid media could be studied readily *in situ* via the droplet probe. In addition, solid fermentation is closer to the natural habitat of fungi, offering the mycelium a support for growth [123] and permitting better oxygen circulation than can be achieved by the high viscosity of liquid fermentation.[124] Previous comparative studies showed a notably higher productivity of pure compounds when microorganisms were grown on solid media, in comparison to liquid cultures.[116, 125-129] with shorter fermentation time and less risk of enzymatic degradation.[130]

MSX59553
MSX79542
A
B
C
A
B
C

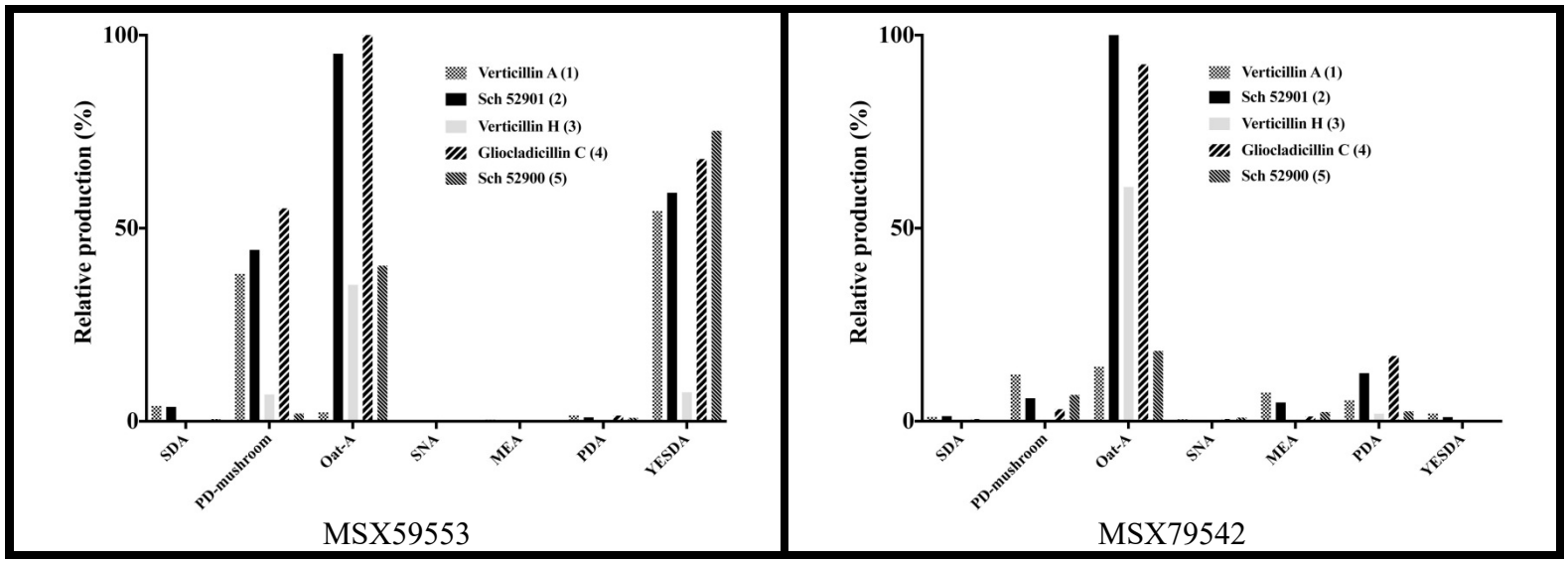

Figure 6. Top: Photos of Strains MSX59553 (top) and MSX79542 (bottom). These fungal cultures were grown on SDA, PD-mushroom, Oat-A, SNA and PDA(**A**)/ MEA(**B**)/ YESDA (**C**) (from left to right respectively) for four weeks. Fungal growths were morphologically distinct based on media, and guttates were observed only on cultures grown on PD-mushroom and Oat-A. **Bottom: Relative Biosynthesis of Verticillin Analogues via Droplet Probe Directly from the Surface of the Strains MSX59553** (bottom left) and MSX79542 (bottom right).

The *in situ* microextractions by droplet probe were analyzed by UPLC-HRMS to identify the targeted verticillin analogues in each culture. Previously, a dereplication strategy [89] demonstrated the effectiveness of direct identification of secondary metabolites from cultures grown in Petri dishes. The peak areas of targeted compounds were averaged to build graphs (Figure 6). For each culture condition, three sampling points were acquired on duplicate plates (n=6). However, error bars were not calculated for two reasons. First, the three different spots represent different fungal growth stages, essentially oldest to youngest when sampling radially from the center. Also, the fungal growth morphology on each media had different traits, such as guttates (liquid droplets) or mycelium (filamentous hyphal growth). Due to this inherent biological variability, the recovery of the 5 μL droplet during microextraction was not always precisely the same (Figure 2S).

The targeted secondary metabolites (Figure 4) were eluted within a retention time windows of 5.30-6.30 min on the 10 min gradient method. Parameters such as retention time, UV profile, mass range within 5 ppm, and fragmentation patterns were used to identify the structurally related analogues.[90] The production of these compounds was compared by measuring the percentage of the relative production of each compound normalized to the largest value. The biosynthetic profile varied according to the respective growth media. Both strains showed essentially zero to slight production of verticillin analogues in SDA, SNA, MEA and PDA media. Interestingly, a recent study on the gene clusters of verticillin biosynthesis noted PDA as a condition where the genes for biosynthesis were not expressed,[32] our phenotypic data (i.e. secondary metabolites)

were supportive of their genotypic data. Of all the conditions examined, Oat-A was the most productive for verticillin biosynthesis in MSX79542 (Figure 6). Similar results were observed with Oat-A in strain MSX59553, although two other media also showed promise (YESD and PD-mushroom).

Production of the targeted secondary metabolites verified by quantification via UPLC-HRMS

We next evaluated the production of verticillins on Oat-A vs. readily available substrates, such as breakfast oatmeal and rice (Figure 3S). The UPLC-HRMS analysis of the *in situ* microextraction on the surface of the three media via the droplet probe were plotted as the relative percentages of the peak normalized according to the compound with highest production (Figure 7 A & B). These results revealed a higher production of the targeted secondary metabolites on oatmeal and Oat-A media compared to the rice. For strain MSX79542, cultures grown on Oat-A showed the highest production, as the fungus expressed guttates (Figure 6S), which have been shown to be concentrated in secondary metabolites.[119-120]

The cultures on Oat-A did not grow as three-dimensional as those grown on rice or breakfast oatmeal. We hypothesized that the three-dimensional character may be beneficial for total verticillin production and thus, the same *in situ* microextracted Petri dishes were extracted in their entirety, and oatmeal and rice had the highest extract amounts (Figure 4S). The peak areas of the compounds of interest were calculated in their respective total defatted mass of the extract. Then, those numbers were normalized according to the compound of highest production to give a more accurate comparison of

the different profiles of verticillin biosynthesis. Regular oatmeal demonstrated the highest amounts of the targeted secondary metabolites (Figure 7 C & D).

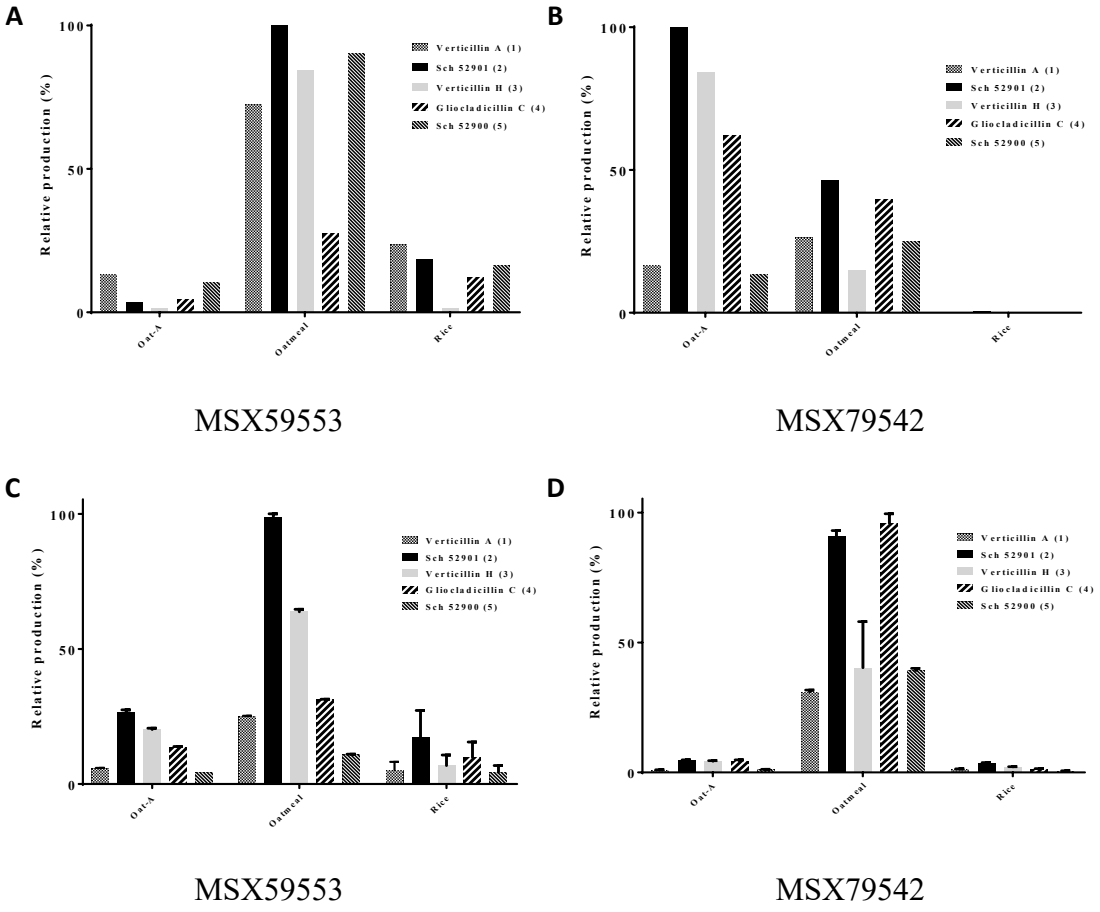

Figure 7. Relative Production of Verticillin Analogues via Droplet Probe Directly from the Surface of Strains MSX59553 (A) and MSX79542 (B) Grown for Four Weeks. Oatmeal agar showed a higher amount of analogues, likely due to the formation of guttates on the surface of the culture. The same cultures grown on the Petri dishes, and used previously for the droplet probe analysis, were fully extracted and then analyzed via UPLC-HRMS to generate graphs (**C**) and (**D**), which represent the relative total production of verticillin analogues by strains MSX59553 and MSX79542, respectively. The relative percentages were normalized by multiplying the peak areas by the weight of their corresponding organic extracts (**Fig 2S** supplementary information). The results from **C** and **D** demonstrate that oatmeal was the best media for total production of verticillin analogues.

In order to make a more accurate comparison and quantify the amounts of verticillins from the organic extracts of the two strains MSX59553 and MSX79542, cultures were fermented in three biological replicates using rice and oatmeal for comparative purposes. Oat-A was excluded from this comparison because the agar media forces the fungus to grow mainly on the surface of the culture, and that contributed to a low extract weight compared to the other cultures grown for the same amount of time (Figure 4S).

Verticillin amounts were calculated via UPLC-HRMS calibration curves prepared using purified analogues. To determine the amounts of verticillin analogues produced in mg per flask of growth, the previous numbers were multiplied by the defatted extract mass of each flask. The defatted weights of organic extracts were higher in the strain grown on oatmeal than when it was grown on rice (Figure 5S). Both fungal strains demonstrated the ability to produce higher amounts of verticillin analogues when grown on oatmeal compared to the rice media. Also, using one way ANOVA, strain MSX59553 expressed significantly higher amounts of secondary metabolites when grown on oatmeal than the same strain grown on rice or strain MSX79542 grown on either rice or oatmeal ($P < 0.005$) (Figure 8 B & C).

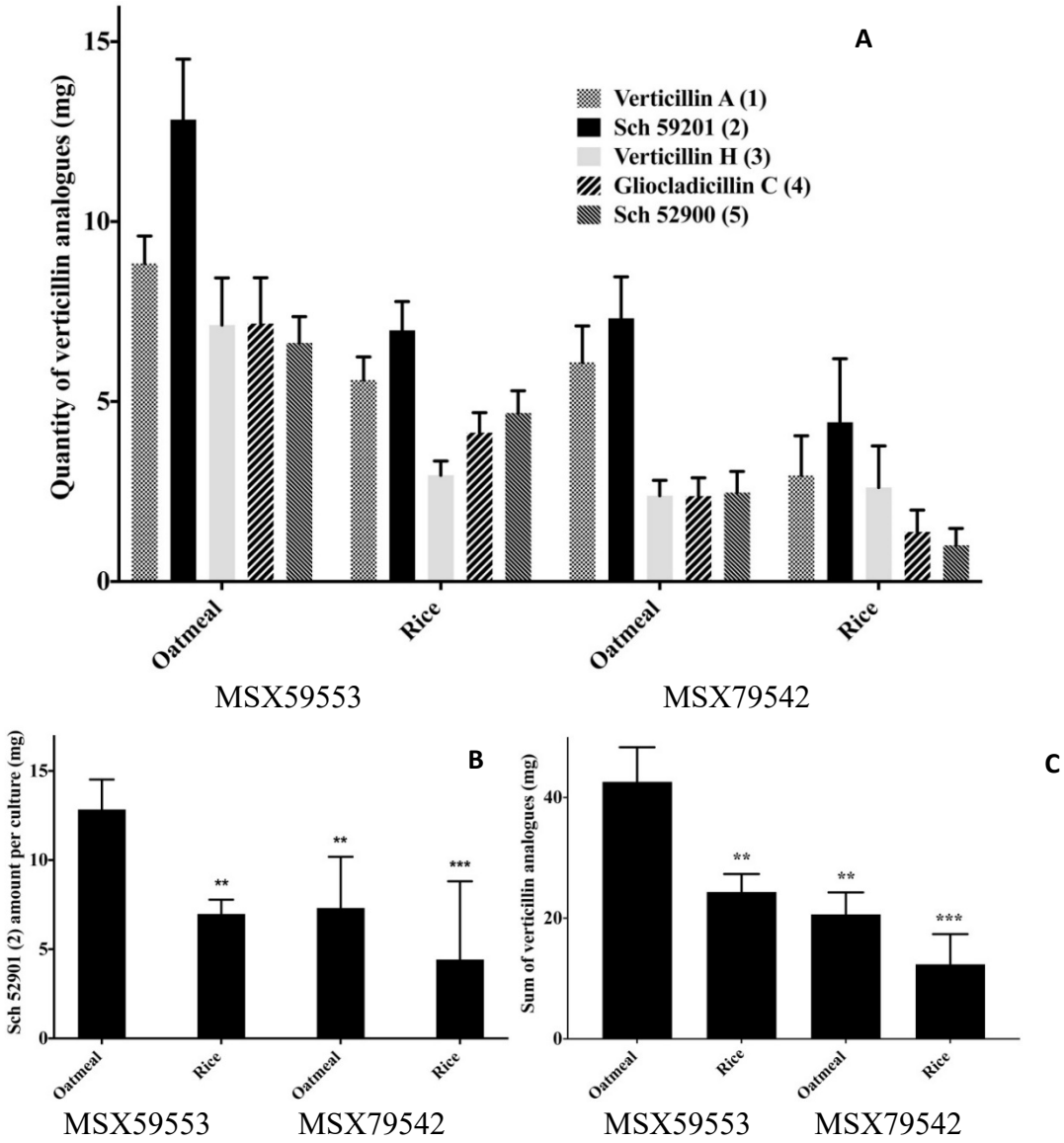

Figure 8. The Amounts of the Secondary Metabolites of Interest in mg Present in Each Culture of Strains MSX59553 and MSX79542. These cultures were grown on rice or oatmeal media for four weeks in three biological replicates (**A**). The quantity of Sch52901 (**2**), the verticillin analogue produced in the highest amount by the fungal strains was calculated per flask. The data plotted are means + SD of three biological replicates per medium and per strain. The quantity of **2** produced by strain MSX59553 grown on oatmeal showed a significant difference relative to the same strain grown on rice and also compared to strain MSX79542 grown on oatmeal and rice respectively (** $P < 0.004$, *** $P < 0.0003$) (**B**). Similarly the sum of all verticillin analogues showed a significant difference between the oatmeal culture of strain MSX59553 and the other growth conditions (** $P < 0.005$, *** $P < 0.0003$) (**C**).

The extraction and isolation of verticillin analogues from strain MSX59553 grown on a large scale on rice versus that on oatmeal for the same amount of time (5 weeks) was compared. When fermenting on oatmeal, there was a yield of 67.3 mg of verticillins **1-5** per g of extract (with a total weight of pure verticillin analogues isolated being 174.8 mg). Alternatively, when rice was used as a medium, there was 63.3 mg of **1-5** per g of extract (with a total weight of 107.6 mg of purified verticillins). Growth of this fungal culture on oatmeal or rice showed enhanced production of the verticillins, substantially exceeding what had been reported in the literature to date.

Profile of secondary metabolites based on different growth times

Duplicate cultures of MSX59553 grown on oatmeal were sampled over 5 weeks to investigate the effect of incubation time on production of secondary metabolites. The amount of verticillin A was calculated from a calibration curve after injecting 0.025 mg/mL of the extract of each flask. This preliminary amount was multiplied by the total mass of the defatted organic extract to normalize the results (Figure 9). The production of verticillins increased up to day seven, after which the production of verticillins plateaued by day 22. Interestingly, a decrease of verticillin A was noticed after day 22 until day 35, which was notable since fungal cultures are routinely grown for approximately 4 weeks in laboratory settings. Thus, our study showed that an average of 11 days was enough time for the biosynthesis, which shortened turnaround time for the scaled-up production of the verticillin analogues.

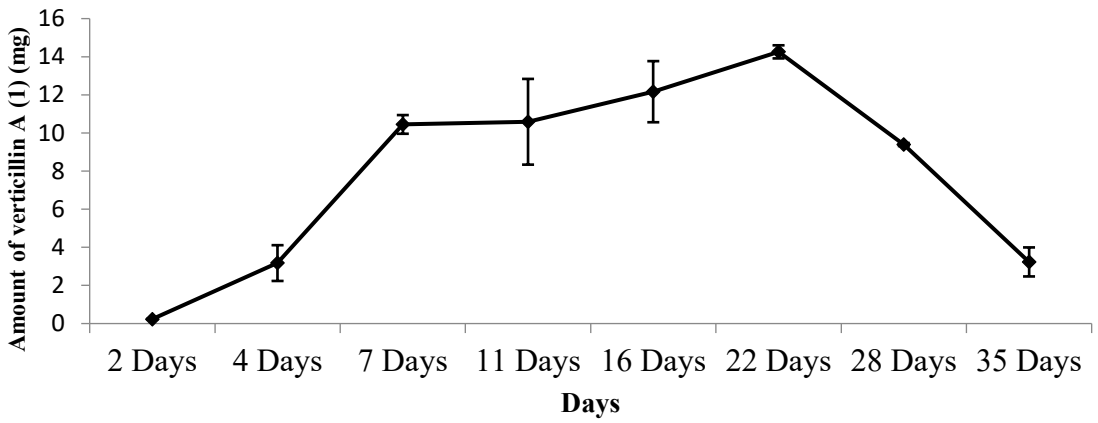

Figure 9. Amounts of Verticillin A (mg) Produced by MSX59553 per Flask Growth During a Period of 35 Days. The cultures were extracted then analyzed using UPLC-HRMS. The compound accumulated up to 22 days and then was apparently destroyed after longer incubation times (presumably, as the stationary growth phase ended). These data are means ± SD of two biological replicates, each analyzed in triplicate (n=6).

Conclusions

The verticillins are a class of fungal metabolites whose biological activity against a suite of anticancer assays has stimulated recent interest. However, our challenge was to supply them on a large enough scale, so as to facilitate further preclinical studies. This study showed that fermentation on Quaker oatmeal significantly enhanced the biosynthesis of verticillin analogues in strain MSX59553; whereas we once could isolate about 10 mg after about 5 weeks of growth on rice medium, we can now produce about 20 mg in 11 days on oatmeal medium. To examine a suite of fermentation conditions efficiently, we demonstrated the use of the droplet probe to measure the chemistry of fungal cultures in grown in Petri dishes *in situ*. Parallel studies of extracts from those Petri dishes using a more traditional natural products extraction approach followed by quantitative UPLC-HRMS analysis showed the same trend, serving to further validate the

reliability of chemical results from droplet probe analyses. For laboratory-scale production, we are confident that a version of the described procedures could be used to supply verticillins on the single to multi-gram scale. However, further research, potentially exploring a suite of options, ranging from liquid fermentations to semi- and/or total synthesis, may be required should the need for kg quantities arise.

Acknowledgments

This research was supported by Grant P01 CA125066 from the National Cancer Institute/National Institutes of Health, Bethesda, MD, USA. The authors thank Dr. Joanna Burdette of the University of Illinois at Chicago and Dr. James Fuchs of Ohio State University for helpful discussions. We also thank Drs. Vilmos Kertesz and Gary J. Van Berkel (Mass Spectrometry and Laser Spectroscopy Group, Chemical Sciences Division, Oak Ridge National Laboratory) for inspiration and guidance with the droplet probe. The high resolution mass spectrometry data were collected at the Triad Mass Spectrometry Laboratory at UNCG.

CHAPTER III

ENGINEERING FLUORINE INTO EPIPOLYTHIODIOXOPIPERAZINE ALKALOIDS (VERTICILLINS) VIA PRECURSOR DIRECTED BIOSYNTHESIS

This chapter is intended for submission to *Organic Letters* and is presented in that style. Coauthors will include Long, J. L., Raja, H. A., Kurina, S., Burdette, J. E., Pearce, C. J., and Oberlies, N. H.

Fluorine and nitrogen have similar natural abundances, yet only 12 secondary metabolites (five compound classes) have been discovered that include a fluorine, and none were fungal derived.[131-132] Interest in the fluorination of drug leads started in the 1950's after the success of 9-α-fluorohydrocortisone,[133] and this was followed by 5-fluorouracil, which is still used in chemotherapy.[134-135] The introduction of even a single fluorine often enhances pharmacological properties,[131, 136] such as potency, pKa, membrane permeability, metabolism, and pharmacokinetics.[137-139] Fluorinated compounds increased from 2% of marketed drugs in the 1970's to approximately 20-30% today.[138, 140] Notably, more than 30% of the most prescribed drugs contain fluorine,[140] including fluoxitine[141] (Prozac), ciprofloxacin[142-143] (Ciprobay), sitagliptin[144] (Januvia), and rosuvastatin (Crestor), which was the 13th most prescribed drug in 2013, surpassing its fluorinated predecessor, atorvastatin (Lipitor).[145]

Despite the advantages of fluorination, its incorporation in natural product derived drug leads is challenging.[146] Several strategies have been developed toward synthetic and

semisynthetic methods for selective fluorination.[147-148] However, this remains difficult in structurally complex natural products, which can be sensitive to degradation.[149]

As an alternative, precursor-directed biosynthesis harnesses the biosynthetic machinery of a microorganism by introducing analogous building blocks to those used naturally.[149-151] For example, incorporating fluorinated amino acids into culture media of the fungus *Beauveria bassiana* resulted in analogues with cytotoxicity against metastatic prostate cancer cells.[152] Another example was flurithromycin, a fluorinated analogue of erythromycin with improved bioavailability and longer half-life.[153-154] Recently, this technique was used for biosynthesizing fluorinated peptaibols.[155]

Given the potential benefit of fluorinating lead natural products, we applied this approach to the verticillins (**1**-**3**), fungal metabolites also termed epipolythiodioxopiperazine (ETP) alkaloids.[26] Verticillin A (**3**)[40] and its conjurers showed nanomolar cytotoxicity against a panel of cancer cell lines.[34, 38, 45, 74] Compound **3** is a selective histone methyltransferases (HMTases) inhibitor.[35] In pancreatic cancer, **3** inhibited the methyltransferase enzyme MLL1 with an IC_{50} value of 0.8 μM resulting in demethylation of histone H3K4me3, consistent with a decrease of PD-L1 (programmed death ligand 1) expression. *In vivo* orthotropic tumors in mice transplanted with either PANC02-H7 or UN-KC-6141 cells had significantly smaller tumor size when treated with a combination of **3** and anti PD-L1.[70] In a separate study, a combined treatment of **3** and 5-fluorouracil in a murine model of metastatic colon carcinoma exhibited significantly smaller tumors compared to control.[35] In total, **3** has shown promise in both *in vitro* and *in vivo* cancer models.

Several ways to fluorinate verticillins could be envisaged. The Movassaghi group has made impressive progress on the synthesis of ETPs. However, they reported the total synthesis of 11,11′-dideoxyverticillin A, lacking key OH moieties.[62, 66] Semisynthesis could suffer from disulfide bridge integrity under the fluorination conditions, resulting in a loss of activity.[65] Taking into consideration the increasing interest in verticillin pharmacology, their amino acid composition and how that fits with NRPS biosynthesis,[42, 156] and the ability to scale their production via fermentation,[33] we hypothesized that verticillins were ideal candidates for precursor-directed biosynthesis by providing fluorinated 5-F-DL-tryptophan (5-F-DL-Trp) to the fungus *Clonostachys rogersoniana* (strain MSX59553).

Strain MSX59553 was grown on oatmeal agar (OMA) with a racemic mixture of 5-F-Trp (375 ppm, Figure S9). Those cultures were analyzed *in situ* via a droplet probe coupled to a UPLC-PDA-HRESIMS-MS/MS system.[33, 89, 103, 106, 109] The microextraction of the culture surface (control vs fluorinated medium) displayed characteristic peaks for verticillin H (**1**) [*m/z* 725.1345 ($[M + H]^+$)], Sch 52901 (**2**) [*m/z* 711.1185 ($[M + H]^+$)], and verticillin A (**3**) [*m/z* 697.1030 ($[M + H]^+$)]. In addition, in the medium containing 5-F-DL-Trp, several peaks for analogues were detected. The substitution of F into the verticillins increased the molecular ion by 17.99 amu for monofluorination, as noted by *m/z* 743.1249, 729.1090, and 715.0933, corresponding to the incorporation of a fluorinated Trp unit in the biosynthesis of **1**-**3**, respectively. Additionally, peaks that were shifted by twice 17.99 amu [i.e. *m/z* 761.1161, 747.0997 and 733.0856] were observed, indicating difluorination into the same three molecules, respectively (Figures S6-S8).

To isolate material for structural characterization and bioassay, the same strain was grown on OMA containing 5-F-DL-Trp (375 ppm). This culture was subjected to a couple transfers to the same fluorinated medium, allowing the microorganism to adapt. Then, the strain was cultured on oatmeal, since it was optimal for lab scale production of verticillins.[33] The growth flasks were supplemented with 500 ppm 5-F-DL-Trp (Figure S4\9**)**, since this concentration was optimal for introducing fluorinated amino acids into peptaibols.[155]

After 28 days of fermentation, the HRESIMS data of the organic extract of the culture confirmed incorporation of 5-F-Trp in **1**-**3** on one or both sides of the dimeric verticillins. Natural product purification yielded seven fluorinated analogues: 9-F-verticillin H (**4**), 9-F-Sch 52901 (**5**), 9′-F-Sch 52901 (**6**), 9-F-verticillin A (**7**), 9,9′-diF-verticillin A (**8**), 9,9′-diF-verticillin H (**9**) and 9,9′-diF-Sch 52901 (**10**). The monofluorinated analogues were in a ratio of about 1:10 relative to the parents; difluorinated analogues were 1:200.

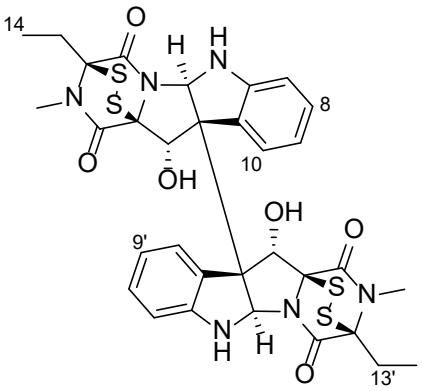

Verticillin H (1)

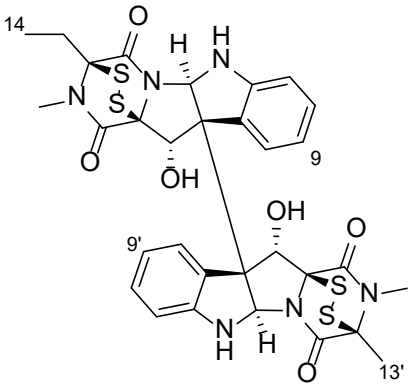

Sch 52901 (2)

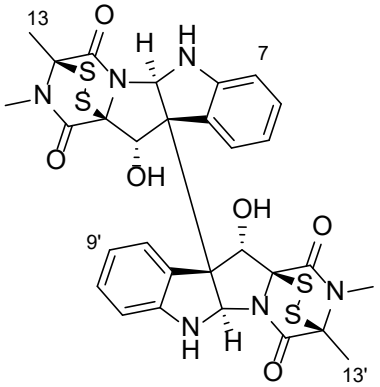

Verticillin A (3)

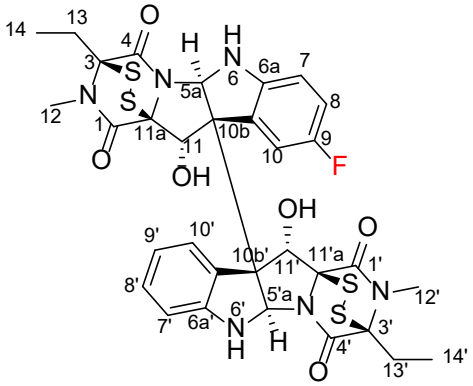

9-F-Verticillin H (4)

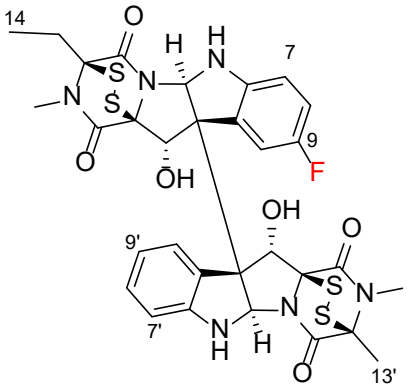

9-F-Sch 52901 (5)

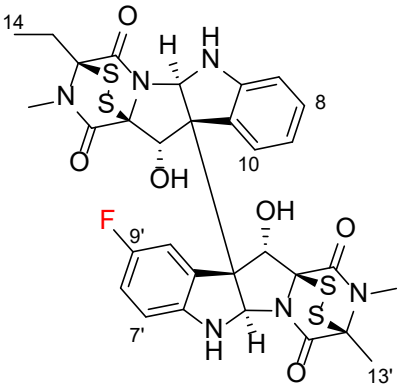

9'-F-Sch 52901 (6)

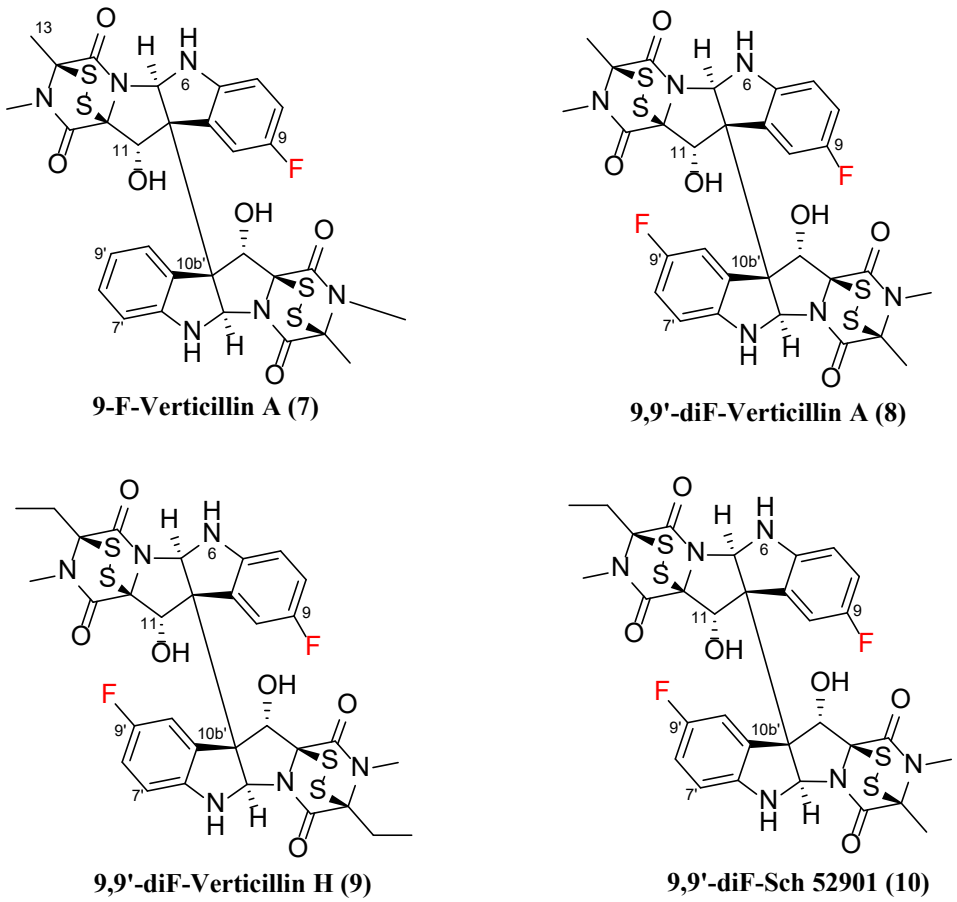

Figure 10. Structures of Verticillins (1-3) and the Fluorinated Analogues (4-10) Obtained via Precursor-Directed Biosynthesis.

Compounds **1-10** were purified as light-yellow amorphous powders. The structures of compounds **1-3** were established by favorable comparisons of the HRESIMS and 1D NMR data to literature.[34, 45] The protonated molecular ion $[M + H]^+$ of compounds **4-7** were noted at *m/z* 743.1231, 729.1071, 729.1064 and 715.0908 respectively. These data corresponded to a gain of 17.99 amu relative to the parents, indicating the replacement of a proton by a fluorine and representing the formulae: $C_{32}H_{31}FN_6O_6S_4$ (**4**), $C_{31}H_{29}FN_6O_6S_4$ (**5**), $C_{31}H_{29}FN_6O_6S_4$ (**6**) and $C_{30}H_{27}FN_6O_6S_4$ (**7**).

The structures of **4-8** were characterized via 1D and 2D NMR data, including ^{19}F NMR spectra (Figures S12-S41). The non-fluorinated parents (i.e. **1** and **3**) of **4** and **7**, respectively, are symmetrical dimers and became asymmetric via monofluorination (Figure 11). This was evident in the aromatic region (δ_H 6.5-8.0 ppm), where H-7, H-7′, H-8, H-8′, H-10 and H-10′ resonated as individual peaks (Figures S13 and S33), and the H-9 signal was replaced by fluorine. Compound **2** is asymmetric, and thus monofluorination resulted in two possible analogues (**5** and **6**), whose aromatic protons exhibited distinct patterns, and as with **4** and **7,** proton H-9 (in **5**) or H-9′ (in **6**) were absent (Figures S19 and S26).

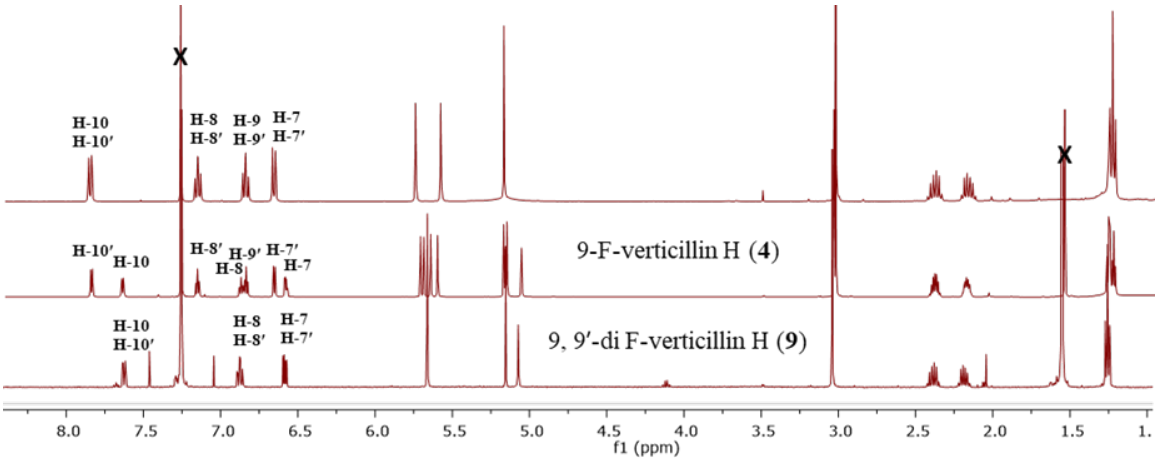

Figure 11. Comparison of the ^{1}H NMR Spectra of Verticillin H (1), 9-F-verticillin H (4), and 9,9′-di F-verticillin H (9). All spectra were recorded in $CDCl_3$ at 500 MHz.

While in lower abundance, the characterization of the difluorinated analogues followed similar logic. For example, compounds **8-10** with *m/z* 733.0826, 761.1135 and 747.0983 respectively, demonstrated a gain of 35.99 amu relative to their parents (**1-3**), corresponding to $C_{30}H_{26}F_2N_6O_6S_4$ (**8**), $C_{32}H_{30}F_2N_6O_6S_4$ (**9**) and $C_{31}H_{28}F_2N_6O_6S_4$ (**10**). In

the aromatic region of the ^{1}H NMR spectra of **8** and **9** (Figure 11, S39 and S44) symmetry was evident, comparable to **3** and **1**, while **10** remained asymmetric. Signals for protons H-9 and H-9′ were absent in compounds **8-10** (Table 2).

Table 2. ^{1}H NMR Data for 4-10 in $CDCl_3$. [700 MHz for **4-8** and 500 MHz for **9-10**].

Position	δ_H, mult (*J* in Hz)						
	(**4**)	(**5**)	(**6**)	(**7**)	(**8**)	(**9**)	(**10**)
1	-	-	-	-	-	-	-
3	-	-	-	-	-	-	-
4	-	-	-	-	-	-	-
5a	5.68, s	5.67, s	5.70, s	5.67, s	5.65, s	5.66, s	5.66, s
6a	-	-	-	-	-	-	-
7	6.58, dd (8.6, 4.4)	6.58, dd (8.6, 4.4)	6.65, dd (7.7, 1.0)	6.58, dd (8.7, 4.4)	6.59, dd (8.6, 4.4)	6.59, dd (8.6, 4.4)	6.59, m (8.8, 4.3)
8	6.86, td (8.6, 2.7)	6.86, td (8.6, 2.6)	7.13, td (7.7, 1.3)	6.86, td (8.7, 2.7)	6.86, td (8.6, 2.6)	6.88, td (8.6, 2.7)	6.86[a], td (8.8, 2.8)
9	-	-	6.81, td (7.7, 1.0)	-	-	-	-
10	7.63, dd (9.4, 2.7)	7.61, dd (9.4, 2.6)	7.81, dd (7.7, 1.3)	7.61, dd (9.4, 2.7)	7.60, dd (9.4, 2.6)	7.60, dd (9.5, 2.7)	7.61[b], dd (9.5, 2.8)
10a	-	-	-	-	-	-	-
10b	-	-	-	-	-	-	-
11	5.16, s	5.15, s	5.15, s	5.14, s	5.13, s	5.15, s	5.14[c], s
11a	-	-	-	-	-	-	-
12	3.02[a], s	3.02, s 3.01, s	3.03, s	3.01[a], s	3.01, s	3.04, s	3.02[d], s
13	2.17, m, 2.38, m	2.17, m 2.37, m	2.18, m 2.39, m	1.88, s, 1.90, s	1.91, s	2.19, m, 2.39, m	2.19, m, 2.39, m
14	1.25[b], t (7.2)	1.22, t (7.2)	1.25, t (7.2)		-	1.26, t (7.1)	1.26, t (7.0)
6-NH	5.05, s	5.05, s	5.15, s	4.99, s	5.01, s	5.66, s	5.05[e], s,
11-OH	5.59, s	5.59, s	5.63, s	5.69, s	5.76, s	5.07, s	5.66[f], s
1′	-	-	-	-	-	-	-
3′	-	-	-	-	-	-	-
4′	-	-	-	-	-	-	-
5a′	5.70, s	5.70, s	5.68, s	5.69, s	5.65, s	5.66, s	5.66, s
6a′	-	-	-	-	-	-	-
7′	6.65, dd (7.6, 1.0)	6.66, dd (7.7, 1.0)	6.58, dd (4.4, 8.6)	6.65, dd (7.7, 1.0)	6.59, dd (8.6, 4.4)	6.59, dd (8.6, 4.4)	6.59, m (8.8, 4.3)
8′	7.15, td (7.6, 1.2)	7.15, td (7.7, 1.2)	6.87, td (8.6, 2.7)	7.14, td (7.7, 0.9)	6.86, td (8.6, 2.6)	6.88, td (8.6, 2.7)	6.88[a], td (8.8, 2.8)
9′	6.83, td (7.6, 1.0)	6.84, td (7.7, 1.0)	-	6.82, td (7.7, 1.0)	-	-	-
10′	7.83, dd (7.6, 1.2)	7.84, dd (7.7, 1.2)	7.64, dd (9.4, 2.7)	7.82, dd (7.7, 0.9)	7.60, dd (9.4, 2.6)	7.60, dd (9.5, 2.7)	7.63[b], dd (9.5, 2.8)
10a′	-	-	-	-	-	-	-
10b′	-	-	-	-	-	-	-
11′	5.14, s	5.13, s	5.13, s	5.12, s	5.13, s	5.15, s	5.15[c], s
11a′	-	-	-	-	-	-	-
12′	3.03[a], s	3.01, s	2.99, s	2.99[a], s	3.01, s	3.04, s	3.04[d], s
13′	2.17, m, 2.38, m	1.90, s	1.89, s	1.88, s, 1.90, s	1.91, s	2.19, m, 2.39, m	1.91, s
14′	1.22[b], t (7.2)				-	1.26, t (7.1)	
6′-NH	5.15, s	5.10, s	4.99, s	5.10, s	5.01, s	5.66, s	5.07[e], s
11′-OH	5.64, s	5.74, s	5.70, s	5.73, s	5.76, s	5.07, s	5.77[f], s

a-f Assignments may be interchangeable

^{19}F NMR experiments are beneficial for such studies,[157] and ^{1}H-^{19}F couplings were supportive of the structural assignments. The ^{1}H NMR spectra of compounds **4-7** (Table 2) showed resonances for seven aromatic protons in the range of 6.58-7.84 ppm, and three of those were coupled with the fluorine on the same ring system (Figures S17, S23, S30 and S37). Difluorinated **8-10** demonstrated only six signals in the aromatic region of the ^{1}H NMR spectra with similar *J* values for ^{1}H-^{19}F couplings (Figures S43, S46 and S49).

The characterization of **4-10** was supported by 2D NMR data (COSY, HSQC and HMBC, Tables S6-12). The position of fluorine was confirmed by the $^{2}J_{CH}$ and $^{3}J_{CH}$ HMBC correlations between the protons on the fluorinated benzene ring and C-9, which was a doublet due to ^{13}C-^{19}F coupling (δ_c 157.6 ppm, *J*=235.3-236.9 Hz). As with the ^{1}H NMR data, the ^{13}C NMR spectra displayed a loss of symmetry for **4** and **7**. Six carbon doublets were observed in the aromatic region (111.1-157.6 ppm), confirming the incorporation of fluorine. Moreover, in the ^{19}F NMR experiment, the δ_F values were in the same range -123.2 to -123.0 ppm with a similar coupling pattern (td), consistent with the pattern observed in the fluorinated building block (δ_F -124.9 ppm, Figure S51). In addition, ^{19}F-HMQC data demonstrated a clear correlation of the fluorine with the doublet carbon at C-9 or C-9′ (Figures S18, S24, S31, S38 and S52). Due to the symmetry in **8** and **9**, one peak with a td splitting pattern was observed in the ^{19}F NMR spectra (Figures S43 and S46). Alternatively, **10** showed two overlapping peaks (td) at -122.9 ppm due to asymmetry (Figure S49). Importantly, the HMBC data showed a $^{3}J_{CH}$

correlation between the aromatic proton H-7 and the doublet carbon peak at δ_c ~158 ppm in **8-10**.

HRESIMS/MS experiments were used to distinguish between the incorporation of the fluorine into **5** vs **6**, since those compounds were asymmetric. The fragmentation of these resulted in *m/z* 380.0555 and *m/z* 348.0452 for **5**, and *m/z* 362.0608 and 366.0388 for **6**, as predicted (Figures S24 and S31).

Table 3. ^{13}C NMR Data for 4-8 in $CDCl_3$. [175 MHz].

Position	δ_C, mult (*J* C-F coupling in Hz)				
	(**4**)	(**5**)	(**6**)	(**7**)	(**8**)
1	167.1	167.1	167.1	166.1	166.0
3	77.4[a]	77.5	77.4	73.0[a]	73.0
4	161.4	161.4	161.4	162.2	162.3
5a	82.0	82.0	81.9	82.0	81.9
6a	144.9, d (1.3)	144.9, d (1.1)	148.7	144.8, d (1.2)	144.8
7	111.1, d (8.5)	111.1, d (8.5)	110.8	111.2, d (8.6)	111.3, d (8.3)
8	116.6, d (24.5)	116.6, d (23.6)	130.1	116.6, d (24.7)	116.7, d (23.9)
9	157.6, d (235.6)	157.6, d (236.3)	120.5	157.6, d (236.2)	157.6, d (236.9)
10	115.5, d (25.4)	115.5, d (25.7)	128.2	115.5, d (25.5)	115.6, d (26.6)
10a	130.8, d (8.5)	130.8, d (8.6)	128.9	130.8, d (8.6)	130.4, d (8.7)
10b	65.9, d (1.9)	65.9, d (1.9)	65.6	66.0, d (1.6)	65.8, d (1.6)
11	83.8	83.7	83.0	83.6	83.4
11a	76.6	76.6	76.7	76.4	76.2
12	28.0	28.0	28.0	27.20[a]	27.2
13	24.6[a]	24.5	24.6	17.4	17.5
14	9.9[a]	9.8	9.8	-	-
1′	167.1	166.1	166.1	166.1	166.0
3′	77.5[a]	72.9	73.0	72.9[a]	73.0
4′	161.4	162.3	162.3	162.3	162.3
5a′	81.9	81.9	82.0	81.9	81.9
6a′	148.8	148.7	144.8, d (1.4)	148.6	144.8
7′	110.8	110.8	111.2, d (8.5)	110.8	111.3, d (8.3)
8′	130.1	130.2	116.6, d (23.8)	130.1	116.7, d (23.9)
9′	120.5	120.5	157.6, d (236.0)	120.5	157.6, d (236.9)
10′	128.2	128.3	115.6, d (25.5)	128.2	115.6, d (26.6)
10a′	128.9	128.9	130.8, d (8.6)	128.9	130.4, d (8.7)
10b′	65.5	65.6	66.0 d (1.9)	65.7	65.8, d (1.6)
11′	83.0	82.8	83.6	82.8	83.4
11a′	76.7	76.4	76.3	76.3	76.2
12′	28.0	27.2	27.2	27.18[a]	27.2
13′	24.5[a]	17.5	17.5	17.423	17.5
14′	9.8[a]	-	-	-	-

[a] Assignments may be interchangeable

The NRPS pathway is characterized by the presence of epimerization domains to catalyze the conversion of L amino acids into D amino acids and *vice versa*,[158-159] suggesting the possible incorporation of both 5-F-Trp enantiomers. The proposed biosynthesis of diketopiperazine rings in gliotoxin,[160] and a study of acetylaranotin,[161] shows that the configuration at the α carbon of Trp is lost via hydroxylation followed by dehydration . To test this, two biological replicates were analyzed using 5-F-D-Trp, 5-F-L-Trp or 5-F-DL-Trp doped separately into OMA media, along with a control. *In situ* analysis via droplet probe demonstrated signals for **1**-**3** in the control, and in all three fluorination experiments, signals for **1**-**10** were observed (Figures S53-S58). Mutually supportive data was noted by traditional natural products extraction of the same plates via measuring relative peak areas of **1**-**10** (Figure S59). As expected based on previous studies,[155] the highest incorporations were observed with 5-F-L-Trp.

The cytotoxicity of **1**-**10** was assessed against three cell lines: melanoma (MDA-MB-435), breast (MDA-MB-231) and ovarian (OVCAR3) cancers.[34, 162-163] The fluorinated analogues were with similar potency to the parent compounds, with IC_{50} values ranging from 30 to 900 nM (Table 4). This indicated that fluorination did not negatively impact cytotoxicity, at least *in vitro*. Studies are planned to examine these compounds *in vivo*.

Table 4. Cytotoxicity of Compounds 1-10.

Compound	IC_{50}(nM)		
	MDA-MB-231	OVCAR 3	MDA-MB-435
Verticillin H (**1**)	71	101	88
Sch 52901 (**2**)	22	30	30
Verticillin A (**3**)	43	37	37
9-F-Verticillin H (**4**)	46	39	49
9-F-Sch 52901 (**5**)	37	37	39
9′-F-Sch 52901 (**6**)	70	104	72
9-F-Verticillin A (**7**)	230	181	237
9,9′-di F-Verticillin A (**8**)	59	75	65
9,9′-di F-Verticillin H (**9**)	844	919	826
9,9′-di F- Sch 52901 (**10**)	105	175	127
Taxol (control)	166	5	0.4

MDA-MB-435: Human melanoma cancer cells, OVCAR3: Human ovarian cancer cells, MDA-MB-231: Human breast cancer cells.

This is the first study using a precursor-directed biosynthetic approach to generate analogues of verticillins and is the first report of fluorination in any manner. Importantly, these compounds displayed nanomolar cytotoxicity *in vitro*. As observed via *in situ* monitoring of the fungal cultures, the incorporation of 5-F-L-Trp was higher than 5-F-D-Trp, but a racemic mixture was used for cost effectiveness and because the configuration at the α carbon was likely ablated during biosynthesis. In addition to the medicinal chemistry advantages that a fluorinated analogue might present, these non-natural natural products may be patentable, which is a current challenge in natural products research.[164]

Experimental Section

General experimental procedures

All solvents were obtained from Fisher Scientific and used without further purification. The 5-F-DL-Tryptophan was purchased from Acros Organics, 5-F-D-

Tryptophan and 5-F-L-Tryptophan were purchased from Biosynth® NMR data were collected in $CDCl_3$ using either a JEOL ECA-500 NMR spectrometer (JEOL USA, Inc.) operating at 500 MHz for ^{1}H, 470 MHz for ^{19}F and 125 MHz for ^{13}C, an Agilent 700 MHz NMR spectrometer (Agilent technologies, Inc., Santa Clara, CA, USA) operating at 700 MHz for ^{1}H and 175 MHz for ^{13}C, or a Bruker AVANCE III 600 (Bruker Corp., USA) operating at 600 MHz spectrometer for ^{1}H and 150 MHz for ^{13}C. Chemical shift values were referenced to the residual solvent signals for $CDCl_3$ (δ_H 7.25 and δ_C 77.2) and conveyed in δ ppm; multiplicity was showed as: s = singlet, d = doublet, t = triplet and m = multiplet; coupling constants were reported in Hz. HRESIMS data were obtained using Thermo QExactive Plus mass spectrometer (Thermofisher, San Jose, CA, USA) with an electrospray ionization source. The higher energy dissociation (HCD) used a normalized energy of 30 eV for all the compounds to obtain MS/MS data. Droplet probe analysis for the *in situ* detection of the biosynthesis of secondary metabolites in fungal cultures was performed using a droplet-LMJ-SSP coupled with a Waters Acquity ultra performance liquid chromatography (UPLC) system (Waters corp.) coupled with a Thermo QE Plus via procedures described previously.[88-89, 103-106, 109] Microextractions were performed using a droplet of 1:1 MeOH:H_2O. Three different spots were extracted in triplicate by delivering 5 µL of the solvent from a syringe to the surface of the culture then aspiring it back after ~2 sec of interaction to be injected into the UPLC-MS system. The UPLC separation was performed using an Acquity BEH C_{18} column (50 mm x 2.1 mm i.d., 1.7 µm) equilibrated at 40 ºC and a flow rate set at 0.3 mL/min. The mobile phase comprised a linear gradient CH_3CN/H_2O with 0.1% HCOOH starting at 15%

CH_3CN to 100% over 8 min. The mobile phase was held for another 1.5 min at 100 % CH_3CN before going back to the starting conditions. Flash column chromatography was carried out with a Teledyne ISCO combiflash Rf connected to ELSD and PDA detectors with UV detection set at 200-400 nm with a specific wavelength set at 300 nm. The HPLC separation was achieved using Varian ProStar HPLC system connected to a ProStar 335 photodiod array detector (PDA) with UV detection set at 240 nm and 300 nm. Preparative normal phase HPLC purification of samples was performed on a silica (5 μm; 250 x 21.2 mm) column using a flow rate of 21.24 mL/min of a mobile phase consisting of EtOAc and Hexanes. Optical rotation data were acquired on a Rudolph Research Autopol III polarimeter (Rudolph Research Analytical, Flanders, NJ, USA). The UV data were acquired using a Varian Cary 100 Bio UV-Vis spectrometer (Varian Inc., Walnut Creek, CA, USA).

Fungal strain identification

Fungal strain MSX59553 from the Mycosynthetix culture collection was utilized in the present study. Strain MSX59553 was isolated by Dr Barry Katz in January 1992 from leaf litter;[33-34, 90] It was identified as *Clonostachys rogersoniana* (Hypocreales, Ascomycota).[33] The sequence data for this fungal strain have been deposited in GenBank and accession numbers are cited in recent publications.[33, 90]

Fermentation, extraction, and isolation

To prepare Petri dishes, fungal strain MSX59553 was grown on oatmeal agar (OMA, Difco). A small piece of agar along with mycelium from the growing edge of the colony was transferred onto oatmeal agar that was supplemented with either 5F-DL-Trp,

5F-D-Trp, or 5F-L-Trp (2 mL of filter sterilized 5F-Trp solution that was added to 150 mL of the oatmeal agar after autoclaving). The fungal strain was cultivated on this fluorine supplemented medium for few weeks and transferred two times during its growth onto newly prepared 5F-DL-Trp supplemented oatmeal agar Petri plates, so as to acclimatize the fungal strain to fluorinated building blocks. The same procedure was followed to prepare Petri dishes that contains separately one of the two stereoisomers of Trp separately.

Subsequently, flasks were prepared for the scale up of the site directed biosynthesis experiment, with the aim of isolating the new fluorinated analogues. A small piece of agar along with fungal mycelium grown on the 5F-DL-Trp fluorinated oatmeal agar was added to a YESD broth with 464 ppm of 5F-DL-Trp (660 µL of the 7500 ppm into 10 mL of YESD; 20 g soy peptone, 20 g dextrose, 5 g yeast extract, 1 L H_2O). The fungus was grown for a period of 3 days at 23 ºC agitated at 100 rpm using an orbital shaker. Fungal colonies grown in YESD broth were transferred into 250 mL Erlenmeyer flasks containing breakfast oatmeal (Old fashion Quaker oats). The oatmeal was prepared by adding 10 g of breakfast oatmeal with 17 mL of DI-H_2O and autoclaved at 221 ºC for 30 min. An additional 1.2 mL of the 7500 ppm 5F-DL-Trp solution was added to the breakfast oatmeal (495 ppm). The flasks were incubated statically at room temperature for approximately 3 weeks until the cultures showed completion of initial growth phase corresponding to the production of secondary metabolites.

After fermentation, 60 mL of 1:1 MeOH:$CHCl_3$ was added to each growth flask, the culture was chopped using a spatula, and then shaken for 16 h at 100 rpm. The extract

was filtrated under vacuum, and 90 mL of $CHCl_3$ and 150 mL of H_2O were added to the eluent. The solvents were transferred into a separatory funnel, and the organic layer was drawn off and evaporated *in vacuo*. This material was reconstituted using 100 mL of 1:1 MeOH:CH_3CN and 100 mL of hexanes and then partitioned in a separatory funnel. The MeOH:CH_3CN layer was drawn off and evaporated *in vacuo*. This defatted organic extract (3.9 g) was adsorbed on Celite 545 (Acros Organics) and fractionated via flash chromatography on a 40 g RediSep Rf Gold Si-gel column using a gradient solvent system of hexanes-$CHCl_3$-MeOH at a flow rate of 40 mL/min over 53.3 column volumes (CV) for a duration of 63.9 min. Fractions were collected every 25.0 mL and pooled according to the UV and ELSD profiles, resulting in six fractions (F_1-F_6). Fraction F_2 (750.11 mg) was observed to contain both the targeted masses of verticillins analogues and the high UV signal at 301 nm, which is characteristic of the presence of verticillins. As such, F_2 was subjected to a second flash chromatography on three stack 4 g RediSep Rf Gold Si-gel column using a gradient solvent system of hexanes-$CHCl_3$-MeOH at a flow rate of 18 mL/min over 155.0 column volumes (CV) for a duration of 41.3 min. Fractions were collected every 5.0 mL and pooled according to the UV and ELSD profiles, resulting in twelve fractions (F'_1-F'_{12}). MS- directed purification showed that fractions F'_3, F'_5 and F'_7 contained both parent and fluorinated analogues of the verticillins. To purify these, fractions F'_3, F'_5 and F'_7 were subjected to preparative normal phase HPLC using Silica column with an isocratic method at 30%, 25%, and 30% of EtOAc, respectively. The separations were performed with a flow rate of 21.24 mL/min over 25, 52 and 54 min for F'_3, F'_5 and F'_7 respectively. This chromatography led to the

isolation of compounds **1** (19.3 mg, t_R = 15.5 min), **4** (2.8 mg, t_R = 16.7 min) and **9** (0.2 mg, t_R = 18.5 min) from F′$_3$, compounds **2** (24.8 mg, t_R = 33.5 min), **5** (2.7 mg, t_R = 36.2 min), **6** (1.8 mg, t_R = 41.0 min) and **10** (0.2 mg, t_R = 46.5 min) from F′$_5$, and compounds **3** (9.3 mg, t_R = 27.0 min), **7** (1.3 mg, t_R = 30.5 min) and **8** (0.1 mg, t_R = 36.5 min) from F′$_7$.

9-F-Verticillin H (**4**). Light yellow powder, $[\alpha]_D^{26}$ + 567 (c 0.3, $CHCl_3$); UV (MeOH) λmax (log ε) 223 (3.22) nm, 309 (2.90) nm; ^{1}H NMR ($CDCl_3$, 700 MHz) δ = 1.22 (t, *J* = 7.2 Hz, 3H), 1.25 (t, *J* = 7.2 Hz, 3H), 2.17 (m, 2H), 2.38 (m, 2H), 3.02 (s, 3H), 3.03 (s, 3H), 5.05 (s, 1H), 5.14 (s, 1H), 5.15 (s, 1H), 5.16 (s, 1H), 5.59 (s, 1H), 5.64 (s, 1H), 5.68 (s, 1H), 5.70 (s, 1H), 6.58 (dd, *J* = 8.6 Hz, 4.4 Hz, 1H), 6.65 (dd, *J* = 7.6 Hz, 1.0 Hz, 1H), 6.83 (td, = 7.6 Hz, 1.0 Hz, 1H), 6.86 (td, *J* = 8.6 Hz, 2.7 Hz, 1H), 7.15 (td, *J* = 7.6 Hz, 1.2 Hz, 1H), 7.63 (dd, *J* = 9.4 Hz, 2.7 Hz, 1H), 7.83 (dd, *J* = 7.6 Hz, 1.2 Hz, 1H); ^{13}C NMR ($CDCl_3$, 175 MHz), δ = 9.8, 9.9, 24.5, 24.6, 28.0, 65.5, 65.9 (d, *J* = 1.9 Hz), 76.6, 76.7, 77.4, 77.5, 81.9, 82.0, 83.0, 83.8, 110.8, 111.1 (d, *J* = 8.5 Hz), 115.5 (d, *J* = 25.4 Hz), 116.6 (d, *J* = 24.5 Hz), 120.5, 128.2, 128.9, 130.1, 130.8 (d, *J* = 8.5 Hz), 144.9 (d, *J* = 1.3 Hz), 148.8, 157.6 (d, *J* = 235.6 Hz), 161.4, 167.1 (Table S6) HRESIMS m/z 743.1231 $[M + H]^+$ (calcd for $C_{32}H_{32}F_1N_6O_6S_4$, *m/z* 743.1245).

9-F-Sch 52901 (**5**). Light yellow powder, $[\alpha]_D^{26}$ + 595 (c 0.2, $CHCl_3$); UV (MeOH) λmax (log ε) 242 (3.67) nm, 310 (3.56) nm; ^{1}H NMR ($CDCl_3$, 700 MHz) δ = 1.22 (t, *J* = 7.2 Hz, 3H), 1.90 (s, 3H), 2.17 (m, 2H), 2.37 (m, 2H), 3.01 (s, 3H), 3.02 (s, 3H), 5.05 (s, 1H), 5.10 (s, 1H), 5.13 (s, 1H), 5.15 (s, 1H), 5.59 (s, 1H), 5.67 (s, 1H), 5.70 (s, 1H), 5.74 (s, 1H), 6.58 (dd, *J* = 8.6 Hz, 4.4Hz 1H), 6.66 (dd, *J* = 7.7 Hz, 1.0 Hz, 1H),

6.84 (td, *J* = 7.7 Hz, 1.0 Hz, 1H), 6.86 (td, *J* = 8.6 Hz, 2.7 Hz, 1H), 7.15 (td, *J* = 7.7 Hz, 1.2 Hz, 1H), 7.61 (dd, *J* = 9.4 Hz, 2.7 Hz, 1H), 7.84 (dd, *J* = 7.7 Hz, 1.2 Hz, 1H); ^{13}C NMR ($CDCl_3$, 175 MHz), δ = 9.8, 17.5, 24.5, 27.2, 28.0, 65.6, 65.9 (d, *J* = 1.9 Hz), 72.9, 76.4, 76.6, 77.5, 81.9, 82.0, 82.8, 83.7, 110.8, 111.1 (d, *J* = 8.5 Hz), 115.5 (d, *J* = 25.7 Hz), 116.6 (d, *J* = 23.6 Hz), 120.5, 128.3, 128.9, 130.2, 130.8 (d, *J* = 8.6 Hz), 144.9 (d, *J* = 1.1 Hz), 148.7, 157.6 (d, *J* = 236.3 Hz), 161.4, 162.3, 166.1, 167.1 (Table S7); HRESIMS m/z 729.1071 $[M + H]^+$ (calcd for $C_{31}H_{30}F_1N_6O_6S_4$, *m/z* 729.1088).

9′-F-Sch 52901 (**6**). Light yellow powder, $[\alpha]_D^{26}$ + 543 (c 0.21, $CHCl_3$); UV (MeOH) λmax (log ε) 236 (3.58) nm, 309 (3.41) nm; ^{1}H NMR ($CDCl_3$, 700 MHz) δ = 1.25 (t, *J* = 7.2 Hz, 3H), 1.89 (s, 3H), 2.18 (m, 2H), 2.39 (m, 2H), 2.99 (s, 3H), 3.03 (s, 3H), 4.99 (s, 1H), 5.13 (s, 1H), 5.15 (s, 2H), 5.63 (s, 1H), 5.68 (s, 1H), 5.70 (s, 2H), 6.58 (dd, *J* = 8.6 Hz, 4.4Hz, 1H), 6.65 (dd, *J* = 7.7 Hz, 1.0 Hz, 1H), 6.81 (td, *J* = 7.7 Hz, 1.0 Hz, 1H), 6.87 (td, *J* = 2.7 Hz, 8.6 Hz, 1H), 7.13 (td, *J* = 7.7 Hz, 1.3 Hz, 1H), 7.64 (dd, *J* = 9.4 Hz, 2.7 Hz, 1H), 7.81 (dd, *J* = 7.7 Hz, 1.3 Hz, 1H); ^{13}C NMR ($CDCl_3$, 175 MHz), δ = 9.8, 17.5, 24.6, 27.2, 28.0, 65.6, 66.0 (d, *J* = 1.9 Hz), 73.0, 76.3, 76.7, 77.4, 81.9, 82.0, 83.0, 83.6, 110.8, 111.2 (d, *J* = 8.5 Hz), 115.6 (d, *J* = 25.5 Hz), 116.6 (d, *J* = 23.8 Hz), 120.5, 128.2, 128.9, 130.1, 130.8 (d, *J* = 8.6 Hz), 144.8 (d, *J* = 1.4 Hz), 148.7, 157.6 (d, *J* = 236.0 Hz), 161.4, 162.3, 166.1, 167.1 (Table S8); HRESIMS m/z 729.1064 $[M + H]^+$ (calcd for $C_{31}H_{30}F_1N_6O_6S_4$, *m/z* 729.1088).

9-F-Verticillin A (**7**). Light yellow powder, $[\alpha]_D^{26}$ + 700 (c 0.13, $CHCl_3$); UV (MeOH) λmax (log ε) 239 (3.90) nm, 309 (3.43) nm; ^{1}H NMR ($CDCl_3$, 500 MHz) δ = 1.88 (s, 3H), 1.90 (s, 3H), 2.99 (s, 3H), 3.01 (s, 3H), 4.99 (s, 1H), 5.10 (s, 1H), 5.12 (s,

1H), 5.14 (s, 1H), 5.67 (s, 1H), 5.69 (s, 2H), 5.73 (s, 1H), 6.58 (dd, *J* = 8.6 Hz, 4.4, 1H), 6.65 (dd, *J* = 7.7 Hz, 1.0 Hz, 1H), 6.82 (td, *J* = *J* = 7.7 Hz, 1.0 Hz, 1H), 6.86 (td, *J* = 8.6 Hz, 2.7 Hz, 1H), 7.14 (td, *J* = 7.7 Hz, 0.9 Hz, 1H), 7.61 (dd, *J* = 9.4 Hz, 2.7 Hz, 1H), 7.82 (dd, *J* = 7.7 Hz, 0.9 Hz, 1H); ^{13}C NMR ($CDCl_3$, 175 MHz), δ = 17.4, 27.18, 27.2, 65.7, 66.0 (d, *J* = 1.6 Hz), 72.9, 73.0, 76.3, 76.4, 81.9, 82.0, 82.8, 83.6, 110.8, 111.2 (d, *J* = 8.6 Hz), 115.5 (d, *J* = 25.5 Hz), 116.6 (d, *J* = 24.7 Hz), 120.5, 128.2, 128.9, 130.1, 130.8 (d, *J* = 8.6 Hz), 144.8 (d, *J* = 1.2 Hz), 148.6, 157.6 (d, *J* = 236.2 Hz), 162.2, 162.3, 166.1 (Table S9); HRESIMS m/z 715.0908 $[M + H]^+$ (calcd for $C_{30}H_{28}F_1N_6O_6S_4$, *m/z* 715.0932).

9,9′-diF-Verticillin A (**8**). Light yellow powder, $[\alpha]_D^{26}$ + 400 (c 0.14, $CHCl_3$); UV (MeOH) λmax (log ε) 239 (3.66) nm, 315 (3.50) nm; ^{1}H NMR ($CDCl_3$, 700 MHz) δ = 1.91 (s, 6H), 3.01 (s, 6H), 5.01 (s, 2H), 5.13 (s, 2H), 5.65 (s, 2H), 5.76 (s, 2H), 6.59 (dd, *J* = 8.6 Hz, 4.4 Hz, 2H), 6.86 (td, *J* = 8.6 Hz, 2.7 Hz, 2H), 7.60 (dd, *J* = 9.4 Hz, 2.7 Hz, 2H); ^{13}C NMR ($CDCl_3$, 175 MHz), δ = 17.5, 27.2, 65.8 (d, *J* = 1.6 Hz), 73.0, 76.2, 81.9, 83.4, 111.3 (d, *J* = 8.3 Hz), 115.6 (d, *J* = 26.6 Hz), 116.7 (d, *J* = 23.9 Hz), 130.4 (d, *J* = 8.7 Hz), 144.8, 157.6 (d, *J* = 236.9 Hz), 162.3, 166.0 (Table S10); HRESIMS m/z 733.0826 $[M + H]^+$ (calcd for $C_{30}H_{27}F_2N_6O_6S_4$, *m/z* 733.0837).

9,9′-diF-Verticillin H (**9**). Light yellow powder, $[\alpha]_D^{26}$ + 1360 (c 0.1, $CHCl_3$); UV (MeOH) λmax (log ε) 234 (3.21) nm, 309 (2.95) nm; ^{1}H NMR ($CDCl_3$, 500 MHz) δ = 1.26 (t, *J* = 7.1 Hz, 6H), 2.19 (m, 1H), 2.39 (m, 1H), 3.04 (s, 6H), 5.07 (s, 2H), 5.15 (s, 2H), 5.66 (s, 4H), 6.59 (dd, *J* = 8.6 Hz, 4.4 Hz, 2H), 6.88 (td, *J* = 8.6 Hz, 2.6 Hz, 2H), 7.60 (dd, *J* = 9.4 Hz, 2.6 Hz, 2H); (Table S11); HRESIMS m/z 761.1135 $[M + H]^+$ (calcd for $C_{32}H_{31}F_2N_6O_6S_4$, *m/z* 761.1150).

9,9′-diF-Sch 52901 (**10**). Light yellow powder, $[\alpha]_D^{26}$ + 1890 (c 0.1, $CHCl_3$); UV (MeOH) λmax (log ε) 226 (3.23) nm, 315 (2.97) nm; ^{1}H NMR ($CDCl_3$, 500 MHz) δ = 1.26 (t, *J* = 7.0 Hz, 3H), 1.91 (s, 3H), 2.19 (m, 1H), 2.39 (m, 1H), 3.02 (s, 3H), 3.04 (s, 3H), 5.05 (s, 1H), 5.07 (s, 1H), 5.14 (s, 1H), 5.15 (s, 1H), 5.66 (s, 3H), 5.77 (s, 1H), 6.59 (m, *J* = 8.8 Hz, 4.4 Hz, 2H), 6.86 (td, *J* = 8.8 Hz, 2.8 Hz, 1H), 6.88 (td, *J* = 8.8 Hz, 2.8 Hz, 1H), 7.61 (m, *J* = 9.4 Hz, 2.8 Hz,, 1H), 7.63 (m, *J* = 9.4 Hz, 2.8 Hz,1H); (Table S12); HRESIMS m/z 747.0983 $[M + H]^+$ (calcd for $C_{31}H_{29}F_2N_6O_6S_4$, *m/z* 747.0994).

Cytotoxicity assay

Human melanoma cancer cells (MDA-MB-435), human breast cancer cells (MDA-MB-231) and human ovarian cancer cells (OVCAR3) were obtained from the American Type Culture Collection (Manassas, VA). The cell lines were cultured in RPMI 1640 medium containing fetal 10% bovine serum, 100 unites/mL penicillin and 100 µg/mL streptomycin. The cells were grown at 37 ºC under 5% CO_2, and then harvested during the log-phase growth by trypsinization followed by two washing to remove all traces of enzymes. Cells were seeded in 96-well clear, flat-bottom plate (Microtest 96, Falcon) at a density of 5000 cells per well. Each plate was incubated overnight at 37 ºC under 5% CO_2. Samples dissolved in DMSO were diluted and added to the appropriate wells to give final concentrations of 20, 4, 0.8, 0.16, and 0.032 µM for pure compounds, and a total volume of 100 µL and 0.5% DMSO per well. The cells with the test samples were then incubated for 72 h at 37 ºC. Cell viability was examined using a commercial absorbance assay (CellTiter 96® AQ_{ueous} One Solution Cell Proliferation Assay, Promega Corp, Madison, WI). IC_{50} values were determined as the concentration required to

diminish cellular growth by 50% compared to the untreated controls after 72 h of continuous exposure. Taxol (Paclitaxel) was used as a positive control.

Acknowledgment

This research was supported via P01 CA125066 from the National Cancer Institute. Mass spectrometry data were acquired in the Triad Mass Spectrometry Laboratory (UNCG). This work was performed, in part, at the Joint School of Nanoscience and Nanoengineering, a member of the Southeastern Nanotechnology Infrastructure Corridor (SENIC) and National Nanotechnology Coordinated Infrastructure (NNCI), which is supported by the National Science Foundation (Grant ECCS-1542174). The authors thank Dr. T. El-Elimat and T. Graf (UNCG) for helpful suggestions. We appreciate Dr F. Zhang (University of Wisconsin) for help from the National Magnetic Resonance Facility at Madison (NMRFAM), which is supported by NIH grants P41 GM103399 and P41 GM66326 (both NIGMS); additional equipment was purchased with funds from the University of Wisconsin, the NIH (RR02781, RR08438), the NSF (DMB-8415048, OIA-9977486, BIR-9214394), and the USDA.

CHAPTER IV

SEMI-SYNTHSIS OF EPIPOLYTHIODIOXOPIPERAZINE ALKALOID ANALOGUES

This chapter is intended for submission to *ACS Medicinal Chemistry Letters* and is presented in that style. Coauthors will include Huntsman, A. C., Doyle, M. G., Burdette, J. E., Pearce, C. J., Fuchs, J. R., and Oberlies, N. H.

Introduction

In 2019, it is estimated that there will be over 1.7 million cases of cancer diagnosed, with over 600 thousand deaths, just in the United States, making it the second leading cause of death in the country.[2] Despite monumental advances in detection and treatment of cancer over the last four decades, some types of cancer, such as pancreatic and ovarian, are still extremely difficult to treat effectively.[165] Many researchers in the natural products community are well versed in the history of medicines from nature, where over 60% of the current anticancer drugs originate.[11, 166] However, what may not be apparent is the number of those that were derived, sometimes semi-synthetically, from a parent natural product. This later group represents 40% of the US FDA small-molecule approved drugs between 1981 and 2014, including 22% of new anticancer drugs.[10] Natural product leads have often been the inspiration for semi-synthetic analogues.[167-168] New compounds that retain the privilege scaffold afforded by nature[169-170] are of importance for exploring structure-activity relationships,[171-173] overcoming challenges such as drug resistance,[174] expanding opportunities for discovery of new drug

candidates,[175] and supplying material on larger scales.[176-179] A key example of semisynthesis was the production of taxotere,[180-181] a 10- deacetyl /erf-butyl carbamate derivative of taxol,[182] which was designed with the goal of yielding a more water soluble analogue with equal antitumor activity.[183] Esterification and linkage via carbamate and carbonate functionalities of the hydroxy at position C-7 on taxol was also proposed for analogous reasons.[179, 184-187] For similar solubility improvements, derivatives of camptothecin (CPT)[188] were synthesized by adding hydrophilic groups to a hydroxy on position C-10 via a carbamate linkage. Two prominent examples that resulted in potent cytotoxic analogues with enhanced aqueous solubility are irinotecan (also known as CPT-11)[189-190] and topotecan.[179, 191-192] Irinotecan has a [4-(1-piperidino)-1-piperidino carbonyloxy] group at C-10 and an ethyl group at C-7, whereas topotecan has a hydroxy and a positively charged dimethyl aminomethyl group at C-10 and C-9, respectively.[179, 189, 193-195] There are many other examples of semi-synthetic analogues of natural products that became FDA approved drugs, with ixabepilone one of the most recent examples[196-197 198], lending validation to this approach.

Verticillins are part of the epipolythiodioxopiperazine alkaloids (ETP) class of fungal secondary metabolites,[24, 30, 38] produced by the filamentous fungi *Verticillium* sp., *Penicillium* sp., and *Gliocladium* sp.[26] This class of compounds is characterized by a *cis*-fused five membered rings and a sulfur bridge.[39] Even in the earliest studies, acetylation of verticillins was shown to enhance the solubility of verticillins compared to parent fungal metabolite (verticillin A).[40-41]

Many studies have underlined the importance of verticillins as a potential anti-cancer agent.[34, 45-46] Recently verticillin A was found to be a selective inhibitor of histone methyl transferases (HMTases) like SUV39H1, SUV39H2, G9a, HTM, MLL1 and GLP.[28] A study by Paschall et al.[35] demonstrated that verticillin A inhibited H3K9 methylation on the *FAS* promoter in colon carcinoma; this mode of action resulted in restoring the Fas expression, and led to cell apoptosis. Moreover, significantly smaller tumor sizes were revealed after treating xenograft mice with a combination of verticillin A and 5-fluorouracil. Metastatic colon carcinoma cells showed to be sensitized to 5-fluorouracil.[35] Similarly, verticillin A inhibited MLL1 in pancreatic cancer cells. MLL1 is responsible of the methylation of histones H3K4me3 resulting in higher PD-L1 expression. Treatment with a combination of verticillin A and anti PD-L caused the reduction of binding to PD-1, thus activation the immune response.[70]

Verticillins illustrates one of the scaffolds that enthrall synthetic chemists because of their dimeric structure that include ten stereocenters, and a sulfur bridges.[62] Based on their retro-biosynthesis hypothesis, the Movassaghi group succeeded in the synthesis of (+)-11,11′-dideoxyverticillin A. The total synthesis was accomplished via enantioselective steps.[62-63] The success of this synthesis strategy gave an insight about synthesis of other ETPs.

A SAR study from the same group demonstrated that the verticillins' high potency is related to the presence of a disulfur bridge at C-3/C-11a, while the removal of the sulfur atoms or the reduction of the sulfur bridge diminish/abolish the activity of verticillins.[49, 65, 67]

Herein, we report a novel series of semisynthetic verticillin analogues by linking diverse groups via ester, carbamate, carbonate, and sulfonate functionalities on the secondary hydroxy group on position C-11. The reactions were monitored with observing the loss of the symmetry via ^{1}H NMR. The structures of the new compounds were supported by ^{1}H and ^{13}C NMR and HRESIMS. Antitumor potential was evaluated *in vitro* via three types of cancer cell lines, and the IC_{50} values were in the order of the nanomolar range.

Results and Discussion

The verticillins class is originally isolated from the fungus *Clonostachys sp.* and demonstrated activity against cancer cell lines *in vitro* and *in vivo*.[27, 34, 70] This class of ETPs was always an inspiration for synthetic chemists. A total synthesis of one of this class analogues, (+)-11,11′-dideoxyverticillin A was achieved by Kim et al.[62] In the current study, verticillins, represented by verticillin H (**1**), was used as an inspiration to generate semisynthetic analogues in an attempt to produce new metabolites with improved solubility.

Starting from the isolated and purified Verticillin H (**1**), different groups were introduced to the position C-11. Several chemical reactions were performed in parallel starting with **1**. The first series of ester derivatives were obtained by reacting **1** with acetic anhydride overnight at room temperature as described for the acetylation of verticillin D,[41] afforded **3** as a major product (47% yield). In a similar way, the reaction of **1** with succinic anhydride overnight at room temperature, afforded **4** (53% yield).

The following ester analogues, **5**, **6**, and **7,** were synthesized by reacting **1** with butyryl chloride, cyclopropanecarbonyl chloride, and pivaloyl chloride, respectively. The reaction yielding to **5** (44% yield) was realized at room temperature for 4 hours, while **6** (82% yield) was obtained after 3 hours at room temperature. These later reactions were realized in an NMR tube and monitored by tracking the desymetrization of the aromatic region δ 6.5-8.0 ppm. The reaction yielding **7** was completed after 22 hours at room temperature with 86% yield, the presence of dimethylaminopyridine in this later reaction was required for full conversion to the desired product.

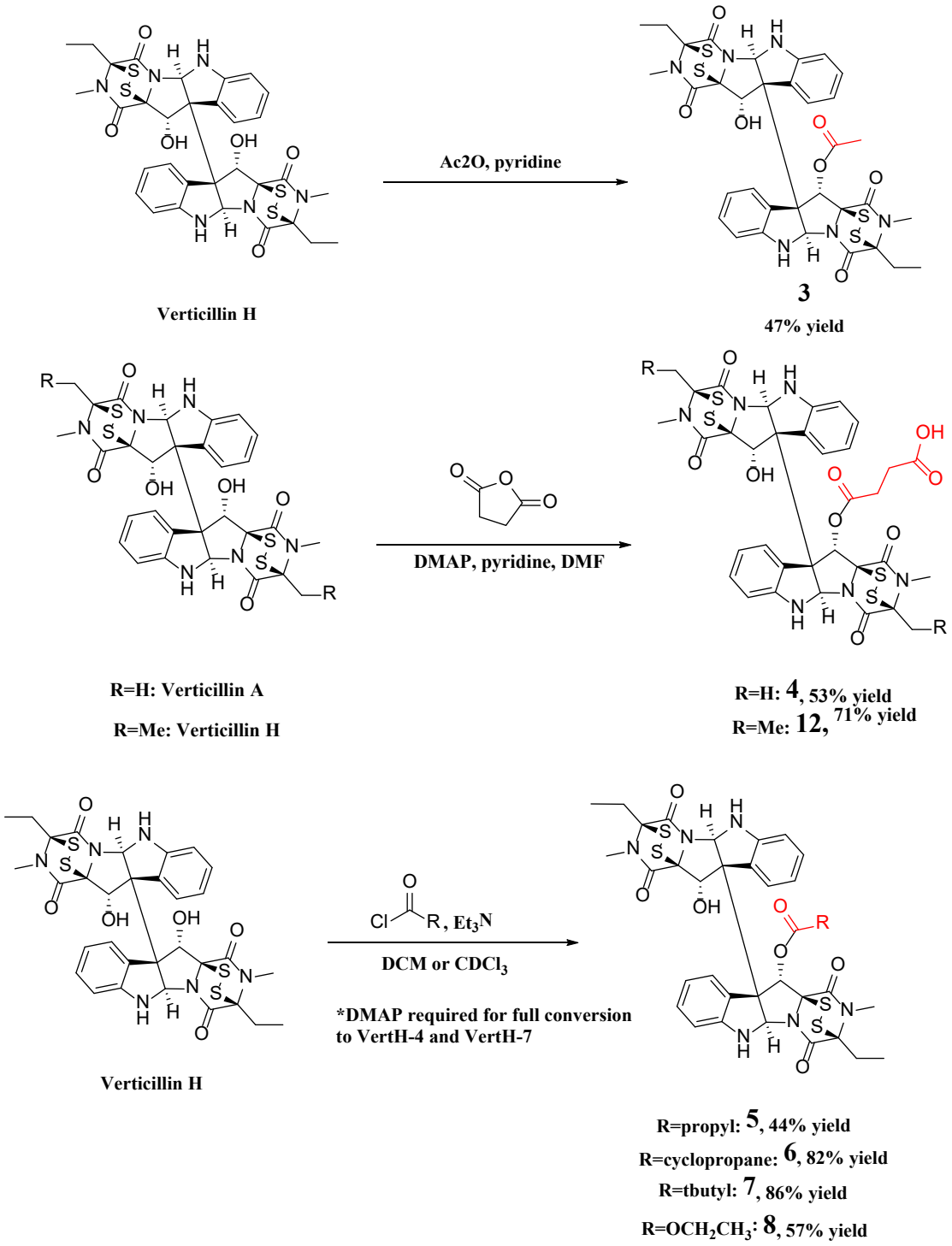

Scheme 1. Semisynthesis of Ester Derivatives 3, 4 and 12 and the Carbonate Derivative 5, 6, 7, and 8. The percent yields were calculated based on isolated product.

Compound **1** was reacted with ethyl chloroformate in the presence of dimethylaminopyridine for 3 hours at room temperature to produce the carbonate analogue **8 (**57% yield). This reaction was realized in an NMR tube in a similar way as the reaction yielding compound **5**, **6** and **7**. The sulfonate derivative **9**, was obtained by reacting **1** with 4-fluorobenzenesulfonyl chloride with the presence of dimethylaminopyridine for 22 hours at room temperature with a yield of 41%.

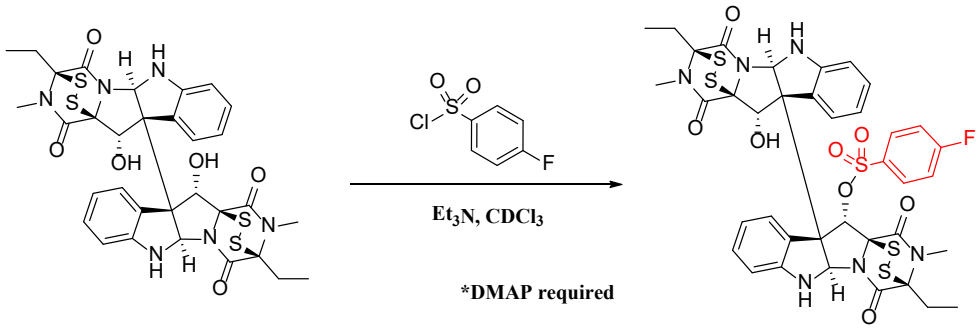

Verticillin H **9** **41% yield**

Scheme 2. Semisynthesis of Sulfonate Derivative 9. The percent yields were calculated based on isolated product.

The carbamate derivatives of **1** were realized in a two steps reaction.[199] First, compound **1** was reacted with carbonyldimidazole in the presence of potassium hydroxide for 2 hours at 50-55 °C (eventually becoming a clear solution) at which time transfer to an NMR tube confirmed consumption of starting material. After transferring back into the reaction vessel, either methylamine or dimethylamine was added respectively, the reaction mixture was stirred overnight at room temperature resulting in 18% yield **10** and 43% yield **11** respectively (Scheme 3).

In nearly all cases, the reaction mixture was then concentrated *in vacuo* providing a residue that was purified by HPLC. For compounds **10** and **11** after *in vacuo* concentration, the reaction mixture was dissolved in ethyl acetate and washed with several portions of water. The combined organics were rinsed with brine, dried over sodium sulfate, and concentrated under vacuum prior to purification by HPLC.

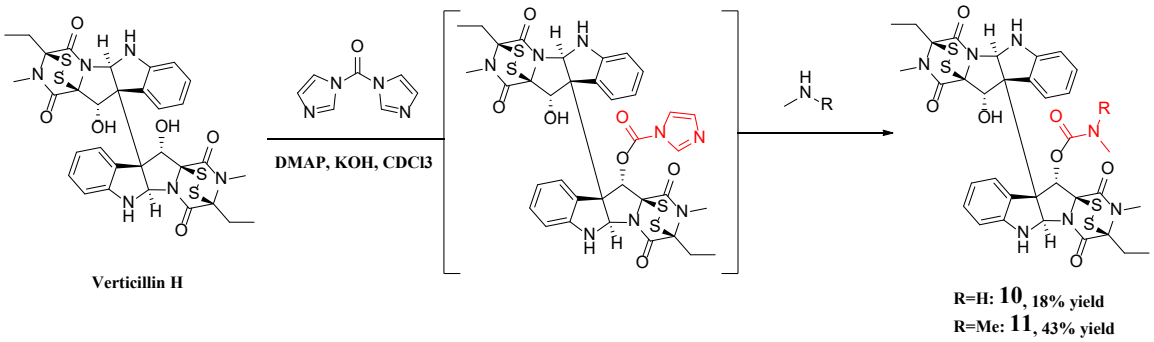

Scheme 3. Semisynthesis of Carbamate Derivatives 10 and 11. The percent yields were calculated based on isolated product.

The succinate derivative reaction was applied on verticillin A (**2**) to successfully generate **12** with a yield of 71%. By this reproduction of the reaction result, we hypothesize the ability of the different verticillin analogues on ongoing effectively through the proposed reactions in a similar way.

In all the previous reactions, the linkage of different groups to **1** was established in only one side of the symmetrical dimer. The presence of a bulky groups on position C-11 was well tolerated on one side resulting in the loss of the symmetry of the compound. The 1D NMR spectra of the ester derivatives (**3**, **4**, **5**, **6**, **7** and **12**), carbonate (**8**), sulfonate (**9**), and the carbamates (**10** and **11**) were characterized by a notable doubling of

signals that illustrated the loss of symmetry of the original compound. A distinct singlet peak in the range between 6.73 and 7.11 ppm was observed in all ^{1}H NMR spectra integrating for one proton, was found to represent H-11. The downfield shift of this peak compared to H-11′ (~ 5 ppm) of the same molecule and the parent compound H-11, proves the linkage of the new chain to OH-11.

More characteristic peaks were noticed in the ^{1}H NMR spectra of the synthesized compounds such as a singlet at 2.46 ppm in **3** with two extra carbons at 22.1 and 168.3 ppm corresponding to the acetate group at OH-11. The NMR and HRESIMS data (*m*/*z* 825.1502 $[M+H]^{+}$) for compound **4** supported a molecular formula of $C_{36}H_{36}N_6O_9S_4$. Two dt at 2.68 and 2.88 ppm and two ddd at 3.06 and 3.18 ppm with four extra carbon shifts, two around ~28 ppm and two at 170.9 and 173.9 ppm demonstrating the presence the succinate group.

Comparison of the NMR data between **1** and **5** showed the appearance of seven new proton peaks at the following chemical shifts; 1.11 (t), 1.93 (m), 2.61 (m), and 2.74 (m) ppm integrating for three, two, one and one proton respectively. The ^{1}H NMR spectrum of derivative **6** demonstrated the presence of multiplet at 1.13, 1.25, 1.48, and 1.96 ppm respectively and additional four carbon shifts at 9.2, 9.5, 13.6, and 172.7 ppm. The NMR and HRESIMS data (*m*/*z* 809.1894 $[M+H]^{+}$) for compound **7** supported a molecular formula of $C_{37}H_{40}N_6O_7S_4$. A singlet at 1.46 ppm integrating for nine protons were observed in the proton spectra corresponding to the three new methyl groups. The carbonate derivative **8** showed the addition of characteristic peaks at 1.49 (t) and 4.54 (q) ppm compared to the proton spectrum of **1,** along with an addition of three shifts in the

^{13}C NMR spectrum at 14.6, 66.0, and 153.7. In compound **9**, two aromatic shifts at 7.22 and 8.11 ppm integrating for two protons each were observed. These peaks correspond to the fluorobenzyl sulfonate group linked to C-11. Moreover, six additional carbon signal were detected in the aromatic region of the ^{13}C NMR spectrum. ^{19}F NMR offered an additional proof of the linkage of the latter group to **1**. The *J* coupling values of the ^{19}F peak (*J* = 8.0 Hz, 4.8 Hz) is shown to be shared with the aromatic peaks at 7.22 ppm (*J* = 8.6 Hz, 8.0 Hz) and 8.11 ppm (*J* = 8.6 Hz, 4.8 Hz). In the carbamate series, **10** showed the appearance of a doubled at 3.06 ppm and a multiplet at 4.86 ppm in the proton NMR. In the ^{1}H NMR of **11**, the dimethyl carbamate derivative showed two singlet shifts were integrating for three protons each at 3.01 and 3.14 ppm.

This set of compounds was evaluated for its *in vitro* cytotoxic properties against the human melanoma cancer cells (MDA-MB-435), human breast cancer cells (MDA-MB-231), and human ovarian cancer cells (OVCAR3). Growth inhibition was measured after a 72h exposure to the compound as previously described[34, 162]. The IC_{50} results of the new derivatives demonstrated a potency of the order of nanomolar (Table 5). Compound **1** and **2** derivatives showed a similar potency compared in the order of nanomolar compared to their parent compound against the three cancer cells suggesting that modifications didn't alter the attributes of the parent structure.

.

Table 5. Cytotoxicity of Compounds 1-12.

Compound	IC_{50}(nM)		
	MDA-MB-231	OVCAR 3	MDA-MB-435
Verticillin H (**1**)	31	229	44
Verticillin A (**2**)	23	36	18
3	21	96	41
4	13	133	21
5	-	-	-
6	12	105	24
7	20	72	21
8	7	137	11
9	49	79	31
10	21	68	22
11	12	19	9
12	12	33	9
Taxol (control)	0.1	171	1.4

MDA-MB-435: Human melanoma cancer cells, OVCAR3: Human ovarian cancer cells, MDA-MB-231: Human breast cancer cells.

In summary, a series of verticillin analogues were synthesized with ester, carbonate, sulfonate, and carbamate linkages. These reactions were monitored essentially via ^{1}H NMR to investigate the completion of the reaction. These compounds retained cytotoxic potency at the nanomolar level.

Experimental Section

General experimental procedures

All solvents were obtained from Fisher Scientific. NMR data were collected in $CDCl_3$ using either a JEOL ECS-400 spectrometer (JEOL USA, Inc.) operating at 400 MHz for ^{1}H and 100 MHz for ^{13}C, or JEOL ECA-500 NMR spectrometer (JEOL USA, Inc.) operating at 500 MHz for ^{1}H, 470 MHz for ^{19}F and 125 MHz for ^{13}C, or an Agilent 700 MHz NMR spectrometer (Agilent technologies, Inc., Santa Clara, CA, USA)

operating at 700 MHz for ^{1}H and 175 MHz for ^{13}C. Chemical shift values were referenced to the residual solvent signals for $CDCl_3$ (δ_H 7.25 and δ_C 77.2) and reported in δ ppm; multiplicity was showed as: s = singlet, d = doublet, t = triplet, q = quartet and m = multiplet; coupling constants were conveyed in Hz. Thermo QExactive Plus mass spectrometer (Thermofisher, San Jose, CA, USA) with an electrospray ionization source was utilized to collect HRESIMS data. The UPLC separation was achieved using an Acquity BEH C_{18} column (50 mm x 2.1 mm i.d., 1.7 µm) equilibrated at 40 ºC and a flow rate set at 0.3 mL/min. The mobile phase comprised a linear gradient CH_3CN/H_2O with 0.1% HCOOH starting at 15% CH_3CN to 100% over 8.5 min. Flash column chromatography was carried out with a Teledyne ISCO combiflash Rf connected to ELSD and PDA detectors with UV detection set at 200-400 nm with a specific wavelength set at 300 nm. The HPLC separation was achieved using Varian ProStar HPLC system connected to a ProStar 335 photodiod array detector (PDA) with UV detection set at 240 nm and 300 nm. Semi-preparative reverse phase HPLC purification of samples was performed on a Luna 5 µm silica (2) (100 A°, 250 x 10.0 mm) column using a flow rate of 4.6 mL/min of a mobile phase consisting of H_2O with 1% formic acid and MeOH.

Cytotoxicity assay

Human melanoma cancer cells (MDA-MB-435), human breast cancer cells (MDA-MB-231) and human ovarian cancer cells (OVCAR3) were produced from the American Type Culture Collection (Manassas, VA). RPMI 1640 medium (fetal 10% bovine serum, 100 unites/mL penicillin and 100 µg/mL streptomycin) was used to culture

cell lines. The cells were grown at 37 ºC under 5% CO_2, then harvested during the log-phase growth by trypsinization followed by two washing to remove all traces of enzymes. 96-Well clear, flat-bottom plate (Microtest 96, Falcon) was used to seed the cells at a density of 5000 cells per well. Each plate was incubated overnight at 37 ºC under 5% CO_2. Sample concentrations of 20, 4, 0.8, 0.16, and 0.032 µM of were prepared by dissolving the pure compounds in DMSO, and a total volume of 100 µL and 0.5% DMSO were added to the appropriate wells. The cells with the test samples were incubated for 72 h at 37 ºC. Cell viability was examined using a commercial absorbance assay (CellTiter 96® AQ_{ueous} One Solution Cell Proliferation Assay, Promega Corp, Madison, WI). IC_{50} values were designated as the concentration required to reduce cellular growth by 50% compared to the untreated controls after 72 h of continuous exposure. Parent's compounds; verticillin H and verticillin A were tested in comparison with the synthetic compounds and Taxol (Paclitaxel) was used as a positive control.

Fermentation, extraction, and isolation

A fungal strains MSX59553 from the Mycosynthetix culture collection identified to be *Clonostachys rogersoniana* was utilized in the present study.[33, 90] Erlenmeyer flasks containing 10 g of breakfast oatmeal were used in fermenting MSX59553 fungal strains over 11 days. Those solid media were extracted with 60 mL of acetone, each flask culture was chopped using a spatula, and then shaken for 16 h at 100 rpm. The extract was filtrated under vacuum then evaporated, the solid extract was reconstituted in 90 mL of EtOAc partitioned against 150 mL of H_2O. The solvents were transferred into a separatory funnel, and the organic layer was drawn off and evaporated *in vacuo*. This

material was re-formed using 100 mL of 1:1 MeOH:CH_3CN and 100 mL of hexanes. The MeOH: CH_3CN layer was drawn off and evaporated *in vacuo*. The defatted organic extract was adsorbed on Celite 545 (Acros Organics) and fractionated via flash chromatography on a 40 g RediSep Rf Gold Si-gel column using a gradient solvent system of hexanes-$CHCl_3$-MeOH at a flow rate of 40 mL/min over 53.3 column volumes (CV) for a duration of 63.9 min. Fractions were collected every 25.0 mL and pooled according to the UV and ELSD profiles, resulting in six fractions (F_1-F_6). Fraction F_1 and $F_3$was observed to contain both the targeted masses of verticillin H and verticillin A, respectively. F_1 and F_3 was subjected to further purifications via partitions of MeOH: CH_3CN against hexanes. The semisynthetic products were purified via reverse phase chromatography with a flow rate of 21.24 mL/min over 20 to 55 min.

Experimental procedures

Compound 3: Following the procedure reported for the acetylation of **Verticillin D**,[41] A solution of **Verticillin H** (**1**) (4 mg, 0.006 mmol), pyridine (0.2 mL), and acetic anhydride (1.5 mL) was stirred overnight at room temperature. The reaction was quenched with water and extracted with ethyl acetate. The combined organics were rinsed with 2M HCl, brine, and then dried over sodium sulfate, and concentrated *in vacuo*. The remaining solid was purified by HPLC to afford **3** (2.2 mg, 0.0028 mmol, 47% yield) as light-yellow powder. ^{1}H NMR ($CDCl_3$, 700 MHz) δ = 1.20 (t, *J* = 7.2 Hz, 3H), 1.21 (t, *J* = 7.2 Hz, 3H), 2.12 (m, 1H), 2.16 (m, 1H), 2.36 (m, 2H), 2.46 (s, 3H), 2.94 (s, 3H), 3.00 (s, 3H), 5.02 (d, *J* = 1.2 Hz, 1H), 5.17 (s, 1H), 5.17 (s, 1H), 5.18 (s, 1H), 5.22 (s, 1H), 5.43 (d, *J* = 1.2 Hz, 1H), 6.64 (d, *J* = 7.6 Hz, 1H), 6.68 (d, *J* = 7.7 Hz, 1H),

6.85 (td, = 7.6 Hz, 1.1 Hz, 1H), 6.88 (td, *J* = 7.7 Hz, 1.0 Hz, 1H), 6.95 (s, 1H), 7.15 (td, *J* = 7.6 Hz, 1.2 Hz, 1H), 7.19 (td, *J* = 7.7 Hz, 1.2 Hz, 1H), 7.65 (d, *J* = 7.7 Hz, 1H), 7.93 (d, *J* = 7.6 Hz, 1H); ^{13}C NMR ($CDCl_3$, 175 MHz), δ = 9.8 (2C), 22.1, 24.5, 24.7, 28.0, 28.5, 65.0, 65.9, 75.2, 76.7, 77.7, 78.3, 80.1, 81.9, 82.5, 83.1, 110.5, 111.1, 120.5, 120.7, 125.9, 128.4, 128.6, 129.0, 130.3, 130.5, 148.5, 149.0, 161.2, 161.3, 164.1, 166.8, 168.3. HRESIMS m/z 767.1433 $[M + H]^+$ (calcd for $C_{34}H_{35}N_6O_7S_4$, *m/z* 767.1450).

Compound 4: General Procedure for Succinates: A suspension of **Verticillin H** (**1**) (17 mg, 0.023 mmol), succinic anhydride (50 equiv., 38 mg), 4-dimethylaminopyridine (0.25 equiv., 0.009 mL of a 0.2 M solution in chloroform-d), and pyridine (50 equiv., 0.030 mL) in dimethylformamide (1 mL) was stirred at room temperature overnight, during which time the mixture became a clear solution. Solvent was then removed by vacuum distillation and the remaining solid was purified by HPLC to afford **4** (10 mg, 0.012 mmol, 53 % yield) as a light-yellow powder. ^{1}H NMR ($CDCl_3$, 700 MHz) δ = 1.20 (t, *J* = 7.4 Hz, 3H), 1.21 (t, *J* = 7.2 Hz, 3H), 2.14 (m, 2H), 2.36 (m, 2H), 2.68 (dt, *J* = 17.5, 4.1 Hz, 1H), 2.88 (dt, *J* = 17.1, 4.1 Hz, 1H), 2.92 (s, 3H), 3.00 (s, 3H), 3.06 (ddd, *J* = 17.1, 12.1, 4.1 Hz, 1H), 3.18 (ddd, *J* = 17.5, 12.1, 4.1 Hz, 1H), 5.02 (d, *J* = 1.9 Hz, 1H), 5.17 (s, 1H), 5.18 (s, 1H), 5.18 (s, 1H), 5.20 (s, 1H), 5.52 (d, *J* = 1.9 Hz, 1H), 6.64 (d, *J* = 7.7 Hz, 1H), 6.67 (d, *J* = 7.8 Hz, 1H), 6.84 (t, = 7.7 Hz, 1H), 6.90 (t, *J* = 7.8 Hz, 1H), 7.00 (s, 1H), 7.14 (t, *J* = 7.7 Hz, 1H), 7.19 (td, *J* = 7.8 Hz, 1.2 Hz, 1H), 7.76 (d, *J* = 7.7 Hz, 1H), 7.92 (d, *J* = 7.8 Hz, 1H); ^{13}C NMR ($CDCl_3$, 175 MHz), δ = 9.7, 9.8 , 24.5, 24.7, 28.1, 28.4, 28.5, 30.1, 65.1, 65.7, 75.0, 77.3, 77.9, 78.3, 80.4, 81.0, 82.5,

83.1, 110.5, 111.0, 120.6, 120.7, 126.1, 128.2, 128.9, 129.2, 130.3, 130.4, 148.4, 148.8, 161.2, 161.2, 164.2, 166.7, 170.9, 173.9. HRESIMS m/z 825.1502 $[M + H]^+$ (calcd for $C_{36}H_{37}N_6O_9S_4$, *m/z* 825.1504).

Compound 5: A solution of **Verticillin H** (**1**) (1 mg, 0.002 mmol), butyryl chloride (50 equiv., 0.01 mL), and triethylamine (70 equiv., 0.02 mL) in dichloromethane (0.25 mL) was stirred at rt for 4 hours before being quenched with water and extracted with ethyl acetate. The combined organic layers were dried over sodium sulfate and concentrated *in vacuo* prior to purification by HPLC to afford **5** (0.7 mg, 0.0009 mmol, 44 % yield) as an off-white powder. ^{1}H NMR ($CDCl_3$, 500 MHz) δ = 1.11 (t, *J* = 7.4 Hz, 3H), 1.20 (t, *J* = 7.2 Hz, 3H), 1.21 (t, *J* = 7.2 Hz, 3H), 1.93 (m, 2H), 2.13 (m, 2H), 2.37 (m, 2H), 2.61 (m, 1H), 2.74 (m, 1H), 2.93 (s, 3H), 3.00 (s, 3H), 5.03 (d, *J* = 1.2 Hz, 1H), 5.16 (s, 1H), 5.18 (s, 1H), 5.19 (s, 1H), 5.22 (s, 1H), 5.42 (d, *J* = 1.2 Hz, 1H), 6.64 (d, *J* = 7.6 Hz, 1H), 6.68 (d, *J* = 7.7 Hz, 1H), 6.86 (td, *J*= 7.7 Hz, 1.1 Hz, 1H), 6.90 (td, *J* = 7.6 Hz, 1.1 Hz, 1H), 7.00 (s, 1H), 7.16 (td, *J* = 7.6 Hz, 1.3Hz, 1H), 7.20 (td, *J* = 7.7 Hz, 1.2 Hz, 1H), 7.70 (d, *J* = 7.6 Hz, 1H), 7.92 (d, *J* = 7.7 Hz, 1H); ^{13}C NMR ($CDCl_3$, 175 MHz), δ = 9.8, 13.9, 18.0, 24.5, 24.8, 28.0, 28.5, 29.7 (2 C), 65.1, 65.9, 75.2, 76.6, 77.7, 78.4, 79.9, 81.7, 82.5, 83.1, 110.5, 111.1, 120.6, 120.7, 126.0, 128.3, 128.7, 129.1, 130.3, 130.4, 148.5, 148.9, 161.2, 161.3, 164.0, 166.8, 171.1. HRESIMS m/z 795.1715 $[M + H]^+$ (calcd for $C_{36}H_{39}N_6O_7S_4$, *m/z* 795.1763).

Compound 6: A solution of **Verticillin H** (**1**) (3 mg, 0.004 mmol), cyclopropanecarbonyl chloride (5 equiv., 0.002 mL), and triethylamine (10 equiv., 0.006 mL) in chloroform-d (1 mL) was added to an NMR tube. The reaction was monitored for

completion by looking for desymmetrization of the aromatic region in the NMR (completion observed as early as 30 minutes). After 3 hours at room temperature, the reaction mixture was then concentrated *in vacuo* providing a residue that was purified by HPLC to afford **6** (2.6 mg, 0.003 mmol, 82% yield) as an off-white powder. ^{1}H NMR ($CDCl_3$, 500 MHz) δ = 1.13 (m, 2H), 1.21 (m, 6H), 1.25 (m, 1H), 1.48 (m, 1H), 1.96 (m, 1H), 2.13 (m, 2H), 2.36 (m, 2H), 2.95 (s, 3H), 3.00 (s, 3H), 5.13 (d, *J* = 1.3 Hz, 1H), 5.18 (s, 1H), 5.20 (s, 2H), 5.22 (s, 1H), 5.36 (d, *J* = 1.3 Hz, 1H), 6.65 (d, *J* = 7.6 Hz, 1H), 6.69 (d, *J* = 7.7 Hz, 1H), 6.85 (t, *J*= 7.6 Hz, 1H), 6.89 (t, *J* = 7.7 Hz, 1H), 6.94 (s, 1H), 7.15 (td, *J* = 7.7 Hz, 1.2Hz, 1H), 7.20 (td, *J* = 7.6 Hz, 1.0 Hz, 1H), 7.84 (d, *J* = 7.6 Hz, 1H), 7.90 (d, *J* = 7.7 Hz, 1H); ^{13}C NMR ($CDCl_3$, 125 MHz), δ = 9.2, 9.5, 9.8, 9.9, 13.6, 24.6, 24.9, 28.1, 28.7, 29.8, 65.3, 66.0, 75.3, 77.9, 78.6, 80.3, 81.7, 82.6, 83.4, 110.6, 111.2, 120.7, 120.8, 126.2, 128.4, 128.9, 129.2, 130.4, 130.6, 148.6, 149.0, 161.3, 161.4, 164.3, 166.9, 172.7. HRESIMS m/z 793.1582 $[M + H]^+$ (calcd for $C_{36}H_{37}N_6O_7S_4$, *m/z* 793.1606).

Compound 7: A solution of **Verticillin H** (**1**) (5 mg, 0.007 mmol), pivaloyl chloride (10 equiv., 0.009 mL), triethylamine (15 equiv., 0.015 mL), and dimethylaminopyridine (0.25 equiv., 0.01 mL of a 0.2 M solution in chloroform-d) in chloroform-d (1 mL) was stirred 22 hours at room temperature, after which transfer to an NMR tube confirmed consumption of starting material. The reaction mixture was then concentrated *in vacuo* providing a residue that was purified by HPLC to afford **7** (4.88 mg, 0.006 mmol, 86 % yield) as an off-white powder. ^{1}H NMR ($CDCl_3$, 400 MHz) δ = 1.21 (m, 6H), 1.46 (s, 9H), 2.14 (m, 2H), 2.36 (m, 2H), 2.92 (s, 3H), 2.98 (s, 3H), 5.13 (s,

1H), 5.16 (s, 1H), 5.17 (s, 2H), 5.19 (s, 1H), 5.30 (s, 1H), 6.63 (d, *J* = 7.6 Hz, 1H), 6.69 (d, *J* = 7.7 Hz, 1H), 6.85 (t, *J*= 7.6 Hz, 1H), 6.91 (t, *J* = 7.7 Hz, 1H), 7.11 (s, 1H), 7.14 (t, *J* = 7.7 Hz, 1H), 7.20 (t, *J* = 7.6 Hz, 1H), 7.83 (d, *J* = 7.6 Hz, 1H), 7.90 (d, *J* = 7.7 Hz, 1H); ^{13}C NMR ($CDCl_3$, 100 MHz), δ = 9.9 (2 C), 24.7, 24.9, 27.7 (3 C), 28.0, 28.6, 29.8, 39.4, 64.8, 66.1, 75.7, 77.9, 78.7, 80.9, 81.1, 82.7, 83.4, 110.7, 111.4, 120.5, 120.8, 125.9, 128.2, 129.1, 129.9, 130.4, 130.5, 148.3, 148.7, 161.4, 161.5, 164.0, 166.9, 176.8. HRESIMS m/z 809.1894 $[M + H]^+$ (calcd for $C_{37}H_{41}N_6O_7S_4$, *m/z* 809.1919).

Compound 8: A solution of **Verticillin H** (**1**) (5 mg, 0.007 mmol), ethyl chloroformate (5 equiv., 0.003 mL), triethylamine (10 equiv., 0.01 mL), and dimethylaminopyridine (0.25 equiv., 0.009 mL of a 0.2 M solution in chloroform-d) in chloroform-d (1 mL) was added to an NMR tube. After 3 hours (consumption of starting material observed after 90 minutes) at room temperature, the reaction mixture was concentrated *in vacuo* providing a residue that was purified by HPLC to afford **8** (2.7mg, 0.004 mmol, 57 % yield) as an off-white powder. ^{1}H NMR (CDCl3, 500 MHz) δ = 1.18 (t, J= 7.2 Hz, 3H), 1.22 (t, J= 7.2 Hz, 3H), 1.49 (t, J= 7.1 Hz, 3H), 2.14 (m, 2H), 2.36 (m, 2H), 2.95 (s, 3H), 3.01 (s, 3H), 4.54 (q, J= 7.1 Hz, 2H), 5.10 (s, 1H), 5.14 (s, 1H), 5.18 (s, 1H), 5.19 (s, 1H), 5.22 (s, 1H), 5.52 (d, J = 1.2 Hz, 1H), 6.65 (m, 2H), 6.75 (s, 1H), 6.88 (m, 2H), 7.16 (m, 2H), 7.79 (d, J = 7.7 Hz, 1H), 7.92 (d, J = 7.8 Hz, 1H); ^{13}C NMR ($CDCl_3$, 125 MHz), δ = 9.9 (2 C), 14.6, 24.6, 24.8, 28.1, 28.6, 29.8, 65.3, 65.6, 66.0, 75.5, 76.7, 77.7, 78.5, 82.0, 82.5, 83.3, 84.0, 110.7, 111.0, 120.8, 121.1, 127.0, 128.4, 128.6, 128.7, 130.5, 148.7, 148.9, 153.7, 161.2, 161.3, 164.4, 167.0. HRESIMS m/z 809.1894 $[M + H]^+$ (calcd for $C_{35}H_{37}N_6O_8S_4$, m/z 809.1919).

Compound 9: A solution of **Verticillin H** (**1**) (6 mg, 0.008 mmol), 4-fluorobenzenesulfonyl chloride (5 equiv., 8 mg), triethylamine (10 equiv., 0.012 mL), and dimethylaminopyridine (0.25 equiv., 0.01 mL of a 0.2 M solution in chloroform-d) in chloroform-d (1 mL) was stirred 22 hours at room temperature, after which transfer to an NMR tube confirmed consumption of starting material. The reaction mixture was then concentrated *in vacou* providing a residue that was purified by HPLC to afford **9** (2.9 mg, 0.003 mmol, 41 % yield) as an off-white powder. ^{1}H NMR ($CDCl_3$, 500 MHz) δ = 1.13 (t, *J*= 7.0 Hz, 3H), 1.21 (t, *J*= 7.2 Hz, 3H), 2.05 (m, 1H), 2.17 (m, 1H), 2.30 (m, 1H), 2.37 (m, 1H), 2.66 (s, 3H), 3.00 (s, 3H), 5.16 (s, 1H), 5.17 (s, 1H), 5.21 (s, 2H), 5.69 (s, 2H), 6.61 (d, *J*= 7.8 Hz, 1H), 6.66 (d, *J*= 7.7 Hz, 1H), 6.73 (s, 1H), 6.85 (t, *J*= 7.8 Hz, 1H), 6.94 (t, *J* = 7.7 Hz, 1H), 7.14 (t, *J* = 7.7 Hz, 1H), 7.22 (m, *J* = 8.6 Hz, 8.0 Hz 3H), 7.87 (d, *J*= 7.8 Hz, 1H), 7.94 (d, *J*= 7.7 Hz, 1H), 8.11 (m, *J* = 8.6 Hz, 4.8 Hz, 2H); ^{13}C NMR ($CDCl_3$, 125 MHz), δ = 9.9 (2 C), 24.7 (2 C), 28.1, 28.4, 66.0, 66.8, 76.4, 77.3, 77.8, 79.6, 80.7, 82.1, 83.6, 88.7, 110.7, 111.0, 115.9, 116.1, 120.5, 120.9, 126.7, 128.4 (2 C), 129.1, 130.5 (2 C), 130.6, 130.7, 148.8, 149.0, 160.8, 161.4, 162.4, 164.5, 166.6 (d, *J*= 194.9 Hz), 166.9. HRESIMS m/z 883.1171 $[M + H]^+$ (calcd for $C_{38}H_{36}FN_6O_8S_5$, m/z 883.1182).

Compound 10: General Procedure for Carbamates.[199] A slurry of **Verticillin H** (**1**) (5 mg, 0.007 mmol), carbonyldiimidazole (15 equiv., 34 mg), potassium hydroxide (cat., 2 mg), and dimethylaminopyridine (0.25 equiv., 0.014 mL of a 0.2 M solution in chloroform-d) in chloroform-d (1 mL) was stirred at 50-55 °C (eventually becoming a clear solution) for 2 hours at which time transfer to an NMR tube confirmed consumption

of starting material. After transferring back into the reaction vessel, methylamine (5 equiv., 0.008 mL) was added and the resulting reaction mixture was stirred overnight at room temperature. The reaction mixture was then concentrated *in vacuo* providing a residue that was dissolved in ethyl acetate and washed with several portions of water (back extracted with ethyl acetate). The combined organics were rinsed with brine, dried over sodium sulfate, and concentrated *in vacuo* prior to purification by HPLC to afford **10** (1 mg, 0.0013 mmol, 18 % yield) as an off-white powder. ^{1}H NMR ($CDCl_3$, 700 MHz) δ = 1.18 (t, *J*= 7.2 Hz, 3H), 1.21 (t, *J*= 7.2 Hz, 3H), 2.12 (m, 2H), 2.36 (m, 2H), 2.93 (s, 3H), 2.99 (s, 3H), 3.06 (d, *J*= 4.8 Hz, 3H), 4.86 (m, 1H), 5.12 (d, *J*=1.9 Hz, 1H), 5.15 (s, 1H), 5.18 (s, 1H), 5.19 (s, 1H), 5.21 (s, 1H), 5.32 (d, *J*= 1.9 1H), 6.64 (d, *J*= 7.7 Hz, 1H), 6.67 (d, *J*= 7.7 Hz, 1H), 6.85 (m, 2H), 6.88 (s, 1H), 7.14 (t, *J*= 7.7 Hz, 1H), 7.18 (t, *J* = 7.7 Hz, 1H), 7.48 (d, *J* = 7.7 Hz, 1H), 7.94 (d, *J*= 7.7 Hz, 1H); ^{13}C NMR ($CDCl_3$, 175 MHz), δ = 9.8 (2 C), 24.6, 24.7, 28.0, 28.5, 28.6, 29.7, 50.9, 65.1, 65.8, 76.1, 77.9, 78.4, 81.4, 81.5, 82.5, 83.2, 110.6, 111.1, 120.2, 120.7, 128.6, 128.8, 129.1, 130.2, 130.4, 148.5, 149.1, 155.2, 161.2, 161.3, 164.3, 166.5. HRESIMS m/z 782.1550 $[M + H]^+$ (calcd for $C_{34}H_{36}N_7O_7S_4$, m/z 782.1559).

Compound 11: Utilizing dimethylamine, in the general procedure for carbamates, **Verticillin H** (**1**) (10 mg, 0.014 mmol) afforded **11** (4.5 mg, 0.006 mmol, 43 % yield) as an off-white powder. ^{1}H NMR ($CDCl_3$, 500 MHz) δ = 1.20 (t, *J*= 7.4 Hz, 6H), 2.13 (m, 2H), 2.36 (m, 2H), 2.92 (s, 3H), 2.98 (s, 3H), 3.01 (s, 3H), 3.14 (s, 3H), 5.14 (d, *J*=2.9 Hz, 1H), 5.20 (s, 2H), 5.21 (s, 1H), 5.24 (s, 1H), 5.33 (d, *J*= 3.0, 1H), 6.65 (d, *J*= 7.8 Hz, 1H), 6.67 (d, *J*= 7.8 Hz, 1H), 6.84 (m, 2H), 6.96 (s, 1H), 7.15 (m, 2H), 7.50 (d, *J* = 7.7

Hz, 1H), 7.96 (d, *J*= 7.7 Hz, 1H); ^{13}C NMR ($CDCl_3$, 125 MHz), δ = 9.9 (2 C), 24.7, 24.8, 28.1, 28.6, 65.2, 65.5, 77.0, 77.2, 77.3, 77.8, 78.2, 78.6, 81.0, 82.1, 82.7, 83.6, 110.9, 111.4, 120.1, 120.9, 126.4, 128.9, 129.0, 129.4, 130.3, 130.5, 148.7, 149.3, 155.7, 161.4, 161.6, 164.5, 166.3. HRESIMS m/z 796.1724 $[M + H]^+$ (calcd for $C_{35}H_{38}N_7O_7S_4$, m/z 796.1715).

Compound 12: Utilizing the general procedure for succination previously described, **Verticllin A** (**1**) (5 mg, 0.008 mmol) afforded **12** (4.5 mg, 0.006 mmol, 71 % yield) as a white powder. ^{1}H NMR ($CDCl_3$, 400 MHz) δ = 1.87 (s, 3H), 1.88 (s, 3H), 2.66 (dt, *J*= 17.3 Hz, 3.7 Hz, 1H), 2.85 (dt, *J*= 17.3 Hz, 3.7 Hz, 1H), 2.90 (s, 3H), 2.97 (s, 3H), 3.04 (dt, *J*= 17.3 Hz, 3.7 Hz, 1H), 3.18 (dt, *J* = 17.3 Hz, 3.7 Hz, 1H), 5.11 (s, 1H), 5.15 (s, 3H), 5.52 (d, *J*= 1.8 Hz, 1H), 6.64 (d, *J* = 7.7 Hz, 1H), 6.67 (d, *J* = 7.7 Hz, 1H), 6.84 (t, *J* = 7.7 Hz, 1H), 6.88 (t, = 7.7 Hz, 1H), 6.98 (s, 1H), 7.16 (m, 2H), 7.73 (d, *J* = 7.7 Hz, 1H), 7.90 (d, *J* = 7.7 Hz, 1H); ^{13}C NMR ($CDCl_3$, 100 MHz), δ = 17.6, 17.8 , 27.4, 27.7, 28.5, 30.2, 65.3, 66.0, 73.4, 73.8, 74.8, 77.3, 80.4, 81.1, 82.4, 83.0, 110.7, 111.2, 120.7, 120.8, 126.2, 128.3, 129.0, 129.3, 130.4, 130.5, 148.4, 148.8, 162.2, 162.3, 163.2, 165.8, 171.0, 174.2. HRESIMS m/z 797.11584 $[M + H]^+$ (calcd for $C_{34}H_{33}N_6O_9S_4$, *m/z* 797.1191).

Acknowledgment

This research was supported via P01 CA125066 from the National Cancer Institute. Mass spectrometry data were acquired in the Triad Mass Spectrometry Laboratory (UNCG). This work was performed, in part, at the Joint School of

Nanoscience and Nanoengineering, a member of the Southeastern Nanotechnology Infrastructure.

CHAPTER V

VERTICILLIN A-EXPANSILE NANOPARTICLES REDUCE TUMOR BURDEN IN HIGH GRADE SEROUS OVARIAN CANCER

This chapter has been modified from the one accepted for publication in *Molecular Cancer Therapeutics* to focus on the expansile nanoparticles work. The chapter is presented in the style of that journal. Coauthors include Salvi, A., Austin, J. R., Kilpatrick, K., Russo, A., Lantvit, D., Calderon-Gierszal, E., Mattes, Z., Pearce, C. J., Grinstaff, M. W., Colby, A. H., Oberlies, N. H., and Burdette, J. E.

Introduction

Ovarian cancer is the fifth leading cause of death among women and is the most lethal tumor type of the female reproductive tract.[200] In 2019, an estimated 22,530 women in United States will be diagnosed with ovarian cancer and about 13,980 women will succumb to the disease.[165] The most common and deadly histological subtype of ovarian cancer is high grade serous ovarian cancer (HGSOC). However, most patients develop chemoresistance and ultimately die from recurrent disease. Chemoresistance is multifaceted and likely arises both from mechanisms of resistance to the current therapy, or through immune cell evasion.[201-204]

One avenue to identify new therapies that may avert the chemoresistance problem is through the investigation of natural product drug leads with both unique chemical structures and modes of action, such as the verticillins.[11] The verticillins are epipolythiodioxopiperazine (ETP) alkaloids, and largely exist as dimers containing both

diketopiperazine moieties and disulfide bridges. This group of secondary metabolites is usually isolated from terrestrial and marine filamentous fungi, such as *Verticillium sp., Penicillium sp.* and *Gliocladium sp*. that belong to Sordariomycetes and Eurotiomycetes.[34, 40] Verticillin A was the first discovered analogue in 1970, and to date, 27 verticillin analogues are described in the literature.[34, 40, 44]

Enabled by recent advances in fungi fermentation and isolation, the role of verticillin A as an anti-cancer agent is actively being investigated.[33-34] Verticillin A selectively inhibits histone methyltransferases (HMTases) such as SUV39H1, SUV39H2, G9a, HTM, MLL1 and GLP.[35, 70] In colon carcinoma, verticillin A inhibited H3K9 methylation on the *FAS* promoter, restored Fas expression, and caused cell death by apoptosis.[35] Furthermore, mice treated with a combination of verticillin A and 5-fluorouracil displayed significantly smaller tumors and sensitized metastatic colon carcinoma cells to 5-fluorouracil.[35] Additionally, verticillin A suppressed metastatic colon cancer cell immune evasion and chemoresistance.[35] In pancreatic cancer cells, verticillin A inhibited MLL1, a HMTase responsible for H3K4 methylation, leading to decreases in H3K4me3 levels and PD-L1 expression. Lower PD-L1 expression led to reduced binding to PD-1 and activation of an immune response along with an enhanced chemotherapeutic response.[70] In a recent study with pancreatic ductal adenocarcinoma cells, verticillin A differentially altered H3K9me3 and H3K4me3 levels leading to expression of pro-apoptotic genes and inhibition of anti-apoptotic genes.[37]

Despite the promising results of verticillin A cytotoxic assays, however, its high toxicity interferes with the healthy cells. Studies performed using peripheral nerve sheath

tumor cells report toxicity and weight loss in mice treated with verticillin A.[30] Therefore, the choice of a delivery system can be important for cancer treatment. Higher concentration of the drug can be provided via a local drug delivery system that delivers directly to the cancer cells.[205] A study of pharmacokinetics and bioavailability of verticillin A in mice showed that intraperitoneal delivery was preferred compared to intravenous and oral administration.[31] To improve the delivery of the drug to the targeted cells, the use of nanoparticles represents an emerging technology.[206-207] Lately, many studies were conducted to ensure a higher dose of drug released from the nanoparticles during a longer period of time, resulting in nanoparticles synthesized by a "control-released" polymer that swells in certain environmental conditions, such as the acidic pH that corresponds to the microenvironment of cancer cells.[207]

Expansile nanoparticles (eNPs) permit the release of the drug in an acidic environment (i.e. pH 4-5) corresponding to the pH of the lysosomes that are formed from endosomes.[208] The swelling of eNPs in acidic pH was assessed using different instrumentations and techniques. The sizes of those eNPs were more than 350 times the original size over a number of days.[208] Another study from the same group showed that the accumulation of paclitaxel-loaded pH-responsive expansile nanoparticles (PTX-eNPs) inside tumor cells permitted the delivery of more than 100 times higher dose of taxol. The retention of eNPs inside the cell permitted the maintenance of a high concentration of the drug until 7 days after its administration, which enhanced animal survivals.[209]

During this study we were able to synthesize 5% loaded Verticillin A-expansile nanoparticles (verticillin A-eNPs). These nanoparticles induced cell death in HGSOC cells. The animals treated with verticillin A-eNPs reduced tumor burden *in vivo* and showed no morphological signs of liver toxicity compared to free verticillin A. Together, these findings validate verticillin A as a potential anti-cancer compound and highlight verticillin A-eNPs as a promising drug delivery strategy.

Materials and Methods

Verticillin A purification and synthesis of expansile nanoparticles

Verticillin A was isolated and characterized from *Clonostachys rogersoniana* (strain MSX59553) as detailed previously following a recently published fermentation optimization strategy.[33-34] The purity of the isolated verticillin A was assessed via UPLC and ^{1}H-NMR. The synthesis of verticillin A-eNPs and eNPs was performed using a miniemulsion polymerization method (Figure 12) as previously described.[209-211] Scanned electron microscope images were taken (Figure S73), and a calibration curve of verticillin A was built to calculate the encapsulation efficiency, which was found to be 76.9% (Figure S73). These data demonstrate the presence of 0.9 mg of verticillin A/ml of the expansile nanoparticles solution. Nanoparticles were stored at 4ºC until the time of dosage.

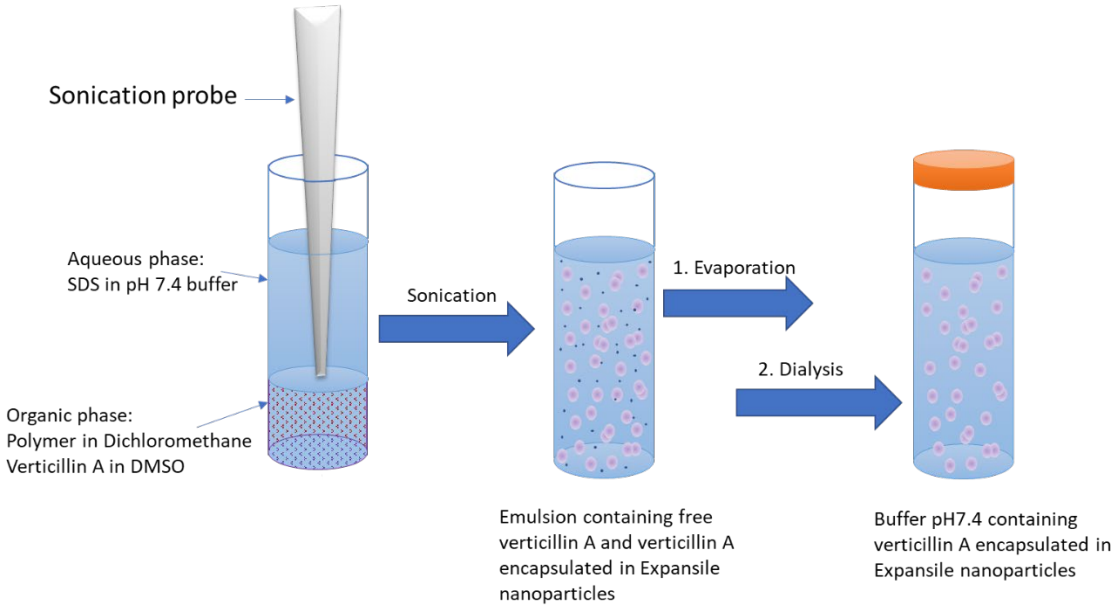

Figure 12. Verticillin A-eNP Synthesis. The synthesis followed a modified procedure developed by Colby et al.[208-209] The aqueous phase contains surfactant while the organic phase contains the pre-polymerized eNP polymer and verticillin A. This solution was emulsified with a probe sonicator to create a suspension of organic phase droplets in the aqueous phase. The organic solvent was evaporated, leaving behind verticillin A encapsulated inside eNPs. Finally, a last step of dialysis was done on the solution to eliminate the verticillin A molecules that escaped encapsulation during the sonication process.

Animals and xenograft experiments

All animals were treated in accordance with NIH Guidelines for the Care and Use of Laboratory Animals and the established Institutional Animal Use and Care protocol at the University of Illinois, Chicago. Xenograft studies utilized NCr *nu*/*nu* athymic female mice 6-8 weeks in age (Taconic). Mice were housed in a temperature and light-controlled environment (12 hours light and 12 hours dark) and provided food and water *ad libitum*. For xenograft experiments, OVCAR8-RFP cells (5 x 10^6) were injected intraperitoneally (IP) per mouse and tumor growth was monitored using Xenogen IVIS® Spectrum *In Vivo*

Imaging System (PerkinElmer) as previously described.[212] Once all the mice formed tumors (~4 weeks), the mice were separated into 2 treatment groups and dosed once every two days with 0.5 mg/kg of verticillin A encapsulated nanoparticles (eNP-VA) and empty nanoparticles (eNP) for a total of 12 days. Mice were IVIS imaged twice weekly (535 nm excitation, and 620 nm emission, Exposure time: 2 seconds, F stop: 2). Living Image 4.0 software was used to quantify the average abdominal radiant efficiency and normalization was performed using Day 0 radiant efficiency. At week 7, all animals were sacrificed, and tumors were collected for histological analysis.

Results

Verticillin A induces cytotoxicity in HGSOC cell lines *in vitro*

Verticillin A has been shown to inhibit the growth of colon cancer, pancreatic cancer, leiomyosarcoma and malignant peripheral nerve sheath tumor cells.[30, 35, 37, 70] In order to determine if verticillin A inhibited growth of ovarian cancer cells, three validated models of HGSOC, OVSAHO, OVCAR4 and OVCAR8 were used. Taxol was used as positive control. Verticillin A was found to inhibit the growth of all three cell lines with IC_{50} values of 60 nM, 47 nM and 45 nM in OVSAHO, OVCAR4 and OVCAR8, respectively (Table 6).

Table 6. IC_{50} Values of OVSAHO, OVCAR4 and OVCAR8 Cells Treated with Verticillin A and Chemotherapeutic Control Taxol. (vehicle: DMSO).

	IC_{50} (nM)		
	OVSAHO	OVCAR4	OVCAR8
Verticillin A	60	47	45
Taxol	80	113	6

In order to determine whether the growth inhibition effects exerted by verticillin A, a 2D foci assay was performed. Cells were treated with verticillin A for 8 hrs and foci were allowed to form for 2 weeks. Treatment with verticillin A completely abrogated foci formation in OVCAR4 and OVCAR8 cells (Figure S74) compared to vehicle control suggesting a cytotoxic effect and not a cytostatic effect.

Verticillin A encapsulated nanoparticles demonstrated reduced liver toxicity relative to free drug

To determine whether verticillin A affected tumor burden *in vivo*, OVCAR8-RFP cells were xenografted IP into female athymic nude mice. Tumors were allowed to form for 4 weeks and once all the mice displayed detectable tumors, the animals were treated with verticillin A and vehicle control (Cremophor EL/EtOH). However, animals treated with verticillin A showed significant gross morphological liver damage at the time of sacrifice (Figure 13). These observations suggested that verticillin A exerted a non-specific cytotoxic effect *in vivo*.

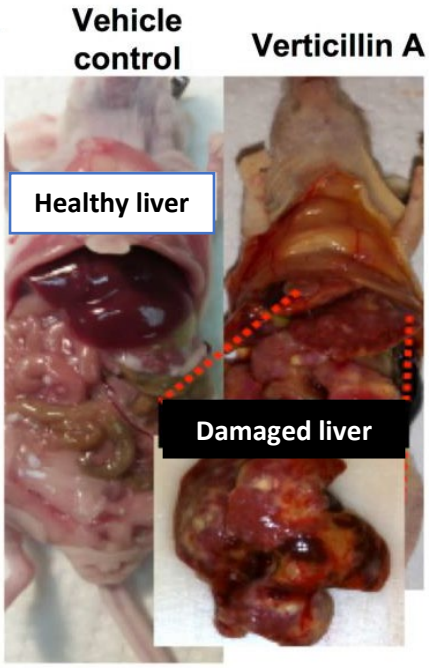

Figure 13. Representative Images Show Liver Damage in Verticillin A Treated Animals. OVCAR8-RFP cells were xenografted IP to form tumors. Mice were dosed with verticillin A and vehicle (Cremophor EL/EtOH) once in 7 days (Dosage: 0.5 mg/kg).

To confirm this, dose response curves were performed using two non-cancerous cell lines. Human ovarian surface epithelial cells IOSE80 and human fallopian tube epithelial secretory cells FT33 were treated with verticillin A and vehicle control (DMSO) for 3 days. Verticillin A inhibited growth of both cancerous and non-cancerous cells indicating a non-specific cytotoxic effect (Figure S75).

To improve the drug specificity towards tumor cells, verticillin A was encapsulated in expansile nanoparticles (verticillin A-eNPs) that have been shown to, following IP administration, localize to IP tumors of ovarian, mesothelial and pancreatic origin.[209, 211, 213-215] Unloaded-eNPs were used as a negative control. These eNPs localize

to tumors via materials-based targeting and, following internalization via macropinocytosis, release the encapsulated verticillin A upon encountering the acidic late endosome, thus reducing non-specific toxicity and increasing drug delivery to the tumor.[209, 211] To determine whether verticillin A loaded nanoparticles were still active, verticillin A-eNPs and eNPs were evaluated in an *in vitro* cytotoxicity assay using 3 HGSOC cell lines (OVSAHO, OVCAR4 and OVCAR8). Verticillin A-eNPs showed potent cytotoxicity with IC_{50} values of 44 nM, 29 nM and 32 nM in OVSAHO, OVCAR4 and OVCAR8 cells respectively (Table 7). Interestingly, IC_{50} values of verticillin A-eNPs were similar to free compound in all three HGSOC cell lines tested, confirming that encapsulation in nanoparticles did not reduce the activity and potency of verticillin A. Unloaded-eNPs did not exert a cytotoxic effect on any of the cell lines.

Table 7. Cytotoxicity Results of Verticillin A Encapsulated Nanoparticles (eNP-VA). OVSAHO, OVCAR4 and OVCAR8 cells were treated with verticillin A and empty nanoparticles (eNP) for 72 hrs.

	IC_{50} (nM)		
	OVSAHO	OVCAR4	OVCAR8
Verticillin A-eNPs	44	29	32

Verticillin A reduces tumor burden *in vivo*

To evaluate the ability of verticillin A-eNPs to reduce *in vivo* tumor burden, OVCAR8-RFP cells were xenografted IP in athymic nude mice and tumors were allowed to form for 4 weeks. The mice were treated with unloaded-eNPs and verticillin A-eNPs every other day for 12 days at a dose of 0.5 mg/kg. Animals treated with verticillin A-eNPs had significantly less tumor burden based on average radiant efficiency measured

with IVIS and had no measurable change in body weight (Figure 14). Interestingly, eNPs and verticillin A-eNPs did not cause the same gross morphological liver damage that was seen in mice treated with free verticillin A suggesting that encapsulation into the eNPs allowed for drug efficacy while reducing liver toxicity.

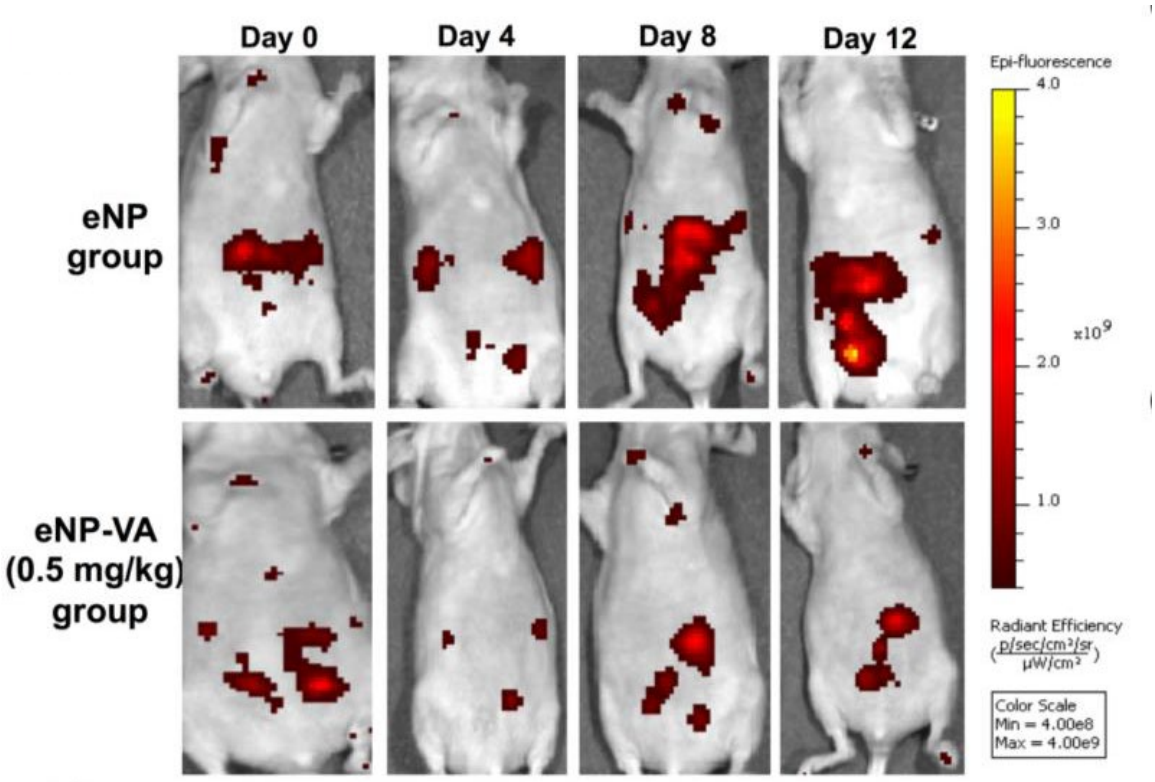

Figure 14. IVIS Images of Tumors in Mice on Days 0, 4, 8 and 12 of Drug Treatment. OVCAR8-RFP cells were xenografted IP to form tumors. Mice were dosed with eNP-VA and eNP once every 2 days for total 12 days (Dosage: 0.5 mg/kg).

Discussion

New therapies are needed to treat HGSOC and metastasis related lethality from the disease. Nearly 60% of all FDA approved anti-cancer drugs are derived from nature, and it remains a promising source for new drug leads, particularly due to the chemical

diversity.[10, 14] This study found that verticillin A, a fungal metabolite, caused cytotoxicity in HGSOC. Encapsulation of verticillin A in eNPs also improved drug specificity, reduced toxicity and, more importantly, caused a significant reduction of tumor burden *in vivo*.

A challenge with chemotherapeutic agents, particularly hydrophobic ones derived from nature, is to identify a delivery method that enables drug to accumulate therapeutic concentrations within the target tissue while minimizing, or averting altogether, adverse systemic toxicities. For example, taxol, which was first reported in 1971, was not considered a promising drug in terms of solubility, toxicity and large-scale production.[179, 182, 216] However, tremendous progress has been made in the past four decades making taxol one of the most effective chemotherapeutic drugs, particularly in frontline therapy for ovarian cancer.[217-218] IP administration of free verticillin A, solubilized in Cremophor EL/EtOH as a means to address its low solubility, resulted in liver toxicity. Shorter studies using verticillin A IP did not report significant liver toxicity, nevertheless, studies performed using peripheral nerve sheath tumor cells report it.[30, 35] To overcome the toxic effects induced by verticillin A, and to enhance solubility, a well-characterized nanoparticle-based drug delivery system, the eNP was used.[209, 211, 219] Previously, eNPs have been used to deliver other cytotoxic natural products (e.g., taxol) with high specificity to peritoneal tumors. As a result of their unique materials-based targeting mechanism, eNPs afford 10 to 100-fold higher intratumoral drug concentrations than are achieved with free drug and show remarkable efficacy (e.g., doubling of survival compared to free drug controls).[211]

In conclusion, encapsulation of verticillin A in an eNP improves drug efficacy, reduces toxicity and highlights the advantages of marrying natural products/anti-cancer research with nanoparticle drug delivery systems to address a clinical challenge. Continued investigation of verticillin A, verticillin analogs, and the eNP delivery system will provide key data for preparing an optimized efficacious formulation worthy of large animal pharmacokinetic studies and bring us one step closer to a promising therapy for ovarian cancer patients.

Acknowledgements

This work was supported in part by grants P01CA125066 and R01CA227433 from the National Cancer Institute of the NIH (Bethesda, MD, USA). IVIS imaging was performed using Xenogen IVIS® Spectrum Imager at University of Illinois, Chicago Research Resource Center's Center for Cardiovascular Research and Physiology Core.

CHAPTER VI

DROPLET PROBE: COUPLING CHROMATOGRAPHY TO THE *IN SITU* EVALUATION OF THE CHEMISTRY OF NATURE

This chapter has been modified from the review paper accepted for publication in *Natural Product Reports* and is presented in that style. Coauthors include Knowles, S. L., Kao, D., Raja, H. A., Kertesz, V., and Oberlies, N. H.

Introduction

The chemistry of nature can be beautiful, inspiring, beneficial and poisonous, deepening on perspective. Since the isolation of the first secondary metabolites roughly two centuries ago[220], much of the chemical research on natural products has been both reductionist and static.[221] Typically, compounds were isolated and characterized from the extract of an entire organism from a single time point. While there could be subtexts to that approach, the general premise has been to determine the chemistry with very little in the way of tools to differentiate spatial and/or temporal changes in secondary metabolite profiles.[222] However, the past decade has seen exponential advances in our ability to observe, measure, and visualize the chemistry of nature *in situ*.[105-106]

In many ways, this review on the droplet-liquid microjunction-surface sampling probe (droplet probe) originates in attempting to carry out similar *in situ* chemistry experiments but on fungal cultures. We believe that the process of studying the chemistry of nature *in situ* is here to stay, and most likely, it will only become both more powerful and more accessible in the future. Quite simply, the ability to probe research questions

that address the timing and/or spatial distribution of natural products are both too tempting and too important to ignore.

Optimized Production of Fungal Metabolites on the Lab Scale

It has long been known that media studies can be used to optimize the production of fungal metabolites, sometimes codified as an OSMAC (one strain, many cultures) approach.[223-224] However, how one goes about that can be quite variable, and we have found that evaluating the chemistry of fungal cultures *in situ* via droplet probe enables scouting growth conditions rapidly, especially when spatial and temporal studies are taken into consideration.

Mevalocidin (spatial considerations)

Mevalocidin[225-226] is a unique phytotoxin that exhibits broad spectrum post emergent herbicidal properties. Since there are no organic herbicides on the market, it is currently being considered for development. As part of a study to improve the production of this compound via fermentation on the laboratory scale, *in situ* sampling via droplet probe permitted a better understanding of the distribution of this herbicidal secondary metabolite in the fungal culture.[227] In addition to the pragmatic goal of increasing yield, what the fungus did with mevalocidin was of interest from a chemical ecology perspective.

The droplet probe facilitated *in situ* sampling of the fungal chemistry on the surface of the cultures (mycelium, guttates, and surrounding agar), which would be challenging to accomplish via traditional natural product extraction methods (Figure. 15). The use of droplet probe was important in understanding that both strains of

Coniolariella sp. (strains MSX56446 and MSX92917) released mevalocidin into their surroundings via guttates (exudates or liquid droplets), where the highest concentration of this secondary metabolite was mapped. Similarly, mevalocidin was also detected in the surrounding agar but not on the surface of the mycelium. Since the fungi that biosynthesize it are both saprobes (i.e. decomposers of dead organic matter), it was fascinating to map that the fungi seem to concentrate mevalocidin in this fashion, so as to exude the phytotoxic compound into their surroundings.[227] Extrapolating, we hypothesized that this imparts an advantage to the fungus, potentially killing (or at least weakening) surrounding plant material, so that the fungus can utilize the dead organic matter for growth and reproduction. Such information could not be obtained without instruments that sampled chemistry *in situ* in this manner.

This general approach has been used several times, where it has been interesting to see where fungal secondary metabolites are concentrated.[228-229] Based on additional literature,[119, 230-232] we suspect that guttates may be a common place for such compounds to be localized.

Verticillins (spatial and temporal considerations)

One of the more prominent examples of using the droplet probe to scout for optimized fermentation conditions comes via our studies on verticillins.[233] This class of compounds (epipolythiodioxopiperazine alkaloids) has been in the literature since the early 1970s.[234] While they have been studied by prominent organic chemists,[65-66, 235] a scalable total synthesis has yet to be reported. Recently, a series of studies on the anticancer activity of the verticillins have been published,[236-240] and there is growing

interest in their potential as selective histone methyl transferase inhibitors. This stimulated several *in vivo* studies,[31, 239-241] and it became obvious that if future progress was to be made, an amplified supply of verticillins was needed. However, based on the initial growth parameters using a rice-based substrate,[236] we found it challenging to scale the supply of this compound.

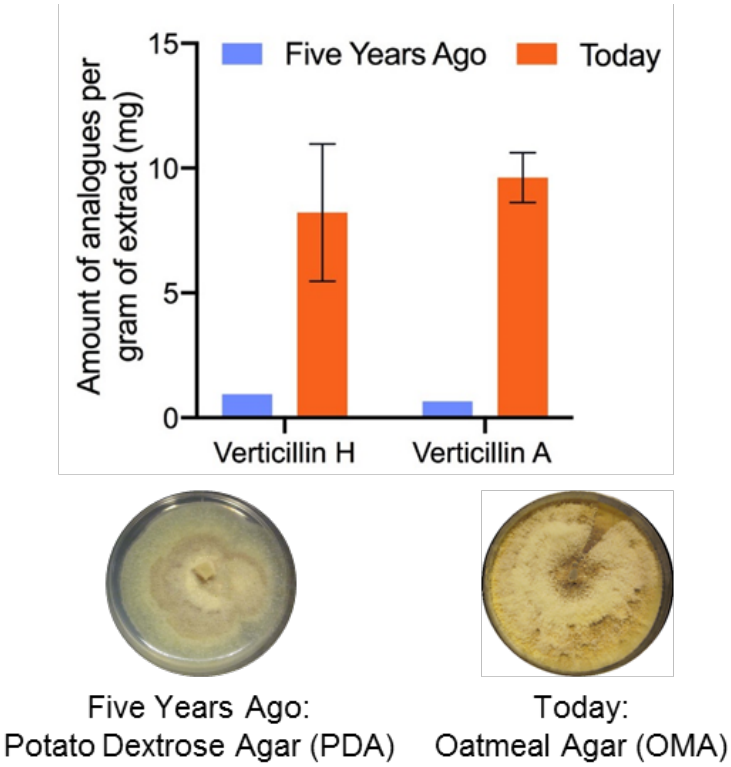

Figure. 15. The Fermentation Conditions Optimized for the Production of Verticillin A and Verticillin H. This was through both strain and media optimization via an OSMAC approach, where the droplet probe played an instrumental role. An average growth of strain MSX59553 yielded about 3 g of extract per flask in the lab. The data in orange are from three biological replicates (+/- SD), indicating about 10 mg of each compound per gram of extract (or 30 mg per flask). Initially, the cultures were generating about 1 mg of each compound per gram of extract (or 3 mg per flask).

Fungal cultures that produced verticillins were examined *in situ* via droplet probe on a suite of different media (Figure. 15), ranging from both rich (i.e. those based on extracts of potatoes, yeast, etc.) and defined (i.e. those that are made via a specific recipe).[233] We were pleased that fermentation on oatmeal-based medium seemed to produce the highest yield of verticillins, a fact that could only be discerned empirically. This observation was then tested in scaled up cultures (including three biological replicates), using a traditional natural products approach to validate the measurements from *in situ* analysis. Not only did the *in situ* results translate well to the pragmatic need for isolating more of the verticillins, but also, a timing study noted their peak production from 7 to 22 days, meaning that cultures could be processed on a weekly to biweekly basis.[233] All told, we went from a challenging provision of a few mg of verticillins to a steady state production of 50 to 100 mg monthly (Figure. 15). Importantly, those materials are now being used in a suite of further studies, including *in vivo* pharmacology, *in vivo* pharmacokinetics, and semi-synthesis; none of those would be possible without the enhanced supply.

Conclusion

In general, the advent of ambient ionization mass spectrometry techniques has made an enormous impact on natural products research, since organisms can be examined *in situ* with limited sample preparation.[242] When it comes to the droplet probe, and with the caveat that we may be biased based on our mycological research, fungi represent ideal candidates for *in situ* mass spectrometry mapping experiments. Compared to plants, microorganisms respond quickly to changes in environment (i.e. media)[243-244] or by the

introduction of other organisms (i.e. co-cultures),[223, 245] thus creating unique profiles of their biosynthesized secondary metabolites. Furthermore, as opposed to many bacteria, fungi are morphologically diverse and often develop unique physical characteristics as the culture grows. The presence of stroma (finger–like projections),[246-247] guttates or liquid exudates [119, 230-231, 248] and mycelium color changes/gradients give rise to several questions about the spatial distribution of the metabolites associated with such features.

Once the droplet probe has sampled the surface of an organism, that extract can then be interfaced with a wide range of analytical tools that are common to natural products laboratories. Chromatographic separation is the most unique aspect, as that is how it differs from the range of ambient ionization techniques that are also used to study the chemistry of nature *in situ*. In turn, chromatographic resolution of the extract from *in situ* sampling via droplet probe serves to enhance the measurements from any detectors added post column, including UV/Vis and HRMS/tandem mass spectrometry.

We have found that it is a great tool for determining ways to enhance the production of secondary metabolites, to probe conditions for the biosynthesis of non-natural natural products, and to examine the generation of new chemical diversity via co-culturing. Opportunities to study the chemistry of a range of materials *in situ* abound, and only time will tell what other questions can be analysed using the droplet probe.

Acknowledgements

SLK and DK were supported by the National Center for Complementary and Integrative Health/National Institutes of Health (NIH), under award numbers T32 AT008938 and F31 AT009264, respectively. VK was supported by the U. S. Department

of Energy, Office of Science, Basic Energy Sciences, Chemical Sciences, Geosciences, and Biosciences Division. Research on bioactive fungal metabolites in NHO's lab is supported by the National Cancer Institute/NIH under grant P01 CA125066.

REFERENCES

(1) Miller, K., D.; Siegel, R., L.; Lin, C., C.; Mariotto, A., B.; Kramer, J., L.; Rowland, J., H.; Stein, K., D.; Alteri, R., Jemal, A., *Ca-Cancer J. Clin.* **2016**, *66*, 271.

(2) Siegel, R. L.; Miller, K. D., Jemal, A., *Ca-Cancer J. Clin.* **2019**, *69*, 7.

(3) Agarwal, R., Kaye, S., B., *Nat. Rev. Cancer* **2003**, *3*, 502.

(4) Whiteside, T., *Oncogene* **2008**, *27*, 5904.

(5) Rueff, J., Rodrigues A, S.,Cancer Drug Resist.; Humana Press, **2016**, p. 1.

(6) Lin, J. H., *Biopolymers* **2016**, *105*, 2.

(7) Holohan, C.; Van Schaeybroeck, S.; Longley, D. B., Johnston, P. G., *Nat. Rev. Cancer* **2013**, *13*, 714.

(8) Newman, D., J., Cragg, G., M., *J. Nat. Prod.* **2007**, *70*, 461.

(9) Salim, A., A.; Chin, Y., W., Kinghorn, A., D. ,Bioactive molecules and medicinal plants; Springer-Verlag Berlin Heidelberg, **2008**, p. XXIII.

(10) Newman, D., J., Cragg, G., M., *J. Nat. Prod.* **2016**, *79*, 629.

(11) Kinghorn, A. D.; Carcache De Blanco, E. J.; Lucas, D. M.; Rakotondraibe, H. L.; Orjala, J.; Soejarto, D. D.; Oberlies, N. H.; Pearce, C. J.; Wani, M. C.; Stockwell, B. R.; Burdette, J. E.; Swanson, S. M.; Fuchs, J. R.; Phelps, M. A.; Xu, L.; Zhang, X., Shen, Y. Y., *Anticancer Res.* **2016**, *36*, 5623.

(12) González-Medina, M.; Owen, J. R.; El-Elimat, T.; Pearce, C. J.; Oberlies, N. H.; Figueroa, M., Medina-Franco, J. L., *Front. Pharmacol.* **2017**, *8*, DOI: 10.3389/fphar.2017.00180.

(13) González-Medina, M.; Prieto-Martínez, F. D.; Naveja, J. J.; Méndez-Lucio, O.; El-Elimat, T.; Pearce, C. J.; Oberlies, N. H.; Figueroa, M., Medina-Franco, J. L., *Future Med. Chem.* **2016**, *8*, 1399.

(14) El-Elimat, T.; Zhang, X.; Jarjoura, D.; Moy, F. J.; Orjala, J.; Kinghorn, A. D.; Pearce, C. J., Oberlies, N. H., *ACS Med. Chem. Lett.* **2012**, *3*, 645.

(15) Andersen, S., Frisvad, J., *J. Appl. Microbiol.* **1994**, *19*, 486.

(16) Ligon, B. L., in *Seminars in pediatric infectious diseases, Vol. 15*, Elsevier, **2004**, p. 52.

(17) Hendrik, G.; Ietida, M.; Pontius, A.; Kehraus, S.; Gross, H., König, G., *Phytochem. Rev.* **2010**, *9*, 537.

(18) Blackwell, M., *Am. J. Bot.* **2011**, *98*, 426.

(19) Hawksworth, D. L., Lücking, R., *Microbiol. Spectrum* **2017**, *5*.

(20) Hibbett, D.; Abarenkov, K.; Kõljalg, U.; Öpik, M.; Chai, B.; Cole, J.; Wang, Q.; Crous, P.; Robert, V., Helgason, T., *Mycologia* **2016**, *108*, 1049.

(21) Bills, G. F., Gloer, J. B., *Microbiol. Spectrum* **2016**, *4*, DOI: 10.1128/microbiolspec.FUNK.

(22) Alberti, F.; Foster, G., D., Bailey, A., M., *Appl. Microbiol. Biotechnol.* **2016**, *101*, 493.

(23) Evidente, A.; Kornienko, A.; Cimmino, A.; Andolfi, A.; Lefranc, F.; Mathieu, V., R., Kiss, R., *Nat. Prod. Rep.* **2014**, *31*, 617.
(24) Iwasa , E.; Hamashima , Y., Sodeoka , M., *Isr. J. Chem.* **2011**, *51*, 420.
(25) Jiang, C. S., Guo, Y. W., *Mini-Reviews in Medicinal Chemistry* **2011**, *11*, 728.
(26) Gardiner, D. M.; Waring, P., Howlett, B. J., *Microbiology* **2005**, *151*, 1021.
(27) Liu., F.; Liu., Q.; Yang., D.; Bollag., W. B.; Robertson., K.; Wu., P., Liu., K., *Cancer Res.* **2011**, *71*, 6807.
(28) Feiyan, L.; Ping, W., Kebin, L., in *United States Patent Application, Vol. US 20140161785A1*, Zhejiang UniversityAugusta University Research Institute Inc United States, **2014**, p. 15.
(29) Niu, S.; Yuan, D.; Jiang, X., Che, Y., *Protein Cell* **2014**, *5*, 945.
(30) Zewdu, A.; Lopez, G.; Braggio, D.; Kenny, C.; Constantino, D.; Bid, H. K.; Batte, K.; Iwenofu, O. H.; Oberlies, N. H.; Pearce, C. J.; Strohecker, A. M.; Lev, D., Pollock, R. E., *Clin. Exp. Pharmacol.* **2016**, *6*, 221.
(31) Wang, J.; Zhu, X.; Kolli, S.; Wang, H.; Pearce, C. J.; Oberlies, N. H., Phelps, M. A., *J. Pharm. Biomed. Anal.* **2017**, *139*, 187.
(32) Wang, Y.; Hu, P.; Pan, Y.; Zhu, Y.; Liu, X.; Che, Y., Liu, G., *Fungal Genet. Biol.* **2017**, *103*, 25.
(33) Amrine, C. S. M.; Raja, H. A.; Darveaux, B. A.; Pearce, C. J., Oberlies, N. H., *J. Ind. Microbiol. Biotechnol.* **2018**, *45*, 1053.
(34) Figueroa, M.; Graf, T. N.; Ayers, S.; Adcock, A. F.; Kroll, D. J.; Yang, J.; Swanson, S. M.; Munoz-Acuna, U.; Carcache de Blanco, E. J.; Agrawal, R.; Wani, M. C.; Darveaux, B. A.; Pearce, C. J., Oberlies, N. H., *J. Antibiot.* **2012**, *65*, 559.
(35) Paschall, A. V.; Yang, D.; Lu, C.; Choi, J.-H.; Li, X.; Liu, F.; Figueroa, M.; Oberlies, N. H.; Pearce, C.; Bollag, W. B.; Nayak-Kapoor, A., Liu, K., *J. Immunol.* **2015**, *195*, 1868.
(36) Lu, C., Liu, K., *Transl. Cancer Res.* **2017**, *6*, S652.
(37) Lu, C.; Yang, D.; Sabbatini, M. E.; Colby, A. H.; Grinstaff, M. W.; Oberlies, N. H.; Pearce, C., Liu, K., *BMC Cancer* **2018**, *18*, 149.
(38) Jordan, T. W., Cordiner, S. J., *Trends Pharmacol. Sci.* **1987**, *8*, 144.
(39) Liu, F.; Wu, S.; Chen, Y.; Yang, L., Wu, P., *Acta Crystallogr., Sect. E: Struct. Rep. Online* **2006**, *62*, 974.
(40) Katagiri, K.; Sato, K.; Hayakawa, S.; Matsushima, T., Minato, H., *J. Antibiot.* **1970**, *23*, 420.
(41) Joshi, B. K.; Gloer, J. B., Wicklow, D. T., *J. Nat. Prod.* **1999**, *62*, 730.
(42) Fox, E. M., Howlett, B. J., *Mycol. Res.* **2008**, *112*, 162.
(43) Minato, H.; Matsumoto, M., Katayama , T., *J. Chem. Soc. D* **1971**, *0*, 44.
(44) Minato, H.; Matsumoto, M., Katayama , T., *J. Chem. Soc., Perkin Trans. 1* **1973**, *17*, 1819.
(45) Chu, M.; Truumees, I.; Rothofsky, M. L.; Patel, M. G.; Gentile, F.; Das, P. R., Puar, M. S., *J. Antibiot.* **1995**, *48*, 1440.
(46) Son, W. B.; Jensen, R. P.; Kauffman, C. A., Fenical, W., *Nat. Prod. Lett.* **1999**, *13*, 213.
(47) Yoshihide, U.; Junko, Y., Atsushi, N., *Heterocycles* **2004**, *63*, 1123.

(48) Dong, J.; He, H.; Shen, Y., Zhang, K., *J. Nat. Prod.* **2005**, *68*, 1510.
(49) Zheng, C. J.; Kim, C. J.; Bae, K. S.; Kim, Y. H., Kim, W. G., *J. Nat. Prod.* **2006**, *69*, 1816.
(50) Jin-Yan, D.; Wei, Z.; Lei, L.; Guo-Hong, L.; Ya-Jun, L., Ke-Qing, Z., *Chin. Chem. Lett.* **2006**, *17*, 922.
(51) Zheng, C. J.; Park, S. H.; Koshino, H.; Kim, Y. H., Kim, W. G., *J. Antibiot.* **2007**, *60*, 61.
(52) Chen, Y.; Guo, H.; Du, Z.; Liu, X. Z.; Che, Y., Ye, X., *Cell Proliferation* **2009**, *42*, 838.
(53) Xingzhong, L.; Shuchun, L.; Che, Y. Y.; sheng, Y.; Huijuan, G., Yali, C., *Vol. CN 200910077302* (Ed.: Institute of Microbiology, C. A. o. S.), Chinese Academy of Sciences, Peop. Rep. China, **2009**.
(54) Dirk, S.; Böttcher, C.; Lee, J., Scheel, D., *J. Antibiot.* **2011**, *64*, 523.
(55) Suhadolnik, R. J., Chenoweth, R. G., *J. Am. Chem. Soc.* **1958**, *80*, 4391.
(56) Winstead, J. A., Suhadolnik, R. J., *J. Am. Chem. Soc.* **1960**, *82*, 1644.
(57) Kirby, W., Robins, J., Academic Press, New York, **1980**, p. 301-326.
(58) Mootz, H., D., Marahiel, M., A., *Curr. Opin. Chem. Biol.* **1997**, *1*, 543.
(59) Marion, A.; Groll, M.; Scharf, D. H.; Scherlach, K.; Glaser, M.; Sievers, H.; Schuster, M.; Hertweck, C.; Brakhage, A. A.; Antes, I., Huber, E. M., *ACS Chem. Biol.* **2017**, *12*, 1874.
(60) Scharf, D. H.; Heinekamp, T.; Remme, N.; Hortschansky, P.; Brakhage, A. A., Hertweck, C., *Appl. Microbiol. Biotechnol.* **2012**, *93*, 467.
(61) Dolan, S. K.; O'Keeffe, G.; Jones, G. W., Doyle, S., *Trends Microbiol.* **2015**, *23*, 419.
(62) Kim, J.; Ashenhurst, J. A., Movassaghi, M., *Science* **2009**, *324*, 238.
(63) Kim, J., Movassaghi, M., *Chem. Soc. Rev.* **2009**, *38*, 3035.
(64) Overman, L. E., Shin, Y., *Org. Lett.* **2007**, *9*, 339.
(65) Boyer, N.; Morrison, K. C.; Kim, J.; Hergenrother, P. J., Movassaghi, M., *Chem. Sci.* **2013**, *4*, 1646.
(66) Kim, J., Movassaghi, M., *Acc. Chem. Res.* **2015**, *48*, 1159.
(67) Rodriguez, P., L., Carrasco, L., *J. Virol.* **1992**, *66*, 1971.
(68) He, J.-S.; Gong, D.-E., Ostergaard, H. L., *J. Immunol.* **2010**, *184*, 555.
(69) Koncz, G.; Hancz, A.; Chakrabandhu, K.; Gogolák, P.; Kerekes, K.; Rajnavölgyi, É., Hueber, A.-O., *J. Immunol.* **2012**.
(70) Lu, C.; Paschall, A. V.; Shi, H.; Savage, N.; Waller, J. L.; Sabbatini, M. E.; Oberlies, N. H.; Pearce, C., Liu, K., *J. Natl. Cancer Inst.* **2017**, *109*, djw283.
(71) O'Hara, B., M.; Klinger, H., P.; Curran, T.; Zhang, Y., D., Blair, D., G., *Mol. Cell. Biol.* **1987**, *7*, 2941.
(72) Scott, R., E., *Pharmacol. Ther.* **1997**, *73*, 51.
(73) Erkel, G.; Gehrt, A.; Anke, T., Sterner, O., *Z. Naturforsch. C* **2002**, *57*, 759.
(74) Zhang, Y.; Chen, Y.; Guo, X.; Zhang, X.; Zhao, W.; Zhong, L.; Zhou, J.; Xi, Y.; Lin, Z., Ding, J., *Anti-Cancer Drugs* **2005**, *16*, 515.
(75) Chen, Y.; Miao, Z.; Zhao, W., Ding, J., *FEBS Lett.* **2005**, *579*, 3683.

(76) Chen, Y.; Zhang, Y.; Li, M.; Zhao, W.; Shi, Y.; Miao, Z.; Zhang, X.; Lin, L., Ding, J., *Biochem. Biophys. Res. Commun.* **2005**, *329*, 1334.
(77) Zheng, L., *J. Natl. Cancer Inst. Monogr.* **2017**, *109*, djw304.
(78) Brahmer , J.; Tykodi , S.; Chow , L.; Hwu , W.-J.; Topalian , S.; Hwu , P.; Drake , C.; Camacho , L.; Kauh , J.; Odunsi , K.; Pitot , H.; Hamid , O.; Bhatia , S.; Martins , R.; Eaton , K.; Chen , S.; Salay , T.; Alaparthy , S.; Grosso , J.; Korman , A.; Parker , S.; Agrawal , S.; Goldberg , S.; Pardoll , D.; Gupta , A., Wigginton , J., *N. Engl. J. Med.* **2012**, *366*, 2455.
(79) Siegel, R. L.; Miller, K. D., Jemal, A., *Ca-Cancer J. Clin.* **2016**, *66*, 7.
(80) Orjala, J.; Oberlies, N. H.; Pearce, C. J.; Swanson, S. M., Kinghorn, A. D.,Bioactive Compounds from Natural Sources, Second Edition; CRC Press, **2011**, p. 37.
(81) Koncz, G.; Hancz, A.; Chakrabandhu, K.; Gogolák, P.; Kerekes, K.; Rajnavölgyi, É., Hueber, A.-O., *J. Immunol.* **2012**, *189*, 2815.
(82) Bennett, J. W., Ciegler, A., M. Dekker, New York, **1983**, p. xii- 478.
(83) Bunch, A. W., Harris, R. E., *Biotechnol. Genet. Eng. Rev.* **1986**, *4*, 117.
(84) Meletiadis, J.; Meis, J. F.; Mouton, J. W., Verweij, P. E., *J. Clin. Microbiol.* **2001**, *39*, 478.
(85) Lilly, V. G., Barnett, H. L., 1 ed., McGraw-Hill Book Company, Inc., New York, **1951**, p. xii - 464
(86) Hewage, R. T.; Aree, T.; Mahidol, C.; Ruchirawat, S., Kittakoop, P., *Phytochemistry* **2014**, *108*, 87.
(87) Hemphill, C. F. P.; Sureechatchaiyan, P.; Kassack, M. U.; Orfali, R. S.; Lin, W.; Daletos, G., Proksch, P., *J. Antibiot.* **2017**, *70*, 726.
(88) Kertesz, V.; Weiskittel, T. M., Van Berkel, G. J., *Anal. Bioanal. Chem.* **2015**, *407*, 2117.
(89) Sica, V. P.; Raja, H. A.; El-Elimat, T.; Kertesz, V.; Van Berkel, G. J.; Pearce, C. J., Oberlies, N. H., *J. Nat. Prod.* **2015**, *78*, 1926.
(90) Paguigan, N. D.; El-Elimat, T.; Kao, D.; Raja, H. A.; Pearce, C. J., Oberlies, N. H., *J. Antibiot.* **2017**, *70*, 553.
(91) El-Elimat, T.; Figueroa, M.; Ehrmann, B. M.; Cech, N. B.; Pearce, C. J., Oberlies, N. H., *J. Nat. Prod.* **2013**, *76*, 1709.
(92) White, T. J.; Bruns, T.; Lee, S. H., Taylor, J. W., Academic Press, San Diego, California, **1990**, p. 315-322.
(93) Gardes, M.; White, T. J.; Fortin, J. A.; Bruns, T. D., Taylor, J. W., *Canadian Journal of Botany* **1991**, *69*, 180.
(94) Raja, H. A.; Miller, A. N.; Pearce, C. J., Oberlies, N. H., *J. Nat. Prod.* **2017**, *80*, 756.
(95) Abreu, L. M.; Moreira, G. M.; Ferreira, D.; Rodrigues-Filho, E., Pfenning, L. H., *Fungal Biol* **2014**, *118*, 1004.
(96) Schroers, H.-J., *Vol. Studies in mycology*, Centraalbureau voor Schimmelcultures, Utrecht, The Netherlands. , **2001**.
(97) Hongsanan, S.; Jeewon, R.; Purahong, W.; Xie, N.; Liu, J.-K.; Jayawardena, R. S.; Ekanayaka, A. H.; Dissanayake, A.; Raspé, O.; Hyde, K. D.; Stadler, M., Peršoh, D., *Fungal Divers.* **2018**, 1.

(98) Moreira, G. M.; Abreu, L. M.; Carvalho, V. G.; Schroers, H.-J., Pfenning, L. H., *Mycol. Prog.* **2016**, *15*, 1031.
(99) Taylor, J. W., *IMA Fungus* **2011**, *2*, 113.
(100) Hawksworth, D. L.; Crous, P. W.; Redhead, S. A.; Reynolds, D. R.; Samson, R. A.; Seifert, K. A.; Taylor, J. W.; Wingfield, M. J.; Abaci, Ö.; Aime, C.; Asan, A.; Bai, F.-Y.; de Beer, Z. W.; Begerow, D.; Berikten, D.; Boekhout, T.; Buchanan, P. K.; Burgess, T.; Buzina, W.; Cai, L.; Cannon, P. F.; Crane, J. L.; Damm, U.; Daniel, H.-M.; van Diepeningen, A. D.; Druzhinina, I.; Dyer, P. S.; Eberhardt, U.; Fell, J. W.; Frisvad, J. C.; Geiser, D. M.; Geml, J.; Glienke, C.; Gräfenhan, T.; Groenewald, J. Z.; Groenewald, M.; de Gruyter, J.; Guého-Kellermann, E.; Guo, L.-D.; Hibbett, D. S.; Hong, S.-B.; de Hoog, G. S.; Houbraken, J.; Huhndorf, S. M.; Hyde, K. D.; Ismail, A.; Johnston, P. R.; Kadaifciler, D. G.; Kirk, P. M.; Kõljalg, U.; Kurtzman, C. P.; Lagneau, P.-E.; Lévesque, C. A.; Liu, X.; Lombard, L.; Meyer, W.; Miller, A.; Minter, D. W.; Najafzadeh, M. J.; Norvell, L.; Ozerskaya, S. M.; Öziç, R.; Pennycook, S. R.; Peterson, S. W.; Pettersson, O. V.; Quaedvlieg, W.; Robert, V. A.; Ruibal, C.; Schnürer, J.; Schroers, H.-J.; Shivas, R.; Slippers, B.; Spierenburg, H.; Takashima, M.; Taşkın, E.; Thines, M.; Thrane, U.; Uztan, A. H.; van Raak, M.; Varga, J.; Vasco, A.; Verkley, G.; Videira, S. I. R.; de Vries, R. P.; Weir, B. S.; Yilmaz, N.; Yurkov, A., Zhang, N., *IMA Fungus* **2011**, *2*, 105.
(101) Rossman, A. Y.; Seifert, K. A.; Samuels, G. J.; Minnis, A. M.; Schroers, H.-J.; Lombard, L.; Crous, P. W.; Põldmaa, K.; Cannon, P. F.; Summerbell, R. C.; Geiser, D. M.; Zhuang, W.-y.; Hirooka, Y.; Herrera, C.; Salgado-Salazar, C., Chaverri, P., *IMA Fungus* **2013**, *4*, 41.
(102) Perdomo, H.; Cano, J.; Gené, J.; García, D.; Hernández, M., Guarro, J., *Mycologia* **2013**, *105*, 151.
(103) Sica, V. P.; Figueroa, M.; Raja, H. A.; El-Elimat, T.; Darveaux, B. A.; Pearce, C. J., Oberlies, N. H., *J. Ind. Microbiol. Biotechnol.* **2016**, *43*, 1149.
(104) Sica, V. P.; Rees, E. R.; Raja, H. A.; Rivera-Chávez, J.; Burdette, J. E.; Pearce, C. J., Oberlies, N. H., *Phytochemistry* **2017**, *143*, 45.
(105) Sica, V. P.; El-Elimat, T., Oberlies, N. H., *Anal. Methods* **2016**, *8*, 6143.
(106) Sica, V. P.; Rees, E. R.; Tchegnon, E.; Bardsley, R. H.; Raja, H. A., Oberlies, N. H., *Front. Microbiol.* **2016**, *7*, DOI: 10.3389/fmicb.2016.00544.
(107) Paguigan, N. D.; Raja, H. A.; Day, C. S., Oberlies, N. H., *Phytochemistry* **2016**, *126*, 59.
(108) Kertesz, V., Van Berkel, G. J., *Anal. Chem.* **2010**, *82*, 5917.
(109) Kertesz, V., Berkel, G. J. V., *Rapid Commun. Mass Spectrom.* **2014**, *28*, 1553.
(110) Khanna, S., Srivastava, A. K., *Process Biochem.* **2005**, *40*, 2173.
(111) Yang, L. H.; Miao, L.; Lee, O. O.; Li, X.; Xiong, H.; Pang, K.; Vrijmoed, L., Qian, P., *Appl. Microbiol. Biotechnol.* **2007**, *74*, 1221.
(112) Fuchser, J., Zeeck, A., *Liebigs Ann.* **1997**, *1997*, 87.
(113) Espeso, E. A.; Tilburn, J.; Arst Jr, H., Penalva, M., *EMBO J.* **1993**, *12*, 3947.
(114) Miao, L.; Kwong, T. F., Qian, P.-Y., *Appl. Microbiol. Biotechnol.* **2006**, *72*, 1063.
(115) Bode, H. B.; Bethe, B.; Höfs, R., Zeeck, A., *ChemBioChem* **2002**, *3*, 619.
(116) Barrios-González, J.; Castillo, T. E., Mejía, A., *Biotechnol Adv.* **1993**, *11*, 525.

(117) Pfefferle, C.; Theobald, U.; Gürtler, H., Fiedler, H.-P., *J. Biotechnol* **2000**, *80*, 135.
(118) Soltero, F. V., Johnson, M. J., *Appl Microbiol.* **1953**, *1*, 52.
(119) Hutwimmer, S.; Wang, H.; Strasser, H., Burgstaller, W., *Mycologia* **2010**, *102*, 1.
(120) Gareis, M., Gareis, E.-M., *Mycopathologia* **2007**, *163*, 207.
(121) Wang, X.; Sena Filho, J. G.; Hoover, A. R.; King, J. B.; Ellis, T. K.; Powell, D. R., Cichewicz, R. H., *J. Nat. Prod.* **2010**, *73*, 942.
(122) Mascarin, G. M.; Jackson, M. A.; Kobori, N. N.; Behle, R. W.; Dunlap, C. A., Júnior, Í. D., *Appl. Microbiol. Biotechnol.* **2015**, *99*, 6653.
(123) Robinson, T.; Singh, D., Nigam, P., *Appl. Microbiol. Biotechnol.* **2001**, *55*, 284.
(124) Elibol, M., Mavituna, F., *Process Biochem.* **1997**, *32*, 417.
(125) Barrios-González, J.; Rodríguez, G. M., Tomasini, A., *J. Ferment. Bioeng.* **1990**, *70*, 329.
(126) Lindenfelser, L., Ciegler, A., *Appl Microbiol.* **1975**, *29*, 323.
(127) Hölker, U., Lenz, J., *Curr. Opin. Microbiol.* **2005**, *8*, 301.
(128) VanderMolen, K. M.; Raja, H. A.; El-Elimat, T., Oberlies, N. H., *AMB Express* **2013**, *3*, 71.
(129) Bills, G. F.; Dombrowski, A. W., Goetz, M. A.,Fungal Secondary Metabolism: Methods and Protocols; Humana Press: New Jersey, **2012**, p. 79.
(130) Hölker, U.; Höfer, M., Lenz, J., *Appl. Microbiol. Biotechnol.* **2004**, *64*, 175.
(131) Yamazaki, T.; Taguchi, T., Ojima, I.,Fluorine in medicinal chemistry and chemical biology; John Wiley & Sons: Wiltshire Great Britain, **2009**, p. 3.
(132) O'Hagan, D., Deng, H., *Chem. Rev.* **2015**, *115*, 634.
(133) Boland, E. W., *Ann. N. Y. Acad. Sci.* **1959**, *82*, 887.
(134) Cohen, S. S.; Flaks, J. G.; Barner, H. D.; Loeb, M. R., Lichtenstein, J., *Proc. Natl. Acad. Sci.* **1958**, *44*, 1004.
(135) Duschinsky, R.; Pleven, E., Heidelberger, C., *J. Am. Chem. Soc.* **1957**, *79*, 4559.
(136) Gillis, E. P.; Eastman, K. J.; Hill, M. D.; Donnelly, D. J., Meanwell, N. A., *J. Med. Chem.* **2015**, *58*, 8315.
(137) Purser, S.; Moore, P. R.; Swallow, S., Gouverneur, V., *Chem. Soc. Rev.* **2008**, *37*, 320.
(138) Müller, K.; Faeh, C., Diederich, F., *Science* **2007**, *317*, 1881.
(139) Meanwell, N. A., *J. Med. Chem.* **2018**, *61*, 5822.
(140) Wang, J.; Sánchez-Roselló, M.; Aceña, J. L.; del Pozo, C.; Sorochinsky, A. E.; Fustero, S.; Soloshonok, V. A., Liu, H., *Chem. Rev.* **2014**, *114*, 2432.
(141) Wong, D. T.; Perry, K. W., Bymaster, F. P., *Nat. Rev. Drug Discovery* **2005**, *4*, 764.
(142) Chin, N.-X., Neu, H. C., *Antimicrob. Agents Chemother.* **1984**, *25*, 319.
(143) Sharma, P. C.; Jain, A.; Jain, S.; Pahwa, R., Yar, M. S., *J. Enzyme Inhib. Med. Chem.* **2010**, *25*, 577.
(144) Kim, D.; Wang, L.; Beconi, M.; Eiermann, G. J.; Fisher, M. H.; He, H.; Hickey, G. J.; Kowalchick, J. E.; Leiting, B.; Lyons, K.; Marsilio, F.; McCann, M. E.; Patel, R. A.; Petrov, A.; Scapin, G.; Patel, S. B.; Roy, R. S.; Wu, J. K.; Wyvratt, M. J.; Zhang, B. B.; Zhu, L.; Thornberry, N. A., Weber, A. E., *J. Med. Chem.* **2005**, *48*, 141.

(145) Zhou, Y.; Wang, J.; Gu, Z.; Wang, S.; Zhu, W.; Aceña, J. L.; Soloshonok, V. A.; Izawa, K., Liu, H., *Chem. Rev.* **2016**, *116*, 422.
(146) Kirk, K. L., *Org. Process Res. Dev.* **2008**, *12*, 305.
(147) Romanov-Michailidis, F.; Guenee, L., Alexakis, A., *Angew. Chem. Int. Ed* **2013**, *125*, 9436.
(148) Halperin, S. D.; Kwon, D.; Holmes, M.; Regalado, E. L.; Campeau, L.-C.; DiRocco, D. A., Britton, R., *Org. Lett.* **2015**, *17*, 5200.
(149) Walker, M. C., Chang, M. C., *Chem. Soc. Rev.* **2014**, *43*, 6527.
(150) Nilanonta, C.; Isaka, M.; Kittakoop, P.; Trakulnaleamsai, S.; Tanticharoen, M., Thebtaranonth, Y., *Tetrahedron* **2002**, *58*, 3355.
(151) Thiericke, R., Rohr, J., *Nat. Prod. Rep.* **1993**, *10*, 265.
(152) Xu, Y.; Zhan, J.; Wijeratne, E. K.; Burns, A. M.; Gunatilaka, A. L., Molnár, I., *J. Nat. Prod.* **2007**, *70*, 1467.
(153) Saverino, D.; Debbia, E. A.; Pesce, A.; Lepore, A. M., Schito, G. C., *J. Antimicrob. Chemother.* **1992**, *30*, 261.
(154) Toscano, L.; Fioriello, G.; Spagnoli, R.; Cappelletti, L., Zanuso, G., *J. Antibiot.* **1983**, *36*, 1439.
(155) Rivera-Chávez, J.; Raja, H. A.; Graf, T. N.; Burdette, J. E.; Pearce, C. J., Oberlies, N. H., *J. Nat. Prod.* **2017**, *80*, 1883.
(156) Süssmuth, R. D., Mainz, A., *Angew. Chem. Int. Ed* **2017**, *56*, 3770.
(157) McAlpine, J. B.; Chen, S.-N.; Kutateladze, A.; MacMillan, J. B.; Appendino, G.; Barison, A.; Beniddir, M. A.; Biavatti, M. W.; Bluml, S.; Boufridi, A.; Butler, M. S.; Capon, R. J.; Choi, Y. H.; Coppage, D.; Crews, P.; Crimmins, M. T.; Csete, M.; Dewapriya, P.; Egan, J. M.; Garson, M. J.; Genta-Jouve, G.; Gerwick, W. H.; Gross, H.; Harper, M. K.; Hermanto, P.; Hook, J. M.; Hunter, L.; Jeannerat, D.; Ji, N.-Y.; Johnson, T. A.; Kingston, D. G. I.; Koshino, H.; Lee, H.-W.; Lewin, G.; Li, J.; Linington, R. G.; Liu, M.; McPhail, K. L.; Molinski, T. F.; Moore, B. S.; Nam, J.-W.; Neupane, R. P.; Niemitz, M.; Nuzillard, J.-M.; Oberlies, N. H.; Ocampos, F. M. M.; Pan, G.; Quinn, R. J.; Reddy, D. S.; Renault, J.-H.; Rivera-Chávez, J.; Robien, W.; Saunders, C. M.; Schmidt, T. J.; Seger, C.; Shen, B.; Steinbeck, C.; Stuppner, H.; Sturm, S.; Taglialatela-Scafati, O.; Tantillo, D. J.; Verpoorte, R.; Wang, B.-G.; Williams, C. M.; Williams, P. G.; Wist, J.; Yue, J.-M.; Zhang, C.; Xu, Z.; Simmler, C.; Lankin, D. C.; Bisson, J., Pauli, G. F., *Nat. Prod. Rep.* **2019**, DOI: 10.1039/C8NP90041H.
(158) Kim, W. E.; Patel, A.; Hur, G. H.; Tufar, P.; Wuo, M. G.; McCammon, J. A., Burkart, M. D., *ChemBioChem* **2019**, *20*, 147.
(159) Tanner, M. E., *Acc. Chem. Res.* **2002**, *35*, 237.
(160) Gu, B.; He, S.; Yan, X., Zhang, L., *Appl. Microbiol. Biotechnol.* **2013**, *97*, 8439.
(161) Guo, C.-J.; Yeh, H.-H.; Chiang, Y.-M.; Sanchez, J. F.; Chang, S.-L.; Bruno, K. S., Wang, C. C. C., *J. Am. Chem. Soc.* **2013**, *135*, 7205.
(162) El-Elimat, T.; Figueroa, M.; Raja, H. A.; Graf, T. N.; Swanson, S. M.; Falkinham III, J. O.; Wani, M. C.; Pearce, C. J., Oberlies, N. H., *Eur. J. Org. Chem* **2015**, *2015*, 109.
(163) El-Elimat, T.; Raja, H. A.; Day, C. S.; Chen, W.-L.; Swanson, S. M., Oberlies, N. H., *J. Nat. Prod.* **2014**, *77*, 2088.

(164) Harrison, C., *Nat. Biotechnol.* **2014**, *32*, 403.
(165) Society, A. C., *Atlanta, Ga: American Cancer Society* **2019**.
(166) Cragg, G. M., Newman, D. J.,Natural Products as Source of Molecules with Therapeutic Potential; Springer, **2018**, p. 309.
(167) Fakhouri, L.; El-Elimat, T.; Hurst, D. P.; Reggio, P. H.; Pearce, C. J.; Oberlies, N. H., Croatt, M. P., *Bioorg. Med. Chem.* **2015**, *23*, 6993.
(168) Altmann, K.-H.; Gaugaz, F. Z., Schiess, R., *Mol. Divers.* **2011**, *15*, 383.
(169) Nicolaou, K.; Pfefferkorn, J.; Roecker, A.; Cao, G.-Q.; Barluenga, S., Mitchell, H., *J. Am. Chem. Soc.* **2000**, *122*, 9939.
(170) Harvey, A. L.; Clark, R. L.; Mackay, S. P., Johnston, B. F., *Expert Opin. Drug Discov.* **2010**, *5*, 559.
(171) Yoshioka, T.; Murakami, K.; Ido, K.; Hanaki, M.; Yamaguchi, K.; Midorikawa, S.; Taniwaki, S.; Gunji, H., Irie, K., *J. Nat. Prod.* **2016**, *79*, 2521.
(172) Bian, L.; Cao, S.; Cheng, L.; Nakazaki, A.; Nishikawa, T., Qi, J., *ChemMedChem* **2018**, *13*, 1972.
(173) Xu, H.; Wang, J.; Sun, H.; Lv, M.; Tian, X.; Yao, X., Zhang, X., *J. Agric. Food Chem.* **2009**, *57*, 7919.
(174) Lee, R. E.; Hurdle, J. G.; Liu, J.; Bruhn, D. F.; Matt, T.; Scherman, M. S.; Vaddady, P. K.; Zheng, Z.; Qi, J., Akbergenov, R., *Nat. Med.* **2014**, *20*, 152.
(175) Patridge, E.; Gareiss, P.; Kinch, M. S., Hoyer, D., *Drug Discov. Today* **2016**, *21*, 204.
(176) Newman, D. J., *Pharmacol. Ther.* **2016**, *162*, 1.
(177) Kung, S. H.; Lund, S.; Murarka, A.; McPhee, D., Paddon, C. J., *Front. Plant Sci.* **2018**, *9*, 87.
(178) McElroy, C., Jennewein, S.,Biotechnology of Natural Products; Springer, **2018**, p. 145.
(179) Oberlies, N. H., Kroll, D. J., *J. Nat. Prod.* **2004**, *67*, 129.
(180) Ringel, I., Horwitz, S. B., *J. Natl. Cancer Inst. Monogr.* **1991**, *83*, 288.
(181) Guenard, D.; Gueritte-Voegelein, F., Potier, P., *Acc. Chem. Res.* **1993**, *26*, 160.
(182) Wani, M. C.; Taylor, H. L.; Wall, M. E.; Coggon, P., McPhail, A. T., *J. Am. Chem. Soc.* **1971**, *93*, 2325.
(183) Commercon, A.; Bezard, D.; Bernard, F., Bourzat, J., *Tetrahedron Lett.* **1992**, *33*, 5185.
(184) Greenwald, R. B.; Pendri, A., Bolikal, D., *J. Org. Chem.* **1995**, *60*, 331.
(185) Mellado, W.; Magri, N. F.; Kingston, D. G.; Garcia-Arenas, R.; Orr, G. A., Horwitz, S. B., *Biochem. Biophys. Res. Commun.* **1984**, *124*, 329.
(186) Magri, N. F., Kingston, D. G., *J. Nat. Prod.* **1988**, *51*, 298.
(187) Vyas, D. M.; Wong, H.; Crosswell, A. R.; Casazza, A. M.; Knipe, J. O.; Mamber, S. W., Doyle, T. W., *Bioorg. Med. Chem. Lett.* **1993**, *3*, 1357.
(188) Wall, M. E.; Wani, M.; Cook, C.; Palmer, K. H.; McPhail, A. a., Sim, G., *J. Am. Chem. Soc.* **1966**, *88*, 3888.
(189) O'Leary, J., Muggia, F., *Eur. J. Cancer* **1998**, *34*, 1500.

(190) Tsuruo, T.; Matsuzaki, T.; Matsushita, M.; Saito, H., Yokokura, T., *Cancer Chemother. Pharmacol* **1988**, *21*, 71.
(191) Kawato, Y.; Furuta, T.; Aonuma, M.; Yasuoka, M.; Yokokura, T., Matsumoto, K., *Cancer Chemother. Pharmacol* **1991**, *28*, 192.
(192) *Oncology (Williston Park, N.Y.)* **2000**, *14*, 652.
(193) Kingsbury, W. D.; Boehm, J. C.; Jakas, D. R.; Holden, K. G.; Hecht, S. M.; Gallagher, G.; Caranfa, M. J.; McCabe, F. L.; Faucette, L. F., Johnson, R. K., *J. Med. Chem.* **1991**, *34*, 98.
(194) Takimoto, C. H., Arbuck, S. G., *Oncology* **1997**, *11*, 1635.
(195) Ulukan, H., Swaan, P. W., *Drugs* **2002**, *62*, 2039.
(196) Walko, C. M., Lindley, C., *Clin. Ther.* **2005**, *27*, 23.
(197) Puhalla, S., Brufsky, A., *Biol.: Targets Ther.* **2008**, *2*, 505.
(198) Fumoleau, P.; Coudert, B.; Isambert, N., Ferrant, E., *Ann. Oncol.* **2007**, *18*, v9.
(199) Rannard, S. P., Davis, N. J., *Org. Lett.* **2000**, *2*, 2117.
(200) Siegel, R. L.; Miller, K. D., Jemal, A., *Ca-Cancer J. Clin.* **2017**, *67*, 7.
(201) Bowtell, D. D.; Böhm, S.; Ahmed, A. A.; Aspuria, P.-J.; Bast Jr, R. C.; Beral, V.; Berek, J. S.; Birrer, M. J.; Blagden, S., Bookman, M. A., *Nat. Rev. Cancer* **2015**, *15*, 668.
(202) Korkmaz, T.; Seber, S., Basaran, G., *Crit Rev Oncol Hematol.* **2016**, *98*, 180.
(203) Bitler, B. G.; Watson, Z. L.; Wheeler, L. J., Behbakht, K., *Gynecol Oncol.* **2017**, *147*, 695.
(204) Herzog, T. J., Monk, B. J., *Gynecol Oncol Res Pract.* **2017**, *4*, 13.
(205) Moses, M., A.; Brem, H., Langer, R., *Cancer Cell* **2003**, *4*, 337.
(206) Shukla, S., Steinmetz, N. F., *Experimental Biology and Medicine* **2016**, *241*, 1116.
(207) Farokhzad, O. C., Langer, R., *Advanced Drug Delivery Reviews* **2006**, *58*, 1456.
(208) Colby, A. H.; Colson, Y. L., Grinstaff, M. W., *Nanoscale* **2013**, *5*, 3496.
(209) Liu, R.; Colby, A. H.; Gilmore, D.; Schulz, M.; Zeng, J.; Padera, R. F.; Shirihai, O.; Grinstaff, M. W., Colson, Y. L., *Biomaterials* **2016**, *102*, 175.
(210) Zubris, K. A. V.; Liu, R.; Colby, A.; Schulz, M. D.; Colson, Y. L., Grinstaff, M. W., *Biomacromolecules* **2013**, *14*, 2074.
(211) Colby, A. H.; Oberlies, N. H.; Pearce, C. J.; Herrera, V. L.; Colson, Y. L., Grinstaff, M. W., *Wiley Interdiscip Rev Nanomed Nanobiotechnol* **2017**, *9*, e1451.
(212) Lewellen, K. A.; Metzinger, M. N.; Liu, Y., Stack, M. S., *J. Vis. Exp.* **2016**, e53316.
(213) Colby, A. H.; Berry, S. M.; Moran, A. M.; Pasion, K. A.; Liu, R.; Colson, Y. L.; Ruiz-Opazo, N.; Grinstaff, M. W., Herrera, V. L., *ACS Nano* **2017**, *11*, 1466.
(214) Herrera, V. L.; Colby, A. H.; Tan, G. A.; Moran, A. M.; O'Brien, M. J.; Colson, Y. L.; Ruiz-Opazo, N., Grinstaff, M. W., *Nanomedicine* **2016**, *11*, 1001.
(215) Gilmore, D.; Schulz, M.; Liu, R.; Zubris, K. A. V.; Padera, R. F.; Catalano, P. J.; Grinstaff, M. W., Colson, Y. L., *Ann. Surg. Oncol.* **2013**, *20*, 1684.
(216) Weaver, B. A., *Mol. Biol. Cell* **2014**, *25*, 2677.
(217) Goldhirsch, A.; Francis, P.; Castiglione-Gertsch, M.; Gelber, R. D., Coates, A. S., *Lancet* **2000**, *356*, 507.
(218) Tuma, R. S., *Oncology Times* **2003**, *25*, 52.

(219) Griset, A. P.; Walpole, J.; Liu, R.; Gaffey, A.; Colson, Y. L., Grinstaff, M. W., *J. Am. Chem. Soc.* **2009**, *131*, 2469.
(220) Dias, D. A.; Urban, S., Roessner, U., *Metabolites* **2012**, *2*, 303.
(221) Schmidt, B.; Ribnicky, D. M.; Poulev, A.; Logendra, S.; Cefalu, W. T., Raskin, I., *Metabolism* **2008**, *57*, S3.
(222) Jones, W. P., Kinghorn, A. D.,Natural products isolation; Springer, **2006**, p. 323.
(223) Hewage, R. T.; Aree, T.; Mahidol, C.; Ruchirawat, S., Kittakoop, P., *Phytochemistry* **2014**, *108*, 87.
(224) Hemphill, C. F. P.; Sureechatchaiyan, P.; Kassack, M. U.; Orfali, R. S.; Lin, W.; Daletos, G., Proksch, P., *J. Antibiot.* **2017**, *70*, 726.
(225) Gerwick, B. C.; Brewster, W. K.; Fields, S. C.; Graupner, P. R.; Hahn, D. R.; Pearce, C. J.; Schmitzer, P. R., Webster, J. D., *J. Chem. Ecol.* **2013**, *39*, 253.
(226) Gerwick III, B. C.; Graupner, P. R.; Fields, S. C.; Schmitzer, P. R., Brewster, W. K., Google Patents, USA, **2008**, p. 12.
(227) Sica, V. P.; Figueroa, M.; Raja, H. A.; El-Elimat, T.; Darveaux, B. A.; Pearce, C. J., Oberlies, N. H., *J. Ind. Microbiol. Biotechnol.* **2016**, *43*, 1149.
(228) Paguigan, N. D.; Raja, H. A.; Day, C. S., Oberlies, N. H., *Phytochemistry* **2016**, *126*, 59.
(229) Raja, H. A.; Paguigan, N. D.; Fournier, J., Oberlies, N. H., *Mycol. Prog.* **2017**, *16*, 535.
(230) Koulman, A.; Lane, G. A.; Christensen, M. J.; Fraser, K., Tapper, B. A., *Phytochemistry* **2007**, *68*, 355.
(231) Wang, X.; Sena Filho, J. G.; Hoover, A. R.; King, J. B.; Ellis, T. K.; Powell, D. R., Cichewicz, R. H., *J. Nat. Prod.* **2010**, *73*, 942.
(232) Gardes, M., Bruns, T. D., *Mol. Ecol.* **1993**, *2*, 113.
(233) Amrine, C. S. M.; Raja, H. A.; Darveaux, B. A.; Pearce, C. J., Oberlies, N. H., *J. Ind. Microbiol. Biotechnol.* **2018**, *45*, 1053.
(234) Katagiri, K.; Sato, K.; Hayakawa, S.; Matsushima, T., Minato, H., *J. Antibiot.* **1970**, *23*, 420.
(235) Kim, J.; Ashenhurst, J. A., Movassaghi, M., *Science* **2009**, *324*, 238.
(236) Figueroa, M.; Graf, T. N.; Ayers, S.; Adcock, A. F.; Kroll, D. J.; Yang, J.; Swanson, S. M.; Munoz-Acuna, U.; De Blanco, E. J. C., Agrawal, R., *J. Antibiot.* **2012**, *65*, 559.
(237) Liu, F.; Liu, Q.; Yang, D.; Bollag, W. B.; Robertson, K.; Wu, P., Liu, K., *Cancer Res.* **2011**.
(238) Lu, C.; Yang, D.; Sabbatini, M. E.; Colby, A. H.; Grinstaff, M. W.; Oberlies, N. H.; Pearce, C., Liu, K., *BMC cancer* **2018**, *18*, 149.
(239) Lu, C.; Paschall, A. V.; Shi, H.; Savage, N.; Waller, J. L.; Sabbatini, M. E.; Oberlies, N. H.; Pearce, C., Liu, K., *J. Natl. Cancer Inst.* **2017**, *109*.
(240) Paschall, A. V.; Yang, D.; Lu, C.; Choi, J.-H.; Li, X.; Liu, F.; Figueroa, M.; Oberlies, N. H.; Pearce, C., Bollag, W. B., *J. Immunol.* **2015**, *195*, 1868.
(241) Zewdu, A.; Lopez, G.; Braggio, D.; Kenny, C.; Constantino, D.; Bid, H.; Batte, K.; Iwenofu, O.; Oberlies, N., Pearce, C., *Clin. Exp. Pharmacol.* **2016**, *6*, 221.
(242) Cooks, R. G.; Ouyang, Z.; Takats, Z., Wiseman, J. M., *Science* **2006**, *311*, 1566.

(243) VanderMolen, K. M.; Darveaux, B. A.; Chen, W.-L.; Swanson, S. M.; Pearce, C. J., Oberlies, N. H., *RSC Adv.* **2014**, *4*, 18329.
(244) Bills, G. F.; Platas, G.; Fillola, A.; Jiménez, M. R.; Collado, J.; Vicente, F.; Martín, J.; González, A.; Bur-Zimmermann, J.; Tormo, J. R., Peláez, F., *J. Appl. Microbiol.* **2008**, *104*, 1644.
(245) Wei, H.; Lin, Z.; Li, D.; Gu, Q., Zhu, T., *Acta Microbiol. Sin.* **2010**, *50*, 701.
(246) Kuhnert, E.; Heitkämper, S.; Fournier, J.; Surup, F., Stadler, M., *Fungal Biol.* **2014**, *118*, 242.
(247) Stadler, M., *Cur. Res. Env. App. Microbiol.* **2011**, *1*, 75.
(248) Figueroa, M.; Jarmusch, A. K.; Raja, H. A.; El-Elimat, T.; Kavanaugh, J. S.; Horswill, A. R.; Cooks, R. G.; Cech, N. B., Oberlies, N. H., *J. Nat. Prod.* **2014**, *77*, 1351.

APPENDIX A

SUPPLEMENTARY TABLES

Table S1. Composition of the Various Agar Media Evaluated in the Current Study.

Table S2. Verticillin Analogues Observed via LC-HRMS Dereplication in a Panel of Fungal Strains from the Mycosynthetix Library (MSX).

Table S3. ^{1}H and ^{13}C NMR Data for Verticillin H (**1**) in $CDCl_3$.

Table S4. ^{1}H and ^{13}C NMR Data for Sch 52901 (**2**) in $CDCl_3$.

Table S5. ^{1}H and ^{13}C NMR Data for Verticillin A (**3**) in $CDCl_3$.

Table S6. ^{1}H, ^{13}C and HMBC NMR Data for 9-F-Verticillin H (**4**) in $CDCl_3$.

Table S7. ^{1}H, ^{13}C and HMBC NMR Data for 9-F-Sch 52901 (**5**) in $CDCl_3$.

Table S8. ^{1}H, ^{13}C and HMBC NMR Data for 9′-F-Sch 52901 (**6**) in $CDCl_3$.

Table S9. ^{1}H, ^{13}C and HMBC NMR Data for 9-F-Verticillin A (**7**) in $CDCl_3$.

Table S10. ^{1}H, ^{13}C and HMBC NMR Data for 9,9′-di F-Verticillin A (**8**) in $CDCl_3$.

Table S11. ^{1}H and HMBC NMR Data for 9,9′-di F-Verticillin H (**9**) in $CDCl_3$.

Table S12. ^{1}H and HMBC NMR Data for 9,9′-di F- Sch 52901 (**10**) in $CDCl_3$.

Table S1. Composition of the Various Agar Media Evaluated in the Current Study.

Name	Abbreviation	Composition per 1000 mL Deionized water (DI-H_2O)
Malt extract agar	**MEA**	12.75 g maltose, 2.75 g dextrin, 2.35 g glycerol, 0.78 g gelatin peptone, 15.0 g agar.
Potato dextrose agar	**PDA**	4 g potato starch, 20 g dextrose, 15 g agar.
Yeast extract dextrose agar	**YESDA**	10 g yeast extract, 20 g soy peptone, 20 g dextrose, 15 g agar.
Spezieller Nahrstoffarmer agar	**SNA**	1 g KH_2PO_4, 1 g KNO_3, 0.5 g $MgSO_4.7H_2O$, 0.5 g KCl, 0.2 g glucose, 0.2 g sucrose, 20 g agar.
Sabouraud dextrose agar	**SDA**	5 g peptic digest of animal tissue, 5 g pancreatic digest of casein, 20 g dextrose, 15 g agar.
Potato dextrose-mushroom	**PD-mushroom**	4 g potato starch, 20 g dextrose, 15 g agar, sterilized pieces of *Leucoagaricus* sp. mushroom.
Oatmeal agar	**Oat-A**	60 g oatmeal, 12.5 g agar.

Table S2. Verticillin Analogues Observed via LC-HRMS Dereplication in a Panel of Fungal Strains from the Mycosynthetix Library (MSX), all of which were grown on a rice based medium. Strains MSX59553 and MSX79542 were chosen for further optimization due to their biosynthetic potential to yield a wide variety of desirable analogues.

Strain ID	Verticillin analogues matched via LC-HRMS dereplication
MSX74391	Sch52900, Gliocladicillin A, Verticillin A, Verticillin H, Sch52901
MSX71844	Verticillin A, Sch52900
MSX58124	Verticillin H, Sch52901, Gliocladicillin C, Sch52900
MSX75296	Verticillin D
MSX75281	Verticillin D
MSX45374	11-Deoxyverticillin A, Gliocladicillin, Verticillin H, Sch52901, Gliocladicillin C, Sch52900
MSX70777	11-Deoxyverticillin A, Sch52900, Sch52901, Verticillin A, Gliocladicillin A, Gliocladicillin C
MSX59553	Verticillin A, Verticillin H, 11-Deoxyverticillin A, Gliocladicillin C, Sch52900, Sch52901
MSX79542	Verticillin A, Verticillin H, 11-Deoxyverticillin A, Gliocladicillin C, Sch52900, Sch52901

.

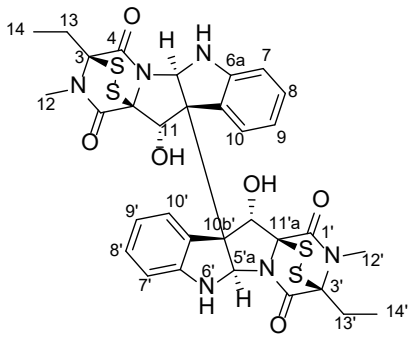

Table S3. **^{1}H and ^{13}C NMR Data for Verticillin H (1) in $CDCl_3$.** [500 MHz for ^{1}H and 125 MHz for ^{13}C].

Position	δ_C	δ_H, mult (*J* in Hz)
1, 1′	167.4	-
3, 3′	77.5	-
4, 4′	161.6	-
5a, 5a′	82.1	5.73, s
6a, 6a′	148.9	-
7, 7′	110.9	6.64, dd (7.8, 0.9)
8, 8′	130.1	7.14, td (7.8, 1.1)
9, 9′	120.6	6.83, td (7.8, 0.9)
10, 10′	128.3	7.84, dd (7.8, 1.1)
10a, 10a′	129.5	-
10b, 10b′	65.8	-
11, 11′	83.3	5.14, s
11a, 11a′	76.9	-
12, 12′	28.1	3.01, s
13, 13′	24.7	2.16, m 2.37, m
14, 14′	9.9	1.21, t (7.2)
6-NH, 6′-NH	-	5.57, s

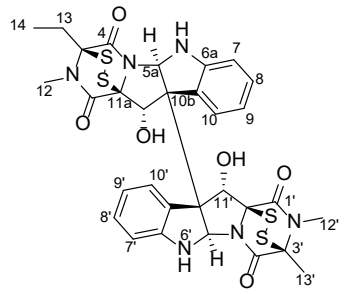

Table S4. ^{1}H and ^{13}C NMR Data for Sch 52901 (2) in $CDCl_3$. [500 MHz for ^{1}H and 125 MHz for ^{13}C].

Position	δ_C	δ_H, mult (*J* in Hz)	Position	δ_C	δ_H, mult (*J* in Hz)
1	162.5[a]	-	1′	161.5[a]	-
3	77.5[a]	-	3′	76.6[a]	-
4	167.3[a]	-	4′	166.3[a]	-
5a	82.1	5.73, s	5a′	82.1	5.73, s
6a	148.8	-	6a′	148.8	-
7	111.0	6.65, dd (7.6, 1.0)	7′	111.0	6.65, dd (7.3, 1.0)
8	128.3	7.15, ddd (7.6, 7.4, 1.1)	8′	128.3	7.13, ddd (7.6, 7.3, 1.1)
9	120.6	6.84, ddd (7.8, 7.4, 1.0)	9′	120.6	6.81, ddd (7.8, 7.6, 1.0)
10	129.5	7.84, dd (7.8, 1.1)	10′	129.5	7.82, dd (7.8, 1.1)
10a	130.1	-	10a′	130.1	-
10b	66.0[a]	-	10b′	65.8[a]	-
11	83.3[a]	5.15, s	11′	83.1	5.15, s
11a	73.0	-	11a′	73.0[a]	-
12	28.1[a]	3.01[a], s	12′	27.3[a]	2.99[a], s
13	17.6	2.16, m 2.36, m	13′	24.7	1.89, s
14	9.9	1.22, t (7.1)	-	-	-
6-NH	-	5.09[b], s	6′-NH	-	5.14[b], s
11-OH	-	5.56[b], s	11′-OH	-	5.67[b], s

[a, b] The assignments may be interchangeable.

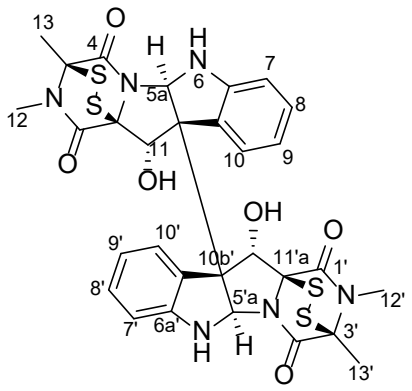

Table S5. ^{1}H and ^{13}C NMR Data for Verticillin A (3) in $CDCl_3$. [500 MHz for ^{1}H and 125 MHz for ^{13}C].

Position	δ_C	δ_H, mult (*J* in Hz)
1, 1′	162.5	-
3, 3′	76.6	-
4, 4′	166.3	-
5a, 5a′	82.1	5.72, s
6a, 6a′	148.8	-
7, 7′	111.0	6.66, dd (7.8, 0.9)
8, 8′	128.3	7.14, td (7.8, 1.1)
9, 9′	120.6	6.82, td (7.8, 0.9)
10, 10′	130.1	7.83, dd (7.8, 1.1)
10a, 10a′	129.5	-
10b, 10b′	66.0	-
11, 11′	83.1	5.14, s
11a, 11a′	73.0	-
12, 12′	27.3	2.99, s
13, 13′	17.6	1.89, s
6-NH, 6′-NH	-	5.09[a], s
11-OH, 11′-OH	-	5.66[a], s

[a] The assignments may be interchangeable.

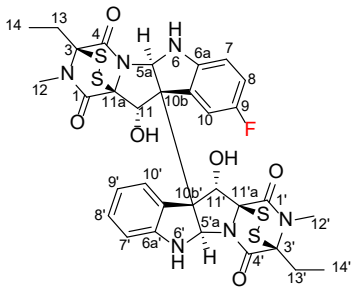

Table S6. **^{1}H, ^{13}C and HMBC NMR Data for 9-F-Verticillin H (4) in $CDCl_3$.** [700 MHz for ^{1}H and 175 MHz for ^{13}C].

Position	δ_C, mult (*J* in Hz)	δ_H, mult (*J* in Hz)	HMBC (^{1}H→^{13}C)	Position	δ_C, mult	δ_H, mult (*J* in Hz)	HMBC (^{1}H→^{13}C)
1	167.1	-		1′	167.1	-	
3	77.4[a]	-		3′	77.5[a]	-	
4	161.4	-		4′	161.4	-	
5a	82.0	5.68, s	4, 10a, 10b, 11, 11a	5a′	81.9	5.70, s	4′, 10a′, 10b′, 11′, 11a′
6a	144.9, d (1.3)	-		6a′	148.8	-	
7	111.1, d (8.5)	6.58, dd (8.6, 4.4)	9, 10a	7′	110.8	6.65, dd (7.6, 1.0)	9′, 10a′
8	116.6, d (24.5)	6.86, td (8.6, 2.7)	6a, 9, 10	8′	130.1	7.15, td (7.6, 1.2)	6a′, 10′
9	157.6, d (235.6)	-		9′	120.5	6.83, td (7.6, 1.0)	7′, 10a′
10	115.5, d (25.4)	7.63, dd (9.4, 2.7)	6a, 8, 9, 10a, 10b	10′	128.2	7.83, dd (7.6, 1.2)	6a′, 8′, 10b′
10a	130.8, d (8.5)	-		10a′	128.9	-	
10b	65.9, d (1.9)	-		10b′	65.5	-	
11	83.8	5.16, s	6a, 10a, 11a	11′	83.0	5.14, s	6a′, 11a′
11a	76.6	-		11a′	76.7	-	
12	28.0	3.02[a], s	1, 3	12′	28.0	3.03[a], s	1′, 3′
13	24.6[a]	2.17, m, 2.38, m	3, 4, 14	13′	24.5[a]	2.17, m, 2.38, m	3′, 4′, 14′
14	9.9[a]	1.25[b], t (7.2)	3, 13	14′	9.8[a]	1.22[b], t (7.2)	3′,13′
6-NH	-	5.05, s	6a, 7, 10a, 10b	6′-NH	-	5.15, s	6a′, 7′, 10a′, 10b′
11-OH	-	5.59, s	10a, 10b, 11a	11′-OH	-	5.64, s	10a′, 10b′, 11a′

[a, b] The assignments may be interchangeable.

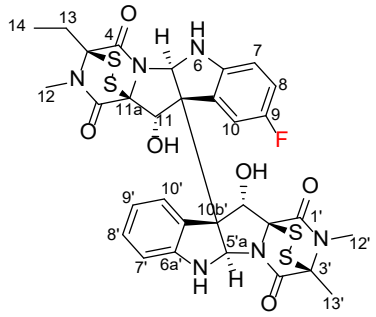

Table S7. ^{1}H, ^{13}C and HMBC NMR Data for 9-F-Sch 52901 (5) in $CDCl_3$. [700 MHz for ^{1}H and 175 MHz for ^{13}C].

Position	δ_C, mult (*J* in Hz)	δ_H, mult (*J* in Hz)	HMBC (^{1}H → ^{13}C)	Position	δ_C,	δ_H, mult (*J* in Hz)	HMBC (^{1}H → ^{13}C)
1	167.1	-		1′	166.1	-	
3	77.5	-		3′	72.9	-	
4	161.4	-		4′	162.3	-	
5a	82.0	5.67, s	4, 10a, 10b, 11, 11a	5a′	81.9	5.70, s	4′, 10a′, 10b ′, 11′, 11a′
6a	144.9, d (1.1)	-		6a′	148.7	-	
7	111.1, d (8.5)	6.58, dd (8.6, 4.4)	9, 10a	7′	110.8	6.66, dd (7.7, 1.0)	9′, 10a′
8	116.6, d (23.6)	6.86, td (8.6, 2.7)	6a, 9, 10	8′	130.2	7.15, td (7.7, 1.2)	6a′, 10′
9	157.6, d (236.3)	-		9′	120.5	6.84, td (7.7, 1.0)	7′, 10a′
10	115.5, d (25.7)	7.61, dd (9.4, 2.7)	6a, 8, 9, 10a, 10b	10′	128.3	7.84, dd (7.7, 1.2)	6a′, 8′, 10b′
10a	130.8, d (8.6)	-		10a′	128.9	-	
10b	65.9, d (1.9)	-		10b′	65.6	-	
11	83.7	5.15, s	6a, 10a, 10b, 11a	11′	82.8	5.13, s	6a′, 10a′, 10b′, 11a′
11a	76.6	-		11a′	76.4	-	
12	28.0	3.02, s 3.01, s	1, 3	12′	27.2	3.01, s	1′, 3′
13	24.5	2.17, m 2.37, m	3, 4, 14	13′	17.5	1.90, s	3′, 4′
14	9.8	1.22, t (7.2)	3, 13				
6-NH	-	5.05, s	5a, 6a, 7, 10a, 10b	6′-NH	-	5.10, s	5a′, 7′, 10b′
11-OH	-	5.59, s	5a, 10b, 11a	11′-OH	-	5.74, s	5a′, 10b′, 11a′

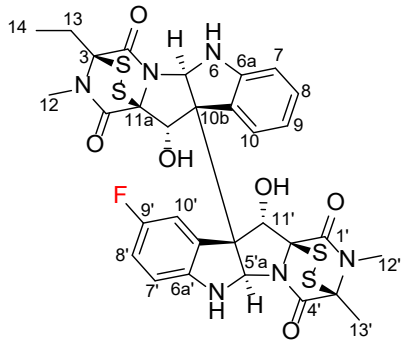

Table S8. ^{1}H, ^{13}C and HMBC NMR Data for 9′-F-Sch 52901 (6) in $CDCl_3$. [700 MHz for ^{1}H and 175 MHz for ^{13}C].

Position	δ_C,	δ_H, mult (*J* in Hz)	HMBC ($^{1}H \rightarrow ^{13}C$)	Position	δ_C, mult (*J* in Hz)	δ_H, mult (*J* in Hz)	HMBC ($^{1}H \rightarrow ^{13}C$)
1	167.1	-		1′	166.1	-	
3	77.4	-		3′	73.0	-	
4	161.4	-		4′	162.3	-	
5a	81.9	5.70, s	10a, 10b, 11	5a′	82.0	5.68, s	10a′, 10b′, 11′
6a	148.7	-		6a′	144.8, d (1.4)	-	
7	110.8	6.65, dd (7.7, 1.0)	9, 10a	7′	111.2, d (8.5)	6.58, dd (4.4, 8.6)	9′, 10a′
8	130.1	7.13, td (7.7, 1.3)	6a, 10	8′	116.6, d (23.8)	6.87, td (8.6, 2.7)	6a′, 9′,10′
9	120.5	6.81, td (7.7, 1.0)	10a	9′	157.6, d (236.0)	-	
10	128.2	7.81, dd (7.7, 1.3)	6a, 8, 10a, 10b	10′	115.6, d (25.5)	7.64, dd (9.4, 2.7)	6a′, 8′, 9′, 10a′, 10b′
10a	128.9	-		10a′	130.8, d (8.6)	-	
10b	65.6	-		10b′	66.0 d (1.9)	-	
11	83.0	5.15, s	6a, 10a, 11a	11′	83.6	5.13, s	6a′, 10a′, 11a′
11a	76.7	-		11a′	76.3	-	
12	28.0	3.03, s	1, 3	12′	27.2	2.99, s	1′, 3′
13	24.6	2.18, m 2.39, m	3, 4	13′	17.5	1.89, s	3′, 4′
14	9.8	1.25, t (7.2)	3				
6-NH	-	5.15, s	10a, 10b	6′-NH	-	4.99, s	10a′, 10b′
11-OH	-	5.63, s	10b, 11, 11a	11′-OH	-	5.70, s	10b′, 11′, 11a′

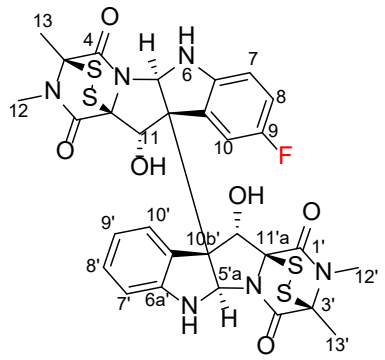

Table S9. ^{1}H, ^{13}C and HMBC NMR Data for 9-F-Verticillin A (7) in $CDCl_3$. [700 MHz for ^{1}H and 175 MHz for ^{13}C].

Position	δ_C, mult (*J* in Hz)	δ_H, mult (*J* in Hz)	HMBC ($^{1}H \rightarrow ^{13}C$)	Position	δ_C, mult	δ_H, mult (*J* in Hz)	HMBC ($^{1}H \rightarrow ^{13}C$)
1	166.1	-		1′	166.1	-	
3	73.0[a]	-		3′	72.9[a]	-	
4	162.2	-		4′	162.3	-	
5a	82.0	5.67, s	4, 10a, 10b, 11, 11a	5a′	81.9	5.69, s	4′, 10a′, 10b′, 11′, 11a′
6a	144.8, d (1.2)	-		6a′	148.6	-	
7	111.2, d (8.6)	6.58, dd (8.6, 4.4)	9, 10a	7′	110.8	6.65, dd (7.7, 1.0)	9′, 10a′
8	116.6, d (24.7)	6.86, td (8.6, 2.7)	6a, 9, 10	8′	130.1	7.14, td (7.7, 0.9)	6a′, 10′
9	157.6, d (236.2)	-		9′	120.5	6.82, td (7.7, 1.0)	7′, 10a′
10	115.5, d (25.5)	7.61, dd (9.4, 2.7)	6a, 8, 9, 10b	10′	128.2	7.82, dd (7.7, 0.9)	6a′, 8′, 10b′
10a	130.8, d (8.6)	-		10a′	128.9	-	
10b	66.0, d (1.6)	-		10b′	65.7	-	
11	83.6	5.14, s	6a, 10a, 10b, 11a	11′	82.8	5.12, s	6a′, 10a′, 10b′, 11a′
11a	76.4	-		11a′	76.3	-	
12	27.20[a]	3.01[a], s	1, 3	12′	27.18[a]	2.99[a], s	1′, 3′
13	17.4	1.88, s, 1.90, s	3, 4	13′	17.4	1.88, s, 1.90, s	3′, 4′
6-NH	-	4.99, s	6a, 7, 10a, 10b	6′-NH	-	5.10, s	6a′, 7′, 10a′, 10b′
11-OH	-	5.69, s	10a, 10b	11′-OH	-	5.73, s	10a′, 10b′

[a] The assignments may be interchangeable.

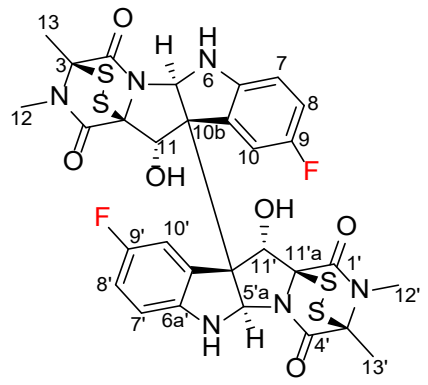

Table S10. **^{1}H, ^{13}C and HMBC NMR Data for 9,9′-di F-Verticillin A (8) in $CDCl_3$.** [700 MHz for ^{1}H and 175 MHz for ^{13}C].

Position	δ_C, mult (*J* in Hz)	δ_H, mult (*J* in Hz)	HMBC (^{1}H→^{13}C)
1, 1′	166.0	-	
3, 3′	73.0	-	
4, 4′	162.3	-	
5a, 5a′	81.9	5.65, s	4, 4′, 10a, 10a′, 10b, 10b′, 11, 11′, 11a, 11a′
6a, 6a′	144.8	-	
7, 7′	111.3, d (8.3)	6.59, dd (8.6, 4.4)	9, 9′, 10a, 10a′
8, 8′	116.7, d (23.9)	6.86, td (8.6, 2.7)	6a, 6a′, 9, 9′, 10, 10′
9, 9′	157.6, d (236.9)	-	
10, 10′	115.6, d (26.6)	7.60, dd (9.4, 2.7)	6a, 6a′, 8, 8′, 9, 9′,10a, 10a′,10b, 10b′
10a, 10a′	130.4, d (8.7)	-	
10b, 10b′	65.8, d (1.6)	-	
11, 11′	83.4	5.13, s	6a, 6a′, 10a, 10a′, 10b, 10b′, 11a, 11a′
11a, 11a′	76.2	-	
12, 12′	27.2	3.01, s	1, 1′, 3, 3′
13, 13′	17.5	1.91, s	3, 3′, 4, 4′
6-NH, 6′-NH	-	5.01, s	5a, 5a′, 10a, 10a′, 10b, 10b′, 11a, 11a′
11-OH, 11′-OH	-	5.76, s	10a, 10a′, 10b, 10b′

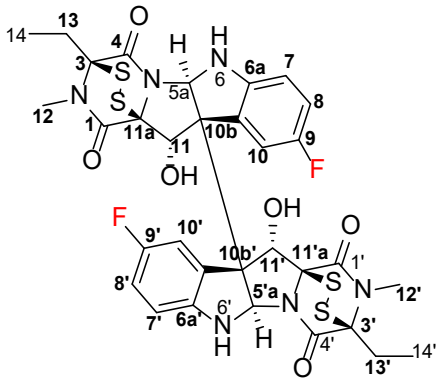

Table S11. **^{1}H and HMBC NMR Data for 9,9′-di F-Verticillin H (9) in $CDCl_3$.** [500 MHz].

Position	δ_H, mult (*J* in Hz)	HMBC (^{1}H → ^{13}C)
1, 1′	-	
3, 3′	-	
4, 4′	-	
5a, 5a′	5.66, s	10a, 10a′, 10b, 10b′, 11, 11′, 11a, 11a′
6a, 6a′	-	
7, 7′	6.59, dd (8.6, 4.4)	9, 9′
8, 8′	6.88, td (8.6, 2.6)	6a, 6a′
9, 9′	-	
10, 10′	7.60, dd (9.4, 2.6)	6a, 6a′
10a, 10a′	-	
10b, 10b′	-	
11, 11′	5.15, s	6a, 6a′, 10a, 10a′, 10b, 10b′, 11a, 11a′
11a, 11a′	-	
12, 12′	3.04, s	1, 1′, 3, 3′
13, 13′	2.19, m, 2.39, m	3, 3′, 4, 4′, 14, 14′
14, 14′	1.26, t (7.1)	3, 3′, 13, 13′
6-NH, 6′-NH	5.66, s	5a, 5a′, 10a, 10a′, 10b, 10b′, 11a, 11a′
11-OH, 11′-OH	5.07, s	10a, 10a′, 10b, 10b′

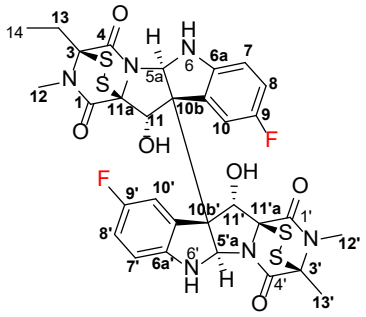

Table S12. **^{1}H and HMBC NMR Data for 9,9′-di F- Sch 52901 (10) in $CDCl_3$.** [500 MHz].

Position	δ_H, mult (*J* in Hz)	HMBC(^{1}H→^{13}C)	Position	δ_H, mult (*J* in Hz)	HMBC(^{1}H→^{13}C)
1	-		1′	-	
3	-		3′	-	
4	-		4′	-	
5a	5.66, s	4, 10a, 10b, 11, 11a	5a′	5.66, s	4′, 10a′, 10b ′, 11′, 11a′
6a	-		6a′	-	
7	6.59, m (8.8, 4.4)	9, 10a	7′	6.59, m (8.8, 4.4)	9′, 10a′
8	6.86[a], td (8.8, 2.8)	6a, 9	8′	6.88[a], td (8.8, 2.8)	6a′, 9′
9	-		9′	-	
10	7.61[b], m (9.4, 2.8)	6a, 9	10′	7.63[b], m (9.4, 2.8)	6a′, 9′
10a	-		10a′	-	
10b	-		10b′	-	
11	5.14[c], s	6a, 10a, 10b, 11a	11′	5.15[c], s	6a′, 10a′, 10b′, 11a′
11a	-		11a′	-	
12	3.02[d], s	1, 3	12′	3.04[d], s	1′, 3′
13	2.19, m, 2.39, m	3, 4, 14	13′	1.91, s	3′, 4′
14	1.26, t (7.0)	3, 13			
6-NH	5.05[e], s,	10a, 10b	6′-NH	5.07[e], s	10a′, 10b′
11-OH	5.66[f], s	5a, 10b, 11a	11′-OH	5.77[f], s	5a′, 10b′, 11a′

[a-f] The assignments may be interchangeable.

APPENDIX B

SUPPLEMENTARY FIGURES

Figure S1. Phylogram of the Most Likely Tree.

Figure S2. *In situ* Microextraction via Droplet Probe Directly from the Surface of Fungal Culture Showing the Spots where the Sampling was Performed.

Figure S3. Photos of the Two Strains MSX59553 (top) and MSX79542 (bottom).

Figure S4. The Amount of the Total Defatted Extracts of Both Strains MSX59553 and MSX79542.

Figure S5. Total Defatted Extracts Weight of Strains MSX59553 and MSX79542.

Figure S6. Full Scan MS Data of Strain MSX59553 Grown on Oatmeal Agar Medium Supplemented with a Racemic Mixture of 5-F-DL-Trp.

Figure S7. Full Scan MS Data of Strain MSX59553 Grown on Oatmeal Agar Medium Supplemented with a Racemic Mixture of 5-F-DL-Trp.

Figure S8. Full Scan MS Data of Strain MSX59553 Grown on Oatmeal Agar Medium Supplemented with a Racemic Mixture of 5-F-DL-Trp.

Figure S9. Culture Conditions for MSX59553 Grown on Oatmeal Agar Medium Supplemented with a Racemic Mixture of 5-F-DL-Trp.

Figure S10. ^{1}H and ^{13}C NMR Spectra of Verticillin H (**1**) in $CDCl_3$.

Figure S11. ^{1}H (upper panel) and ^{13}C (lower panel) NMR Spectra of Sch 52901 (**2**) in $CDCl_3$.

Figure S12. ^{1}H (upper panel) and ^{13}C (lower panel) NMR Spectra of Verticillin A (**3**) in $CDCl_3$.

Figure S13. ^{1}H (upper panel) and ^{13}C (lower panel) NMR Spectra of 9-F-verticillin H (**4**) in $CDCl_3$.

Figure S14. ^{1}H-^{1}H COSY NMR Spectrum of 9-F-verticillin H (**4**) in $CDCl_3$.

Figure S15. ^{1}H-^{13}C HSQC NMR spectrum of 9-F-verticillin H (**4**) in $CDCl_3$.

Figure S16. ^{1}H-^{13}C HMBC NMR Spectrum of 9-F-verticillin H (**4**) in $CDCl_3$.

Figure S17. ^{1}H (upper panel) and ^{19}F (lower panel) NMR Spectra of 9-F-verticillin H (**4**) in $CDCl_3$.

Figure S18. ^{13}C NMR (lower panel) and ^{19}F-^{13}C HMQC NMR Spectra of 9-F-verticillin H (**4**) in $CDCl_3$

Figure S19. ^{1}H (upper panel) and ^{13}C (lower panel) NMR Spectra of 9-F-Sch 52901 (**5**) in $CDCl_3$.

Figure S20. ^{1}H-^{1}H COSY NMR Spectrum of 9-F-Sch 52901 (**5**) in $CDCl_3$.

Figure S21. ^{1}H-^{13}C HSQC NMR Spectrum of 9-F-Sch 52901 (**5**) in $CDCl_3$.

Figure S22. ^{1}H-^{13}C HMBC NMR Spectrum of 9-F-Sch 52901 (**5**) in $CDCl_3$.

Figure S23. ^{1}H (upper panel) and ^{19}F (lower panel) NMR Spectra of 9-F-Sch 52901 (**5**) in $CDCl_3$.

Figure S24. ^{13}C (lower panel) NMR and ^{19}F-^{13}C HMQC NMR Spectra of 9-F-Sch 52901 (**5**) in $CDCl_3$.

Figure S25. Full Scan MS Data of 9-F-Sch 52901 (**5**).

Figure S26. ^{1}H and ^{13}C NMR Spectra of 9′-F-Sch 52901 (**6**) in $CDCl_3$.

Figure S27. ^{1}H-^{1}H COSY NMR Spectrum of 9′-F-Sch 52901 (**6**) in $CDCl_3$.

Figure S28. (^{1}H-^{13}C HSQC NMR Spectrum of 9′-F-Sch 52901 (**6**) in $CDCl_3$.

Figure S29. ^{1}H-^{13}C HMBC NMR Spectrum of 9′-F-Sch 52901 (**6**) in $CDCl_3$.

Figure S30. ^{1}H (upper panel) and ^{19}F (lower panel) NMR Spectra of 9′-F-Sch 52901 (**6**) in $CDCl_3$.

Figure S31. ^{13}C NMR (lower panel) and ^{19}F-^{13}C HMQC NMR Spectra of 9′-F-Sch 52901 (**6**) in $CDCl_3$.

Figure S32. Full Scan MS Data of 9-F-Sch 52901 (**6**).

Figure S33. ^{1}H (upper panel) and ^{13}C (lower panel) NMR Spectra of 9-F-verticillin A (**7**) in $CDCl_3$.

Figure S34. ^{1}H-^{1}H COSY NMR Spectrum of 9-F-verticillin A (**7**) in $CDCl_3$.

Figure S35. ^{1}H-^{13}C HSQC NMR Spectrum of 9-F-verticillin A (**7**) in $CDCl_3$.

Figure S36. ^{1}H-^{13}C HMBC NMR Spectrum of 9-F-verticillin A (**7**) in $CDCl_3$.

Figure S37. ^{1}H (upper panel) and ^{19}F (lower panel) NMR Spectra of 9-F-verticillin A (**7**) in $CDCl_3$.

Figure S38.^{13}C NMR (lower panel) and ^{19}F-^{13}C HMQC NMR Spectra of 9-F-verticillin A (**7**) in $CDCl_3$.

Figure S39. ^{1}H (upper panel) and ^{13}C (lower panel) NMR Spectra of 9,9′-di F-verticillin A (**8**) in $CDCl_3$.

Figure S40. ^{1}H-^{1}H COSY NMR Spectrum of 9,9′-di F-verticillin A (**8**) in $CDCl_3$.

Figure S41. ^{1}H-^{13}C HSQC NMR Spectrum of 9,9′-di F-verticillin A (**8**) in $CDCl_3$.

Figure S42. ^{1}H-^{13}C HMBC NMR Spectrum of 9,9′-di F-verticillin A (**8**) in $CDCl_3$.

Figure S43. ^{1}H (upper panel) and ^{19}F (lower panel) NMR Spectra of 9,9′-di F-verticillin A (**8**) in $CDCl_3$.

Figure S44. ^{1}H NMR Spectrum of 9,9′-di F-verticillin H (**9**) in $CDCl_3$.

Figure S45. ^{1}H-^{13}C HMBC NMR Spectrum of 9,9′-di F-verticillin H (**9**) in $CDCl_3$.

Figure S46. ^{1}H (upper panel) and ^{19}F (lower panel) NMR Spectra of 9,9′-di F-verticillin H (**9**) in $CDCl_3$.

Figure S47. ^{1}H NMR Spectrum of 9,9′-di F-Sch 52901 (**10**) in $CDCl_3$.

Figure S48. ^{1}H-^{13}C HMBC NMR Spectrum of 9,9′-di F-Sch 52901 (**10**) in $CDCl_3$.

Figure S49. ^{1}H (upper panel) and ^{19}F (lower panel) NMR Spectra of 9,9′-di F-Sch 52901 (**10**) in $CDCl_3$.

Figure S50. ^{1}H (upper panel) and ^{13}C (lower panel) NMR Spectra of 5-F-Tryptophan in D_2O.

Figure S51. ^{19}F NMR Spectra of 5-F-Tryptophan in D_2O.

Figure S52. ^{19}F-^{13}C HMQC NMR Spectrum of 5-F-Tryptophan in D_2O.

Figure S53. Full Scan MS Data of Strain MSX59553 Grown on Oatmeal Agar Medium Supplemented with 5-F-D-Trp.

Figure S54. Full Scan MS Data of Strain MSX59553 Grown on Oatmeal Agar Medium Supplemented with 5-F-D-Trp.

Figure S55. Full Scan MS Data of Strain MSX59553 Grown on Oatmeal Agar Medium Supplemented with 5-F-D-Trp.

Figure S56. Full Scan MS Data of Strain MSX59553 Grown on Oatmeal Agar Medium Supplemented with 5-F-L-Trp.

Figure S57. Full Scan MS Data of Strain MSX59553 Grown on Oatmeal Agar Medium Supplemented with 5-F-L-Trp.

Figure S58. Full Scan MS Data of Strain MSX59553 Grown on Oatmeal Agar Medium Supplemented with 5-F-L-Trp.

Figure S59. Relative Production of Fluorinated Verticillin Analogues via UPLC-HRMS Analysis of Extracted Petri Dishes Used Previously for the Droplet Probe Analysis.

Figure S60. ^{1}H (upper panel) and ^{13}C (lower panel) NMR Spectra of **3** in $CDCl_3$.

Figure S61. ^{1}H (upper panel) and ^{13}C (lower panel) NMR Spectra of **4** in $CDCl_3$.

Figure S62. ^{1}H (upper panel) and ^{13}C (lower panel) NMR Spectra of **5** in $CDCl_3$.

Figure S63. ^{1}H (upper panel) and ^{13}C (lower panel) NMR Spectra of **6** in $CDCl_3$.

Figure S64. ^{1}H (upper panel) and ^{13}C (lower panel) NMR Spectra of **7** in $CDCl_3$.

Figure S65. ^{1}H (upper panel) and ^{13}C (lower panel) NMR Spectra of **8** in $CDCl_3$.

Figure S66. ^{1}H (upper panel), ^{13}C (lower panel) NMR Spectra of **9** in $CDCl_3$.

Figure S67. ^{13}C NMR Spectra of **9** in $CDCl_3$ Showing the Split Carbon by the ^{19}F.

Figure S68. ^{19}F NMR Spectrum of **9** in $CDCl_3$.

Figure S69. ^{1}H (upper panel) and ^{13}C (lower panel) NMR Spectra of **10** in $CDCl_3$.

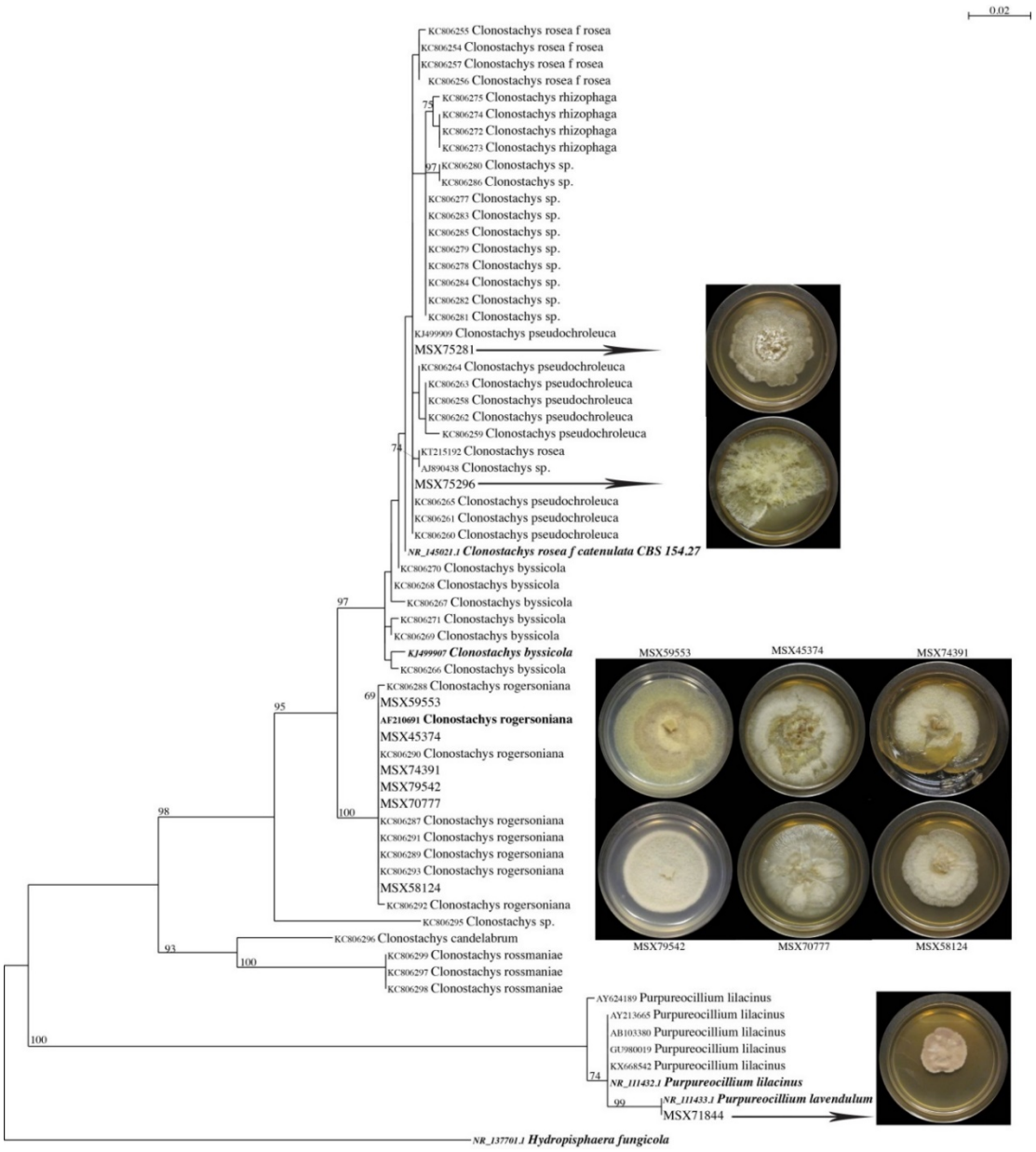

Figure S1. Phylogram of the Most Likely Tree (-lnL = 1766.04) from a RAxML analysis of 67 *Clonostachys* strains based on ITS region (470 bp). Numbers refer to RAxML bootstrap support values ≥ 70% based on 1000 replicates. Type strains are highlighted in bold italics, authentic strains (bold). Three-week old cultures of MSX strains on Potato Dextrose Agar media are shown on right. Eight strains (MSX75281, MSX75296, MSX59553, MSX45374, MSX74391, MSX79542, MSX70777, MSX58124) are identified as members of the genus *Clonostachys,* while one strain MSX71844 is identified as *Purpureocillium lavendulum.* Bar indicates nucleotide substitutions per site.

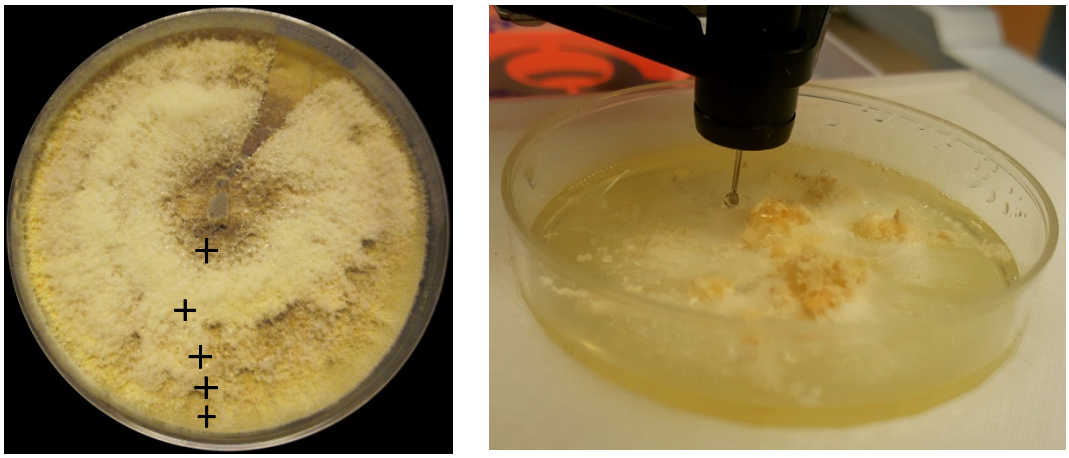

Figure S2. *In situ* Microextraction via Droplet Probe Directly from the Surface of Fungal Culture Showing the Spots where the Sampling was Performed (black crosses, left). From the central spot towards the edge, the fungal colony goes from the oldest to the youngest. The size of the droplet (~3 to 5 µL) is shown in a black circle (right).

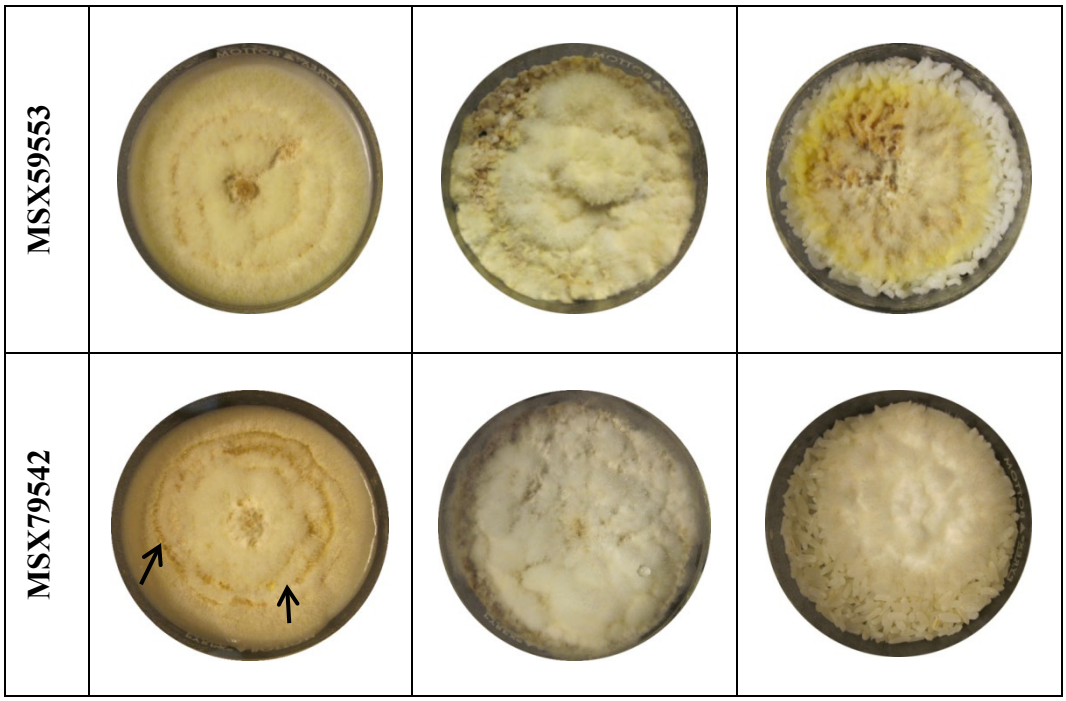

Figure S3. Photos of the Two Strains MSX59553 (top) and MSX79542 (bottom) grown on oatmeal agar, oatmeal, and rice (from left to right). Guttates were found only on the oatmeal agar culture of MSX79542 (black arrows). The cultures were grown for 4 weeks at room temperature then analyzed by droplet probe prior to their extraction.

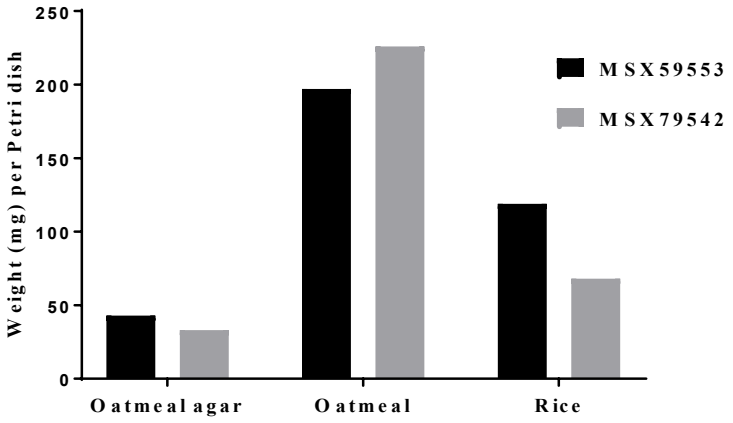

Figure S4. The Amount of the Total Defatted Extracts of Both Strains MSX59553 and MSX79542. The cultures were grown on Petri dishes in three different media (oatmeal agar, oatmeal, and rice).

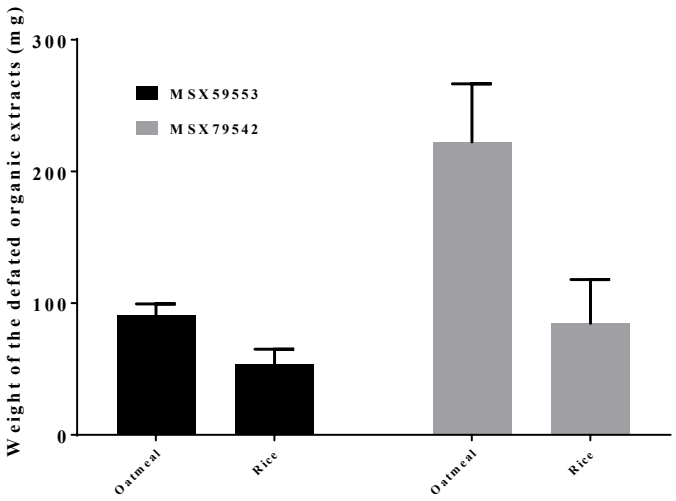

Figure S5. Total Defatted Extracts Weight of Strains MSX59553 and MSX79542 grown in flasks in two different media (oatmeal and rice) in three biological replicates.

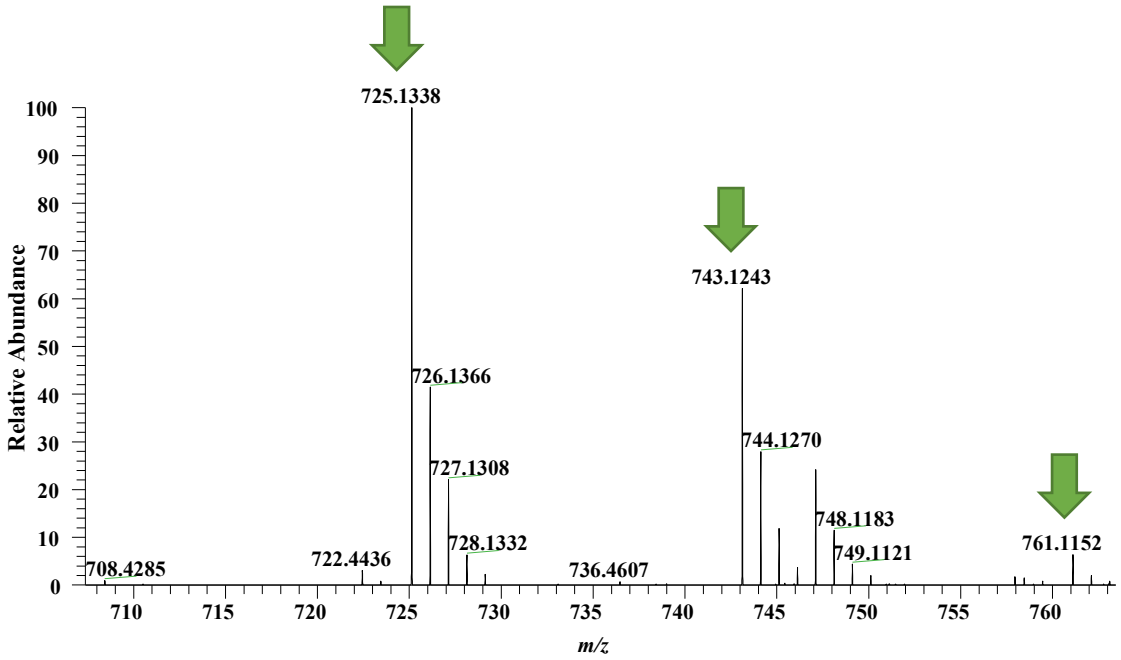

Figure S6. Full Scan MS Data of Strain MSX59553 Grown on Oatmeal Agar Medium Supplemented with a Racemic Mixture of 5-F-DL-Trp. The plates were microextracted *in situ* using a droplet probe coupled to a hyphenated system (UPLC-PDA-HRMS-MS/MS). The peaks indicated with green arrows (*m/z* 725.1338, 743.1243, 761.1152) correspond to the mass of verticillin H (**1**), the incorporation of one fluorine atom, and the incorporation of two fluorine atoms in the molecule, respectively.

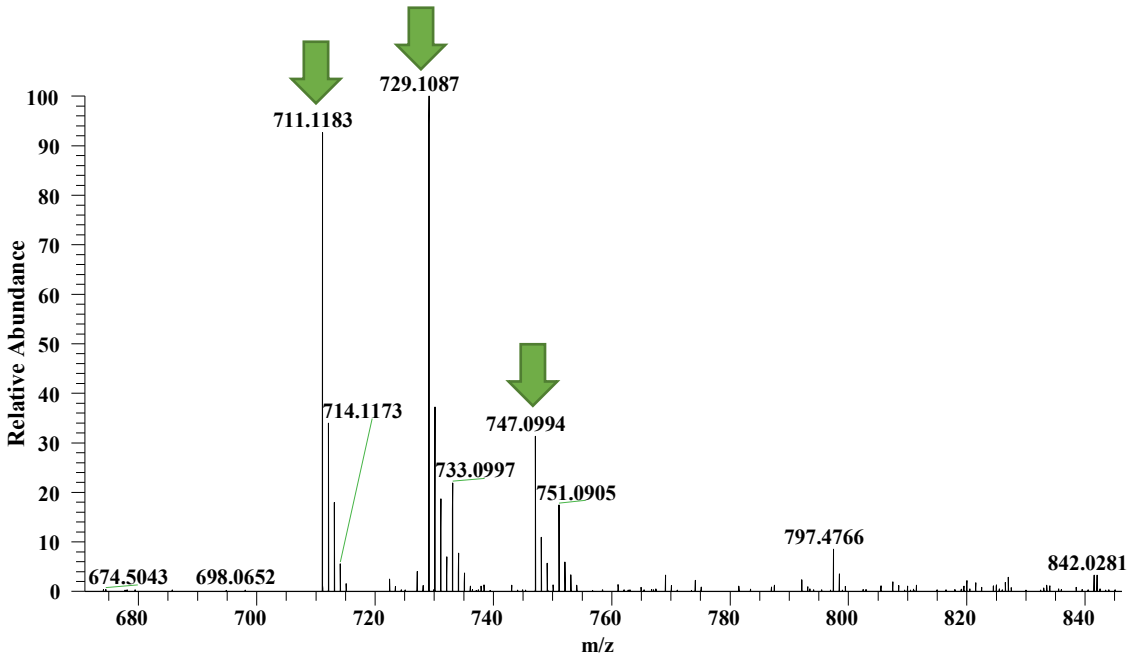

Figure S7. Full Scan MS Data of Strain MSX59553 Grown on Oatmeal Agar Medium Supplemented with a Racemic Mixture of 5-F-DL-Trp. The plates were microextracted *in situ* using a droplet probe coupled to a hyphenated system (UPLC-PDA-HRMS-MS/MS). The peaks indicated with green arrows (*m/z* 711.1183, 729.1087, 747.0994) correspond to the mass of Sch 52901 (**2**), the incorporation of one fluorine atom, and the incorporation of two fluorine atoms in the molecule, respectively.

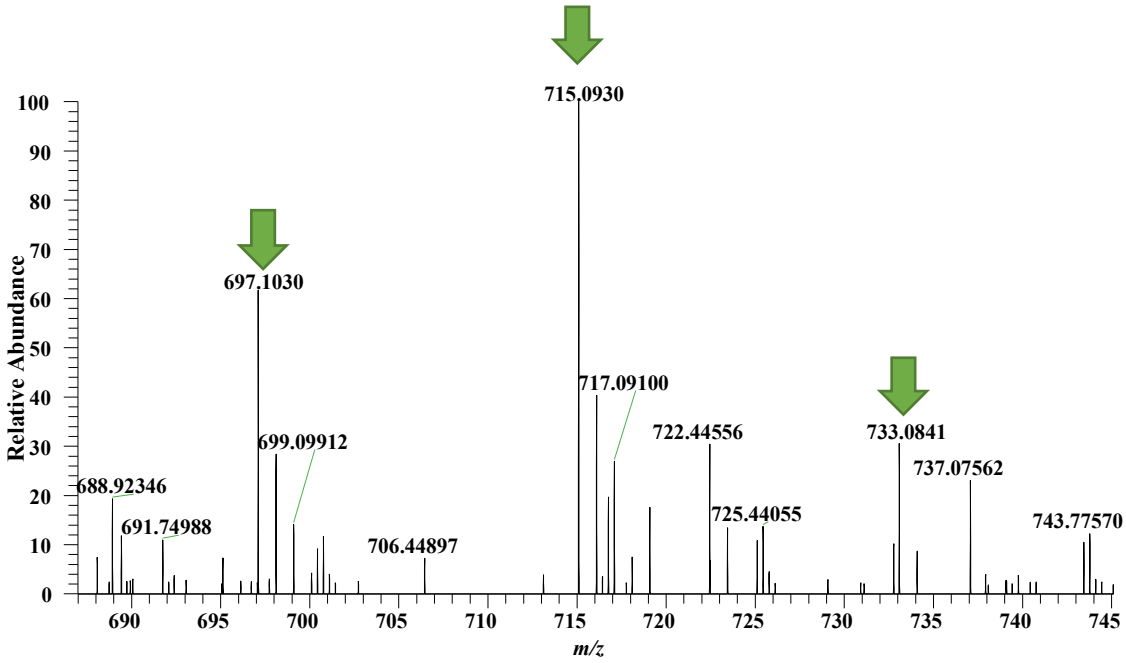

Figure S8. Full Scan MS Data of Strain MSX59553 Grown on Oatmeal Agar Medium Supplemented with a Racemic Mixture of 5-F-DL-Trp. The plates were microextracted *in situ* using a droplet probe coupled to a hyphenated system (UPLC-PDA-HRMS-MS/MS). The peaks indicated with green arrows (*m/z* 697.1030, 715.0930, 733.0841) correspond to the mass of verticillin A (**3**), the incorporation of one fluorine atom, and the incorporation of two fluorine atoms in the molecule, respectively.

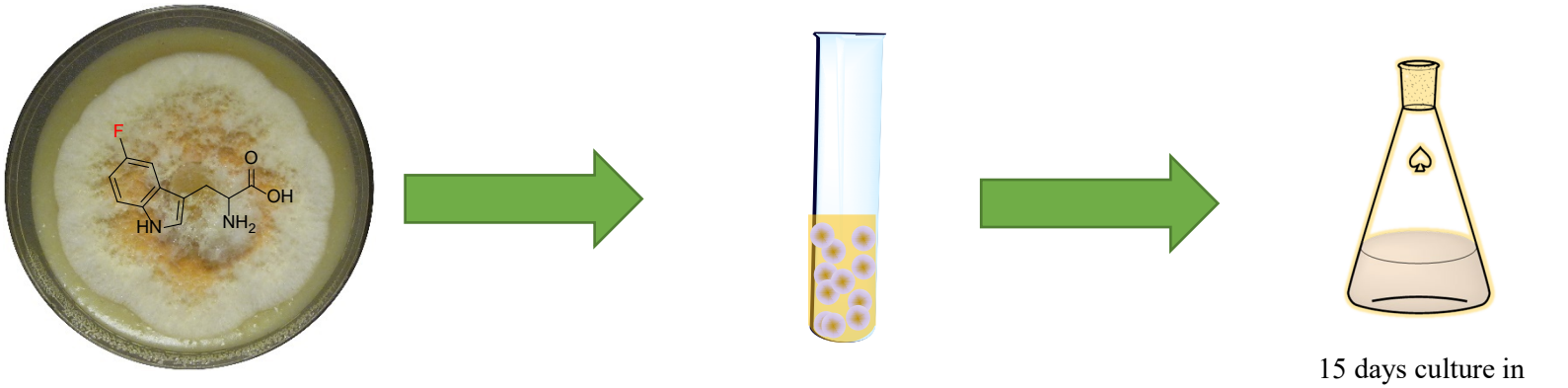

Figure S9. Culture Conditions for MSX59553 Grown on Oatmeal Agar Medium Supplemented with a Racemic Mixture of 5-F-DL-Trp. The plate was used to inoculate 10 mL of YESD to be used to grow cultures on oatmeal supplemented with 375 ppm of 5-F-DL-Trp.

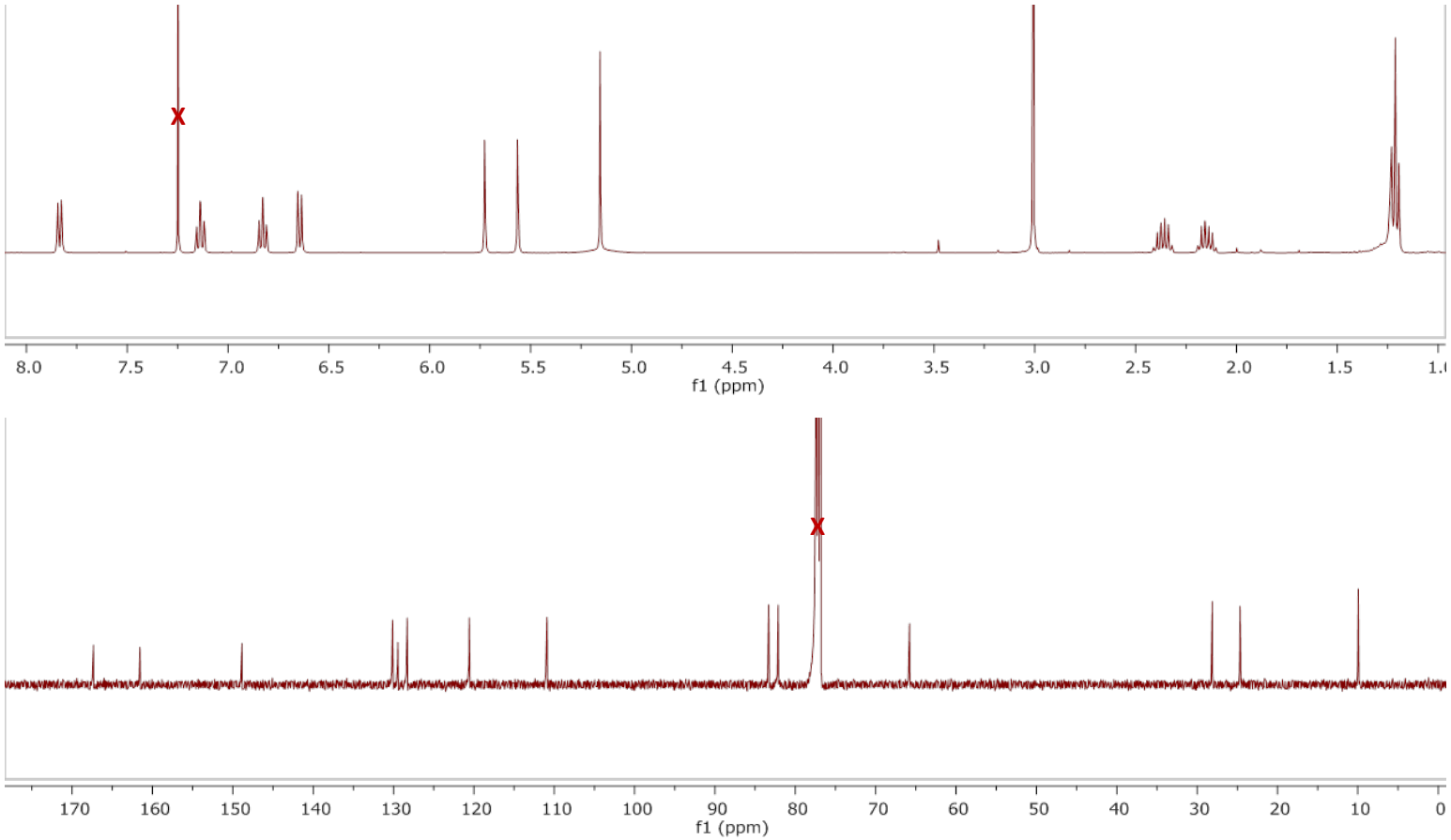

Figure S10. ^{1}H and ^{13}C NMR Spectra of Verticillin H (1) in $CDCl_3$ [500 MHz for ^{1}H and 125 MHz for ^{13}C].

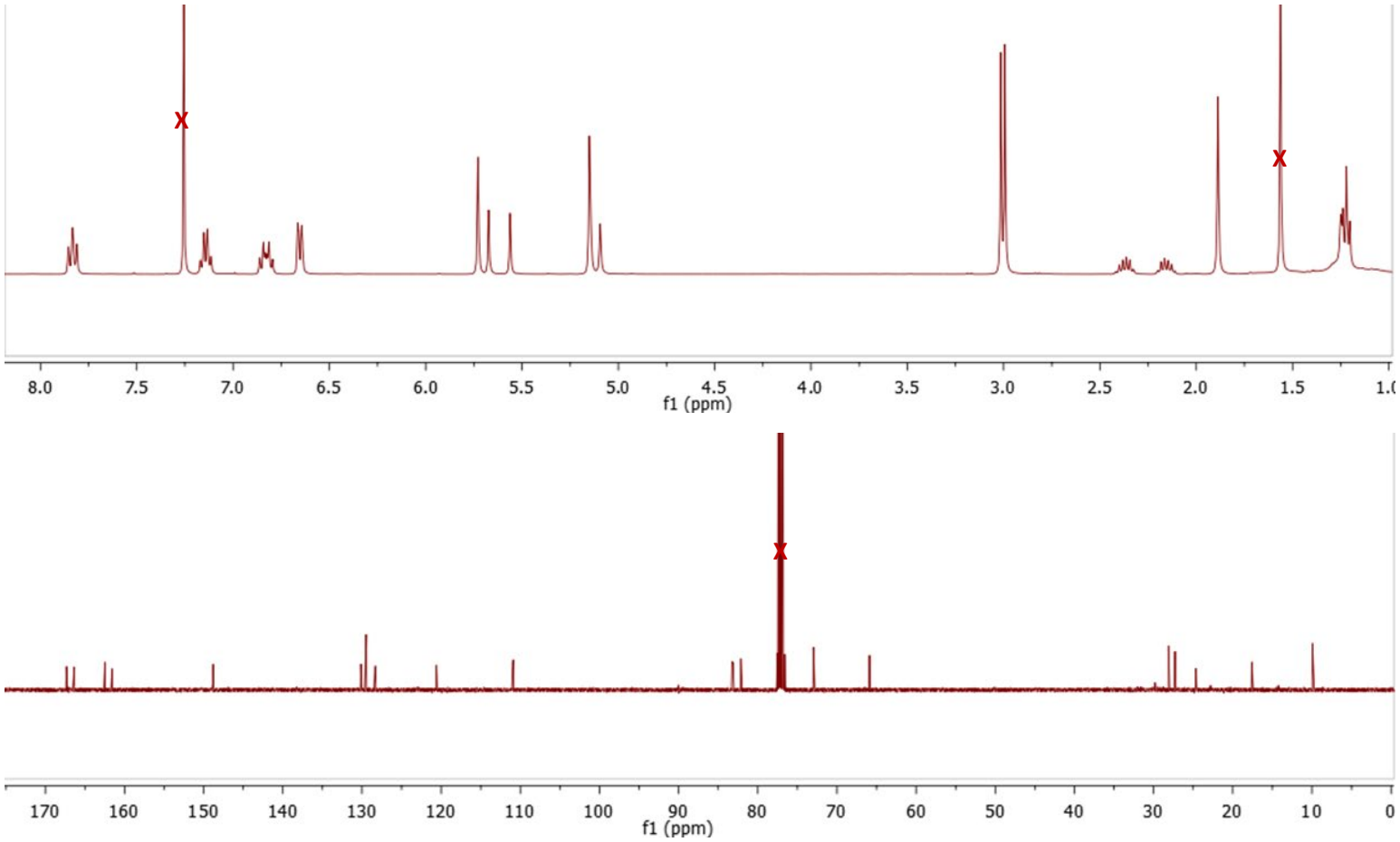

Figure S11. ^{1}H (upper panel) and ^{13}C (lower panel) NMR Spectra of Sch 52901 (2) in $CDCl_3$ [500 MHz for ^{1}H and 125 MHz for ^{13}C].

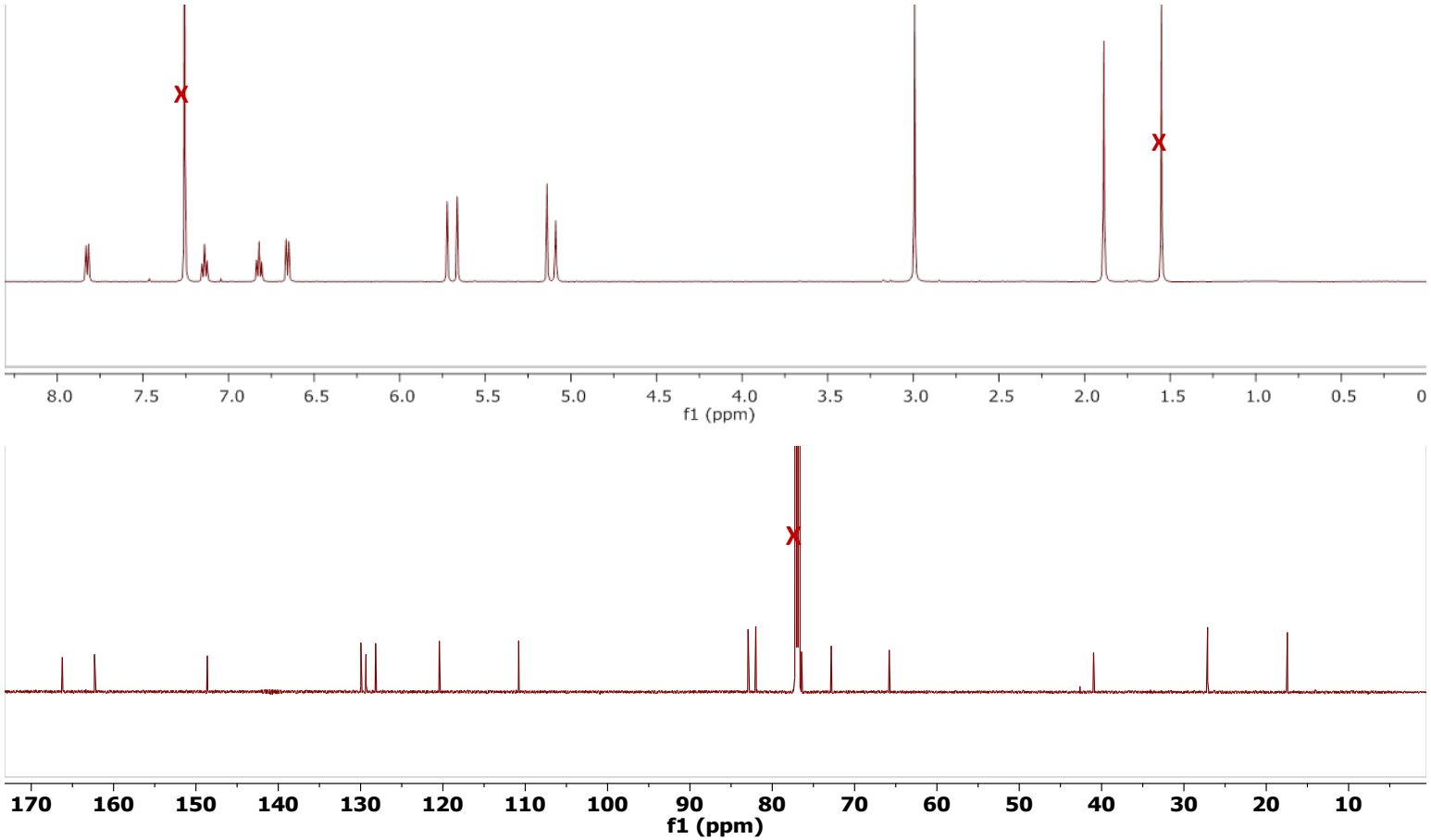

Figure S12. ^{1}H (upper panel) and ^{13}C (lower panel) NMR Spectra of Verticillin A (3) in $CDCl_3$ [500 MHz for ^{1}H and 125 MHz for ^{13}C].

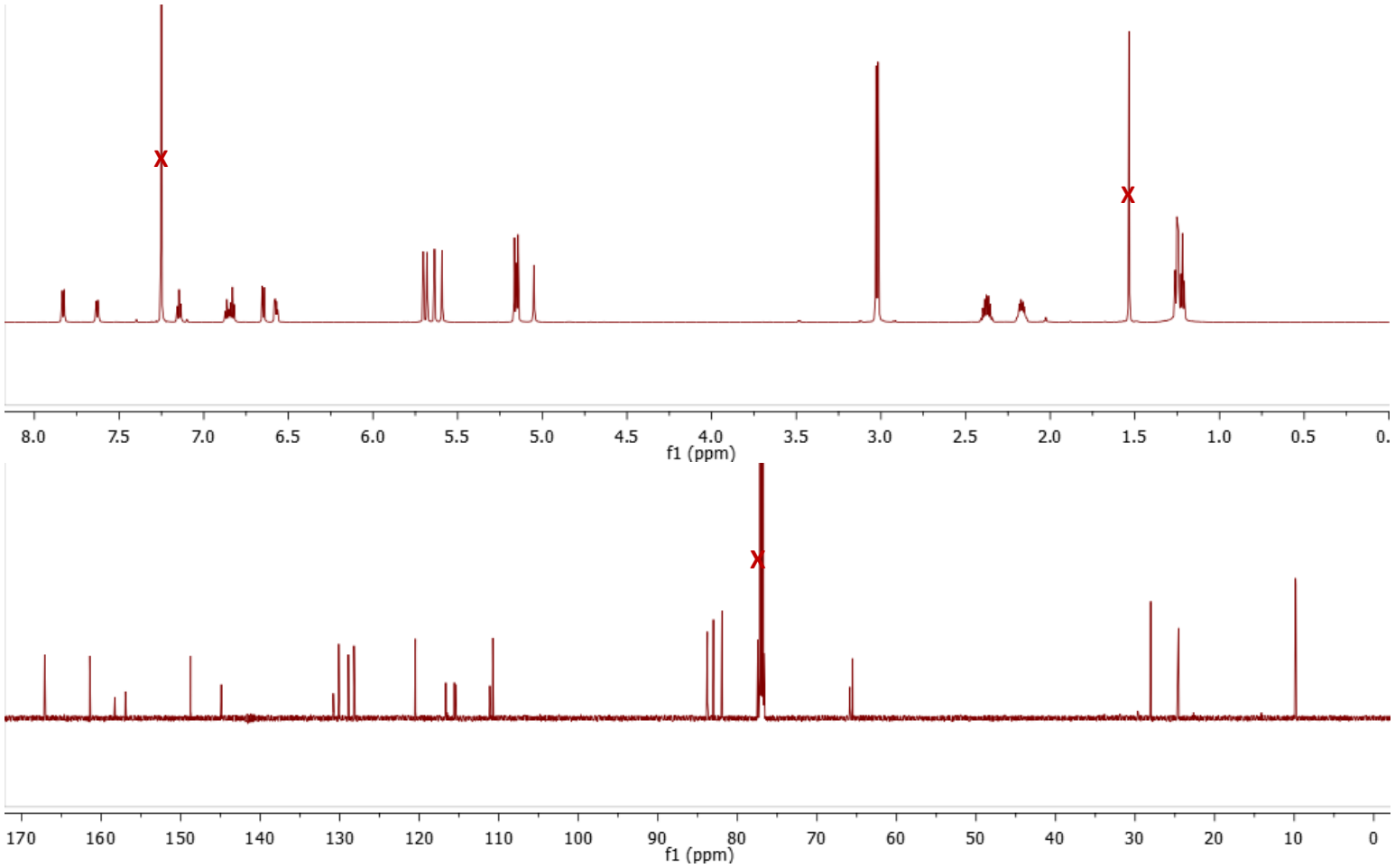

Figure S13. ^{1}H (upper panel) and ^{13}C (lower panel) NMR Spectra of 9-F-verticillin H (4) in $CDCl_3$ [700 MHz for ^{1}H and 175 MHz for ^{13}C].

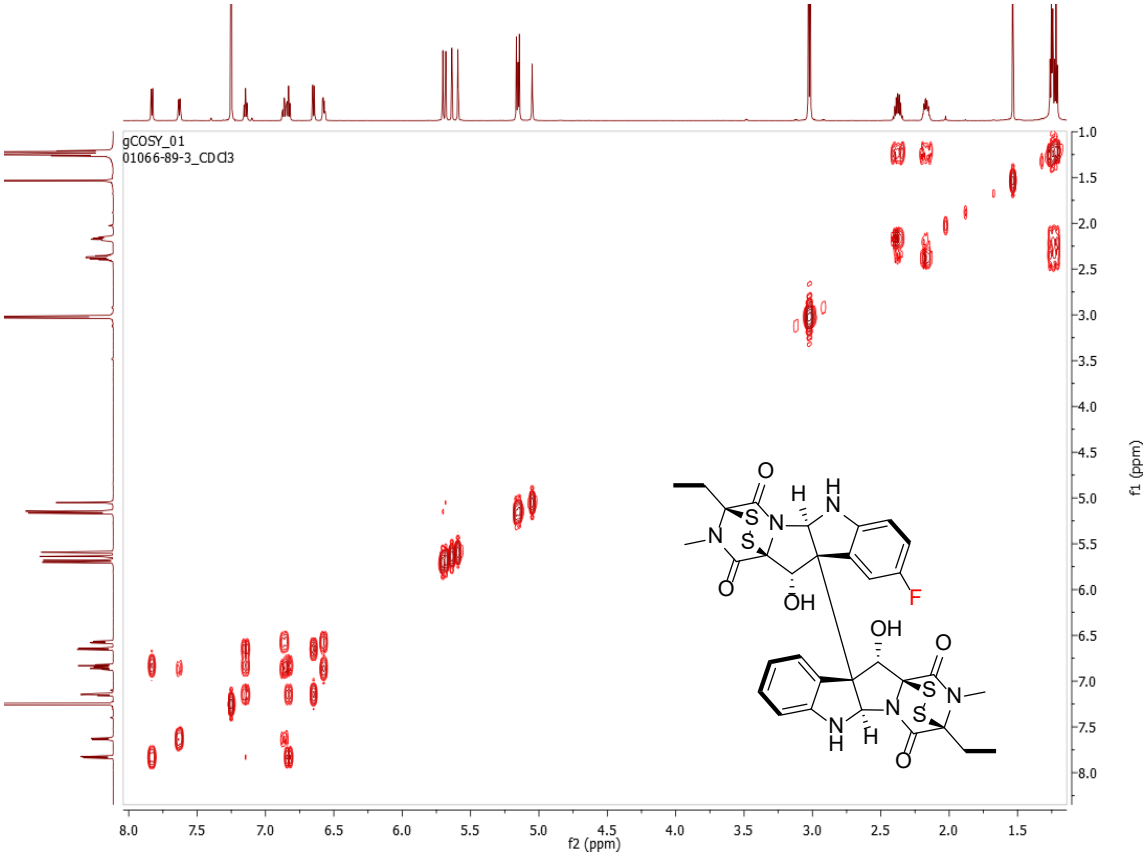

Figure S14. ^{1}H-^{1}H COSY NMR Spectrum of 9-F-verticillin H (4) in $CDCl_3$ (700 MHz).

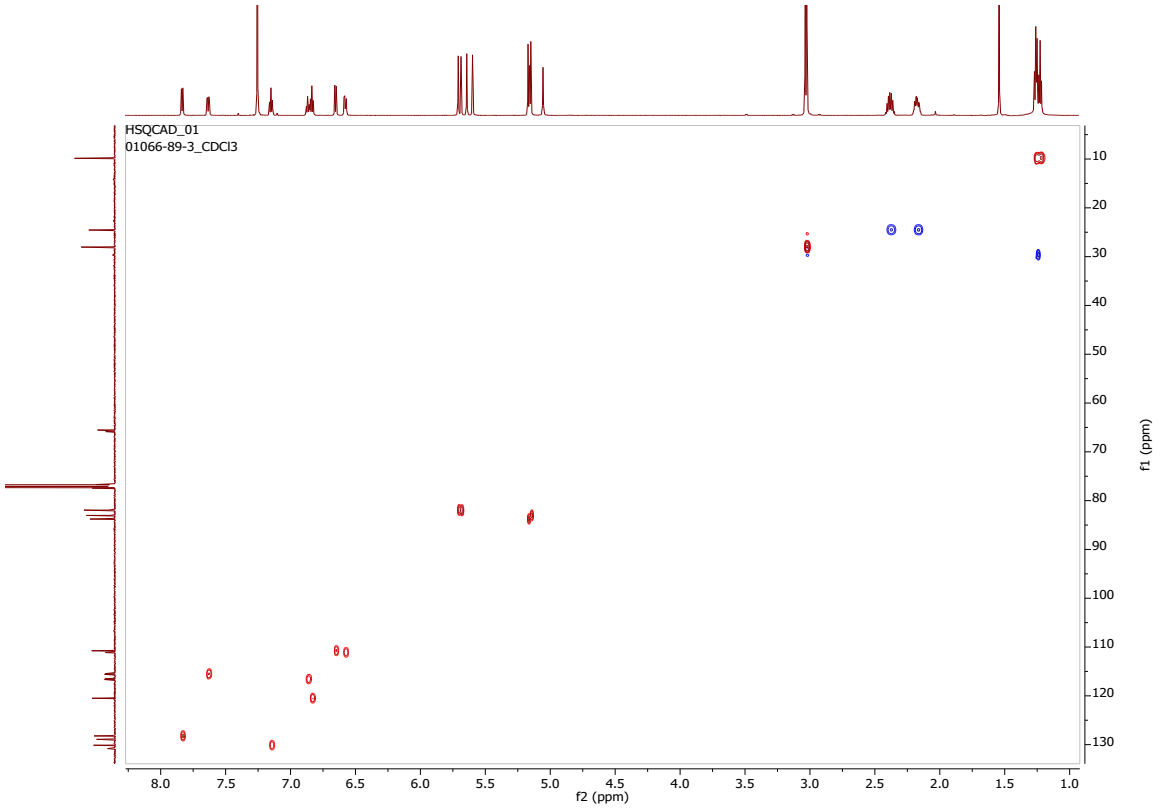

Figure S15. ^{1}H-^{13}C HSQC NMR spectrum of 9-F-verticillin H (4) in $CDCl_3$ (700 MHz).

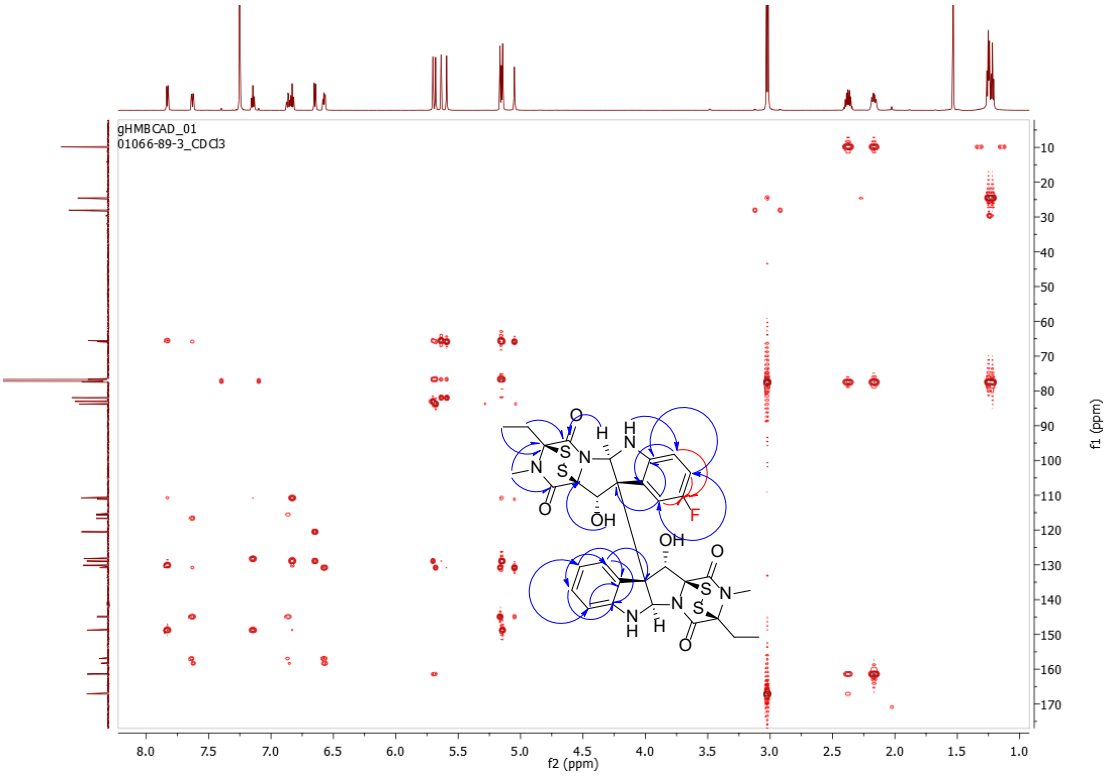

Figure S16. ^{1}H-^{13}C HMBC NMR Spectrum of 9-F-verticillin H (4) in $CDCl_3$ (700 MHz). The red arrows show the correlations between the protons in positions H-7, H-8 and H-10 with the characteristic carbon at C-9 that contains the fluorine atom.

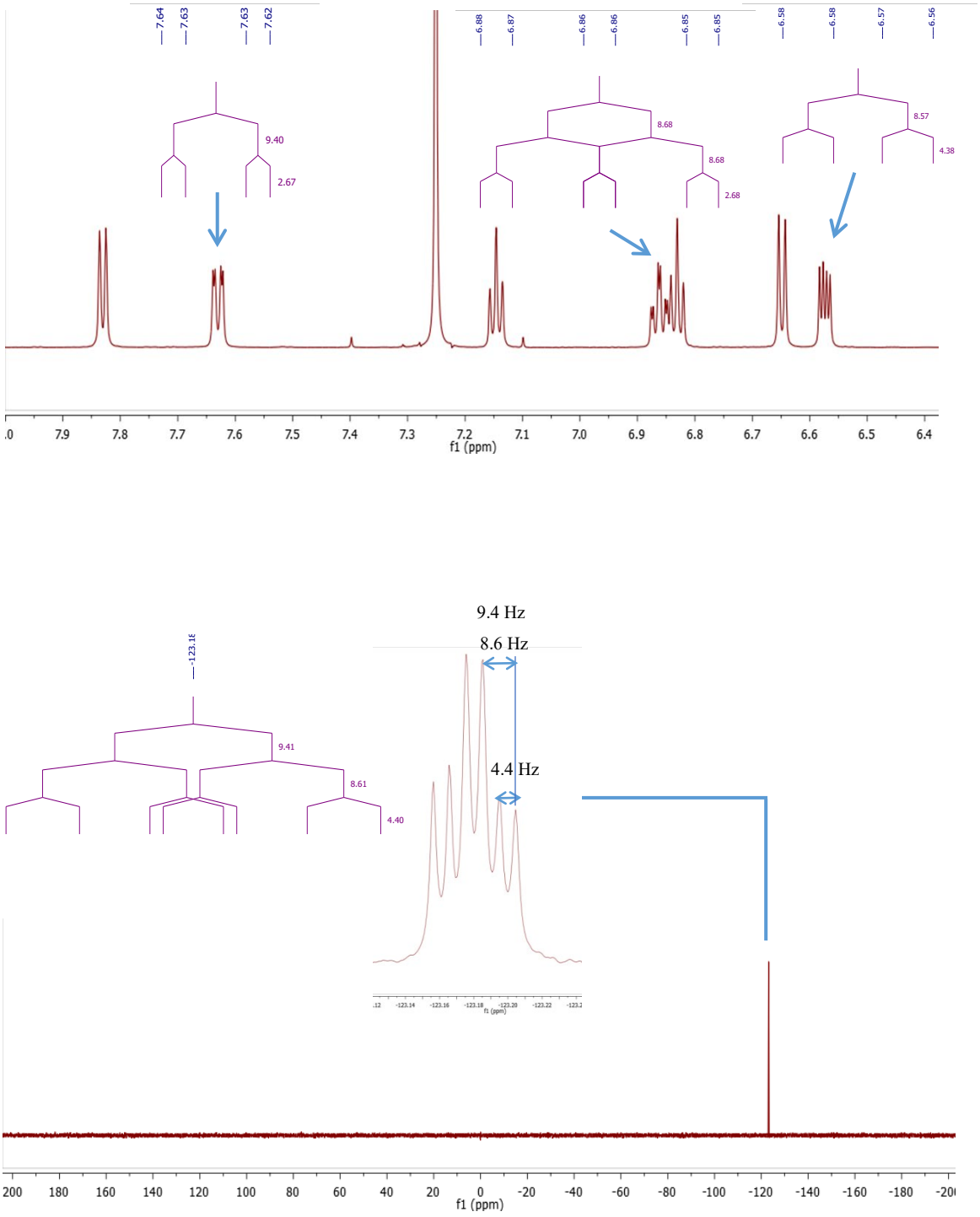

Figure S17. ^{1}H (upper panel) and ^{19}F (lower panel) NMR Spectra of 9-F-verticillin H (4) in $CDCl_3$ [700 MHz for ^{1}H and 470 MHz for ^{19}F].

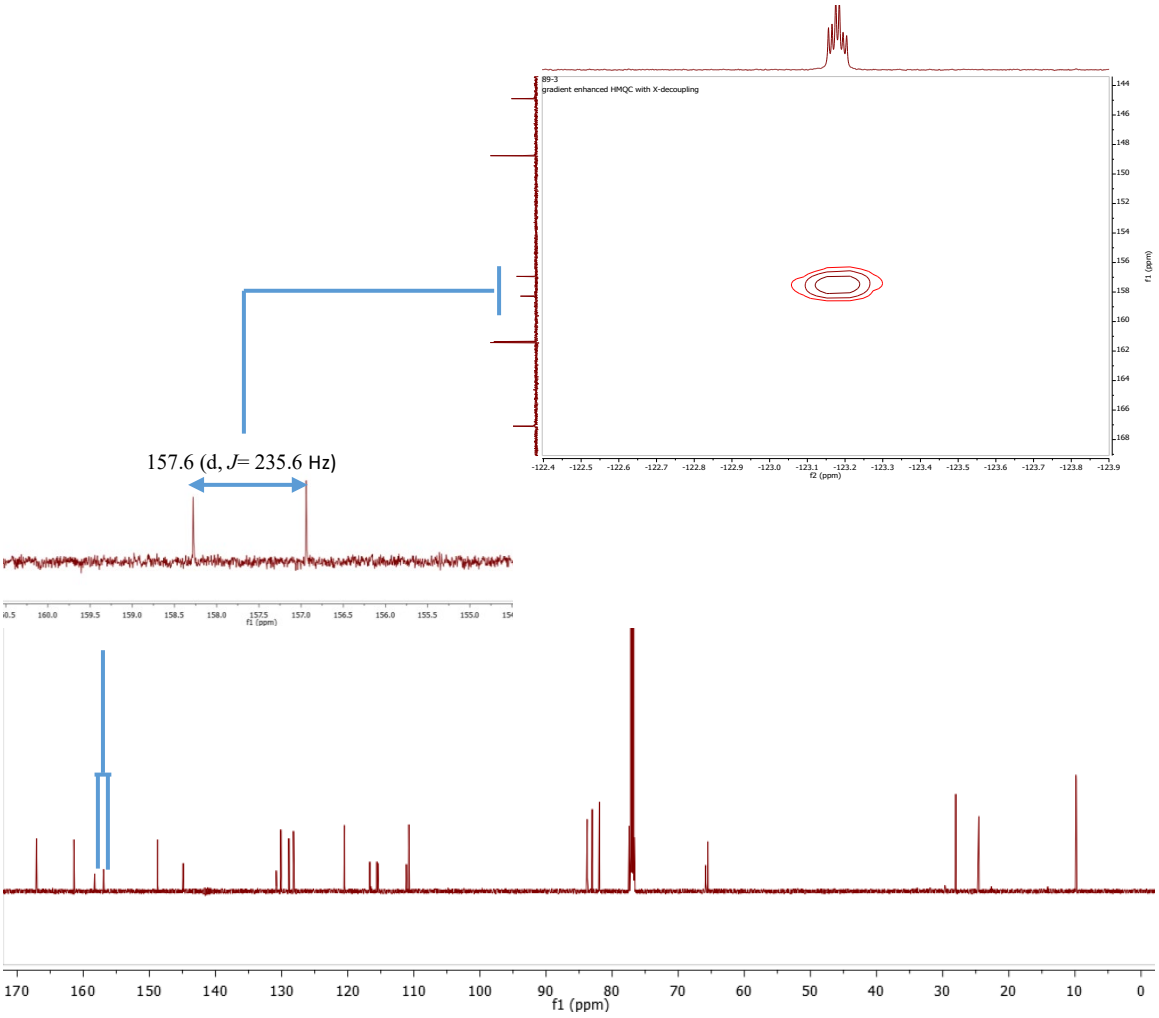

Figure S18. ^{13}C NMR (lower panel) and ^{19}F-^{13}C HMQC NMR Spectra of 9-F-verticillin H (4) in $CDCl_3$ [175 MHz for ^{13}C and 470 MHz for ^{19}F].

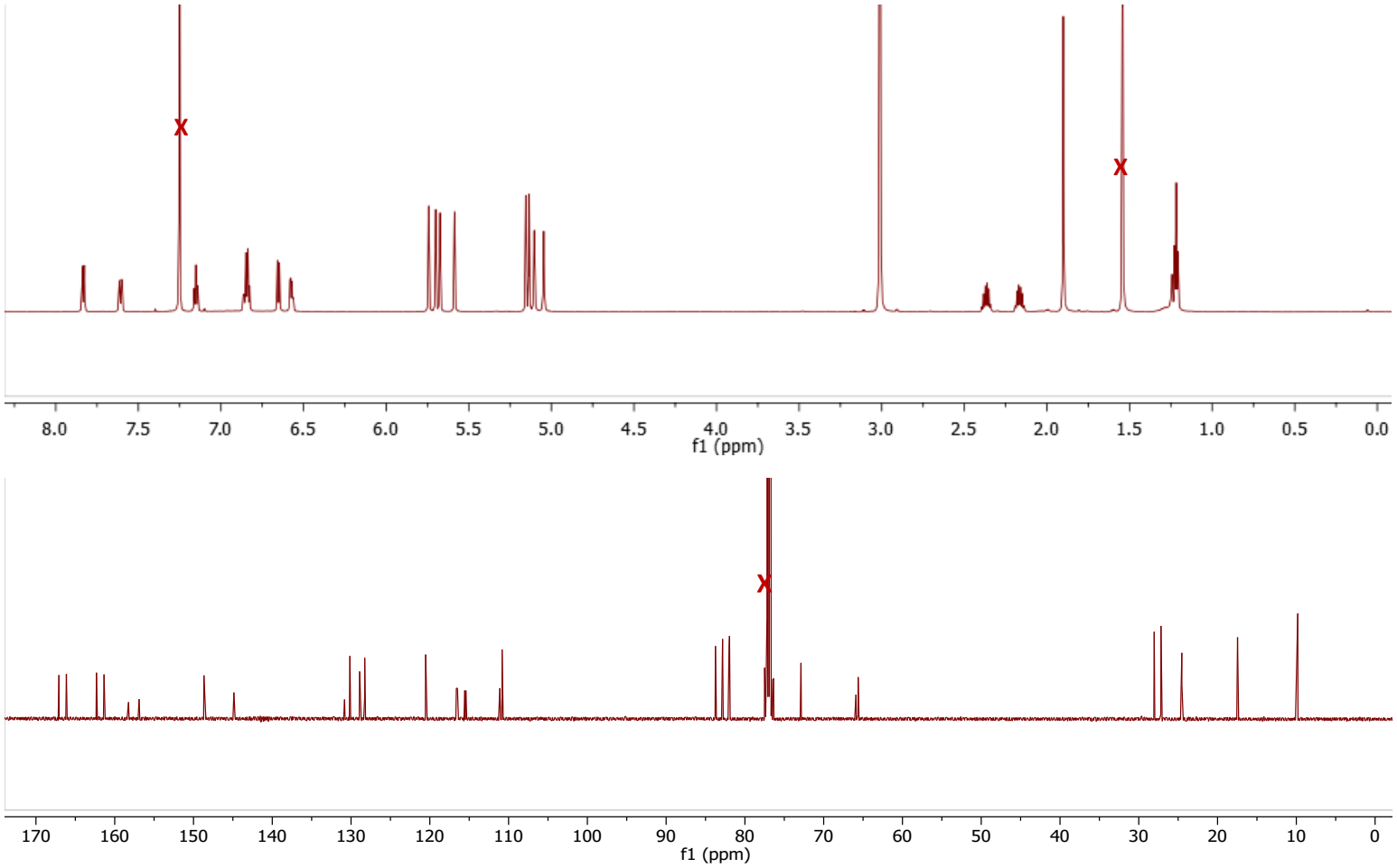

Figure S19. ^{1}H (upper panel) and ^{13}C (lower panel) NMR Spectra of 9-F-Sch 52901 (5) in $CDCl_3$ [700 MHz for ^{1}H and 175 MHz for ^{13}C].

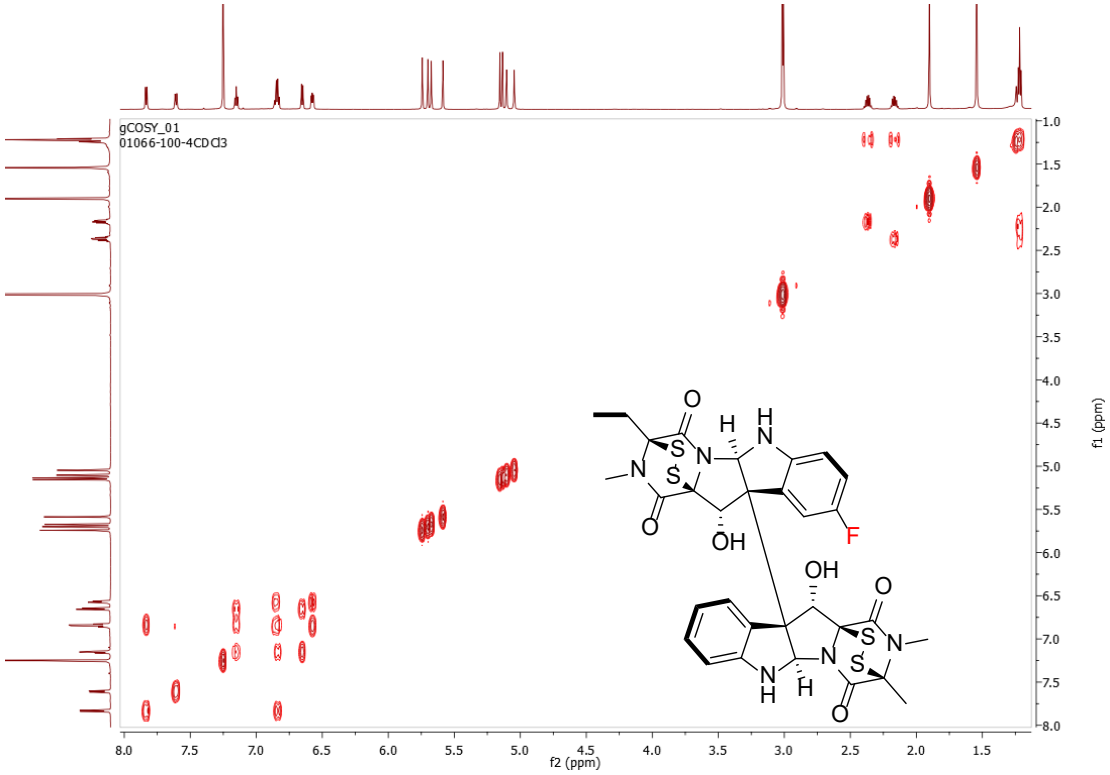

Figure S20. ^{1}H-^{1}H COSY NMR Spectrum of 9-F-Sch 52901 (5) in $CDCl_3$ (700 MHz).

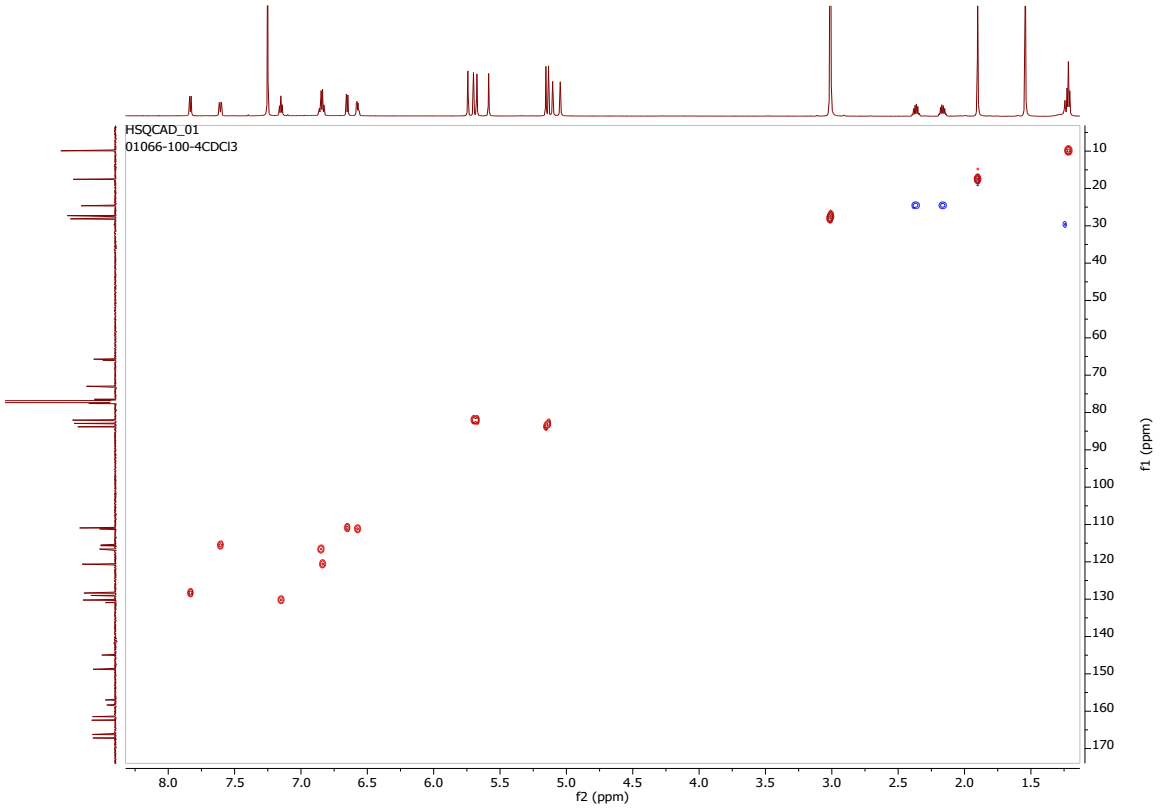

Figure S21. ^{1}H-^{13}C HSQC NMR Spectrum of 9-F-Sch 52901 (5) in $CDCl_3$ (700 MHz).

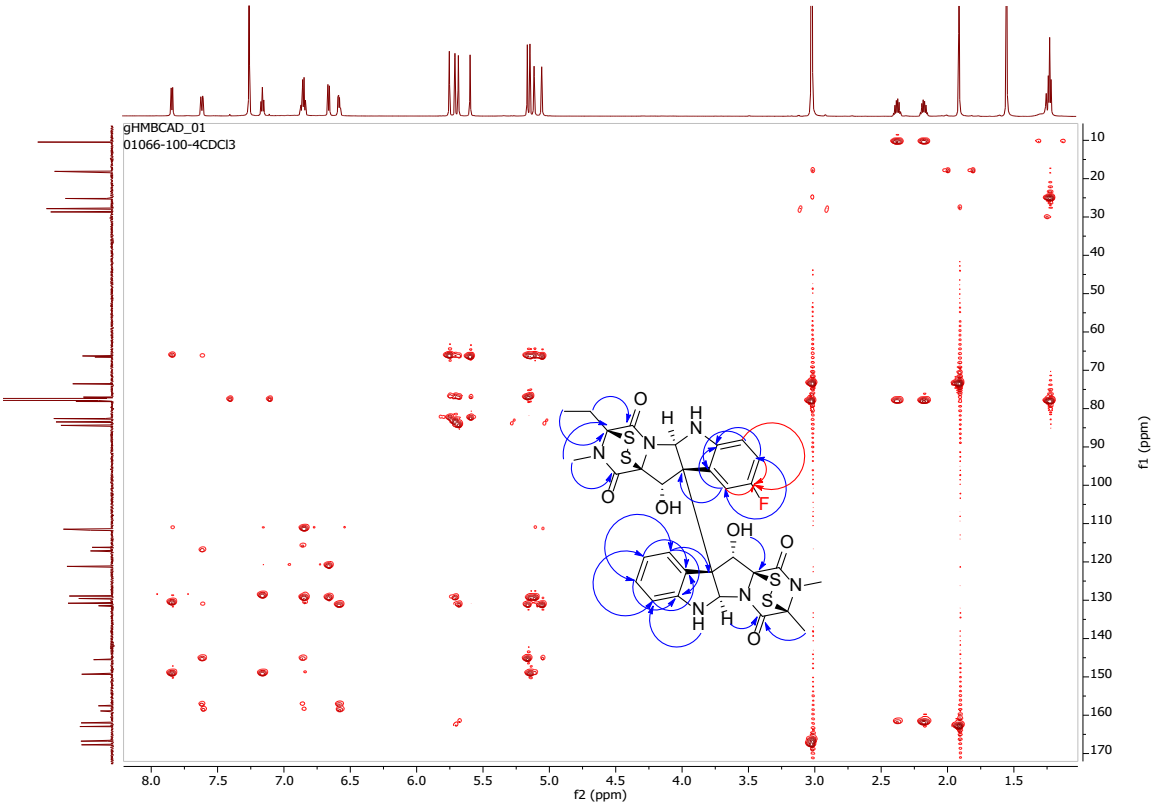

Figure S22. ^{1}H-^{13}C HMBC NMR Spectrum of 9-F-Sch 52901 (5) in $CDCl_3$ (700 MHz). The red arrows show the correlations between the protons in positions H-7, H-8 and H-10 with the characteristic carbon at C-9 that contains the fluorine atom.

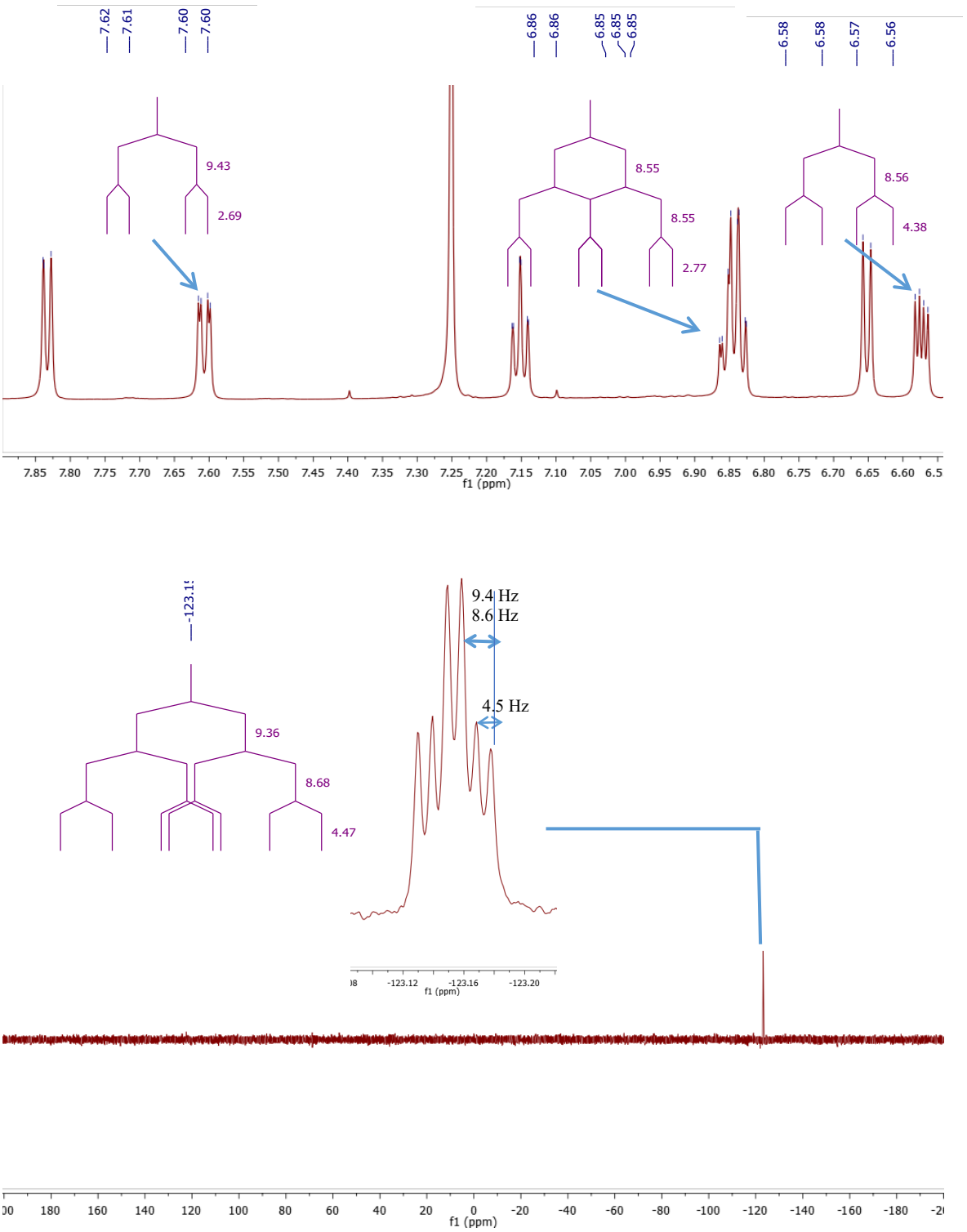

Figure S23. ^{1}H (upper panel) and ^{19}F (lower panel) NMR Spectra of 9-F-Sch 52901 (5) in $CDCl_3$ [700 MHz for ^{1}H and 470 MHz for ^{19}F].

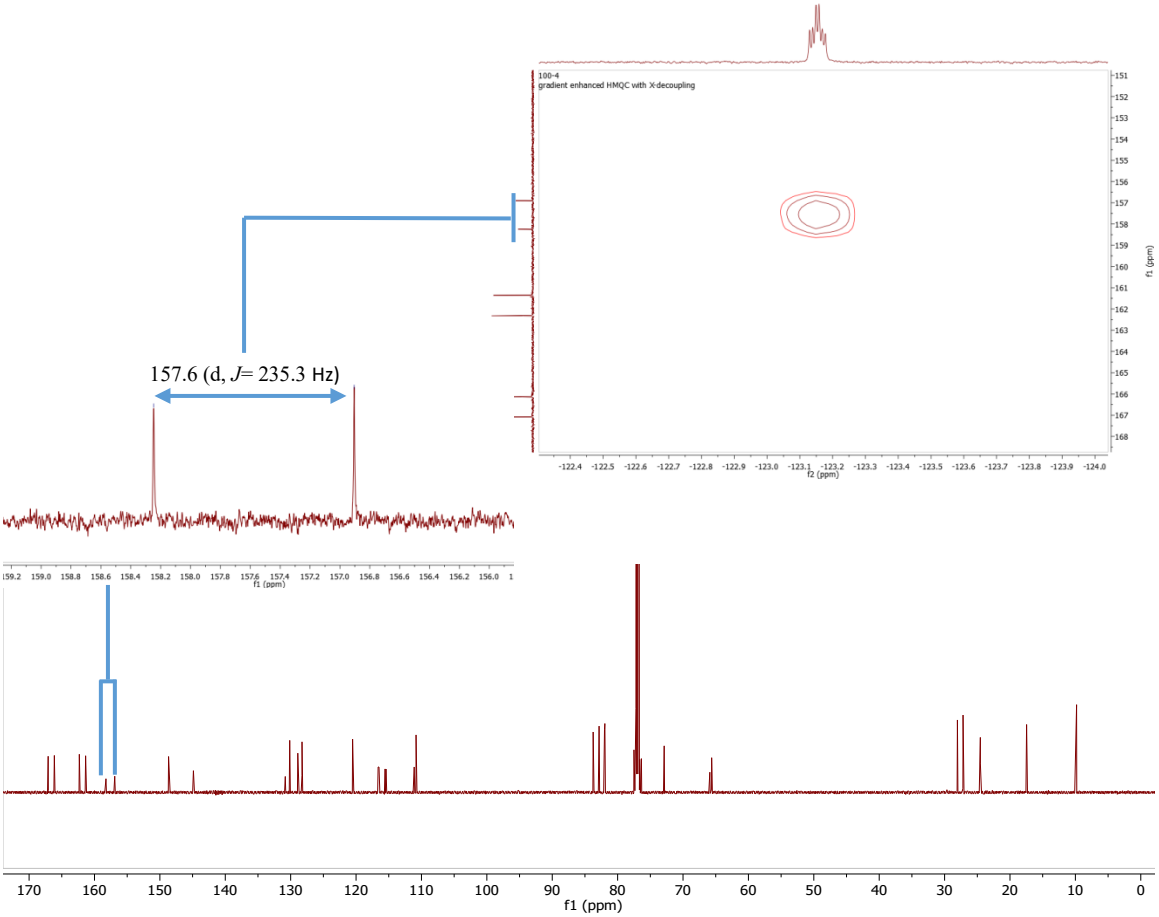

Figure S24. ^{13}C (lower panel) NMR and ^{19}F-^{13}C HMQC NMR Spectra of 9-F-Sch 52901 (5) in $CDCl_3$ [175 MHz for ^{13}C and 470 MHz for ^{19}F].

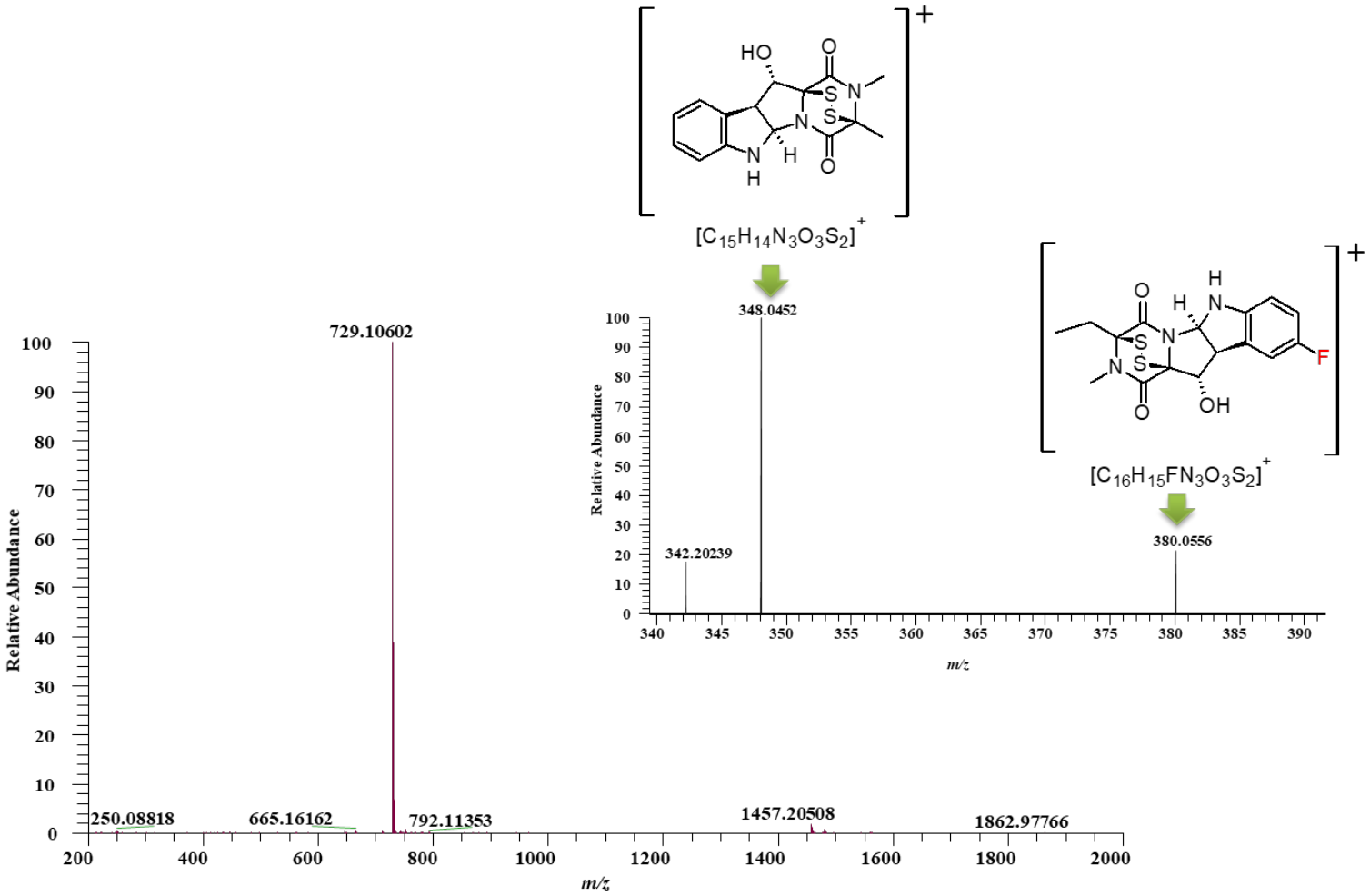

Figure S25. Full Scan MS Data of 9-F-Sch 52901 (5) with *m/z* 729.1060. HRMS-MS/MS fragmentation showed *m/z* 348.0452 and *m/z* 380.0556 (green arrow) indicating the incorporation of the fluorine to a specific monomer of Sch 52901 (**2**).

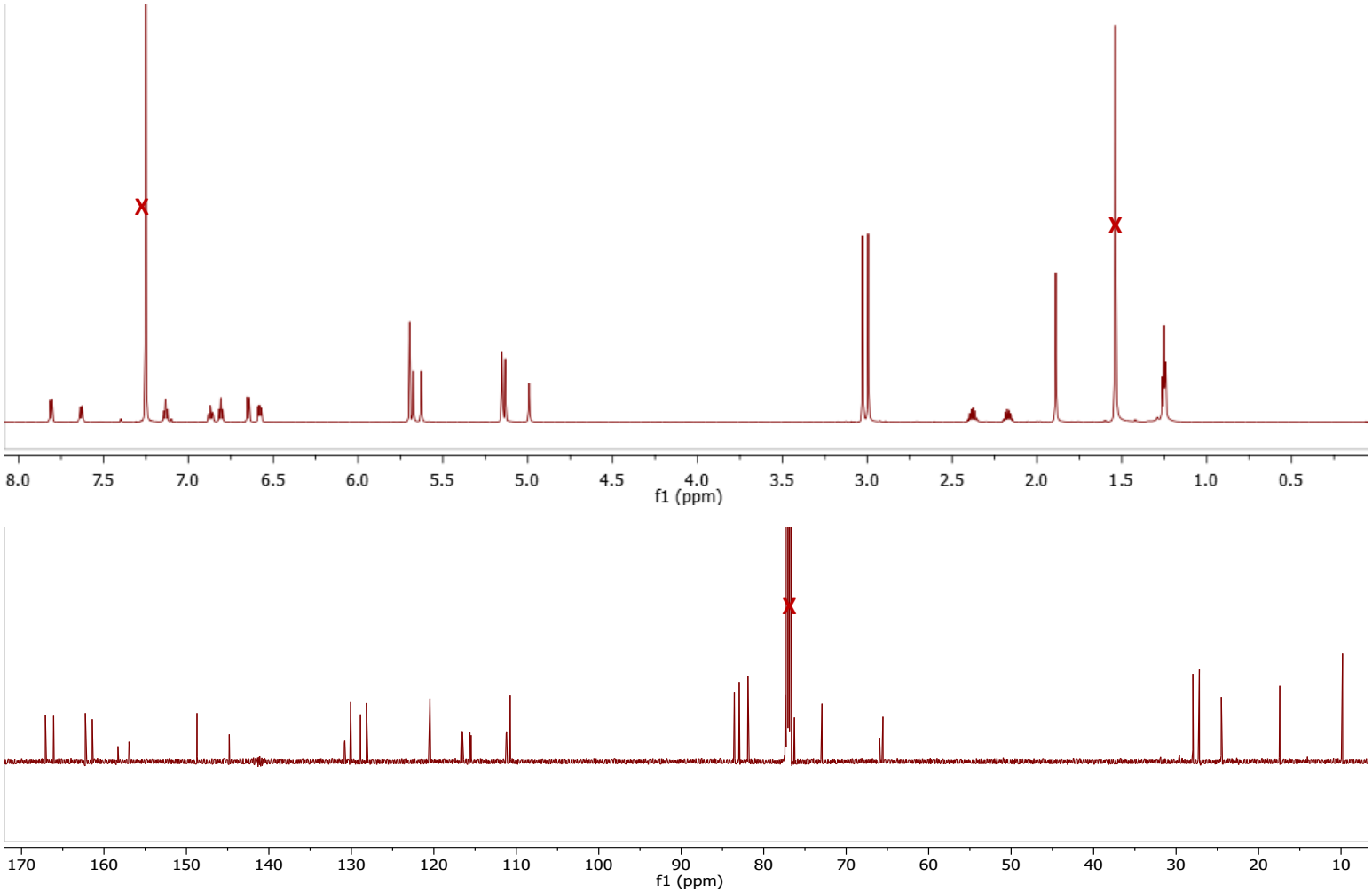

Figure S26. ^{1}H and ^{13}C NMR Spectra of 9′-F-Sch 52901 (6) in $CDCl_3$ [700 MHz for ^{1}H and 175 MHz for ^{13}C].

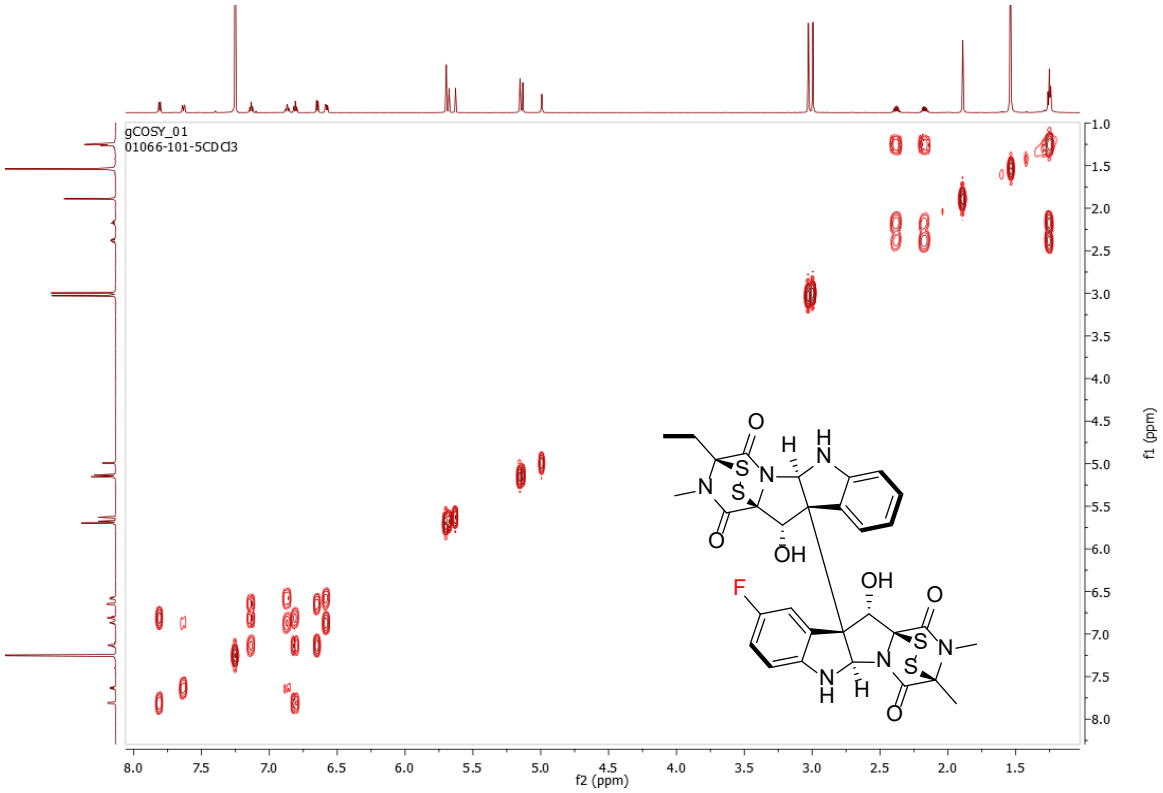

Figure S27. ^{1}H-^{1}H COSY NMR Spectrum of 9′-F-Sch 52901 (6) in $CDCl_3$ (700 MHz).

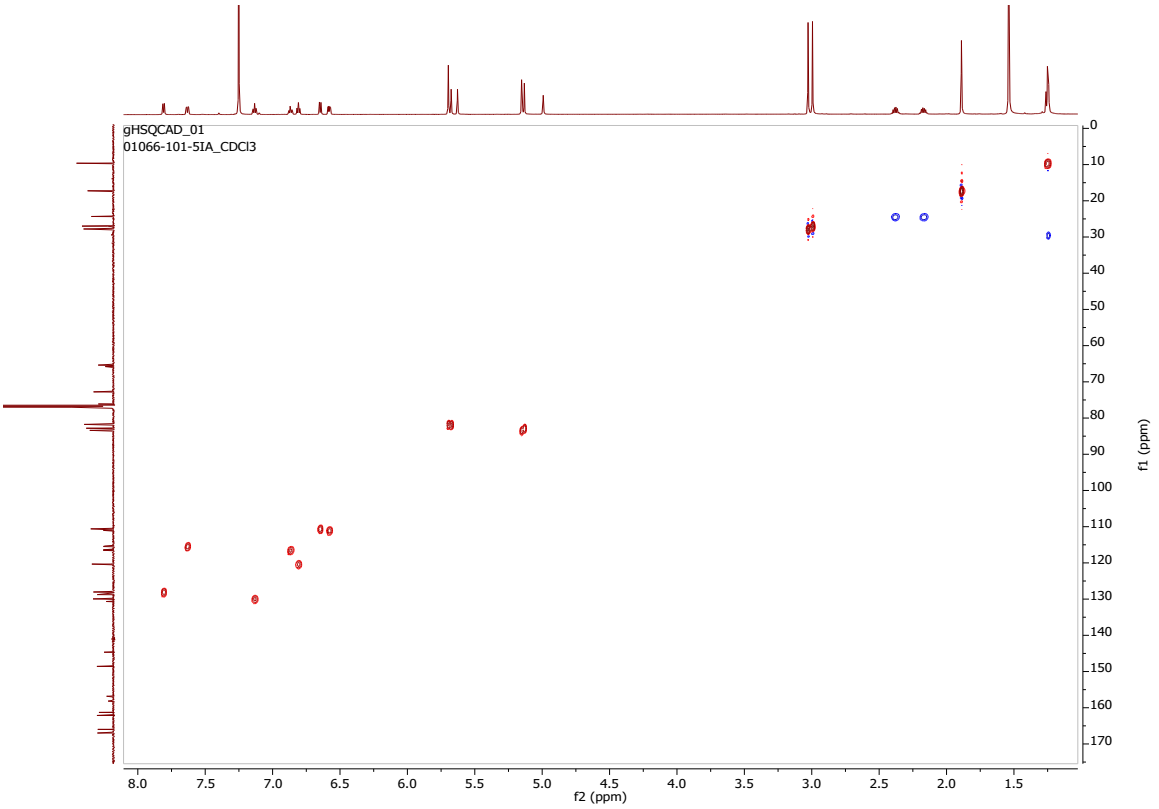

Figure S28. ^{1}H-^{13}C HSQC NMR Spectrum of 9′-F-Sch 52901 (6) in $CDCl_3$ (700 MHz).

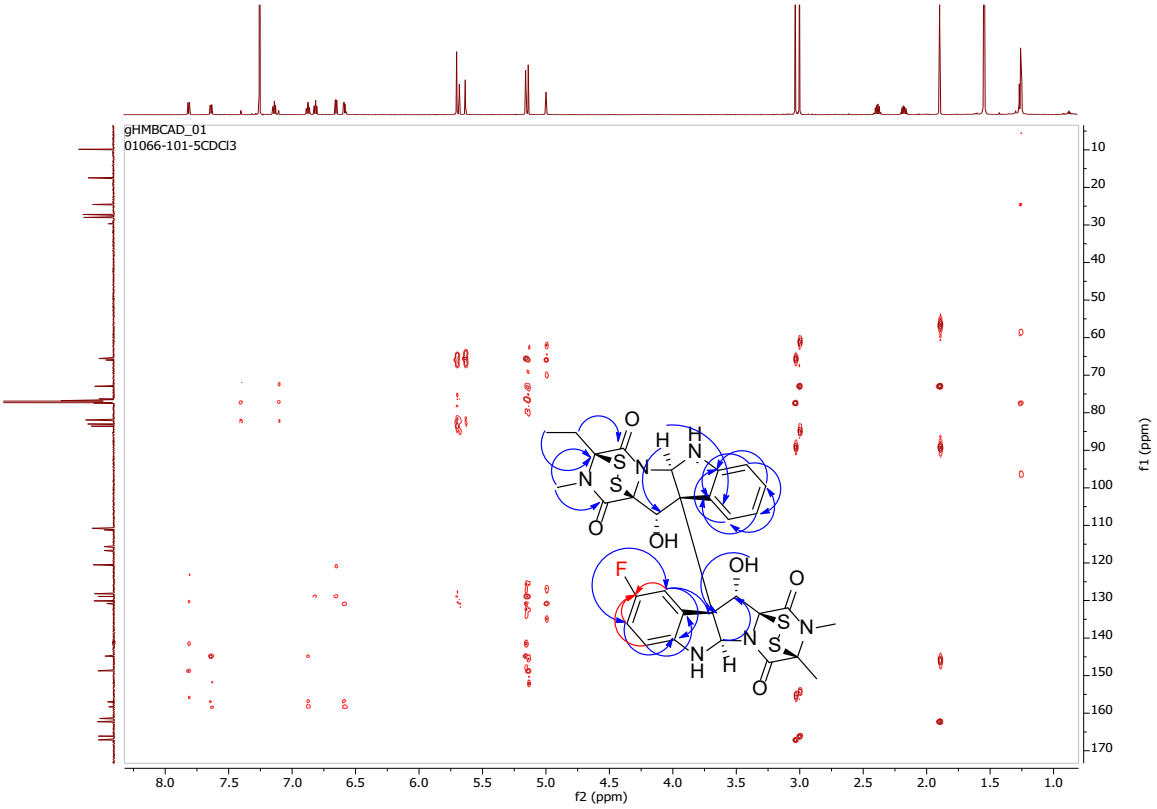

Figure S29. ^{1}H-^{13}C HMBC NMR Spectrum of 9′-F-Sch 52901 (6) in $CDCl_3$ (700 MHz) The red arrows show the correlations between the protons in positions H-7′, H-8′ and H-10′ with the characteristic carbon at C-9′ that contains the fluorine atom.

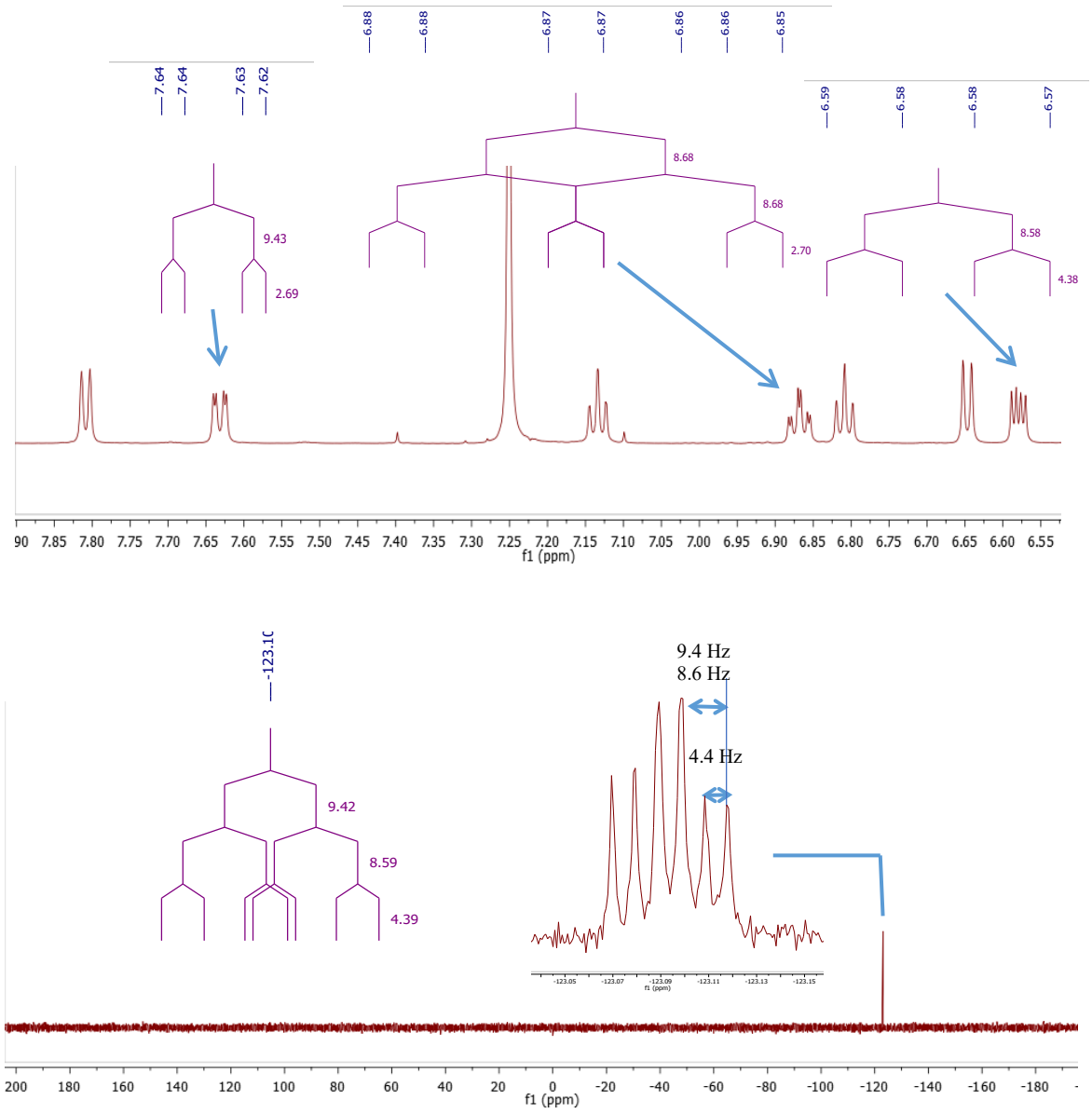

Figure S30. ^{1}H (upper panel) and ^{19}F (lower panel) NMR Spectra of 9′-F-Sch 52901 (6) in $CDCl_3$ [700 MHz for ^{1}H and 470 MHz for ^{19}F].

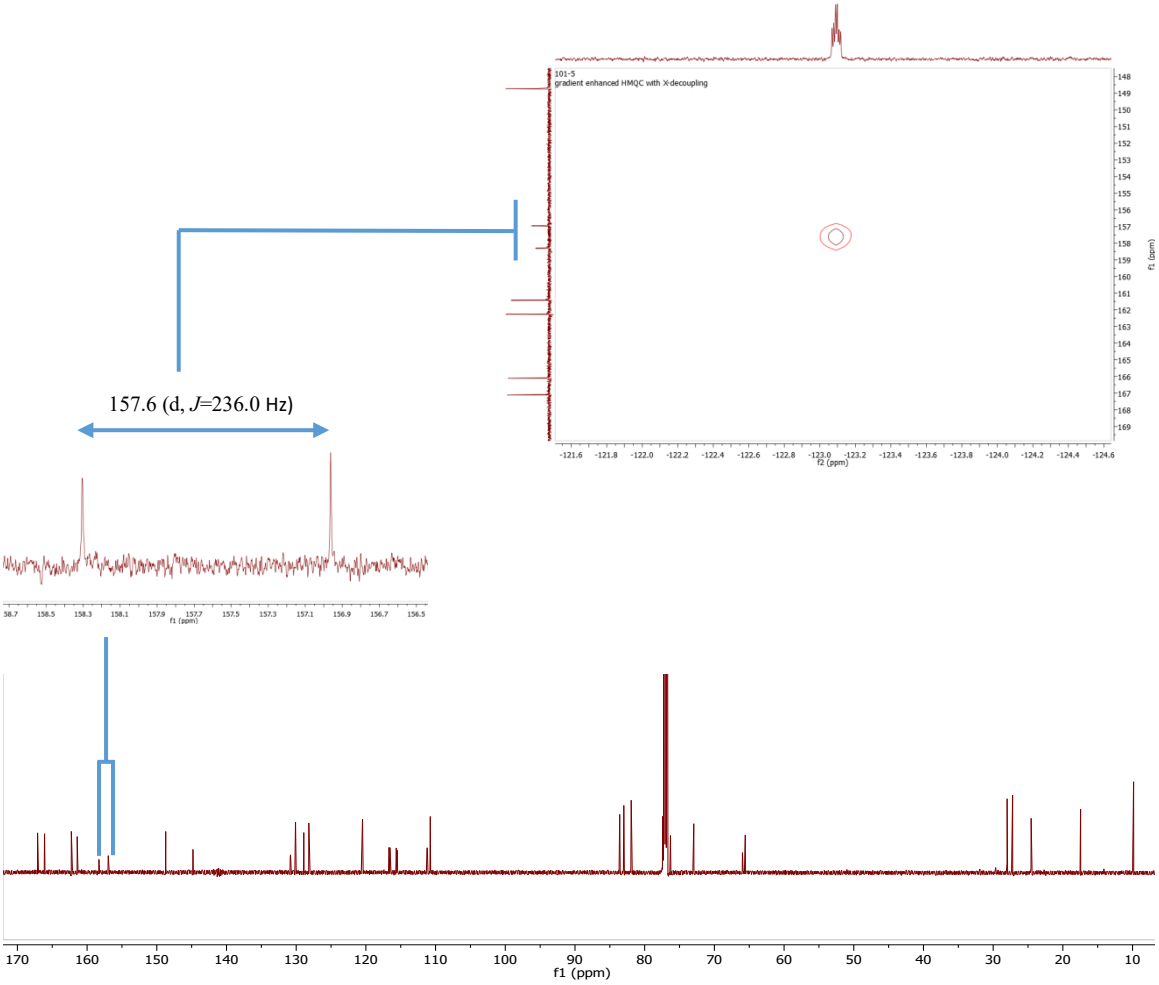

Figure S31.^{13}C NMR (lower panel) and ^{19}F-^{13}C HMQC NMR Spectra of 9′-F-Sch 52901 (6) in $CDCl_3$ [175 MHz for ^{13}C and 470 MHz for ^{19}F].

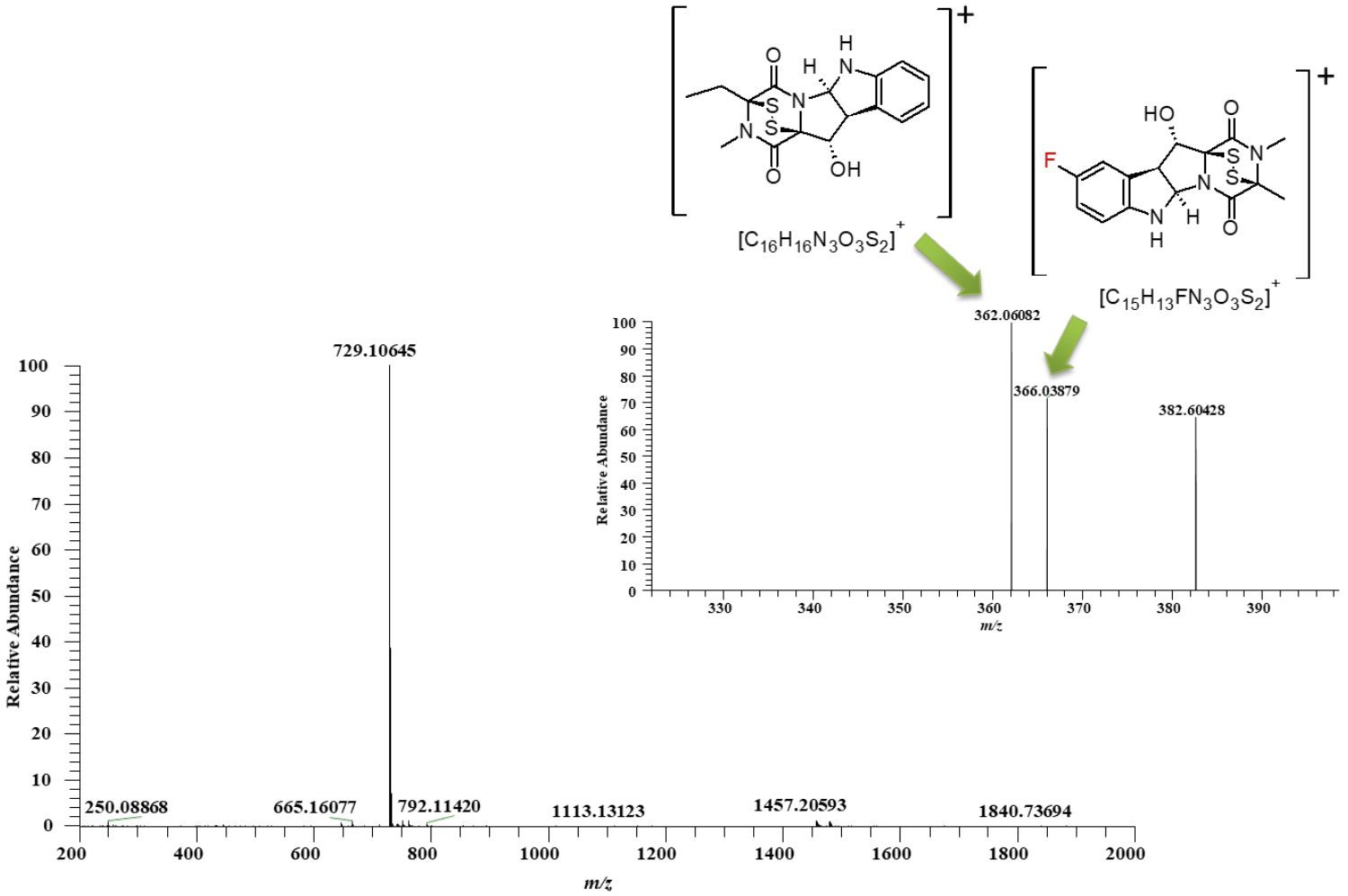

Figure S32. Full Scan MS Data of 9-F-Sch 52901 (6) with *m/z* 729.1065. HRMS-MS/MS fragmentation showed *m/z* 362.0608 and *m/z* 366.0388 (green arrow) indicating the incorporation of the fluorine to a specific monomer of Sch 52901 (**2**).

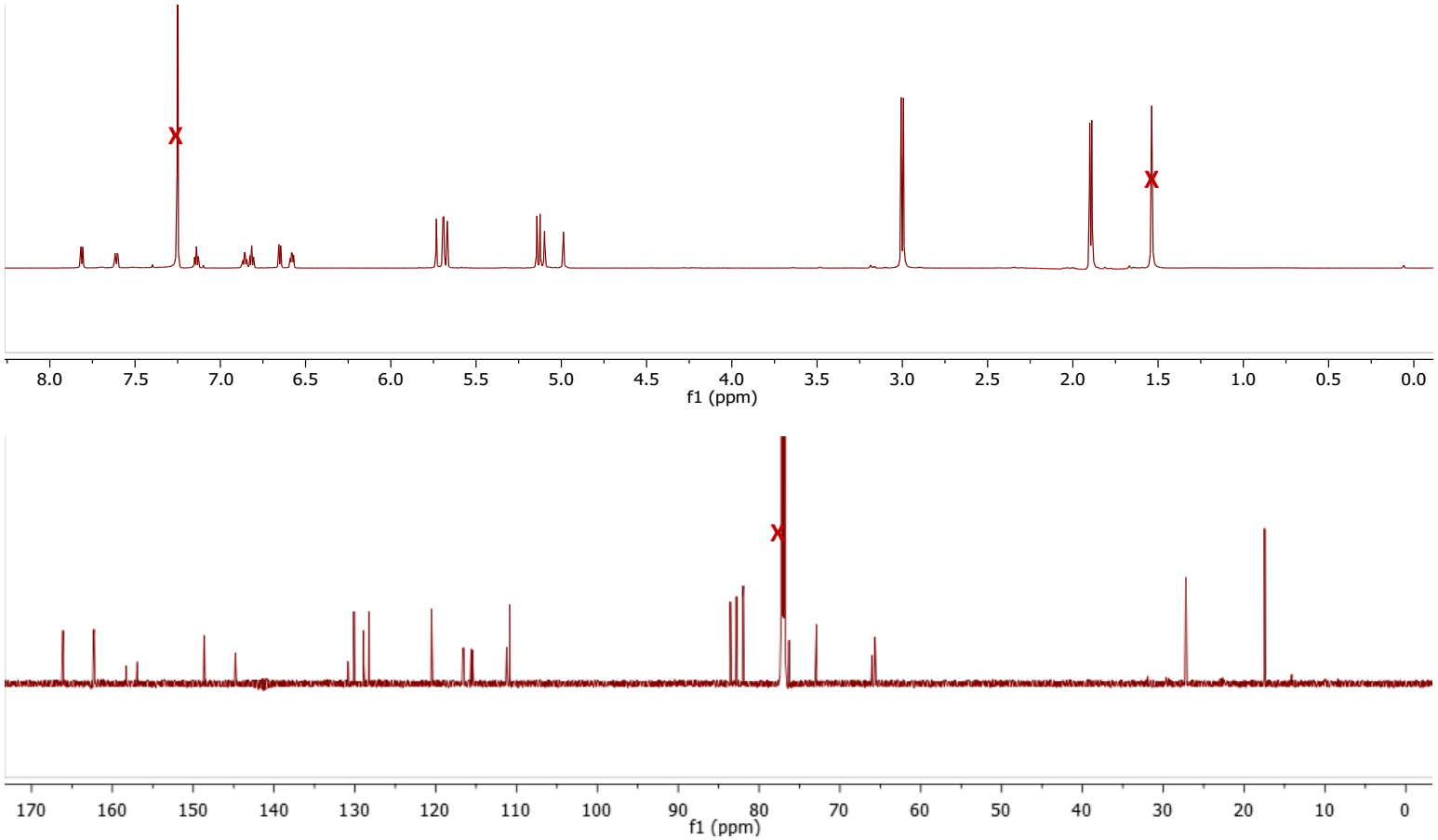

Figure S33. ^{1}H (upper panel) and ^{13}C (lower panel) NMR Spectra of 9-F-verticillin A (7) in $CDCl_3$ [700 MHz for ^{1}H and 175 MHz for ^{13}C].

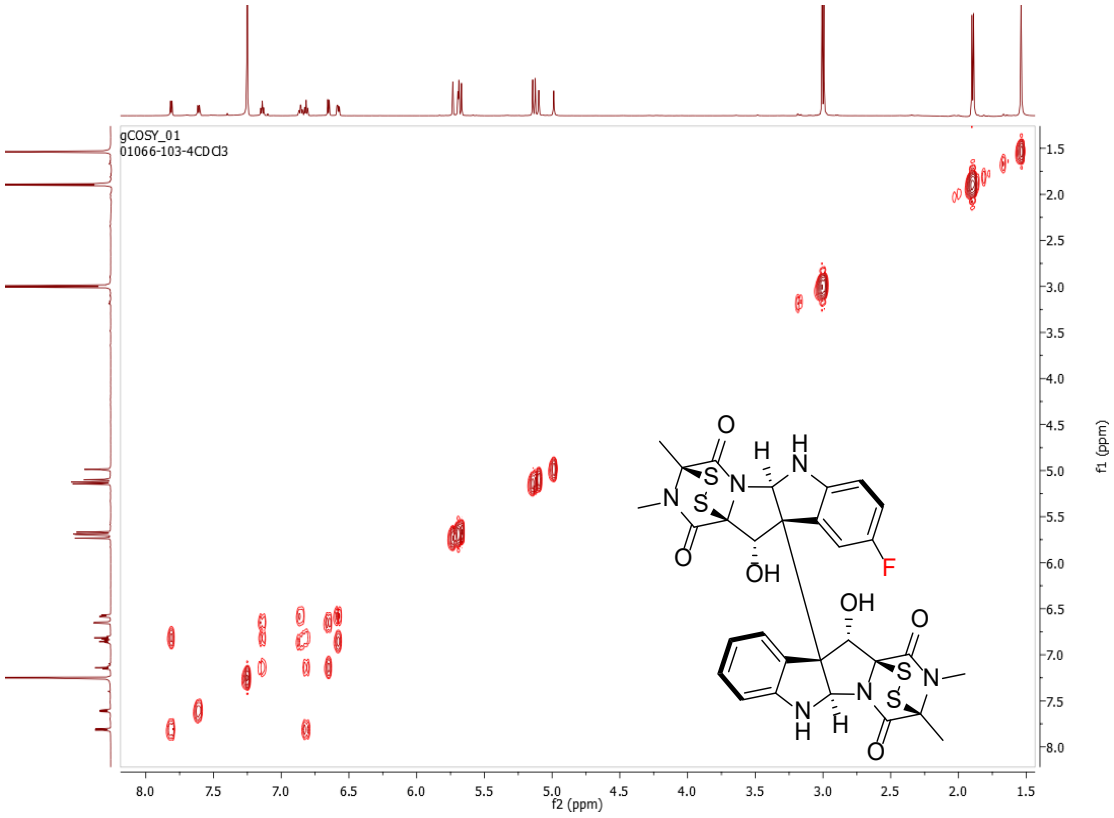

Figure S34. ^{1}H-^{1}H COSY NMR Spectrum of 9-F-verticillin A (7) in $CDCl_3$ (700 MHz).

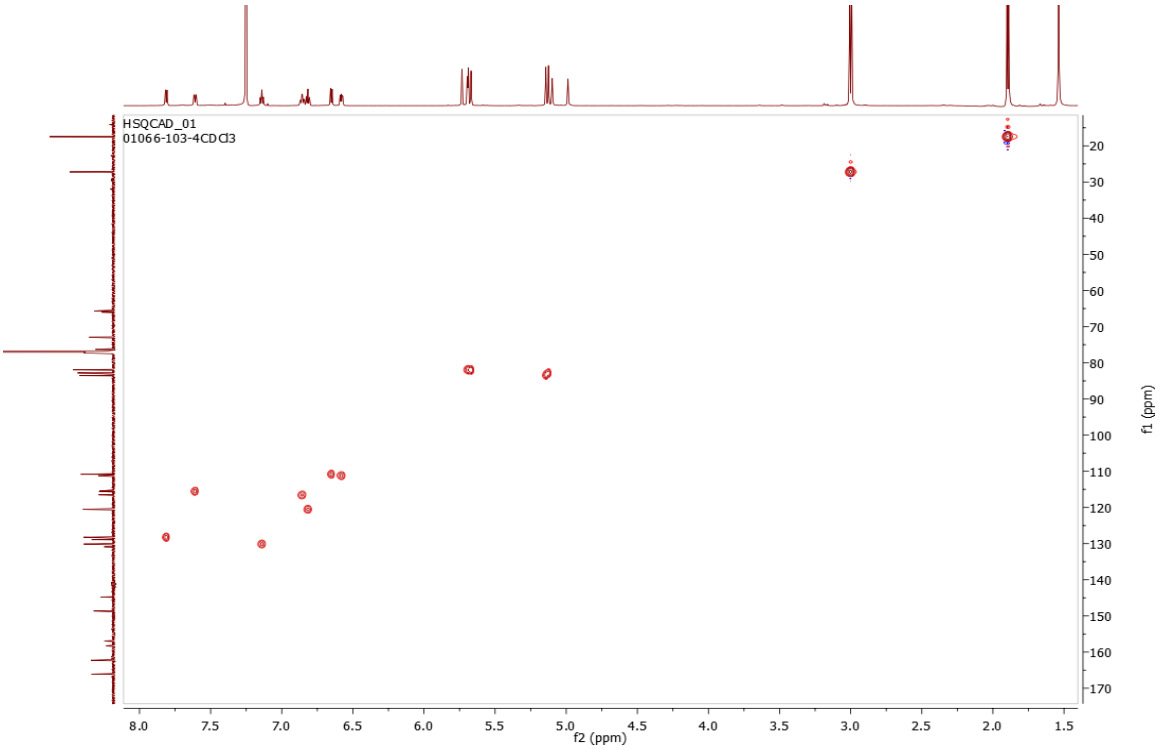

Figure S35. ^{1}H-^{13}C HSQC NMR Spectrum of 9-F-verticillin A (7) in $CDCl_3$ (700 MHz).

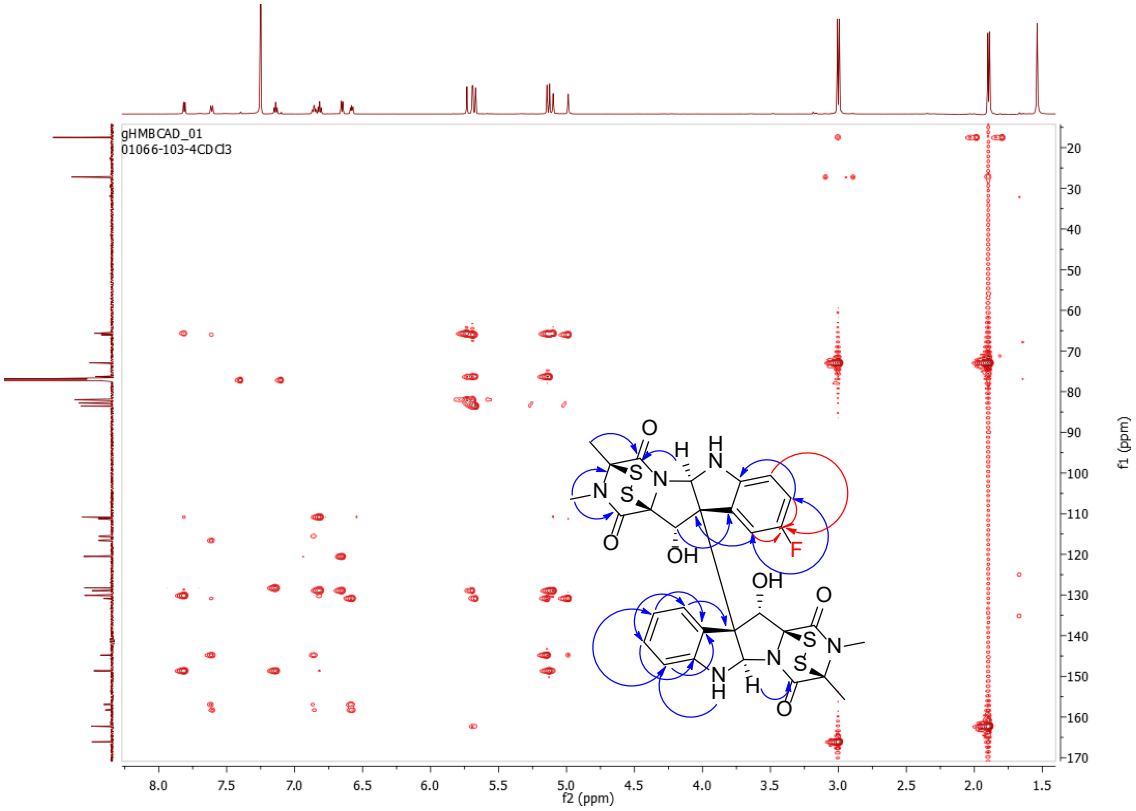

Figure S36. ^{1}H-^{13}C HMBC NMR Spectrum of 9-F-verticillin A (7) in $CDCl_3$ (700 MHz). The red arrows show the correlations between the protons in positions H-7, H-8 and H-10 with the characteristic carbon at C-9 that contains the fluorine atom.

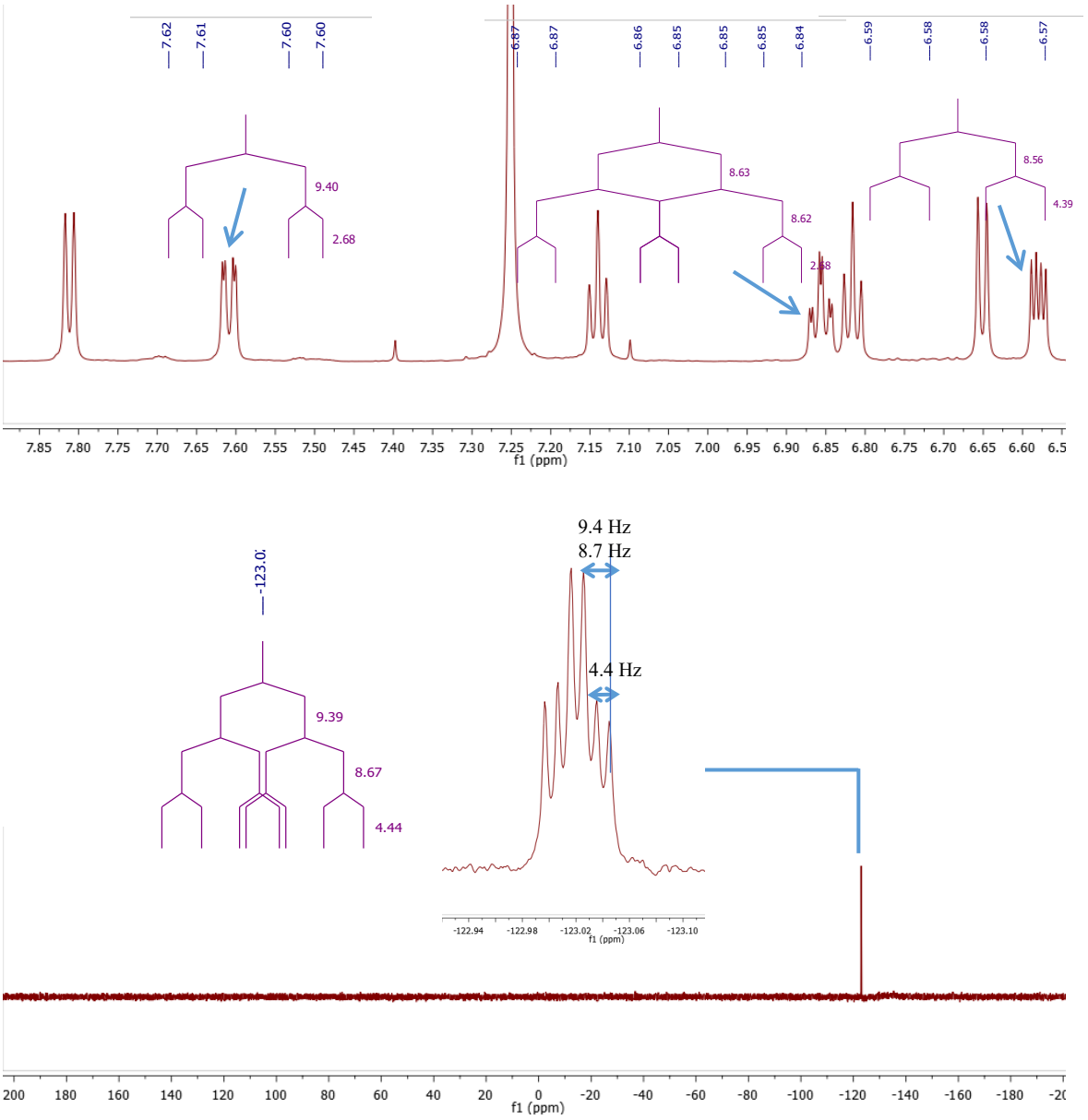

Figure S37. ^{1}H (upper panel) and ^{19}F (lower panel) NMR Spectra of 9-F-verticillin A (7) in $CDCl_3$ [700 MHz for ^{1}H and 470 MHz for ^{19}F].

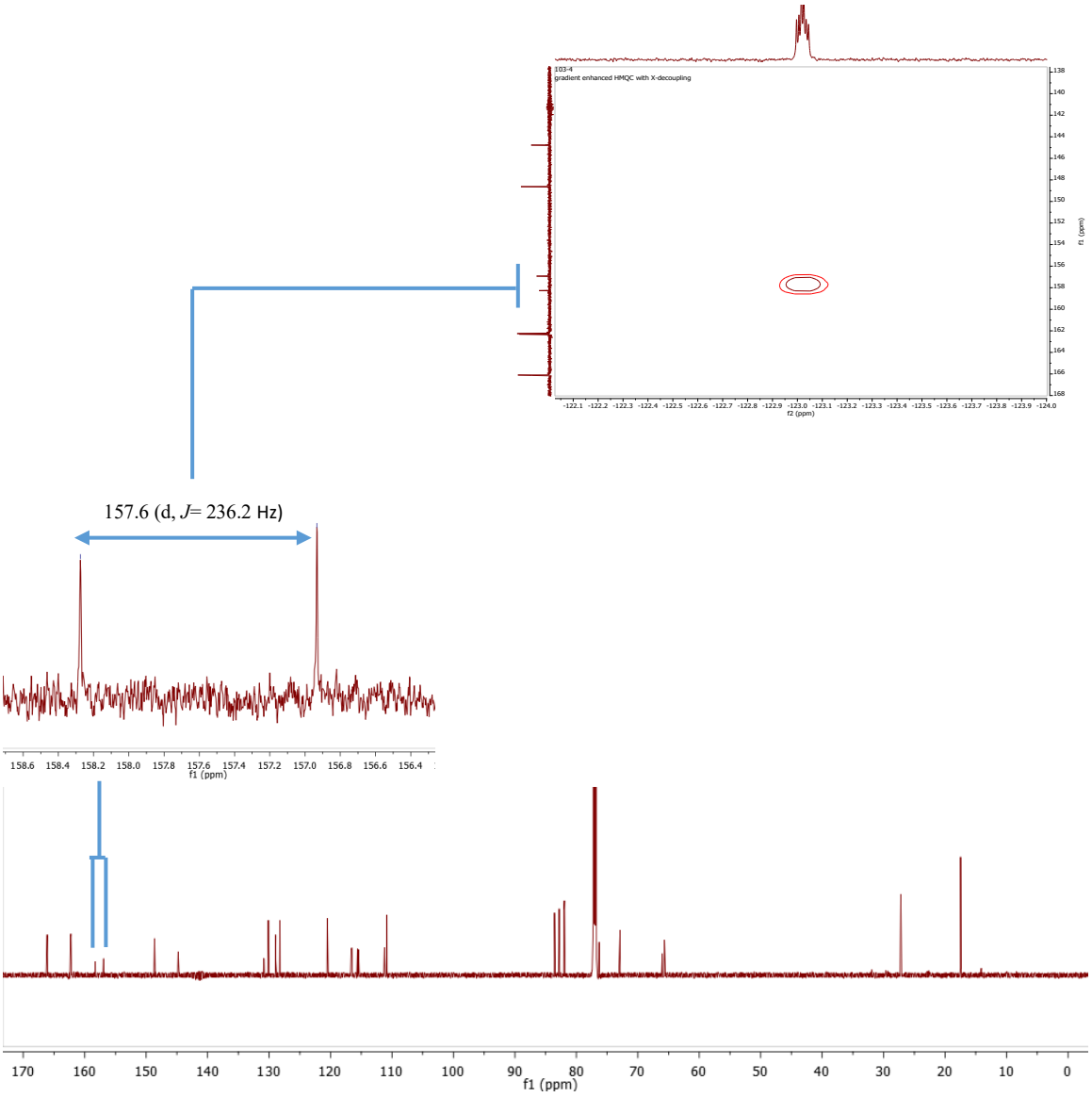

Figure S38.^{13}C NMR (lower panel) and ^{19}F-^{13}C HMQC NMR Spectra of 9-F-verticillin A (7) in $CDCl_3$ [175 MHz for ^{13}C and 470 MHz for ^{19}F].

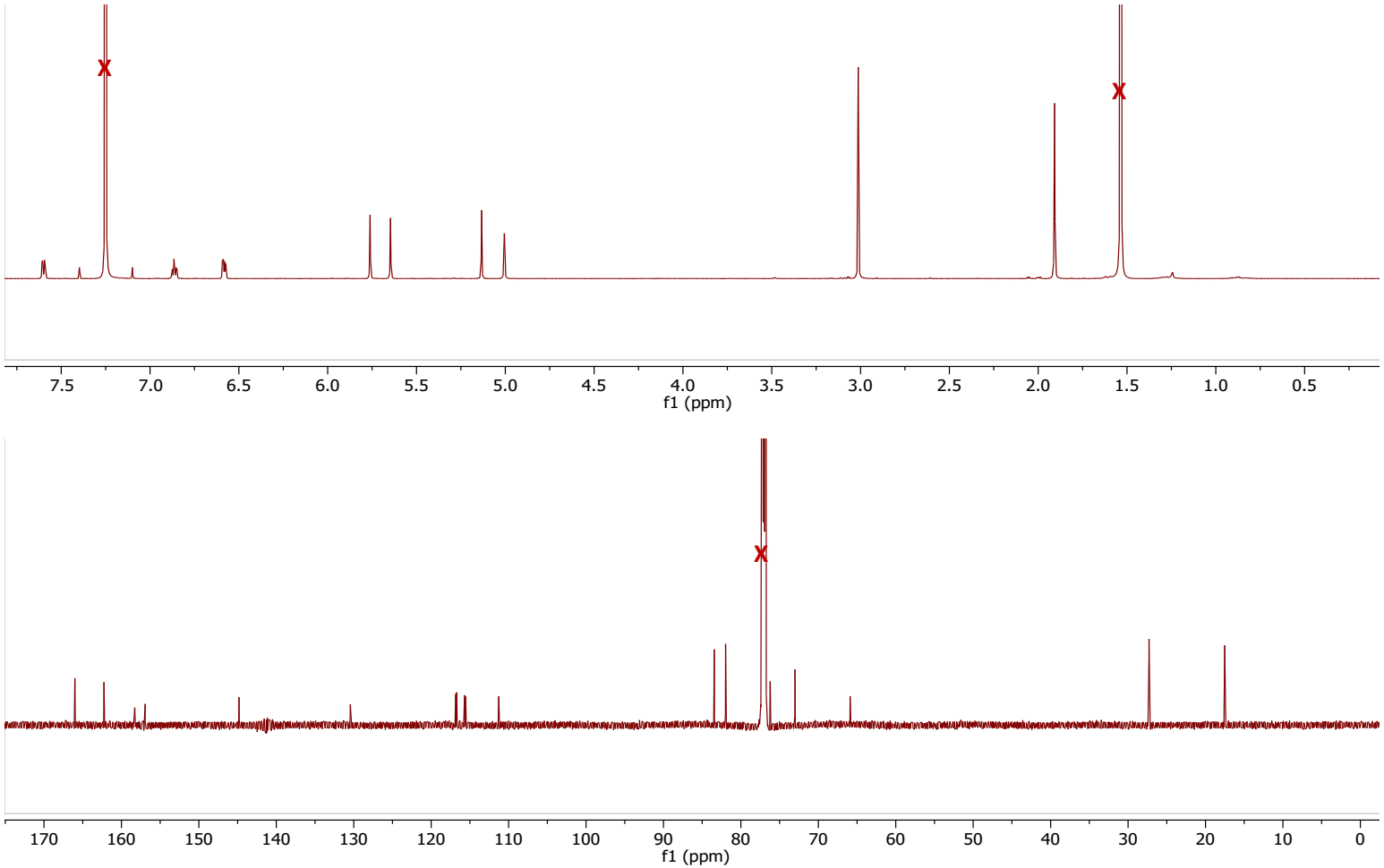

Figure S39. ^{1}H (upper panel) and ^{13}C (lower panel) NMR Spectra of 9,9′-di F-verticillin A (8) in $CDCl_3$ [700 MHz for ^{1}H and 175 MHz for ^{13}C].

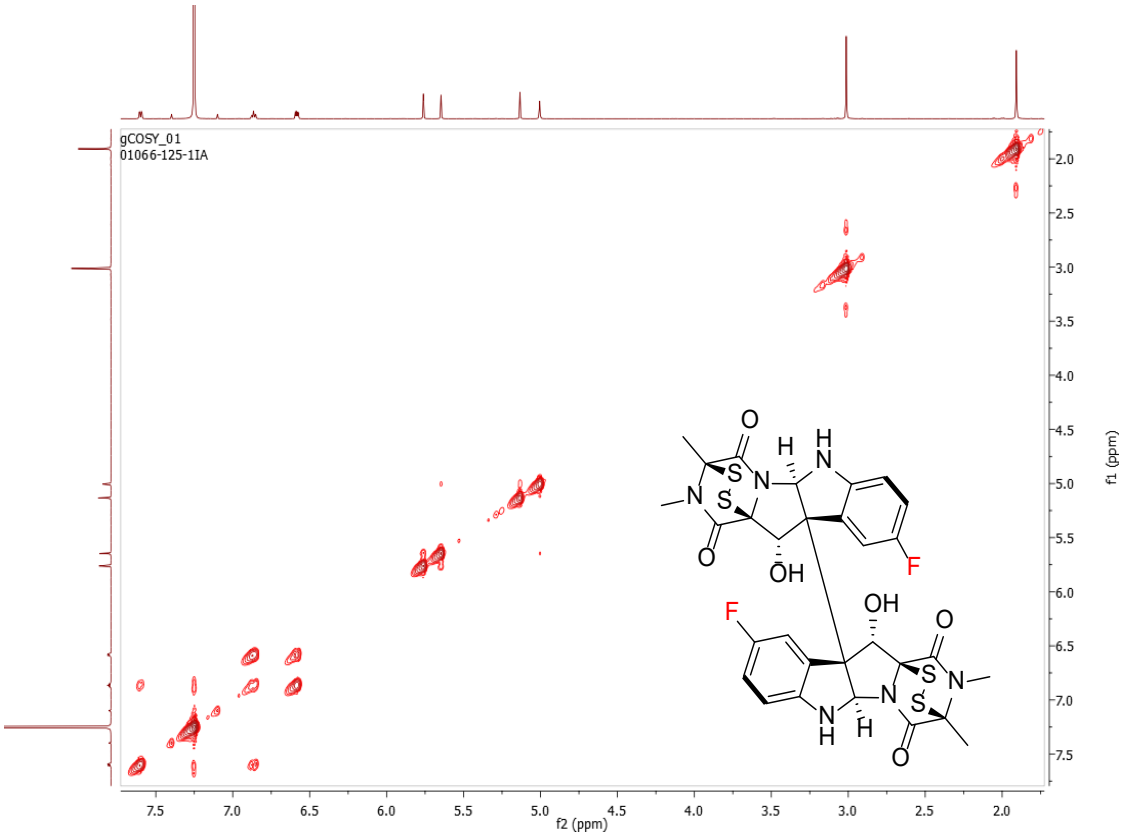

Figure S40. ^{1}H-^{1}H COSY NMR Spectrum of 9,9′-di F-verticillin A (8) in $CDCl_3$ (700 MHz).

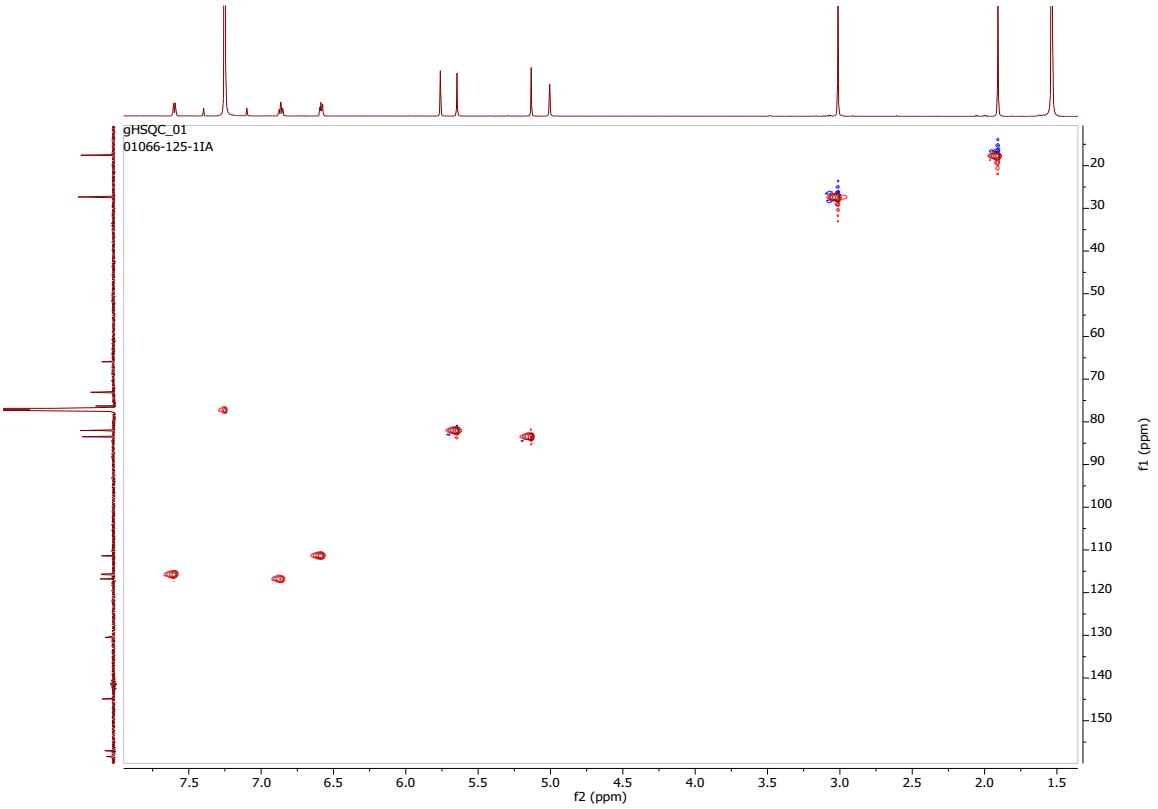

Figure S41. ^{1}H-^{13}C HSQC NMR Spectrum of 9,9′-di F-verticillin A (8) in $CDCl_3$ (700 MHz).

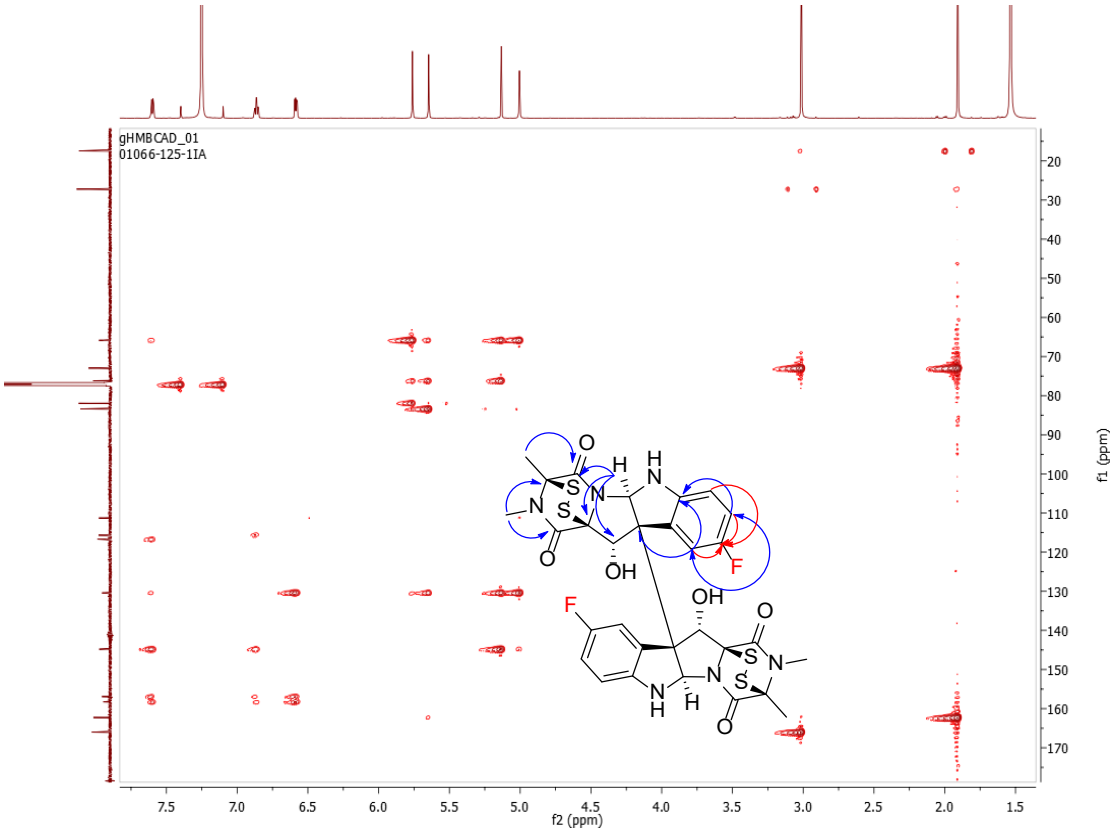

Figure S42. ^{1}H-^{13}C HMBC NMR Spectrum of 9,9′-di F-verticillin A (8) in $CDCl_3$ (700 MHz). The red arrows show the correlations between the protons in positions H-7, H-8, and H-10 with the characteristic carbon at C-9 that contains the fluorine atom. Those correlations are true for the other half of the dimer.

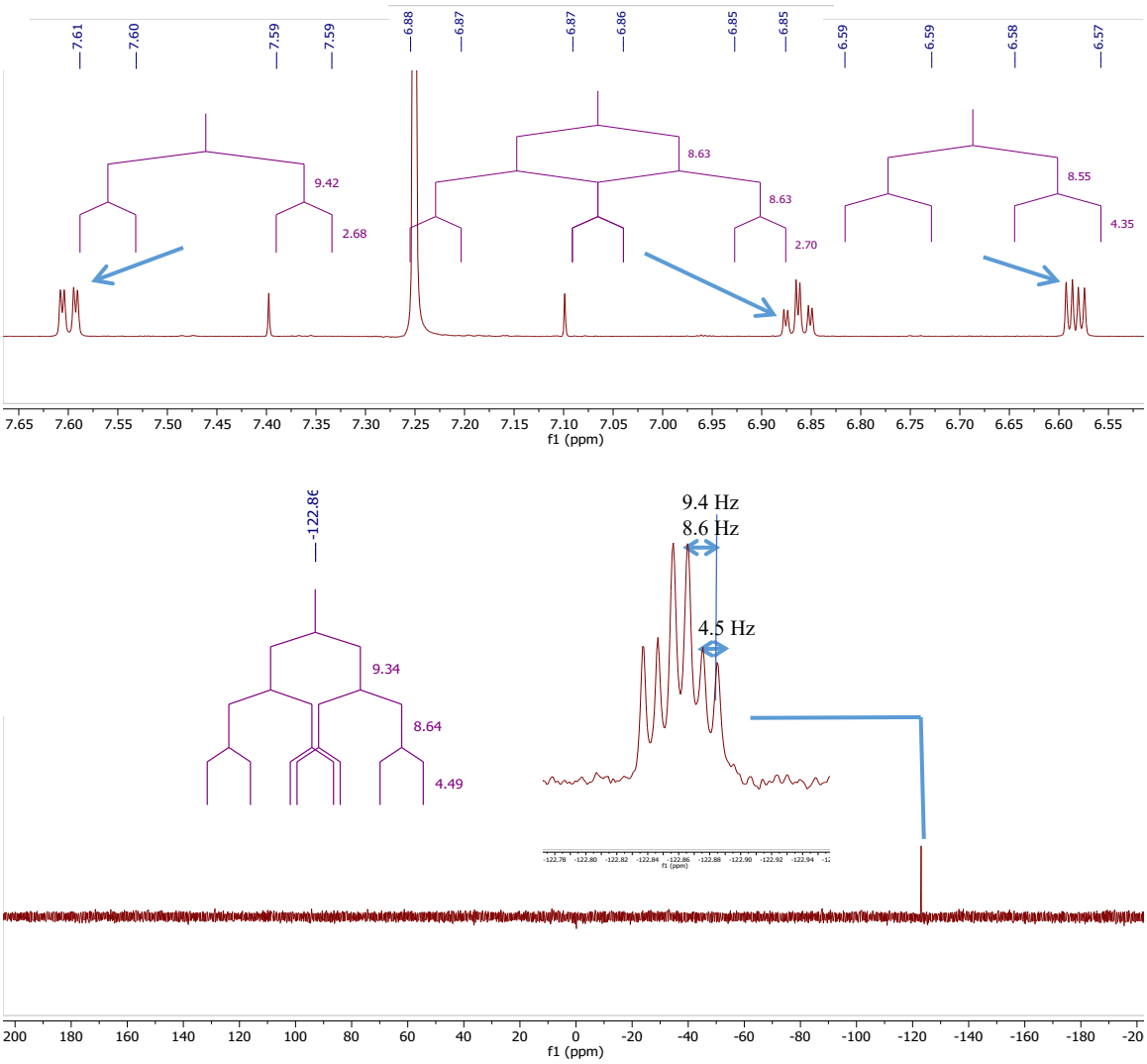

Figure S43. ^{1}H (upper panel) and ^{19}F (lower panel) NMR Spectra of 9,9′-di F-verticillin A (8) in $CDCl_3$ [700 MHz for ^{1}H and 470 MHz for ^{19}F].

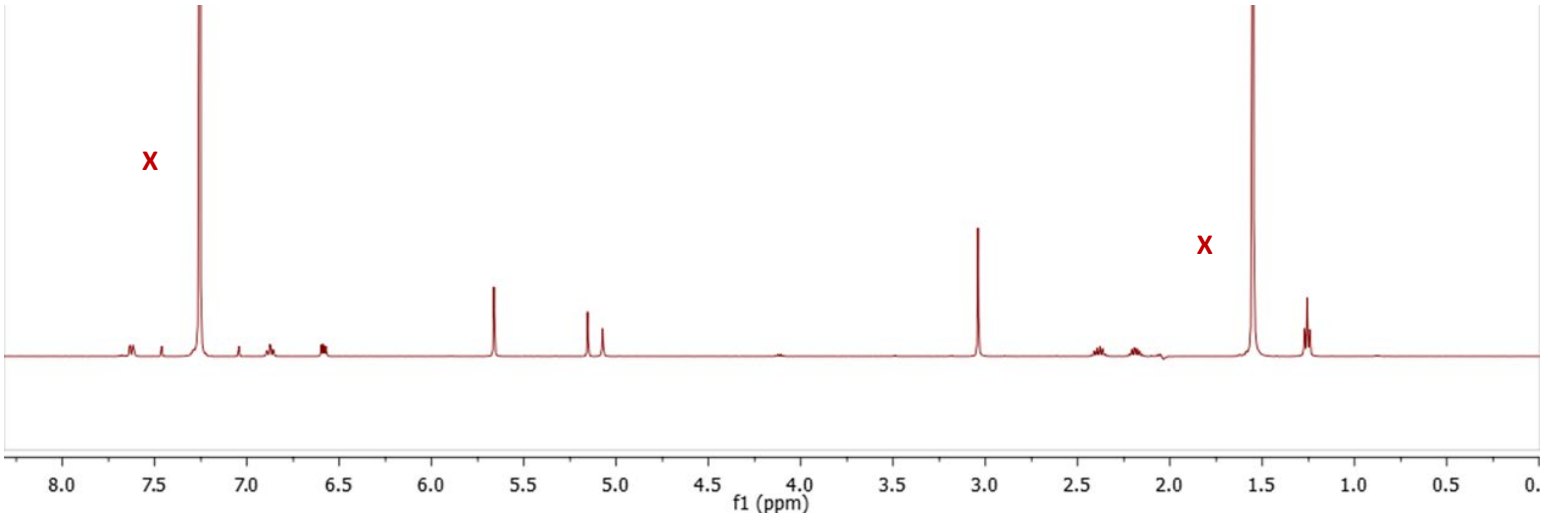

Figure S44. ^{1}**H NMR Spectrum of 9,9′-di F-verticillin H (9) in** $CDCl_3$ [500 MHz].

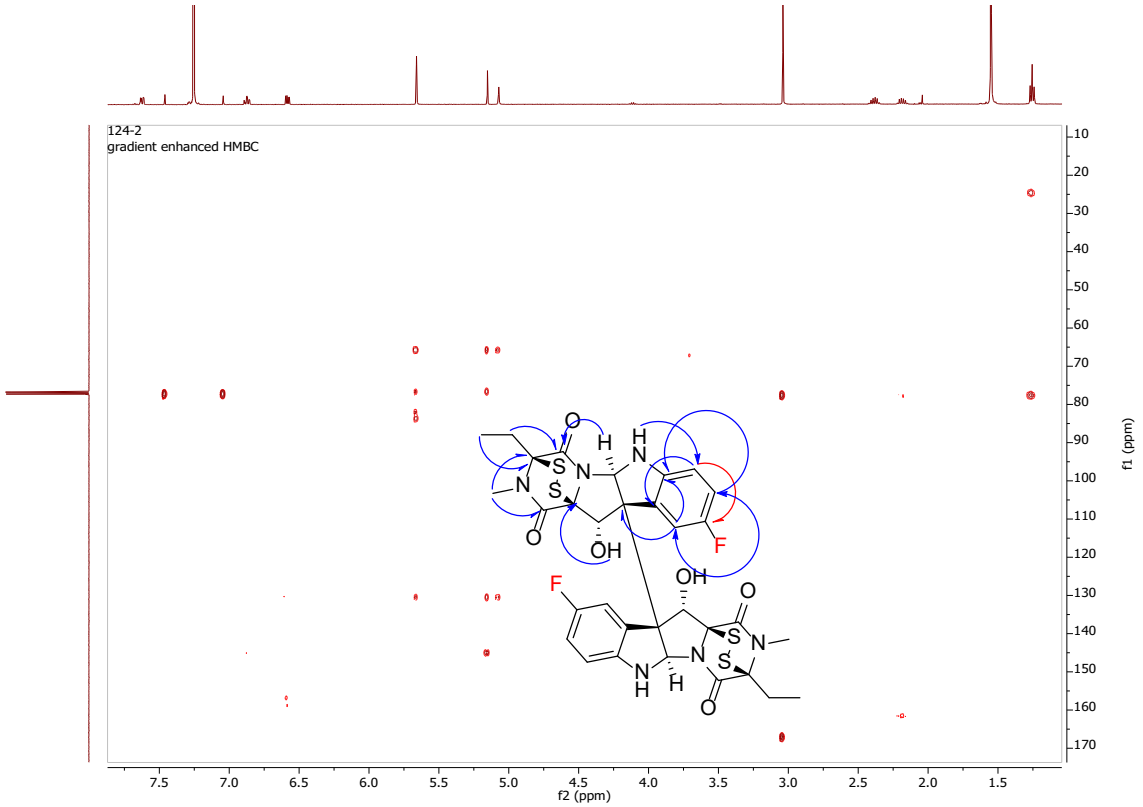

Figure S45. ^{1}H-^{13}C HMBC NMR Spectrum of 9,9′-di F-verticillin H (9) in $CDCl_3$ (500 MHz). The red arrow shows the correlation between the protons in position H-7 with the characteristic carbon at C-9 that contains the fluorine atom. Those correlations are true for the other half of the dimer.

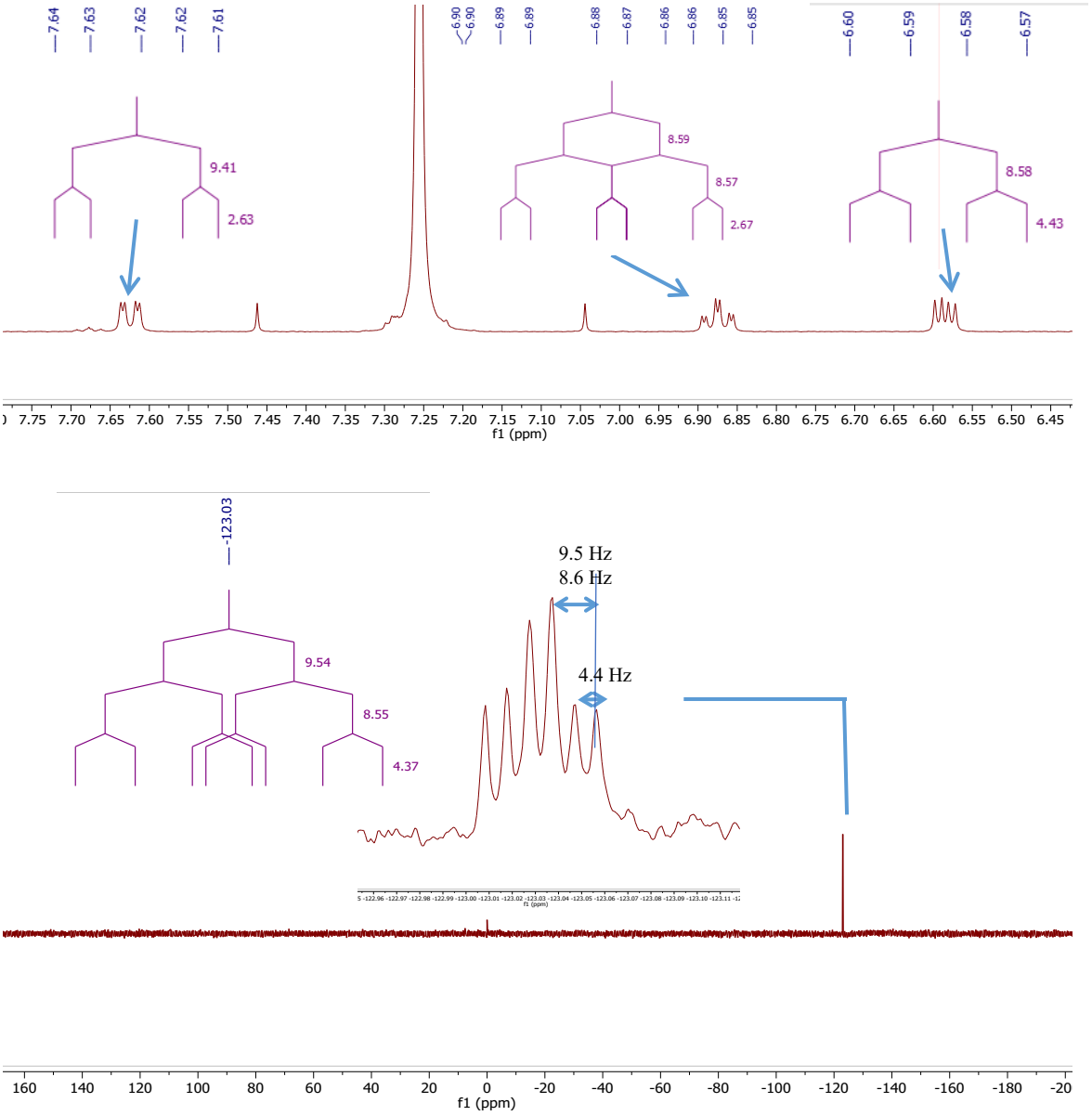

Figure S46. ^{1}H (upper panel) and ^{19}F (lower panel) NMR Spectra of 9,9′-di F-verticillin H (9) in $CDCl_3$ [500 MHz for ^{1}H and 470 MHz for ^{19}F].

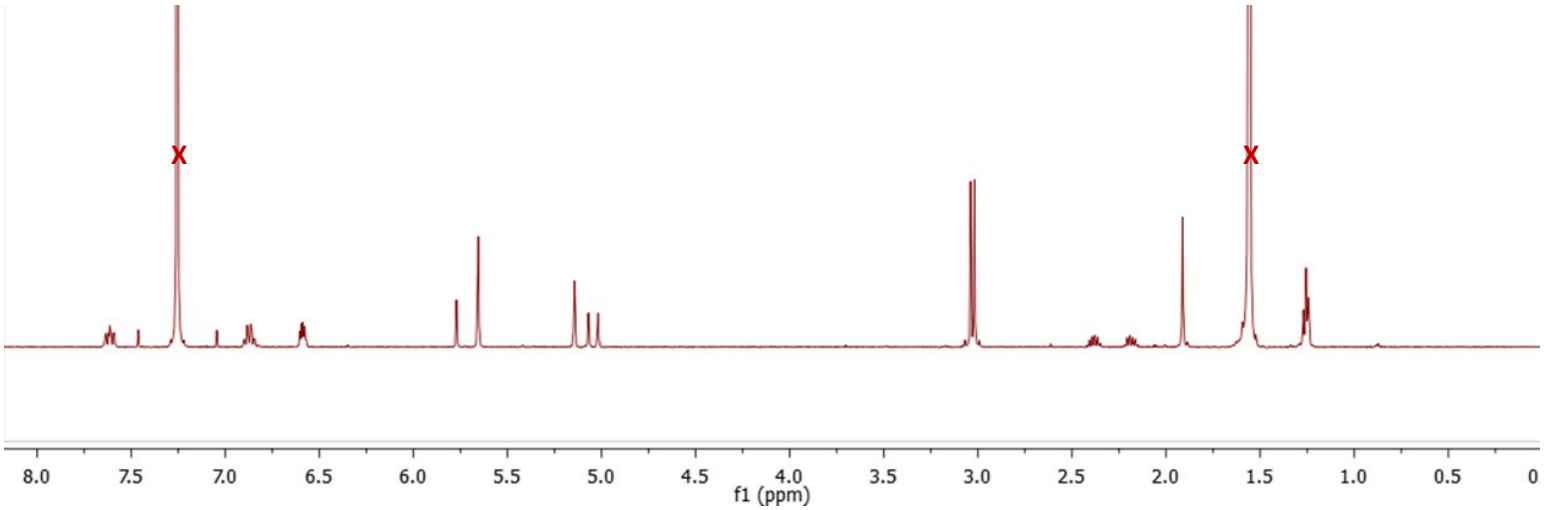

Figure S47. ^{1}H NMR Spectrum of 9,9′-di F-Sch 52901 (10) in $CDCl_3$ [500 MHz].

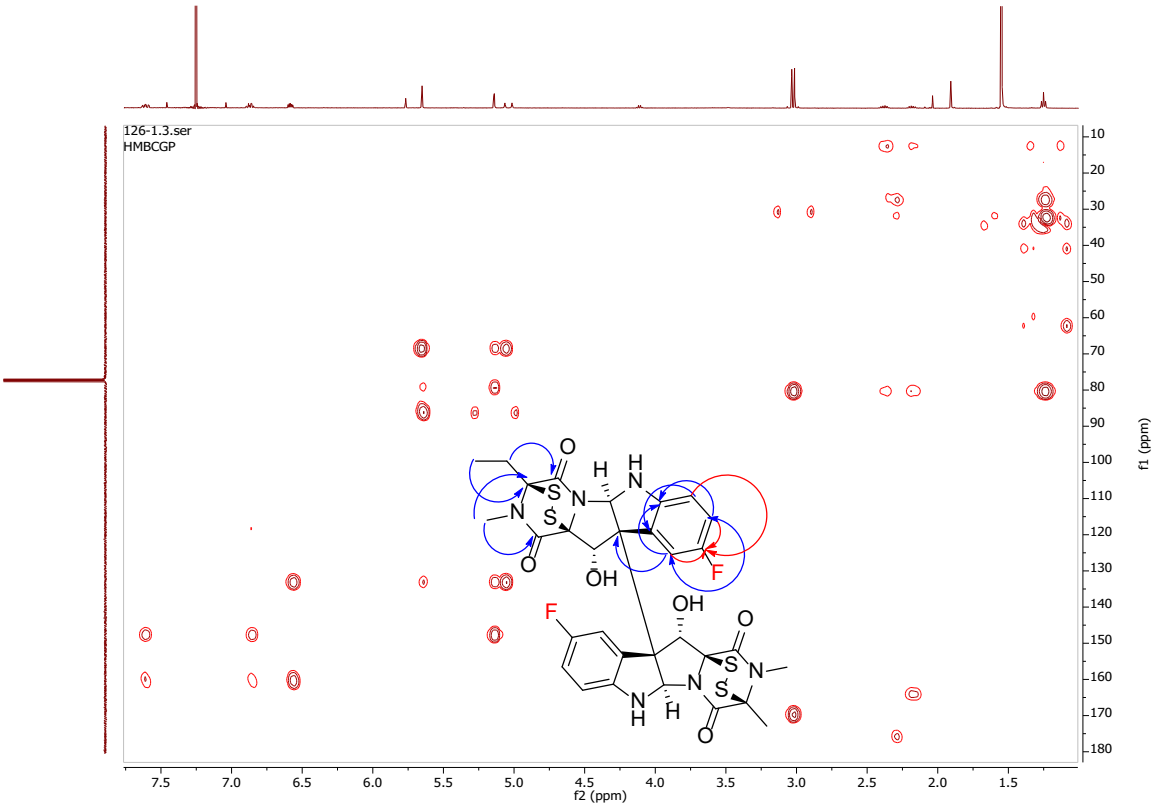

Figure S48. ^{1}H-^{13}C HMBC NMR Spectrum of 9,9′-di F-Sch 52901 (10) in $CDCl_3$ (500 MHz). The red arrows show the correlation between the protons in positions H-7 H-8, and H-10 with the characteristic carbon at C-9 that contains the fluorine atom. Those correlations are true for the other half of the dimer.

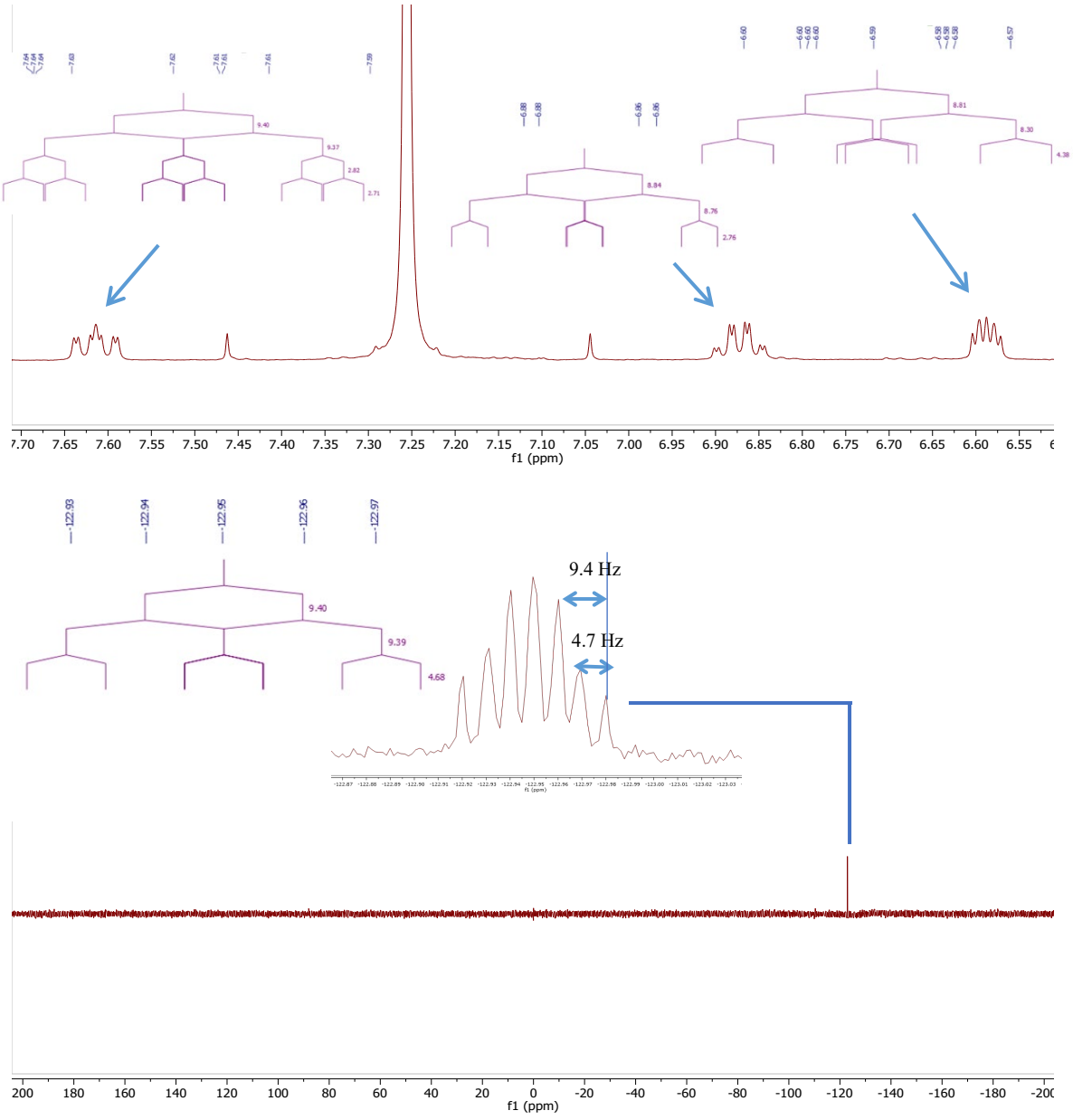

Figure S49. ^{1}H (upper panel) and ^{19}F (lower panel) NMR Spectra of 9,9′-di F-Sch 52901 (10) in $CDCl_3$ [500 MHz for ^{1}H and 470 MHz for ^{19}F].

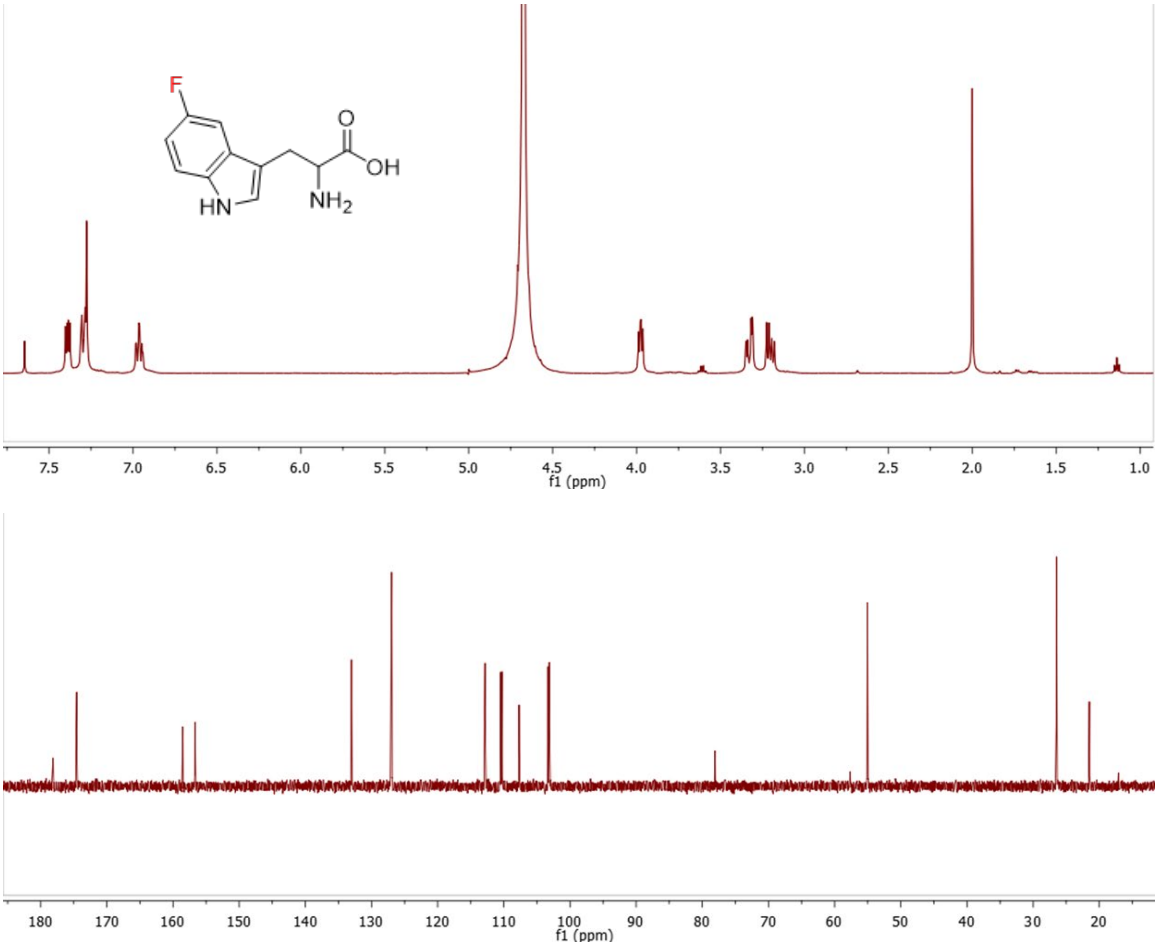

Figure S50. ^{1}H (upper panel) and ^{13}C (lower panel) NMR Spectra of 5-F-Tryptophan in D_2O [500 MHz for ^{1}H and 125 MHz for ^{13}C].

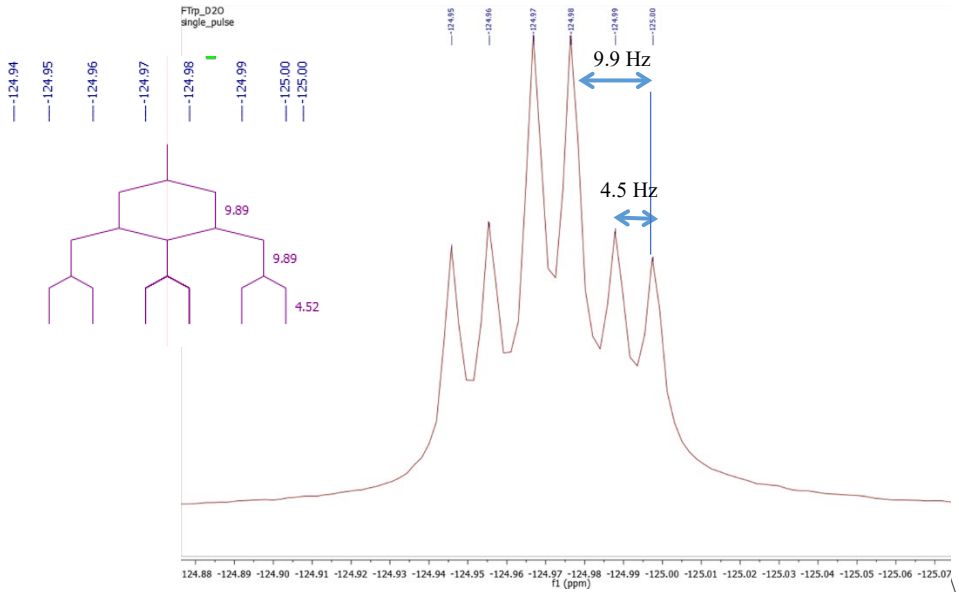

Figure S51. ^{19}F NMR Spectra of 5-F-Tryptophan in D_2O [470 MHz].

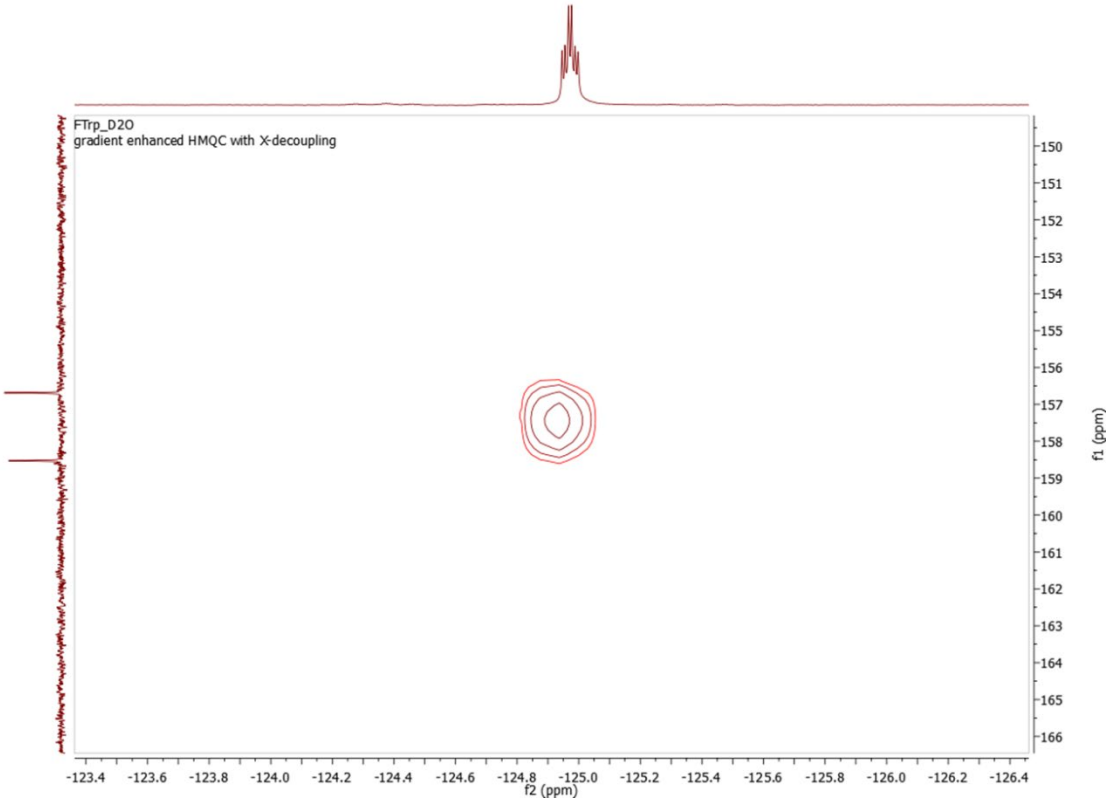

Figure S52. ^{19}F-^{13}C HMQC NMR Spectrum of 5-F-Tryptophan in D_2O [175 MHz for ^{13}C and 470 MHz for ^{19}F].

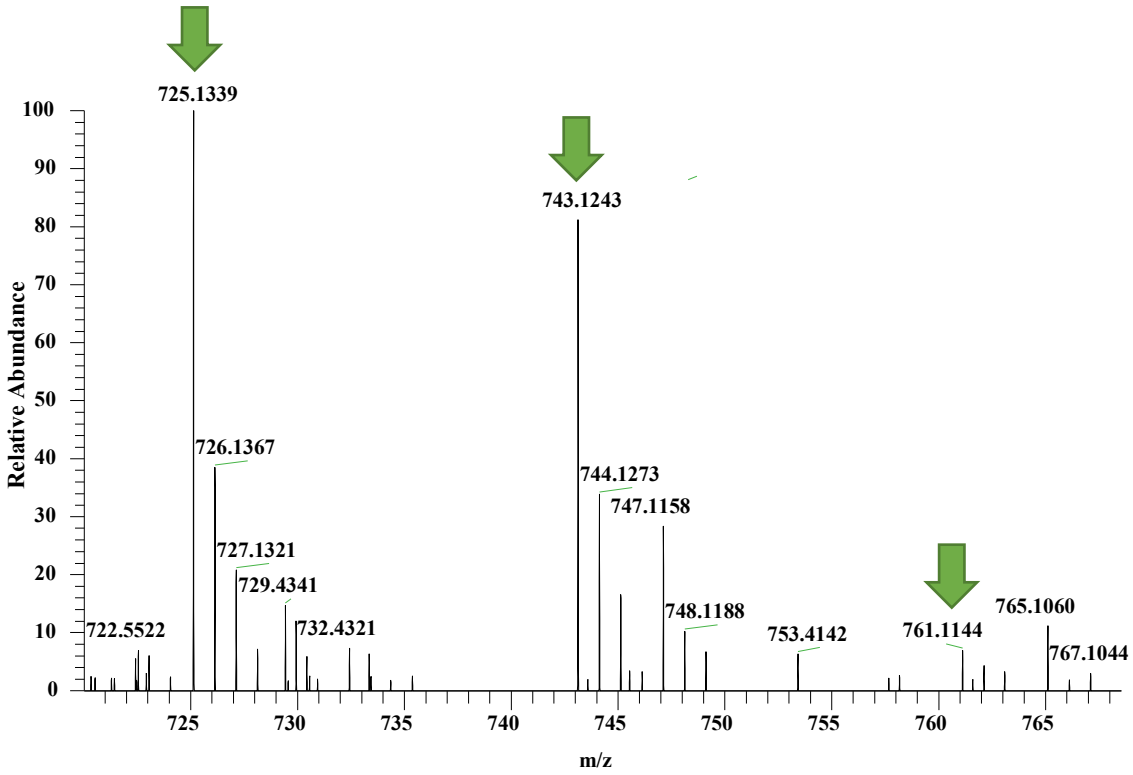

Figure S53. Full Scan MS Data of Strain MSX59553 Grown on Oatmeal Agar Medium Supplemented with 5-F-D-Trp. The plates were microextracted *in situ* using a droplet probe coupled to a hyphenated system (UPLC-PDA-HRMS-MS/MS). The peaks indicated with green arrows (*m/z* 725.1339, 743.1243, 761.1144) correspond to the mass of verticillin H (**1**), the incorporation of one fluorine atom, and the incorporation of two fluorine atoms in the molecule, respectively.

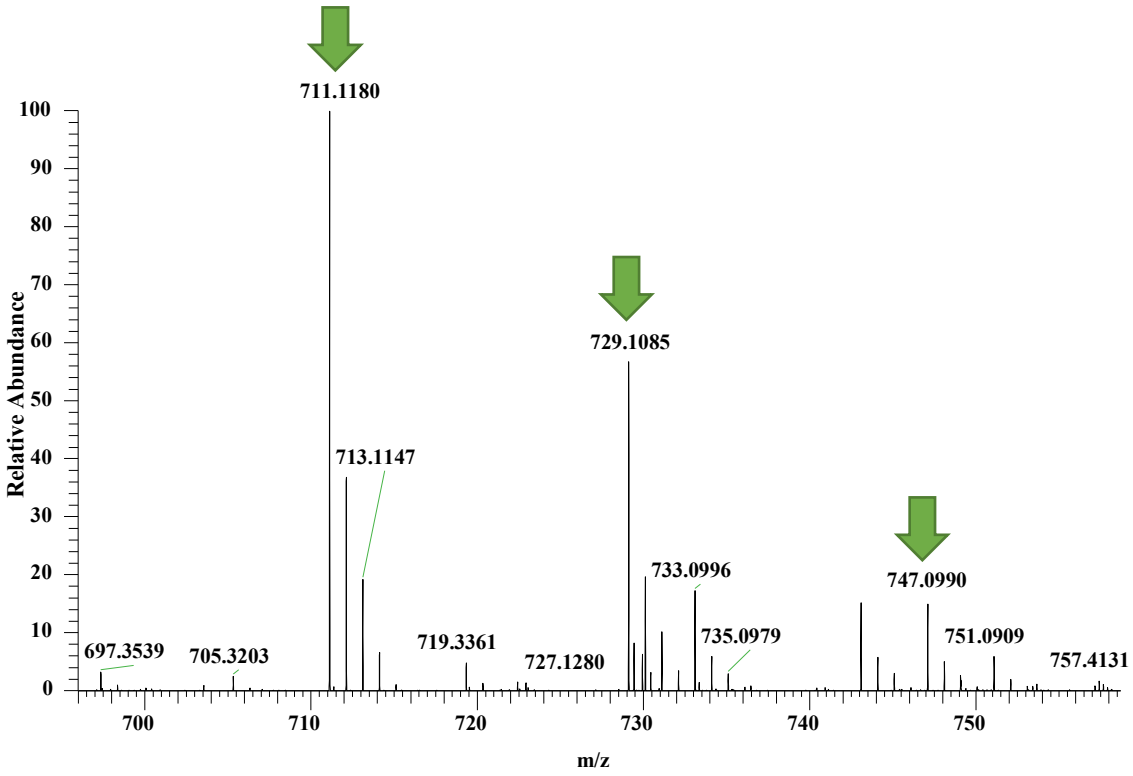

Figure S54. Full Scan MS Data of Strain MSX59553 Grown on Oatmeal Agar Medium Supplemented with 5-F-D-Trp. The plates were microextracted *in situ* using a droplet probe coupled to a hyphenated system (UPLC-PDA-HRMS-MS/MS). The peaks indicated with green arrows (*m/z* 711.1180, 729.1085, 747.0990) correspond to the mass of Sch 52901 (**2**), the incorporation of one fluorine atom, and the incorporation of two fluorine atoms in the molecule, respectively.

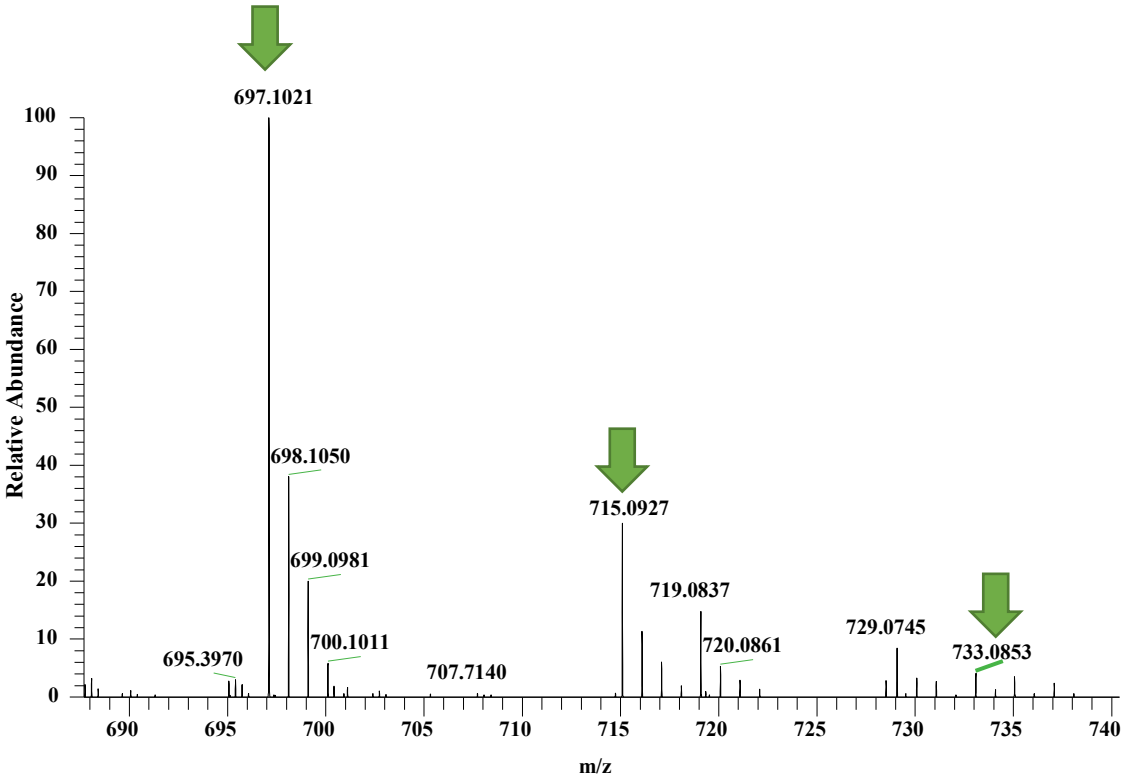

Figure S55. Full Scan MS Data of Strain MSX59553 Grown on Oatmeal Agar Medium Supplemented with 5-F-D-Trp. The plates were microextracted *in situ* using a droplet probe coupled to a hyphenated system (UPLC-PDA-HRMS-MS/MS). The peaks indicated with green arrows (*m/z* 697.1021, 715.0927, 733.0853) correspond to the mass of verticillin A (**3**), the incorporation of one fluorine atom, and the incorporation of two fluorine atoms in the molecule, respectively.

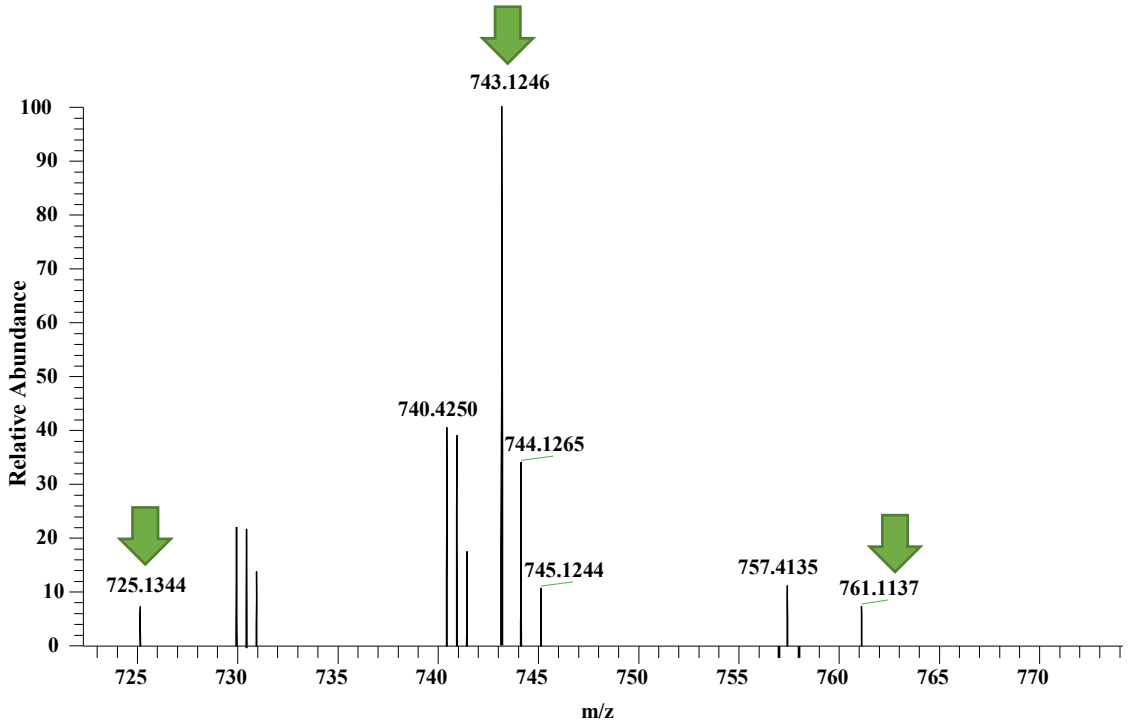

Figure S56. Full Scan MS Data of Strain MSX59553 Grown on Oatmeal Agar Medium Supplemented with 5-F-L-Trp. The plates were microextracted *in situ* using a droplet probe coupled to a hyphenated system (UPLC-PDA-HRMS-MS/MS). The peaks indicated with green arrows (*m/z* 725.1344, 743.1246, 761.1137) correspond to the mass of verticillin H (**1**), the incorporation of one fluorine atom, and the incorporation of two fluorine atoms in the molecule, respectively.

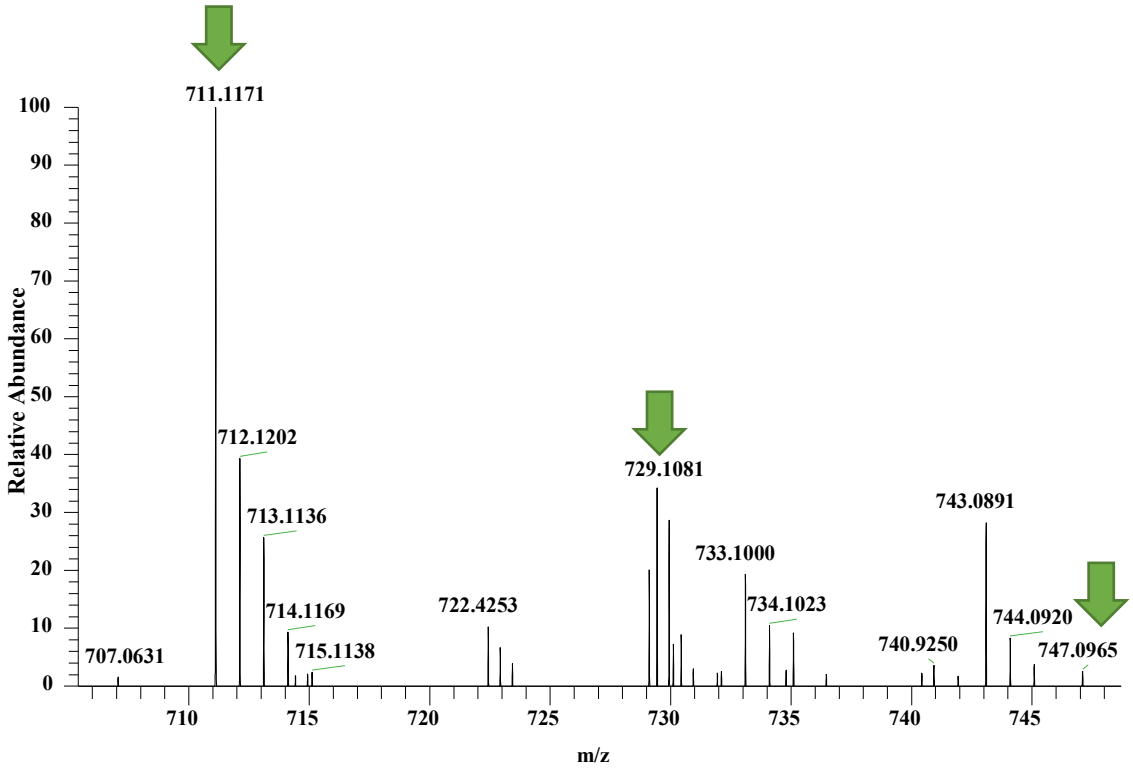

Figure S57. Full Scan MS Data of Strain MSX59553 Grown on Oatmeal Agar Medium Supplemented with 5-F-L-Trp. The plates were microextracted *in situ* using a droplet probe coupled to a hyphenated system (UPLC-PDA-HRMS-MS/MS). The peaks indicated with green arrows (*m/z* 711.1171, 729.1081, 747.0965) correspond to the mass of Sch 52901 (**2**), the incorporation of one fluorine atom, and the incorporation of two fluorine atoms in the molecule, respectively.

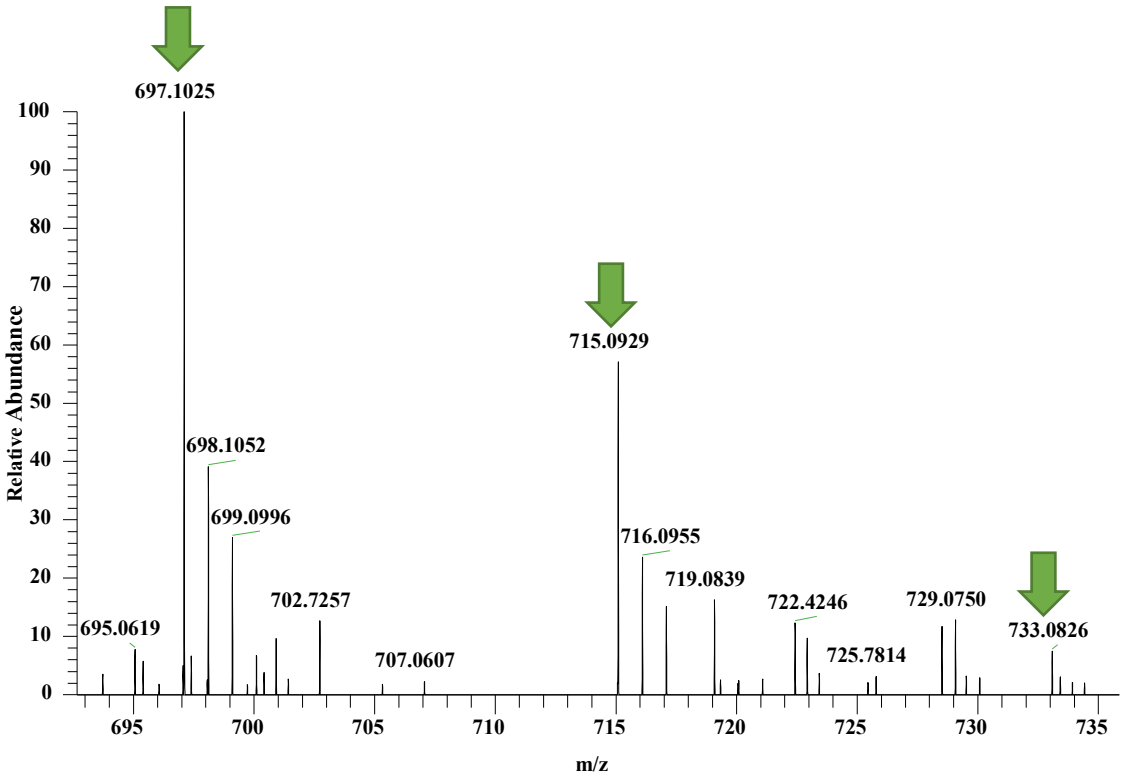

Figure S58. Full Scan MS Data of Strain MSX59553 Grown on Oatmeal Agar Medium Supplemented with 5-F-L-Trp. The plates were microextracted *in situ* using a droplet probe coupled to a hyphenated system (UPLC-PDA-HRMS-MS/MS). The peaks indicated with green arrows (*m/z* 697.1025, 715.0929, 733.0826) correspond to the mass of verticillin A (**3**), the incorporation of one fluorine atom, and the incorporation of two fluorine atoms in the molecule, respectively.

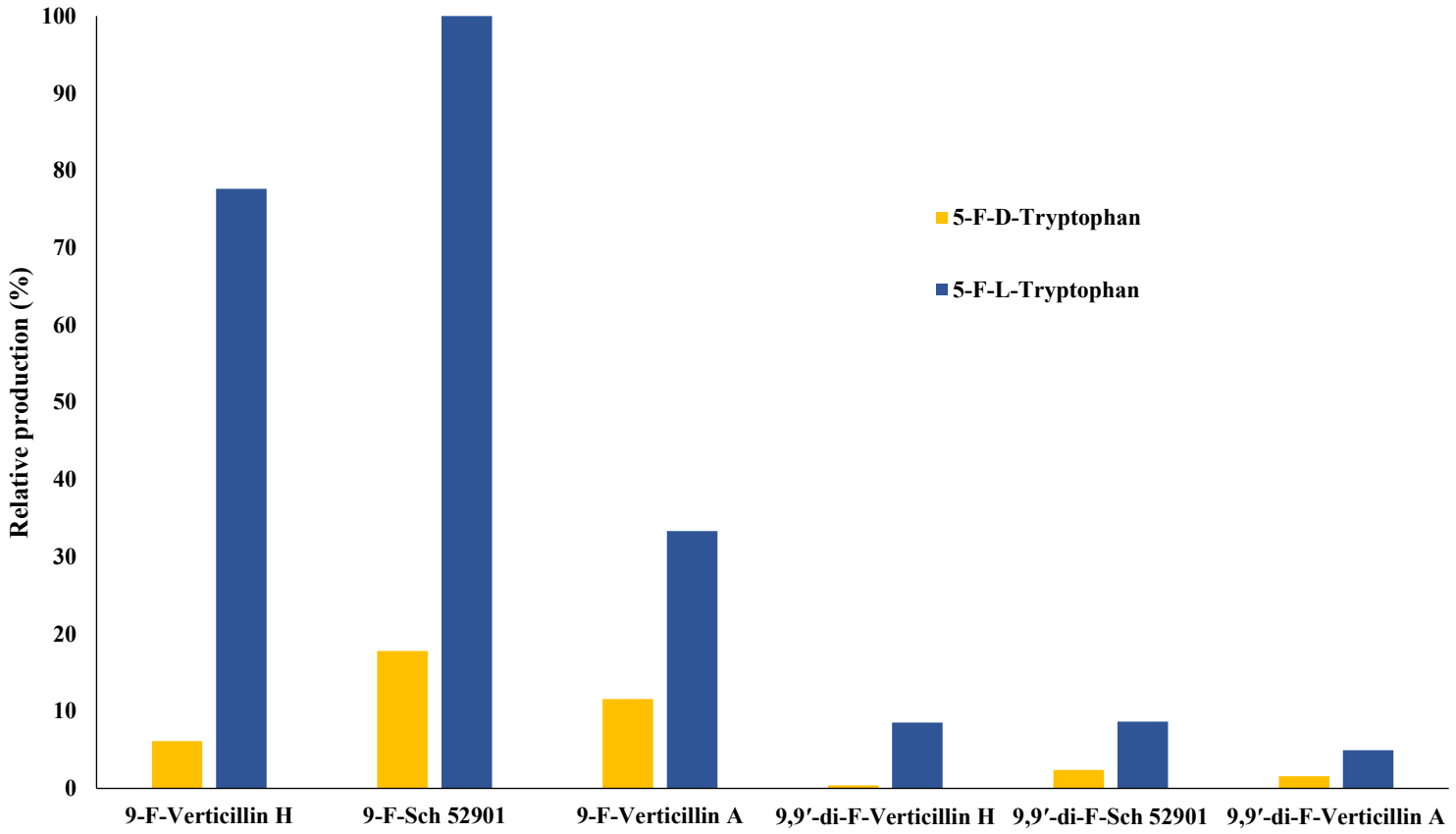

Figure S59. Relative Production of Fluorinated Verticillin Analogues via UPLC-HRMS Analysis of Extracted Petri Dishes used Previously for the Droplet Probe Analysis. The *in-situ* extraction observed a detection of the expected masses of the fluorinated verticillin analogues in both 5-F-D-Trp and 5-F-L-Trp supplemented media. The relative percentages were normalized by multiplying the peak areas by the weight of their corresponding organic extracts. The results demonstrate that the 5-F-$_{L}$-Trp was the building block that was preferably incorporated in the total production of the fluorinated verticillin analogues.

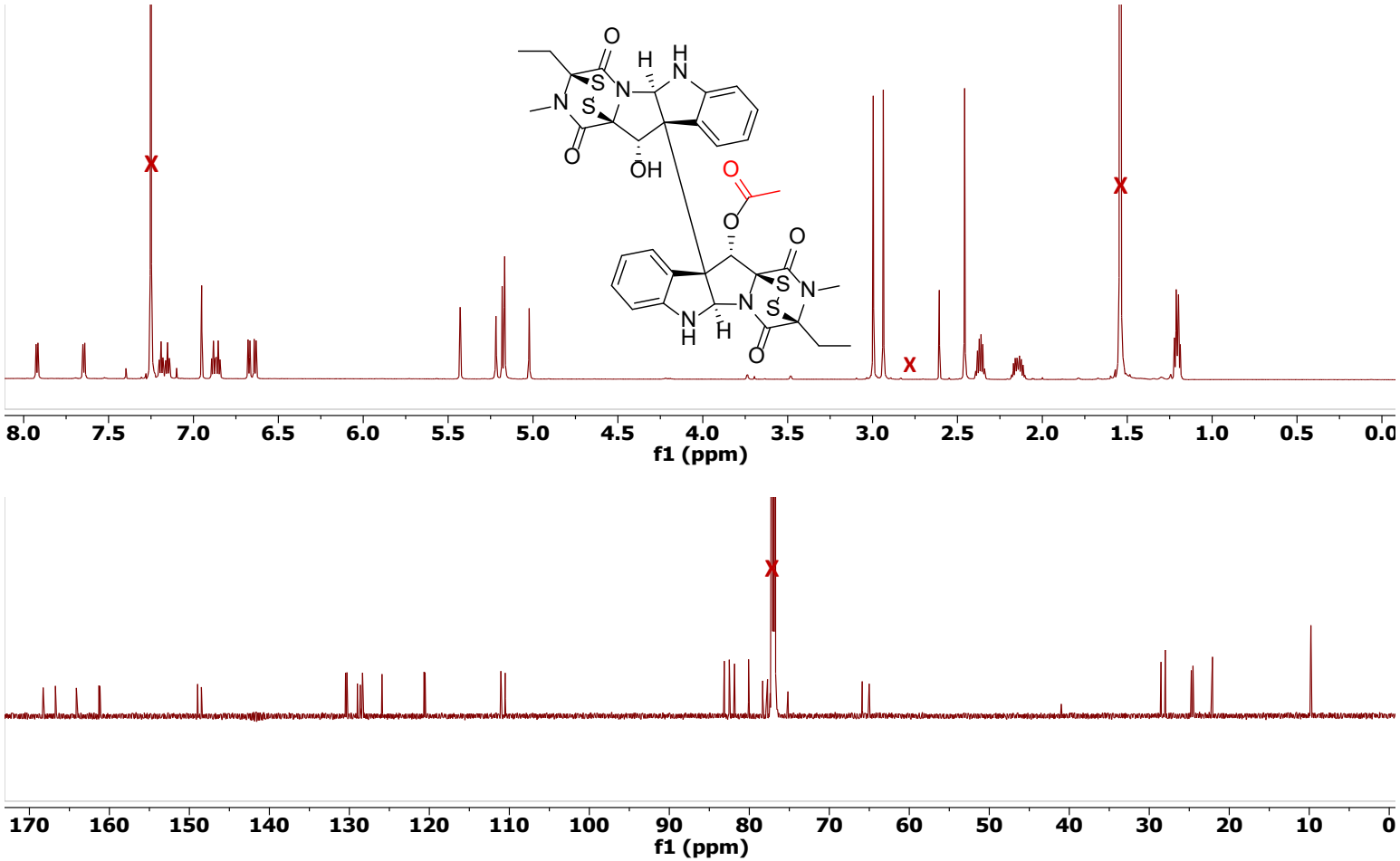

Figure S60. ^{1}H (upper panel) and ^{13}C (lower panel) NMR Spectra of 3 in $CDCl_3$ [700 MHz for ^{1}H and 175 MHz for ^{13}C].

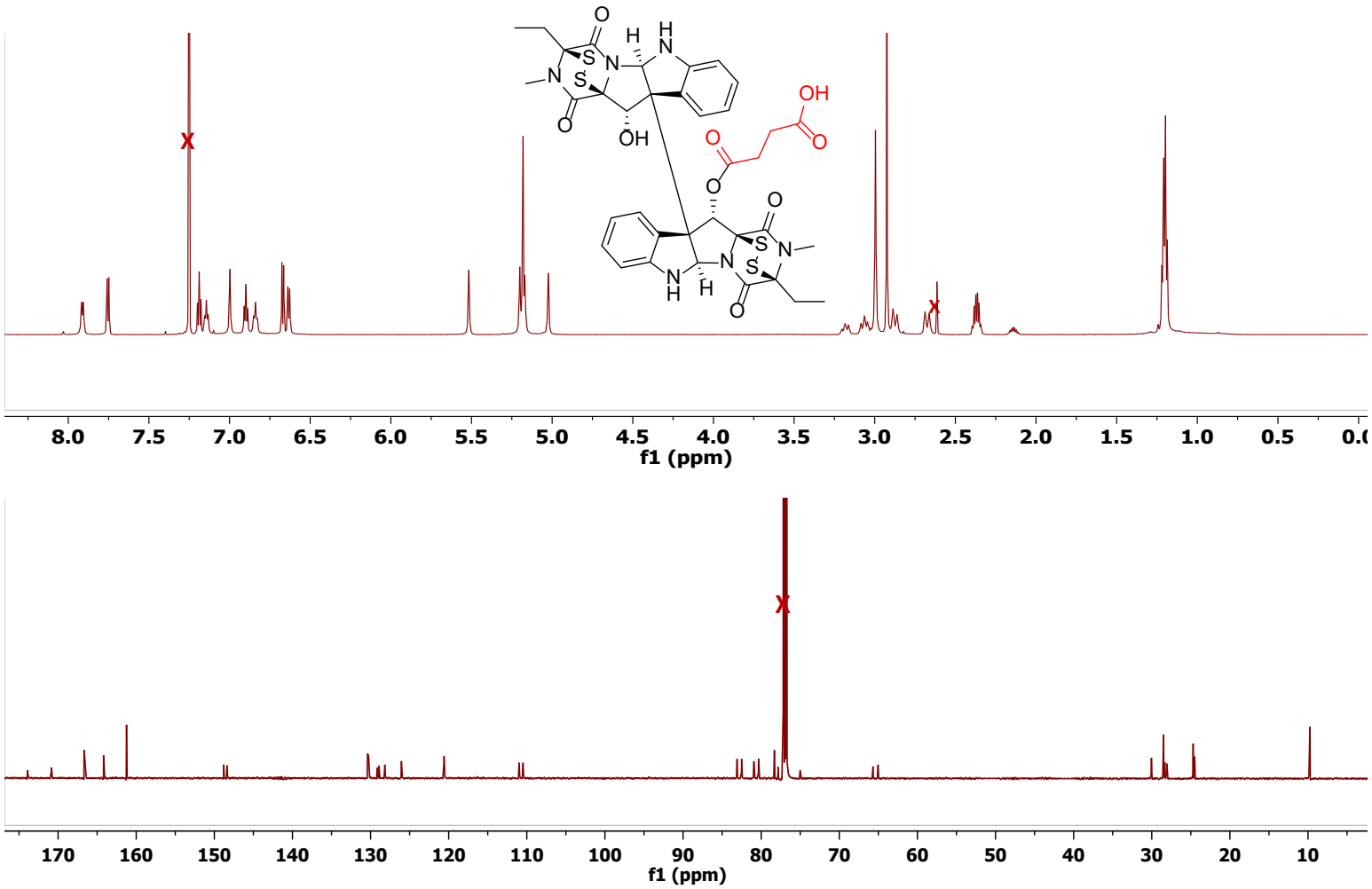

Figure S61. ^{1}H (upper panel) and ^{13}C (lower panel) NMR Spectra of 4 in $CDCl_3$ [700 MHz for ^{1}H and 175 MHz for ^{13}C].

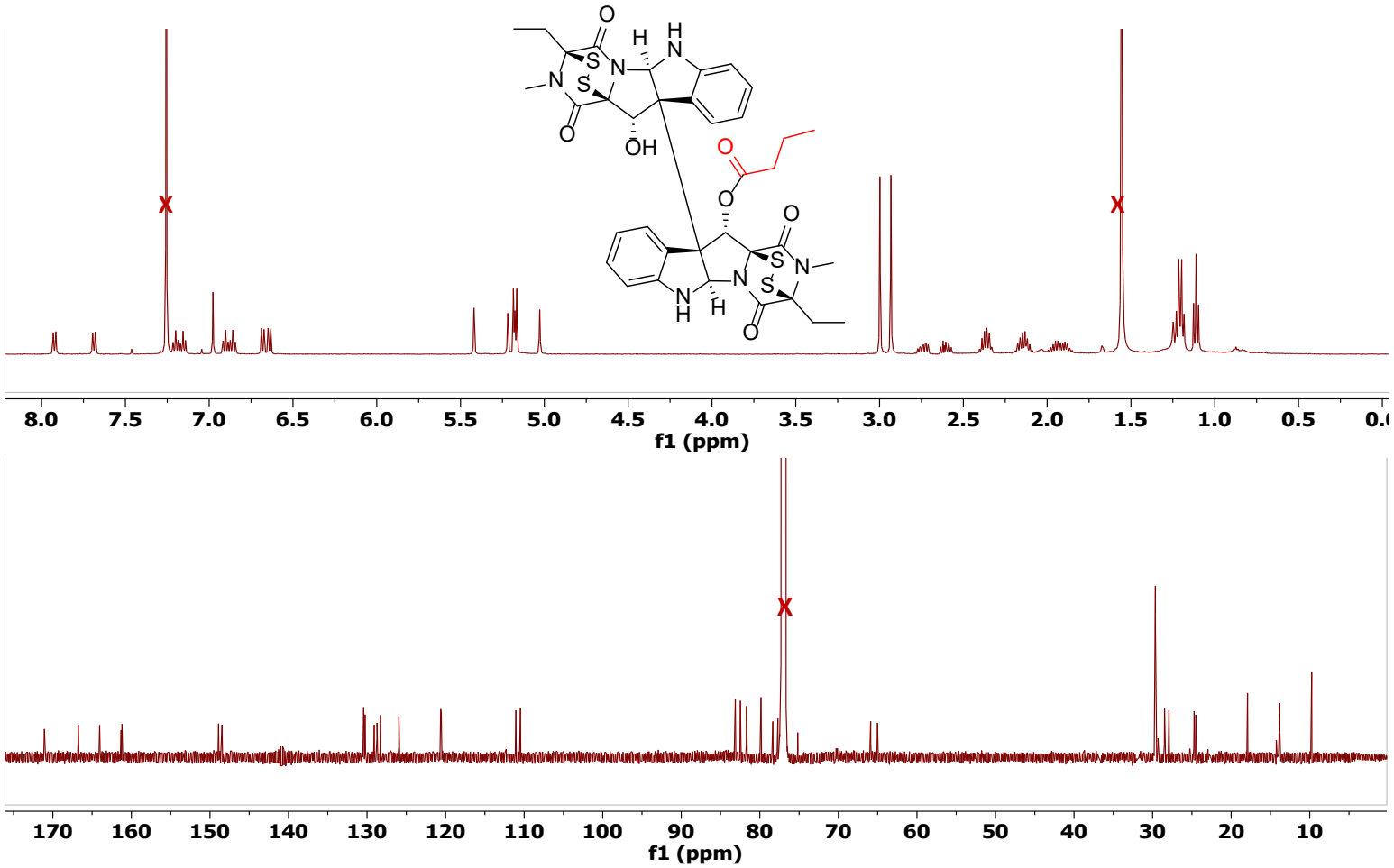

Figure S62. ^{1}H (upper panel) and ^{13}C (lower panel) NMR Spectra of 5 in $CDCl_3$ [500 MHz for ^{1}H and 175 MHz for ^{13}C].

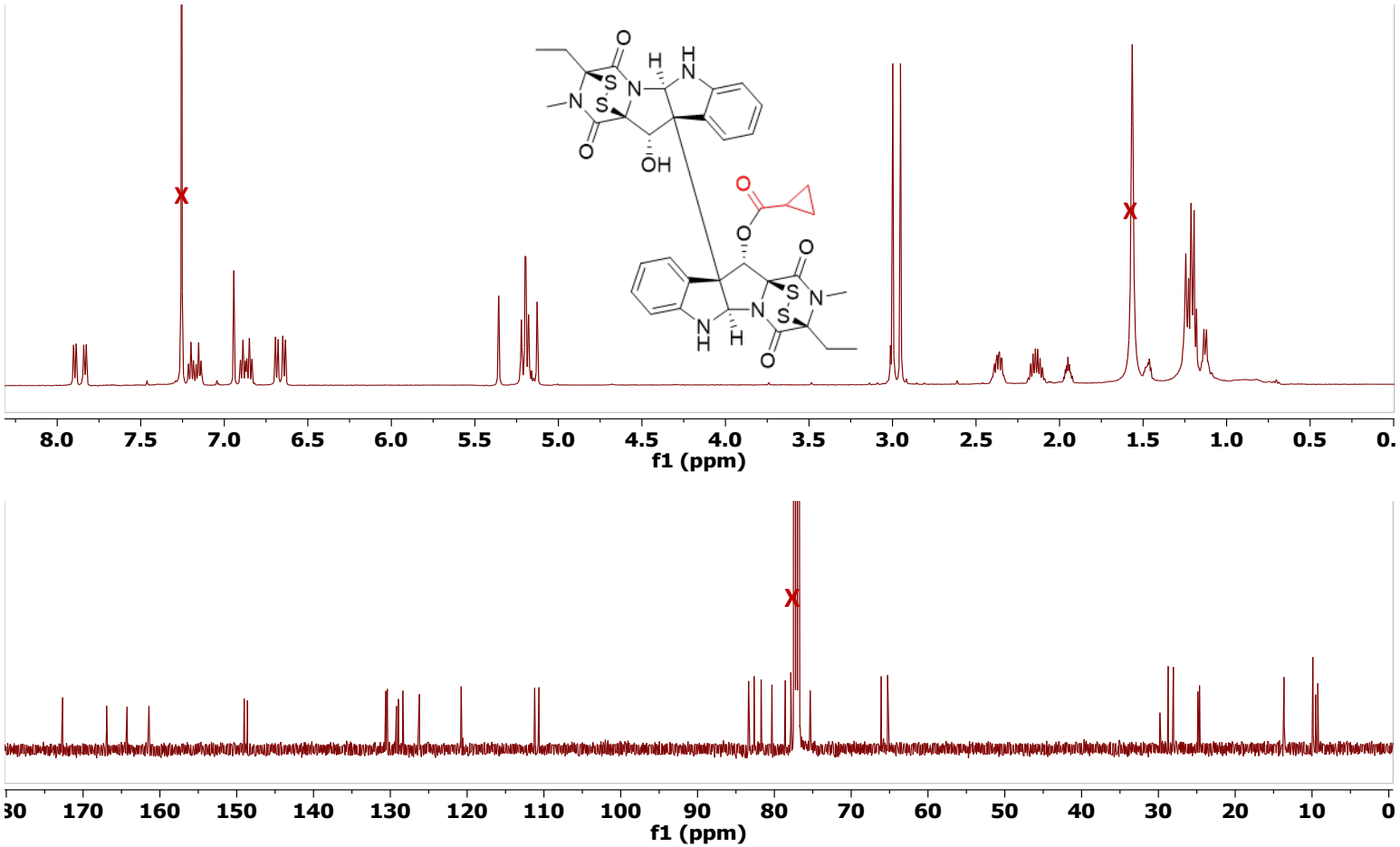

Figure S63. ^{1}H (upper panel) and ^{13}C (lower panel) NMR Spectra of 6 in $CDCl_3$ [500 MHz for ^{1}H and 125 MHz for ^{13}C].

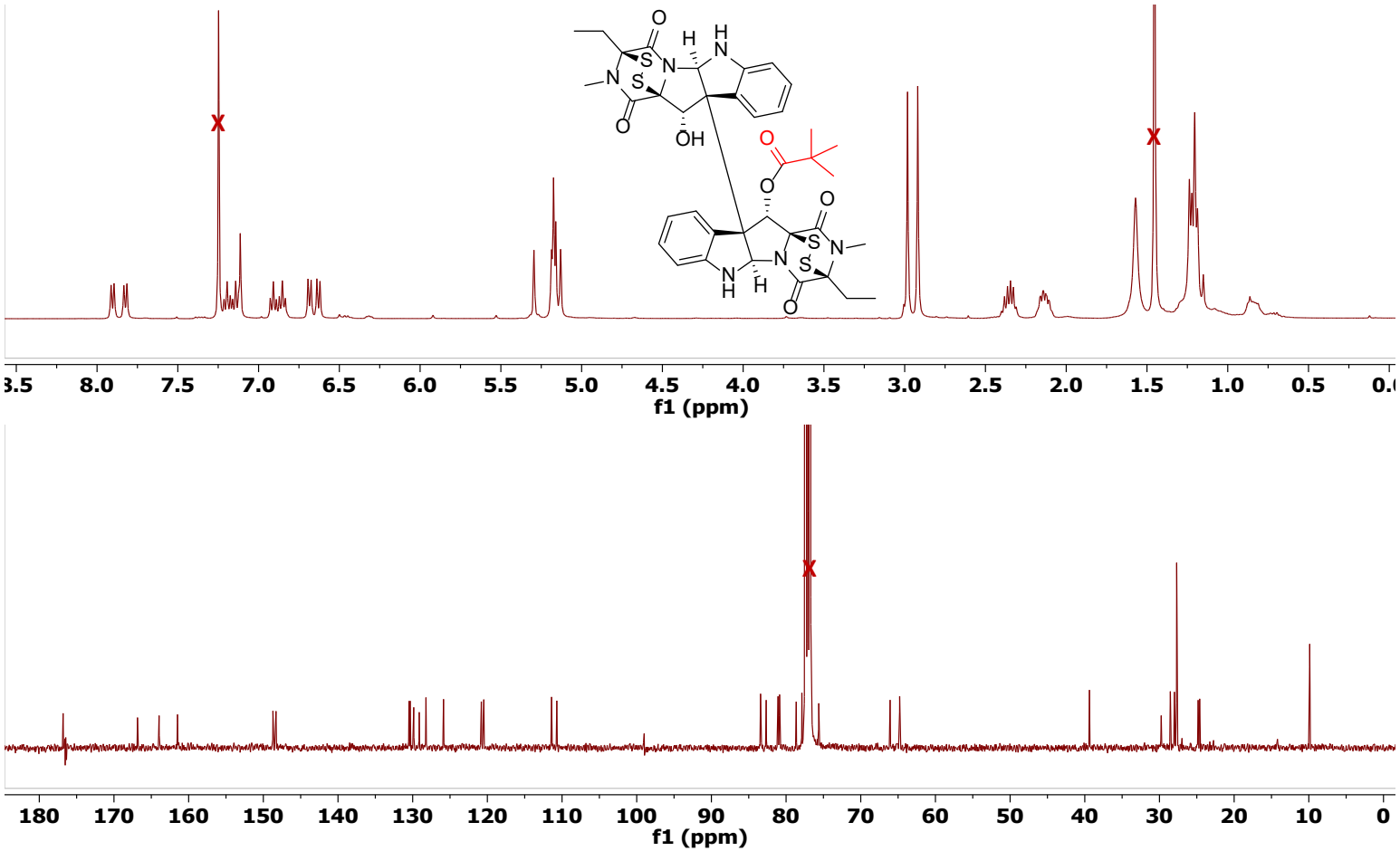

Figure S64. ^{1}H (upper panel) and ^{13}C (lower panel) NMR Spectra of 7 in $CDCl_3$ [400 MHz for ^{1}H and 100 MHz for ^{13}C].

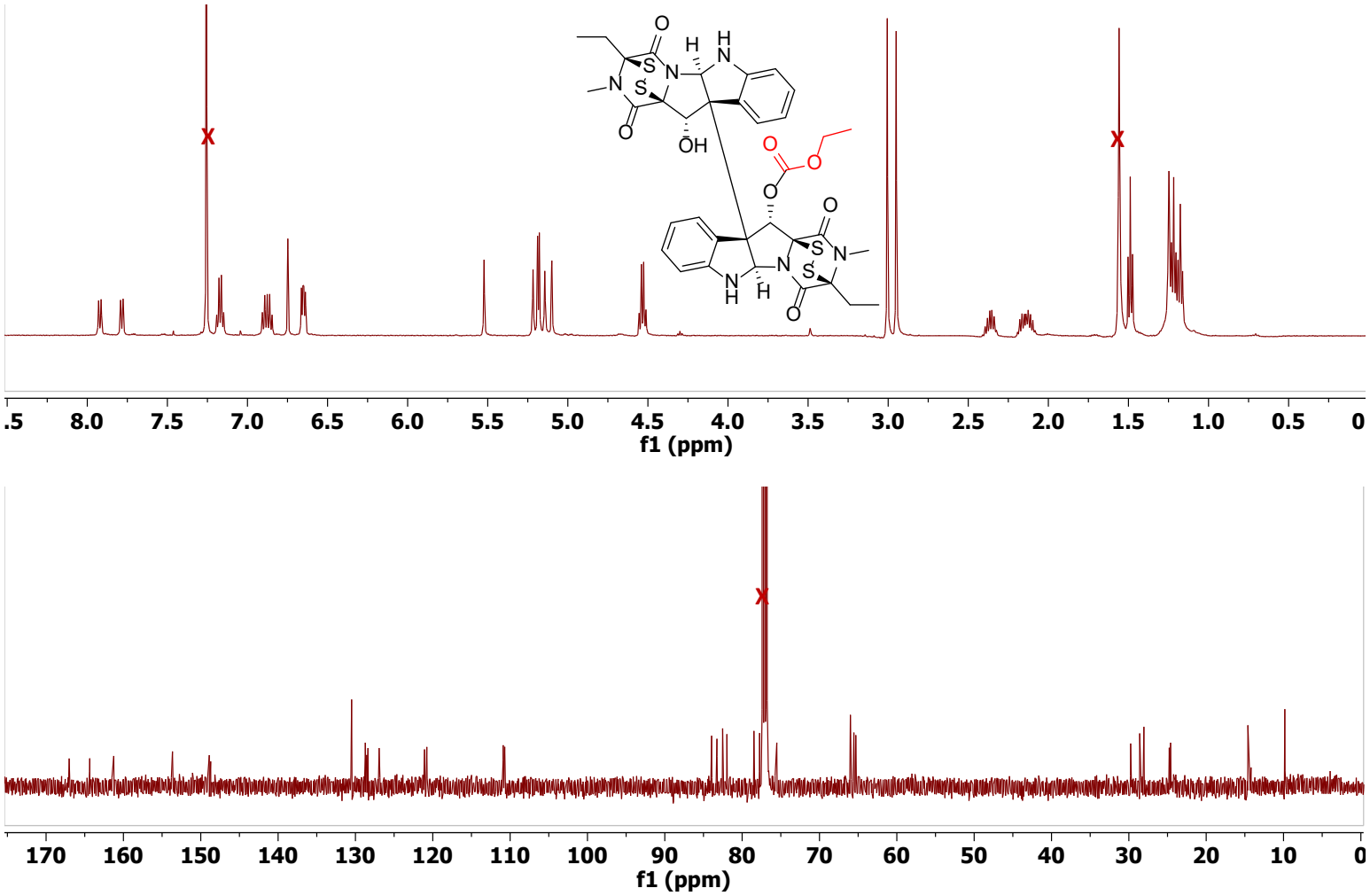

Figure S65. ^{1}H (upper panel) and ^{13}C (lower panel) NMR Spectra of 8 in $CDCl_3$ [500 MHz for ^{1}H and 125 MHz for ^{13}C].

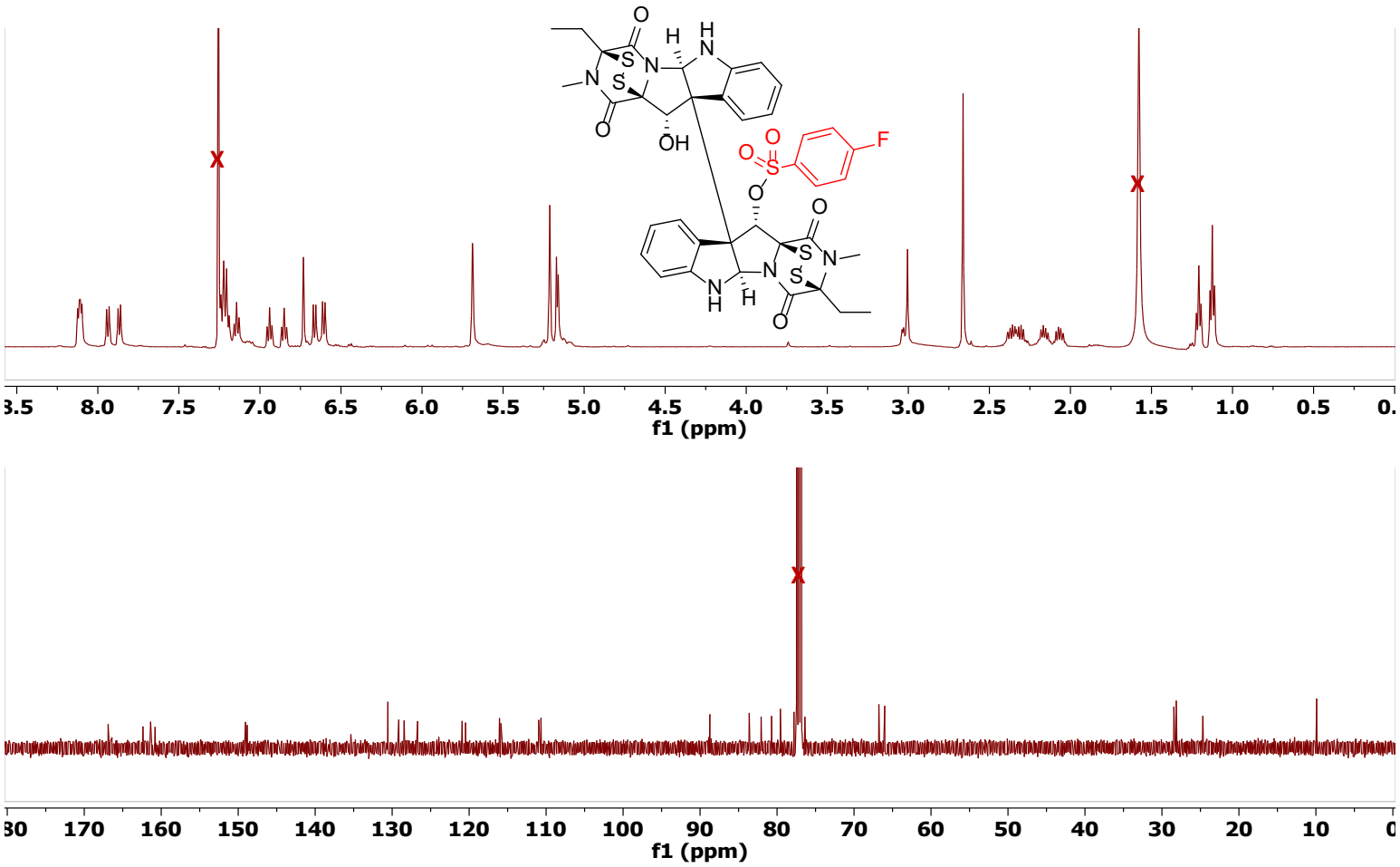

Figure S66. ^{1}H (upper panel), ^{13}C (lower panel) NMR Spectra of 9 in $CDCl_3$ [500 MHz for ^{1}H, and 125 MHz for ^{13}C].

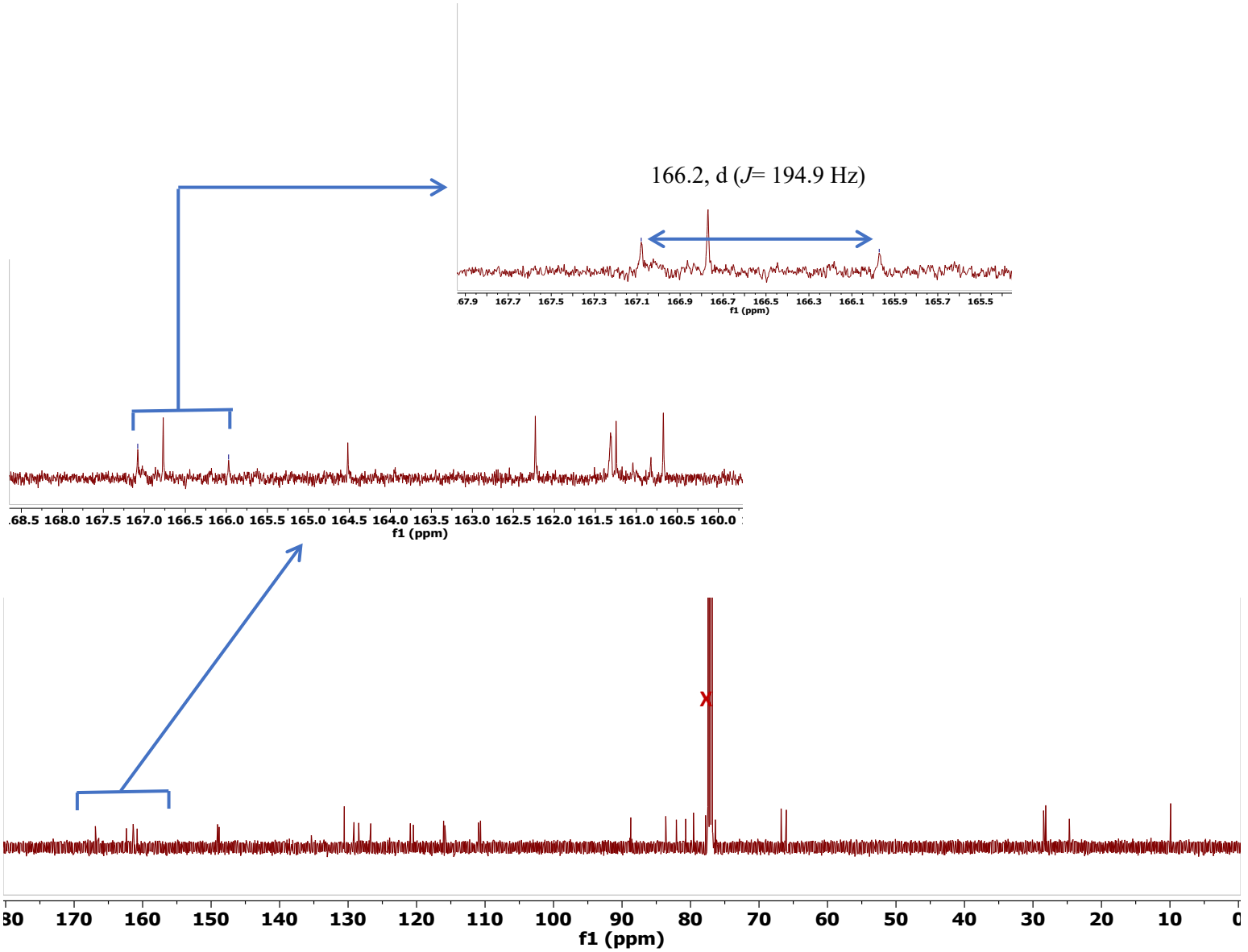

Figure S67. ^{13}C NMR Spectra of 9 in $CDCl_3$ Showing the Split Carbon by the ^{19}F [125 MHz for ^{13}C].

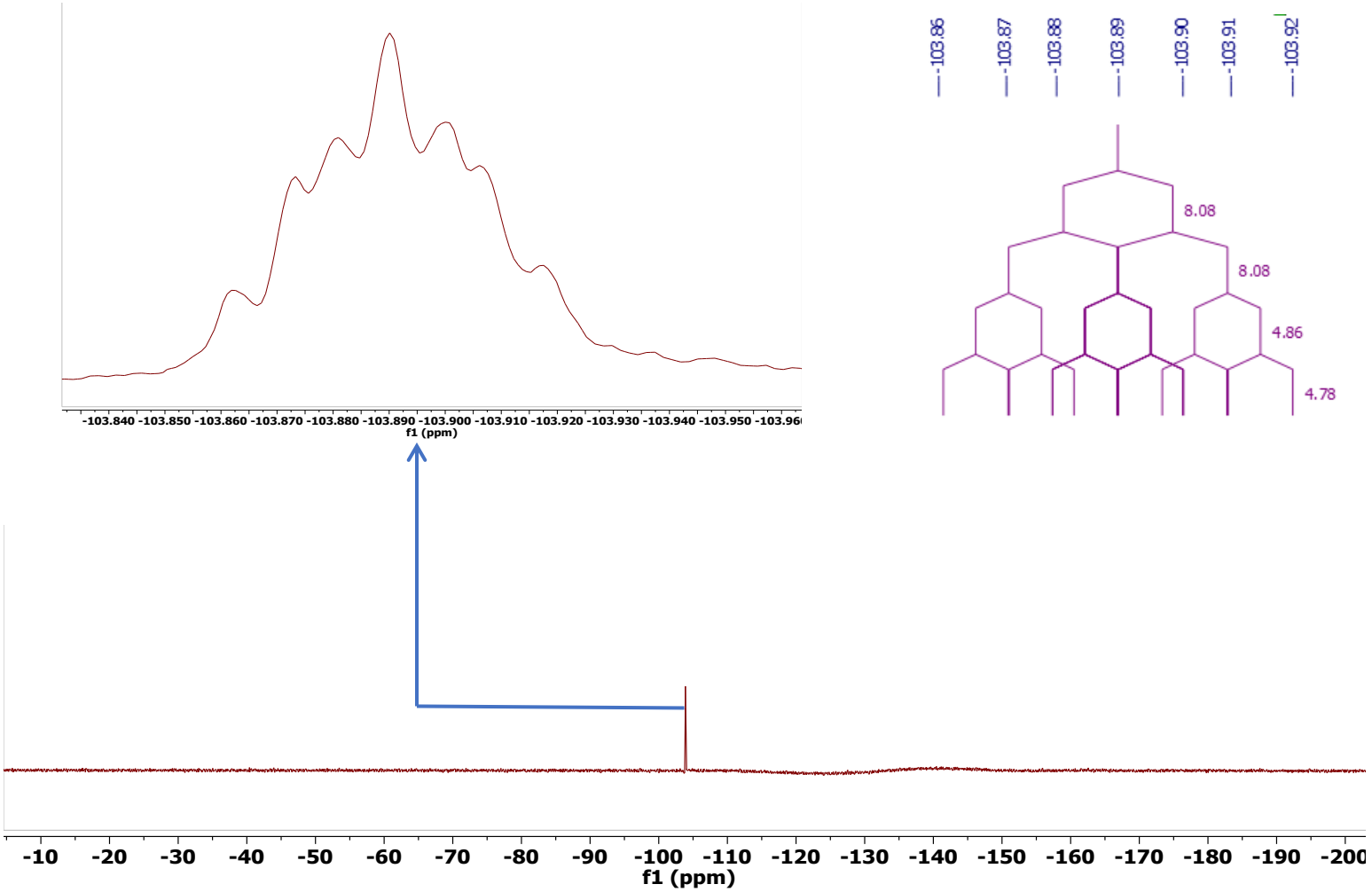

Figure S68. ^{19}F NMR Spectrum of 9 in $CDCl_3$ [470 MHz for ^{19}F].

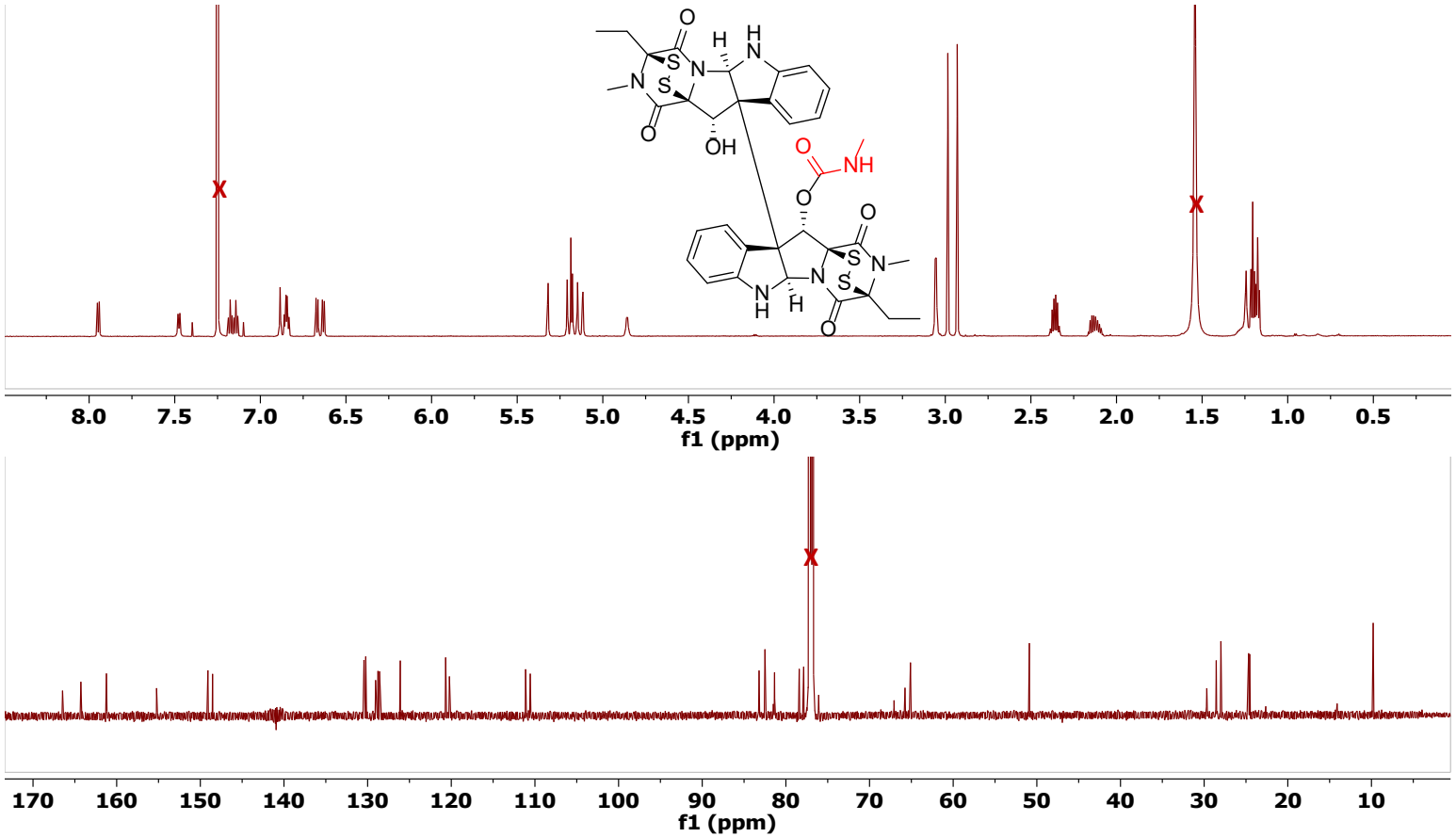

Figure S69. ^{1}H (upper panel) and ^{13}C (lower panel) NMR Spectra of 10 in $CDCl_3$ [500 MHz for ^{1}H and 175 MHz for ^{13}C]

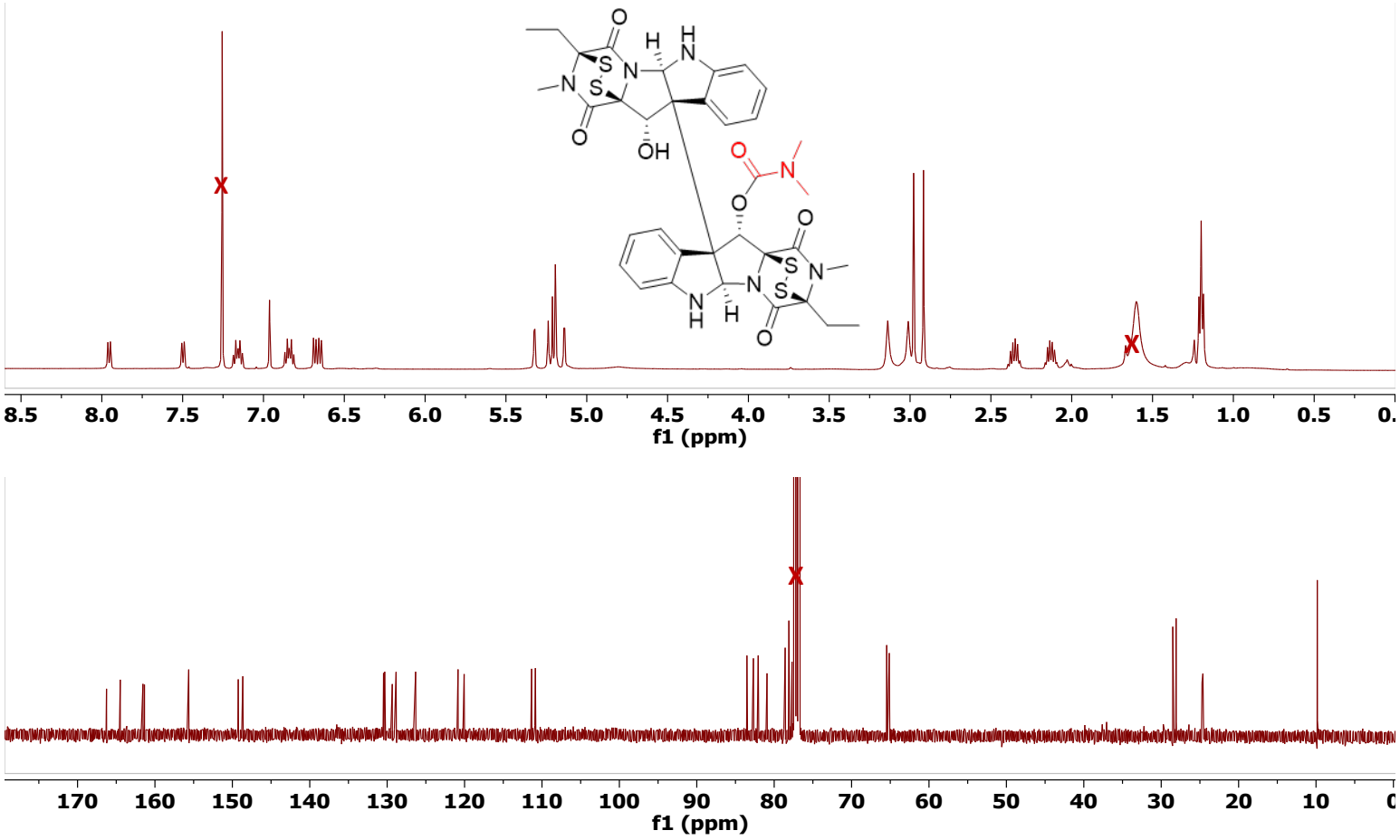

Figure S70. ^{1}H (upper panel) and ^{13}C (lower panel) NMR Spectra of 11 in $CDCl_3$ [500 MHz for ^{1}H and 175 MHz for ^{13}C]

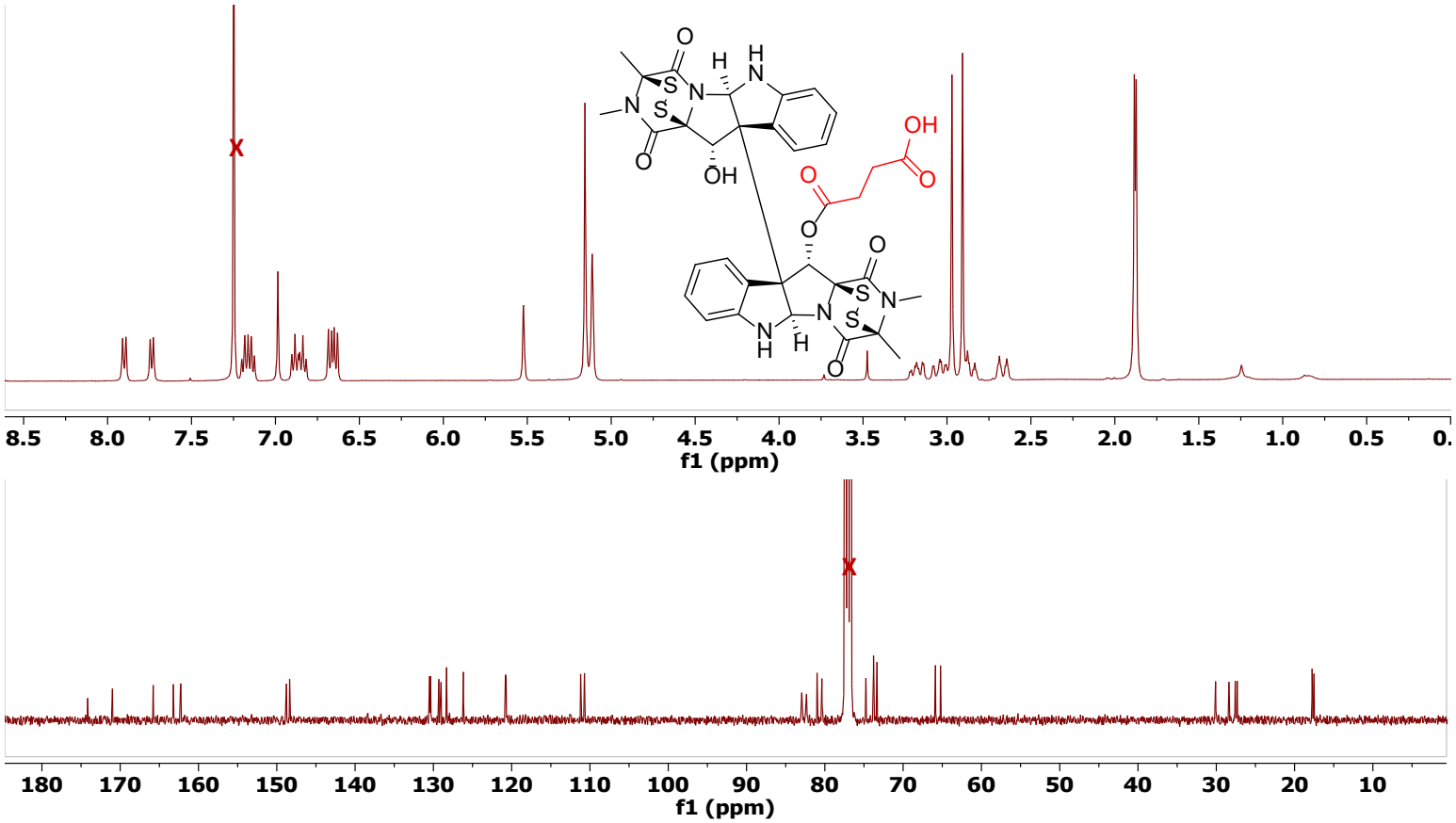

Figure S71. ^{1}H (upper panel) and ^{13}C (middle panel) NMR Spectra of 12 in $CDCl_3$ [400 MHz for ^{1}H and 100 MHz for ^{13}C]

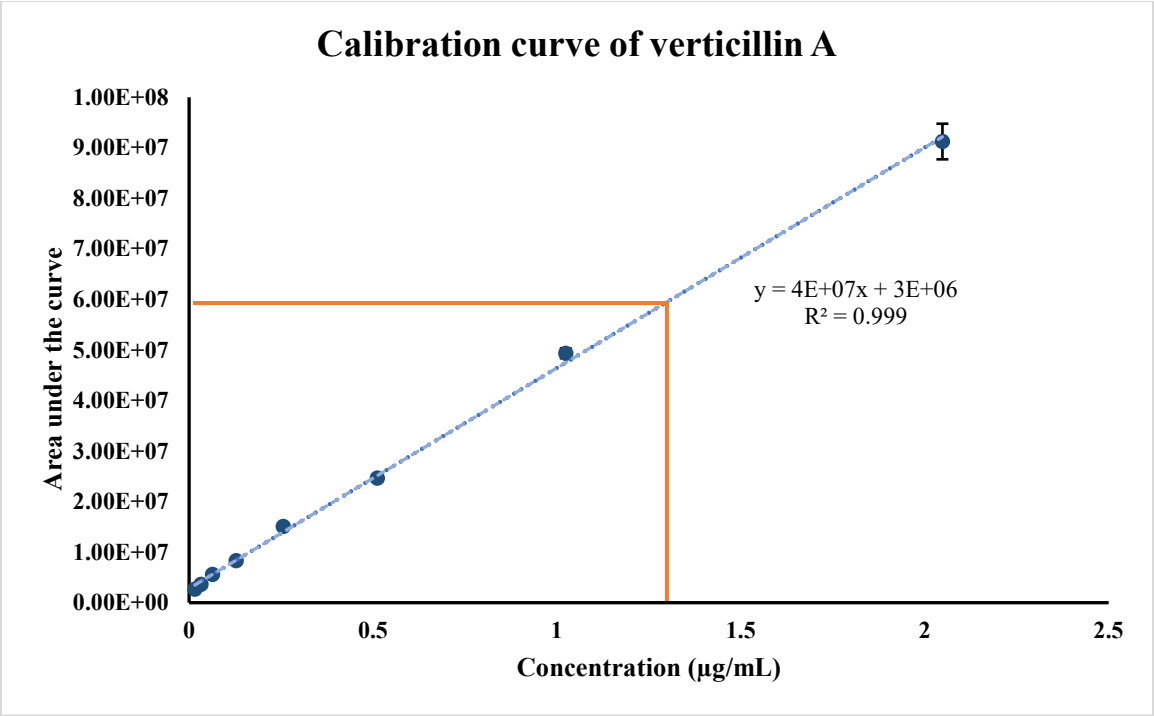

Figure S72. Calibration Curve for Verticillin A. Measured via UPLC-HRMS, using a Waters Acquity UPLC system coupled with a Thermo Q-Exactive Plus mass spectrometer. The instrument was operated under positive mode using selected ion monitoring (SIM) of verticillin A [$(M+H)^+$, *m/z* of 697.10]. To build the calibration cure (above), 3 µL of each concentration was analyzed in triplicate. These data represent means ± SD, and the orange line shows the amount of verticillin A in the diluted solution (1.29 µg/mL). In sum total, there were 0.91 mg of verticillin A per mL of eNP solution, representing an encapsulation efficiency of 76.9%.

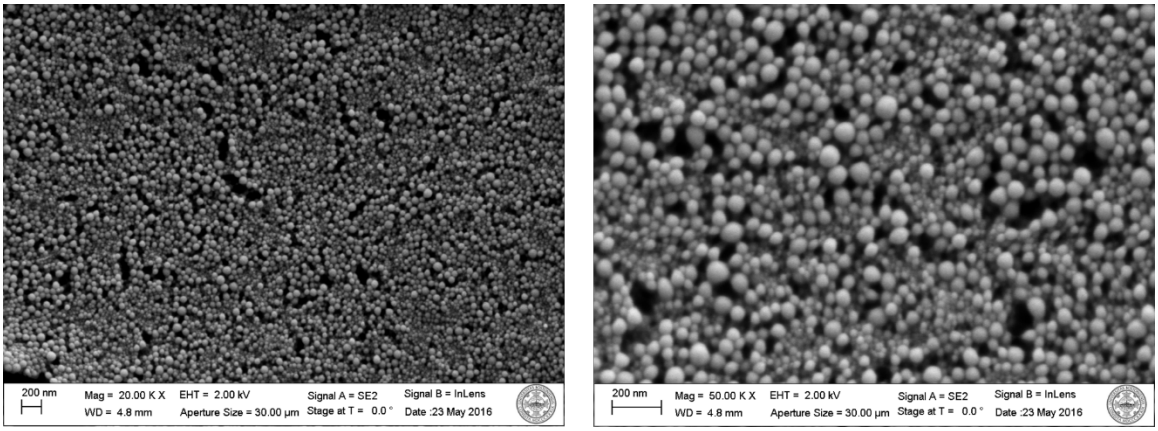

Figure S73. Scanning Electron Micrograph of Verticillin A Expansile Nanoparticles (eNP). Showing spherical particles of approximately 100 nm at pH 7.4. The right picture is a zoom in of a spot shown on the left picture. In both pictures, the scale bar = 200 nm.

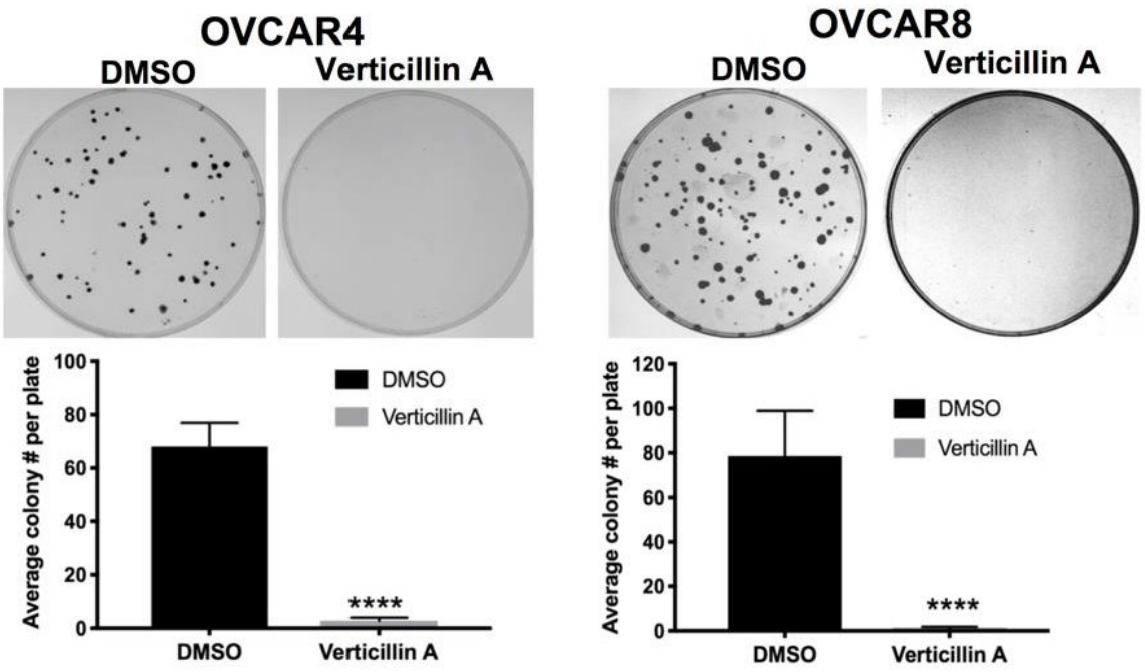

Figure S74. 2D Foci Assay on OVCAR4 and OVCAR8 Cells. The cells were treated with vehicle and verticillin A (50 nM) for 8 hrs. Following drug incubation, media was changed, and cells were incubated for 2 weeks to form colonies. Representative images of 2D foci assay performed in OVCAR4 and OVCAR8 cells are shown. Each experiment was performed in three biological replicates, and data represent mean ± SEM. Significance tested by Student's t-test in comparison to vehicle control. $p<0.05$ was considered statistically significant (* $p<0.05$; ** $p<0.01$; *** $p<0.001$; **** $p<0.0001$).

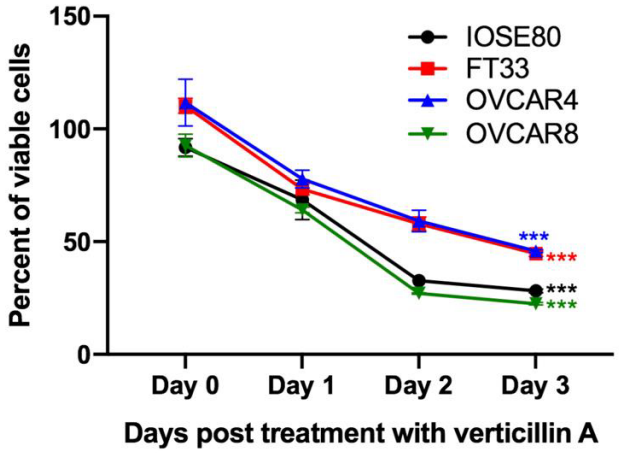

Figure S75. Cell Viability Test of Normal and Cancer Cells Treated with Verticillin A. Four ovarian cell lines (IOSE80, FT33, OVCAR4 and OVCAR8) were treated with vehicle (DMSO) and verticillin A (50 nM) for 72 hrs. Each experiment was performed in three biological replicates, and data represent mean ± SEM. Statistics were generated with Student's t-test for Day 0 and Day 3 within each cell line. $p<0.05$ was considered statistically significant (* $p<0.05$; ** $p<0.01$; *** $p<0.001$; **** $p<0.0001$).